Targeting PI3K pathway to enhance cisplatin cytotoxicity in lung cancer models

Thesis submitted for the degree of

Doctor of Philosophy

At the University of Leicester

By

Wenjing Liao

Department of Cancer Studies

University of Leicester

2016

ABSTRACT

Targeting PI3K pathway to enhance cisplatin cytotoxicity in lung cancer models

Wenjing Liao

Lung cancer is a leading cause of cancer deaths and is commonly diagnosed in both males and females. The cause of lung cancer is mainly attributable to cigarette smoking and aging, accounting for more than half of all lung cancer deaths. Non-small cell lung cancer (NSCLC) is the most common subtype of lung cancer (about 80%) compared to small cell lung cancer (SCLC) and it is normally subclassified into squamous cell carcinoma, adenocarcinoma and large cell carcinoma. Cisplatin-based treatments are the main first-line regimens for any stage of NSCLC, although platinum has over a 40-year history of use in clinical practice. Recently, molecularly targeted agents have been developed for improvement of treatment outcomes in patients with advanced lung cancers, such as EGFR-and ALK-targeted drugs. However, the acquired resistance to these agents eventually impairs sensitivity to treatment. Studies have shown that PI3K/Akt signaling activation is associated with resistance to the targeted treatments, and highlights a role for targeting PI3K/Akt signaling to restore sensitivity to targeted therapies. Moreover, Akt inhibition has been shown to promote sensitivity to cisplatin treatment.

In this project, both cisplatin and various agents which target Akt directly or indirectly, were tested on 2D NSCLC cell cultures for assessment of potencies. Single-agent treatment showed that the mutant P53 cell line (H596) showed the greatest sensitivity to cisplatin treatment compared to two WT P53 cell lines (A549 and H460). This was similarly observed in a patient-derived tissue explant model which showed that P53 mutant cases were more sensitive to cisplatin treatment than those WT P53 cases. In 2D adherent cell culture and 3D organotypic co-culture of cancer cells with fibroblasts, Akt activity was activated in response to cisplatin treatment, which was similarly observed in one explant case. Moreover, decreased Akt phosphorylation was significantly correlated with increased PARP cleavage in WT P53 cases only.

Both PI3K- and Akt-targeted treatments were shown to be highly potent on 2D culture and 3D spheroid models compared to other cisplatin-based regimens. Further analysis of molecular biomarkers by In-Cell western assay corroborated this, with induction of caspase-3-dependent cell death significantly higher when cisplatin treatment was combined with PI3K- or Akt-targeting drugs. The increase in apoptosis was concurrently observed with decreases in pAkt levels. P53 and PTEN levels were not induced by combination treatments compared to cisplatin alone, suggesting that functional P53 might not be required for induction of cell death.

ACKNOWLEDGEMENTS

This PHD project is certainly unable to be operated without friendly support from a number of staff at CSMM department.

Firstly, I give my sincere gratitude to Dr Lynne Howells for her earnest and tireless help with my project arrangement, guideline and thesis modification in the third year. I also thank Dr James Howard Pringle for his help with project research in the previous two years and suggesting for the thesis modification. Moreover, I would express my sincere thankfulness to Dr Don JL Jones for his help to arrange a new supervisor for me in the third year, when Dr Pringle has retired. Lastly, I am thankful to the departmental leaders including Prof Karen Brown for their providing of equipment and lab consumables for carrying on study.

Secondly, I am thankful to those colleagues who helped me with my experiments. The first needs to be mentioned is Dr Ellie Karekla, who helped me with the study on explants model. Next, I would like to thank Gintare Smagurauskaite, Almahdi Jaber and Abdlrzag M.Ehdode for their generous lending chemicals to me when I was running out of materials by the end of study. Of course, there are many other staff who used to help with my study, whom I do not forget to express my thankfulness

Then, I would give my thankfulness to the core histology service staff- Angie, Linda and Janine for proving tissues-associated materials.

Above all, I would like to give my heartfelt gratitude to my beloved mother, father, grandpa and other family members for their generous providing of funds to finish a PHD project and continually encouraged me to complete the project.

TABLE OF CONTENTS

ABBREVIATIONS

AAH	Atypical adenomatous hyperplasia
ADC	Adenocarcinoma
AIS	Adenocarcinoma *in situ*
AC	Atypical carcinoid
ALK	Anaplastic lymphoma kinase (*ALK* refers to gene)
AKT	V-Akt murine thymoma viral oncogene homolog (Akt refers to protein)
ATM	Ataxia-telangiectasia mutated protein kinase
ATP	Adenosine-5'-triphosphate
ANOVA	Analysis of variance
AIF	Apoptosis-inducing factor
BRAF	Serine/threonine-protein kinase BRAF *(BRAF* refers to gene)
BCL-2	B-cell lymphoma 2
BAD	Bcl-2-associated death promoter
BAK	Bck-2 homologous antagonist/killer
BAX	Bcl2-like protein 4
BSA	Bovine serum albumin
CDKN2A	Cyclin-dependent kinase inhibitor 2A
CT	Computed tomography
CTLA-4	Cytotoxic T-lymphocyte antigen-4
CK	Cytokeratin
CAFs	Cancer-associated fibroblasts
CI	Combination index
DNA	Deoxyribonucleic acid
DDR2	Discoidin domain receptor tyrosine kinase 2 (*DDR2* refers to gene)
DDR	DNA damage response
2D/3D	2/3 Dimensional
DMF	Dimethylformamide
DMSO	Dimethylsulfoxide
DMEM	Dulbecco's modified eagle's medium-high glucose
EBUS	Endobronchial ultrasound

EUS	Endoscopic (oesophageal) ultrasound
ECM	Extracellular matrix
EGFR	Epidermal growth factor receptor (*EGFR* refers to gene)
ERBB2	The gene encoding HER2
ERK	Mitogen-activated protein kinase (also known as MAPK)
EMA	European medicines agency
EDTA	Ethylenediaminetetraacetic acid
Fa	Fraction affected by dose
FGFR1	Fibroblast growth factor receptor 1 (*FGRF1* refers to gene)
FDA	US food and drug administration
FBS	Fetal bovine serum
5-FU	Fluorouracil
RAL-GEF	Guanine nucleotide exchange factors of the RAS-like small guanosine-5'-triphosphate (GTP)-binding protein regulators (GTPases)
GTP	Guanosine-5'-triphosphate
GAPDH	Glyceraldehyde 3-phosphate dehydrogenase (*GAPDH* refers to gene)
HNSCC	Head and neck squamous cell carcinoma
HPV	Human papillomavirus
HER2	Human epidermal growth factor receptor 2
HGFR	Hepatocyte growth factor receptor
HSP	Heat shock protein
HGD	Human genomic DNA
H&E	Hematoxylin and eosin
hr	hour
IKKα	IkappaB kinase alpha
IHC	Immunohistochemistry
ICW	In-cell western assay
IMS	Industrial methylated spirits
IAA	Isoamyl alcohol
IC50	Half maximal inhibitory concentration
IV	Intravenous(ly)
KRAS	V-Ki-ras2 Kirsten rat sarcoma viral oncogene homolog (KRAS refers to protein)
KGM	Keratinocyte growth medium
LPA	Lepidic predominant adenocarcinoma

LNA	Locked nucleic acid
MRI	Magnetic resonance imaging
MIA	Minimally invasive adenocarcinoma
M	Mean
MEK1/MAPKK	Mitogen-activated protein kinase kinase 1 (*MEK1*/*MAPKK1* refers to gene)
MET	Mesenchymal-epithelial transition receptor tyrosine kinase (*MET* refers to gene)
MDM2	Mouse double minute-2
α-MEM	α Modified eagle's medium
MDR	Multidrug resistance
mTORC2/PDK2	Mammalian target of rapamycin complex 2
MMPs	Matrix metalloproteases
NSCLC	Non-small cell lung cancer
NOS	Not otherwise specified
NOTCH1	Notch homolog 1
NA	Non-applicable
NF-κB	Nuclear factor kappa B
OS	Overall survival
OSA	Osteosarcoma
ORR	Objective response rate
PET	Positron emission tomograph
PFS	Progression free survival
PIK3CA	Phosphatidylinositol 3-kinase, catalytic, α polypeptide (*PIK3CA* refers to gene)
PTEN	Phosphatase and tensin homolog deleted on chromosome ten (PTEN refers to protein)
PKB	Protein kinase B
PIP2	Phosphatidylinositol 4,5-bisphosphate
PIP3	Phosphatidylinositol (3,4,5)-trisphosphate
PD-1	Programmed death-1
PDK1	3-Phosphoinositide-dependent protein
PBS	Phosphate buffered saline
PH	Potential of hydrogen
PARP	Poly (ADP-ribose) polymerase
PCR	Polymerase chain reaction

PMAIP1	Phorbol-12-myristate-13-acetate-induced protein 1 (or NOXA)
PUMA	P53 upregulated modulator of apoptosis
QoL	Quality of life
ROS1	*ROS* proto-oncogene 1, encoding a receptor tyrosine kinase (ROS1)
RET	*RET* proto-oncogene encoding a receptor tyrosine kinase (RET)
RALB	RAS like proto-oncogene B encoding RALB
SCLC	Small cell carcinoma
SD	Standard deviation
SDS	Sodium dodecyl sulfate
STAT3	Signal transducer and activator of transcription 3
SDF-1	Stromal cell-derived factor 1
SCC	Squamous cell carcinoma
TME	Tumor microenvironment
RTK	Receptor tyrosine kinase
TBK1	Tank binding kinase 1 (*TBK1* refers to gene)
TLR	Toll-like receptors
TAAs	Tumor associated antigens
UHL	University hospitals of leicester
WHO	World health organization
WT	Wildtype

LIST OF FIGURES

Chapter One:

Chapter Two:

Chapter Three:

Chapter Five:

LIST OF TABLES

Chapter One:

Chapter Three:

Chapter Four:

LIST OF PUBLICATIONS

Karekla , E. et al., 2017. Ex vivo explant cultures of non-small cell lung carcinoma enable evaluation of primary tumor responses to anticancer therapy. *Cancer Research* (see appedix 7.3).

1. CHAPTER ONE: INTRODUCTION

1.1LUNG CANCER AND NON-SMALL-CELL LUNG CANCER

1.1.1 CANCER

Cancer is a leading cause of disease worldwide with approximately 14.1 million new cases diagnosed and 8.2 million deaths due to cancer in 2012 (WHO Media Centre , 2015) (Worldwide Cancer Factsheet, 2014) (Torre, et al., 2015). The most common types of cancer diagnosed worldwide in both men and women include lung, colorectum and stomach cancer (Worldwide Cancer Factsheet, 2014). Lung cancer accounts for 13% of total cancer diagnoses with an estimated 1.8 million new cases occurred in 2012 (Torre, et al., 2015). Lung cancer represents the commenest tumor types in both men and women. Amongst the global male population, the incidence of lung cancer in Asia (35.1 per 100,100) is substantively below that in Europe and North America, whereas for females, breast cancer represents the high incidence and most prevalant type of cancer around the world (Stewart, 2014).

1.1.2 SUBTYPES OF LUNG CANCER

Lung cancer is generally classified into two main subtypes, which are non-small cell lung cancer (NSCLC) and small cell carcinoma (SCLC). NSCLC accounts for the majority of lung cancer cases (85%) and is commonly subcassified into three histological subtypes: squamous cell carcinoma, adenocarinoma and large cell carcinoma (About Lung Cancer, 2016). Adenocarcinoma (40%) and squamous cell carcinoma (30%) account for most of the NSCLC cases (About Lung Cancer, 2016).

1.1.3 MORTALITY AND SURVIVAL FOR LUNG CANCER

Lung cancer is the leading cause of cancer deaths in men worldwide. For women, lung cancer is the leading cause of cancer deaths in more developed countries compared with less developed counterparts (Torre, et al., 2015). Taken as a whole, lung cancer represents one of the leading causes of cancer deaths worldwide with around 1.4 in 2010 and 1.6 million deaths in 2012 (The Cancer Genome Atlas Research Network, 2012) (WHO Media Centre , 2015). Lung cancer has a poorer 5-year survival rate than other frequently diagnosed cancers, such as prostate (mainly in males), breast (mainly in females) and colorectum cancers (Worldwide Cancer Factsheet, 2014).The 5-year survival rate for lung

cancer is lower in the UK than in the USA or the rest of Europe (Lung Cancer Fact Sheet - 2015 - Europe, 2015). SCLC tends to have a lower survival rate than NSCLC with median survival less than 4 months without treatment (Sankaranarayanan , et al., 2011).

1.2RISK FACTORS FOR LUNG CANCER

1.2.1 TOBACCO CONSUMPTION

Tobacco use is the most important risk factor for cancer and particularly for lung cancer, accounting for around 20% of global cancer deaths and 70% of lung cancer deaths worldwide (WHO Media Centre , 2015). China has the largest population of smokers across the world with an estimated 301 million people currently smoking and smoking habit accounts for about half of all smoking-male deaths in China (Lung Cancer Fact Sheet - 2016 - Asia, 2016). As smoking is associated with a high incidence of lung cancer, elimination of smoking initiation and an increase in smoking cessation would help to reduce the number of lung cancer cases. Due to an increasing number of female smokers, lung cancer is rapidly becoming an equally commonly diagnosed type of cancer in women as in men (Torre, et al., 2015). Smoking-associated lung cancer can also be caused by second-hand smoke. Passive smoking is responsible for one in four persons getting lung cancer and may also increase the risk of cancers of the larynx (voice box) and pharynx (upper throat) (Passive Smoking, 2016).

Cigarette smoke has been discovered so far to contain more than 7000 chemical compounds. The majority of the known carcinogens amongst these chemicals have been associated with initiation of cancer, by binding to deoxyribonucleic acid (DNA) and initiating genetic mutations, oxidative stress and epigenetic changes (Stewart, 2014).

1.2.2 NON-CIGARETTE ASSOCIATED RISK FACTORS

A large number of lung cancer cases are also diagnosed in non-smokers. Occupational and environmental carcinogens such as asbestos, arsenic, radon and polycyclic aromatic hydrocarbons can increase the risk of lung cancer (Torre, et al., 2015). In the USA and UK, radon gas is the leading cause of non-smoking-related lung cancers (Why Non-smokers Sometimes Get Lung Cancer, 2015) (Other Risk Fctors-Exposure to Radon Gas, 2014). Recently, air pollution has also been determined as a cause of lung cancer and in some East Asian countries more than 20% of deaths are attributable to ambient fine particles (Torre, et al., 2015). Virus infection (i.e. human papillomavirus (HPV)) may

also correlate with lung cancer development, but this association remains controversial (van Boerdonk , et al., 2013) (Lin , et al., 2016).

1.2.3 AGING

Cancer can be considered an age-related disease because the incidence of most cancers increase with age (WHO Media Centre , 2015) (White, et al., 2014). Lung cancer is often diagnosed in an aging population and on average each year around 3 in 5 lung cancer diagnoses in the UK between 2011 and 2013 were at 70 years and over (Lung Cancer Incidence by Age, 2016). Aging is also responsible for a high motality rate of lung cancer. In the UK between 2012 and 2014, elderly people aged 75 and over accounted for around half of all lung cancer deaths on average each year (Lung Cancer Mortality by Age, 2016). The diagnoses at advanced stages that tended to correlate with a poorer surival rate often occured in the elderly group, elevating the contribution of lung cancer deaths within his population.

1.2.4 HISTOLOGY

The recent update (2015) in WHO (World Health Organization) classification of lung cancer reviewed that some histologic subtypes are not only important for classification of lung cancer but also relate to the prognosis of lung cancer (Travis, et al., 2015). Adenocarcinoma with micropapillary or solid subtypes were found to be associated with risk of recurrence and poor prognosis of lung cancer (Spira, et al., 2015) (Travis, et al., 2015). Classification of tumor grades amongst subtypes of lung cancer can also be applied to determine tumor prognosis, as the majority of high grades of lung cancer, such as micropapillary and solid subtypes tend to show a poorer prognosis than the low-grade counterparts. The numerical grades of lung cancer can be generally classified into low, intermediate and high grades (Travis, et al., 2015).

1.3DIAGNOSIS OF LUNG CANCER

Lung cancer is a complex disease which can involve mutiple types of morphology and histology. Hence, the accurate diagnosis of lung cancer morphologically and histologically is of great importance in order to adequately inform the guildlines for appropriate staging and treatment. There are two main types of diagnostic measures for lung cancer; morphological diagnosis with imaging techiques; histological and cytological diagnosis with histological stains (Travis, et al., 2013).

1.3.1 IMAGING TECHNIQUES FOR DETECTION OF LUNG CANCER

Over the past three decades, several useful imaging techniques have been developed and applied for the diagnosis of lung cancer. Low-dose computed tomography (CT) scanning is useful for the detection of tumors in people with past or current smoking history at a high-risk for developing lung cancer (Bach, et al., 2012) (Spira, et al., 2015). CT combined with positron emission tomography (PET) is currently more widely used in clinical trials to assess how advanced primary lesions are, and for diagnosing distant metastases including lymph node involvement (National Collaborating Centre for Cancer (UK), 2011). Magnetic resonance imaging (MRI) tends to be applied for detecting cancers closer to the top of lung (also known as pancoast tumors or superior sulcus tumors) and and is suitable to detect cancers that have spread into the ribs or spine (Cancer Research UK, 2014) (Figure 1.1).

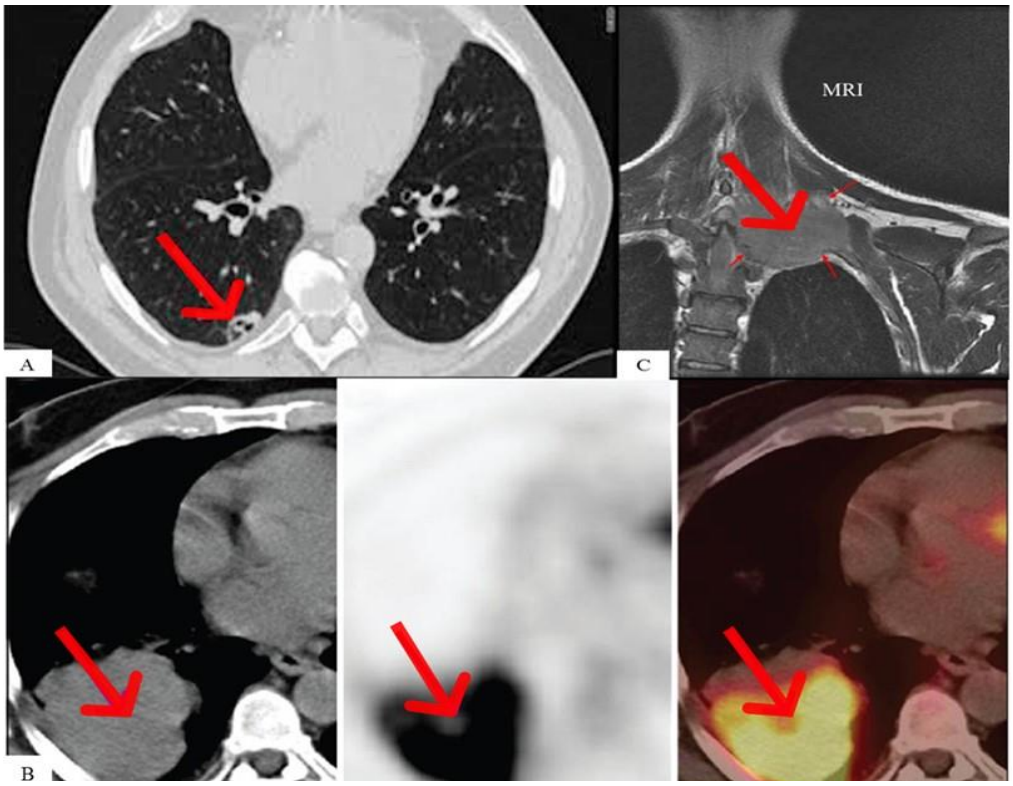

Figure 1. 1 Scanning images for diagnosis of lung cancer

The different scanning techniques for diagnosing lung cancer include low-dose CT scan (A) (Glatter, 2015), CT combined with PET (CT/PET) (Sharma, et al., 2013) and MRI scan (Pumonary Imaging, 2010). Figure (B) shows in the order from left to right CT, PET and CT/PET and (C) shows the detection of a pancoast tumor on the top of the lung. The red arrow in each image shows the tumor of interest.

1.3.2 HISTOLOGICAL AND CYTOLOGICAL DIAGNOSIS OF LUNG CANCER

1.3.2.1. Small Biopsies and Cytology Specimens

New criteria for lung cancer diagnosis based on small biopsies and cytology specimens have been proposed in the latest version of the WHO classification (Travis, et al., 2015). The diagnosis of around 60% of lung cancer patients at advanced stages is usually established based on these small specimens, which are also expected to be used to diagnose those lung patients at early stages along with the introduction of lung cancer sceening (Travis, et al., 2015). The small tissue samples are also used for molecular testing (Travis, et al., 2015).

1.3.2.2. Lung Cancer Subtyping for Diagnosis

Lung cancer subtypes classification is critical as it is beneficial when guiding patient-specific treatment modalities. The different NSCLC subtypes exhibit typical histologic features, which can be briefly described as follows: for lung squamous cell carcinoma,

unequivocal keratinization and well-formed classical bridges are observed; for lung adenocarcinoma, acinar, papillary, lepidic, micropapillary features are observed; the recent WHO classification classifies those NSCLC not otherwise specified (NOS) tumors without clear adenocarcinoma, squamous or neuroendocrine morphology or staining pattern as large cell carcinoma (Travis, et al., 2015). The typical histological patterns of the two main types of NSCLC are shown below (Figure 1.2). The lung cancers with combined histological features of different subtypes of NSCLC were also reviewed in the WHO classification, including adenosquamous carcinoma and adenocarcinomas predominant pattern (including nearly all subtypes of adenocarcinoma) (Travis, et al., 2015).

The diagnosis of lung cancer is sometimes unable to be determined based on the classic morphological and histologic features, and so immunohistochemical techniques assessing subtype-specific biomarkers are more beneficial for classifying those poorly differentiated NSCLCs (Fasano, et al., 2015) (Travis, et al., 2015).

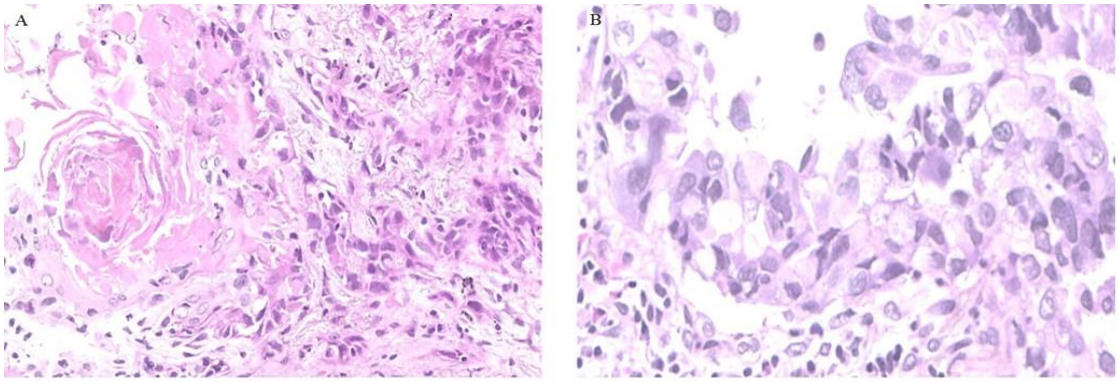

Figure 1. 2 The typical histological patterns of the two main subtypes of NSCLC

The histological appearance of the two common subtypes of NSCLC (squamous cell carcinoma and adenocarcinoma) shown above as (A) intercellular bridges and keratin pearl formation for squamous cell carcinoma (taken from LT105 case) and (B) mucus formation feature for adenocarcinoma (taken from LT104 case).

1.3.2.3. Sampling Tumor Tissues Using Minimally Invasive Procedures

There are several useful techniques for assisting lung cancer biopsies, including endobronchial ultrasound (EBUS), endoscopic (oesophageal) ultrasound (EUS) and mediastinoscopy (Cancer Research UK, 2014) (National Collaborating Centre for Cancer (UK), 2011). The currently applied precedures for obtaining sample tissues from lung cancer patients include bronchoscopic, needle and core biopsies (Sackett, et al., 2010) (Travis, et al., 2015). The cytological specimens are usually collected from sputum of patients and are more helpful to diagnose cancers intiating in the major airway of the lung, such as squamous cell carcinoma than other types of lung cancer (Sputum cytology, 2016).

1.3.3 LUNG CANCER STAGES AND DIAGNOSIS

1.3.3.1. The Old and Latest Updated Version of the TNM System

Tumor staging is usually given at the diagnosis of cancer. It provides more information about tumor sizes and progression and is beneficial to guide the appropriate treatment options for patients (Staging, 2015). Staging of cancer is also the most important predictor of survival (Mirsadraee, et al., 2012). The TNM staging system was first used in the classification of lung cancer (Mountain, 1986). In this system, 'T' represents primary tumor with numeric suffixes describing increasing size and involvement or both; 'N' stands for regional lymph nodes involvement with suffixes to describe levels of metastatic disease and 'M' for distant metastasis with suffixes to describe the absence or presence of metastasis to distant sites. The latest version of TNM staging system was released in 2009 and the changes in the new version took effect in January 2010 (American Joint Committee on Cancer, 2009) (Union for International Cancer Control, 2011). As shown in Table (1.1), the new version of the TNM system shows greater detail in the classification of tumor staging than did the old system. Since 2010, the staging of small cell carcinoma was also included in the application of the system (Union for International Cancer Control, 2011).

Table 1. 1 Comparison of the old and new TNM staging system for classification of lung cancer stages

The old version of TNM system was taken from the article (Mountain, 1986) and the new version of the system was the latest update of the system, taking effect in January 2010 (American Joint Committee on Cancer, 2009). The new version of the staging system is more comprehensive than the old version in the contents of description of TNM system and classification of tumor staging. 'T' represents primary tumor; TX: tumor cannot be assessed or tumor only present in sputum or bronchial washings; T0: no evidence of primary tumor; TIS: carcinoma *in situ* and the rest of numeric suffixes-containg 'T' describes primary tumor with increasing size and involvment or both. The numeric suffixes-containing 'N' symbols describe regional lymph nodes with levels of metastatic disease. The numeric suffixes-containing M symbols describe distant metastasis with the absence or presence of metastasis to distant sites.

The Older Version of TNM Staging System for Classification of Lung Cancer Stages (1986)				The Latest Version of TNM Staging System for Classification of Lung Cancer Stages (2010)			
Staging	The TNM System			Staging	The TNM System		
Occult Carcinoma	TX	N0	M0	Occult Carcinoma	TX	N0	M0
Stage 0	TIS	Carcinoma in situ		Stage 0	TIS	N0	M0
Stage I	T1	N0	M0	Stage Ia	T1a	N0	M0
	T2	N0	M0		T1b	N0	M0
				Stage Ib	T2a	N0	M0
Stage II	T1	N1	M0	Stage IIa	T2b	N0	M0
					T1a	N1	M0
					T1b	N1	M0
					T2a	N1	M0
	T2	N1	M0	Stage IIb	T2b	N1	M0
					T3	N0	M0
Stage IIIa	T3	N0	M0	Stage IIIa	T1a	N2	M0
					T1b	N2	M0
					T2a	N2	M0
	T3	N1	M0		T2b	N2	M0
					T3	N1	M0
					T3	N2	M0
	T1-3	N2	M0		T4	N0	M0
					T4	N1	M0
Stage IIIb	Any T	N3	M0	Stage IIIb	T1a	N3	M0
					T1b	N3	M0
					T2a	N3	M0
					T2b	N3	M0
	T4	Any N	M0		T3	N3	M0
					T4	N2	M0
					T4	N3	M0
Stage IV	Any T	Any N	M1	Stage IV	Any T	Any N	M1a
					Any T	Any N	M1b

1.3.3.2. Classification of Lung Cancer Incidence and Five-year Survival using the TNM System

The majority (70~80%) of patients with lung cancer are diagnosed at advanced stages (III and IV), whereas those with early stage disease only account for approximately 20-30% (Langer, et al., 1996) (Cancer Research UK, 2016).

The five-year survival rate for NSCLC decreases dramatically with increasing stage, falling from 58% (median of stage IA and IB) to 7.5% at stage IV. Five-year survival rate for SCLC decreased from around 30% at stage I to 1% at stage IV (Survival for non small cell lung cancer by stage, 2014). The summarized data of the five-year survival rate for lung cancer based on the combined NSCLC and SCLC data is shown in Figure 1.3. Taken together, the five-year survival rate for lung cancer is 44% at stage I and this dramatically reduced to 4.25% at stage IV.

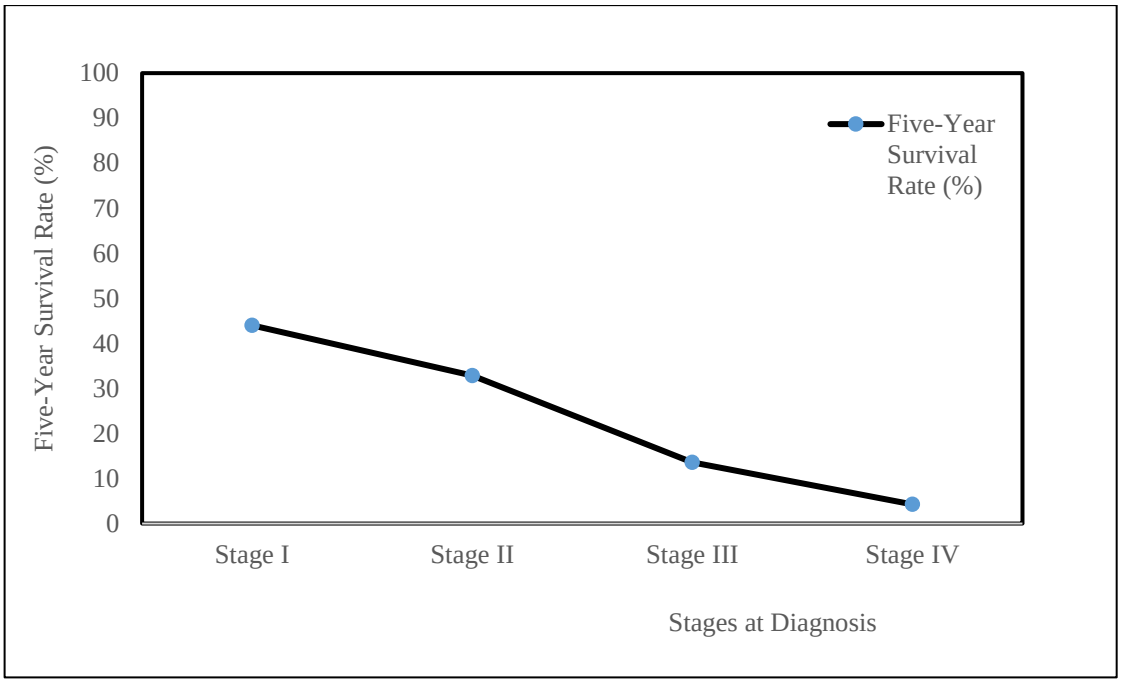

Figure 1. 3 Five-year survival rate for lung cancer

Graph shows combined data for five-year survival of NSCLC and SCLC patients, which is classified by stage (I, II, III and IV). The five-year survival rate of patients with these two main subtypes of lung cancer steadily decreased from 44% at stage I to 4.25% at stage IV (Survival for NCLC and SCLC by Stage, 2014).

1.4PULMONARY CELL TYPES AND PATHOGENESIS OF LUNG CANCER

1.4.1. PULMONARY CELL TYPES CLASSIFICATION

The complexity of lung cancer is contributed to not only by the emergence of multiple mutations, but also by the diversity of cell types that constitute normal lung physiology within the upper and lower respiratory airways. Within the upper airway, the trachea (windpipe) and bronchi contain mainly columnar pseudostratified ciliated cells, goblet cells, basal cells and neuroendocrine cells; In the lower airway, the epithelial cell types include columnar ciliated cells (cuboidal not pseudostratified), clara cells and neuroendocrine cells, in addition to alveolar type I and II pneumocytes (Figure 1.4). NSCLCs can therefore be divided into numerous subtypes in addition to the three basic subtypes (adenocarcinoma, squamous cell carcinoma and large cell carcinoma), with classification being subject to some ambiguity. For example, all neuroendocrine-associated lung cancers have been grouped into the category of neuroendocrine tumors; type II pneumocytes or clara cells are the main precursor cells developing into atypical adenomatous hyperplasia (AAH) (primarily non-mucinous), adenocarcinoma *in situ* (AIS)

(primarily non-mucinous), minimally invasive adenocarcinoma (MIA) (primarily non-mucinous) and lepidic predominant adenocarcinoma (LPA) (non-mucinous lepidic predominant adenocarcinoma) (Travis, et al., 2011). The lung squamous cell carcinoma tends to arise from the central airways of the lung, and adenocarcinoma are mostly developed from the peripheral area of lung.

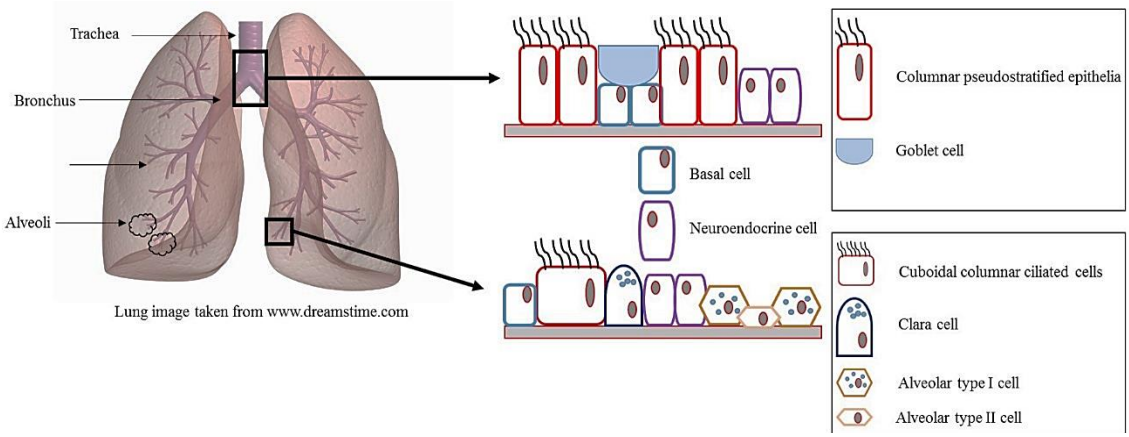

Figure 1. 4 The main composition of the lung and the epithelial cell types within it.
The lung architecture consists of the windpipe (trachea), bronchus (upper airway), bronchioles and alveoli (lower airway). The main specific types of epithelial cells in the upper airway include columnar pseudostratified ciliated cells, goblet cells (squared in diagram), and in the lower airway include cuboidal columnar ciliated cells, clara cells, alveolar type 1 and II pneumocytes (squared in diagram). Neuroendocrine cells and basal cells exist in both upper and lower airways.

1.4.2. PATHOGENESIS OF LUNG CANCER

The development of lung cancer is associated with the original cell type from which the cancer has developed and a subsequent programmed progression from its preneoplastic or preinvasive lesions. The 2015 WHO classification of lung cancer recently updated the preinvasive lesions for adenocarcinoma that are AAH and AIS (Travis, et al., 2015). The progression from preneoplastic lesion to invasive adenocarcinoma (lepidic subtype) involves three stages, which are AAH to AIS, AIS to MIA and MIA to invasive adenocarcinoma (lepidic dominant) (BMJ Best Practice , 2016). For lung squamous cell carcinoma, carcinoma *in situ* remains the only type of preinvasive lesion as shown in the 2004 classification (Travis, et al., 2015) and the classical progression from preneoplasia to invasive squamous cell carcinoma develops from a multistage process from hyperplasia-metaplasia-dysplasia-carcinoma *in situ* (stage 0) to squamous cell carcinoma (Funai, et al., 2003) (Greenberg, et al., 2002). For large cell carcinoma, the new WHO

classification restricted the diagnosis for this subtype and there is no further subtyping for lung large cell carcinoma and no definition for its preinvasive lesions (Travis, et al., 2015).

1.4.2.1. Oncogenesis of Lung Cancer

The initiation of lung cancer is associated with cancer biology and requires a multistep progression, which is attributed to the accumulation of many genetic alterations. The frequency of occurrence of genetic mutations can be accelerated by many lung cancer risk factors (e.g. tobacco smoke) that can expose the lung to a multitude of chemical carcinogens (Borczuk, et al., 2009). Tobacco smoke is the main risk factor for lung cancer by causing DNA alterations that lead to oncogene activation, tumor suppressor gene silencing and widespread loss of heterozygosity (Borczuk, et al., 2009). The way in which radiation contributes to carcinogenesis is also via causing genetic instability in cells (Little , 2000). Carcinogenesis is often associated with defects in cell cycle regulation and DNA repair capacity, which contributes to the promotion of lung cancer (Wu , et al., 2005). The subsequent progression of neoplasia is highly dependent on the tumor microenvironment (TME), as cancer-associated stroma involves a variety of essential elements, including fibroblasts, myofibroblasts, extracellular matrix (ECM) and immune and inflammatory cells (Chen , et al., 2015). Prior to the formation of neoplasia, naïve stromal cells play a critical role in maintaining physiological homeostasis of normal tissue. However, development of the cancerous environment promotes transformation and activation of normal stromal cells, further contributing to evolution of the tumor microenvironment (Chen , et al., 2015). The TME is important not just for supporting tumor initiation and progression but also in development of the metastatic niche, thus enhancing occurrence of metastasis (Chen , et al., 2015).

1.4.2.2. Classification of Genomic Alterations of Lung Cancer by Subtypes

For NSCLC, the two main subtypes of squamous cell carcinoma and adenocarcinoma are the most studied for gene mutation frequencies, and so subsequent discussions will focus on these subtypes only. *TP53* mutation (the gene encoding a nuclear phosphoprotein of 53 kDa (P53)) occurs in almost every type of cancer at rates varying between 10% (e.g. in hematopoietic malignancies) and close to 100% (e.g. in high-grade serous carcinoma of the ovary) (Rivlin, et al., 2011). *TP53* is also commonly diagnosed in NSCLC. The other frequently diagnosed mutations in NSCLC include *EGFR* (10-35%) (the gene encoding epidermal growth factor receptor (EGFR), v-ki-ras2 kirsten rat sarcoma viral

oncogene homolog (*KRAS* encoding KRAS protein) (15-25%), *FGRF1* (20%) (the gene encoding fibroblast growth factor receptor 1 (FGFR1)) amplification, *PIK3CA* (1-3%) (the gene encoding phosphatidylinositol 3-kinase, catalytic, α polypeptide (PI3K)), phosphatase and tensin homolog deleted on chromosome ten (*PTEN* encoding PTEN protein) (4-8%) and *HER2* (2-4%) (*ERBB2,* the gene encoding human epidermal growth factor receptor 2 (HER2)) (Lovly, et al., 2016). Adenocarcinoma has been identified with *TP53* (46%), *EGFR* (14%), *KRAS* (33%), *BRAF* (10%) (the gene encoding serine/threonine-protein kinase BRAF), *PIK3CA* (7%), and *MET* (7%) (the gene encoding hepatocyte growth factor receptor (HGFR)) mutations (The Cancer Genome Atlas Research Network, 2014) (Figure 1.5). The identification of common mutations in adenocarcinoma has been successfully developed for targeted therapy, such as mutations in *EGFR* and translocated *ALK* (the gene encoding anaplastic lymphoma kinase (ALK), *ROS* proto-oncogene 1 (*ROS1* encoding a receptor tyrosine kinase ROS1) or *RET* proto-oncogene (*RET* encoding a receptor tyrosine kinase RET) (The Cancer Genome Atlas Research Network, 2014) (Travis, et al., 2015). In squamous cell carcinoma (Figure 1.5), the more common genomic mutations include *TP53* (81%), cyclin-dependent kinase Inhibitor 2A (*CDKN2A*) (15%), *PIK3CA* (16%), *PTEN* (8%) and notch homolog 1 (*NOTCH1*) (8%) and *DDR2* (the gene encoding discoidin domain receptor tyrosine kinase 2 (DDR2)); In addition to that, squamous cell carcinoma was also identified with alterations in copy numbers of the genes such as *FGRF1* and *FDGFRA* (the gene encoding platelet derived growth factor receptor α (PDGFRA)) amplification, and *CDKN2A* deletion (The Cancer Genome Atlas Research Network, 2012). The potential targets developed for treatment of squamous cell carcinoma are *FGFR1* and *DDR2* (The Cancer Genome Atlas Research Network, 2012).

SCLC has not been extensively examined for genetic alterations and there is no specific targeted treatment developed for SCLC treatment; a report showing that an oncogenic somatic mutation in the *RET* gene (encoding amino acid 918) was identified in SCLC tumors, which is associated with an increase in intracellular signaling and cell growth (Haymarket Media, 2014).

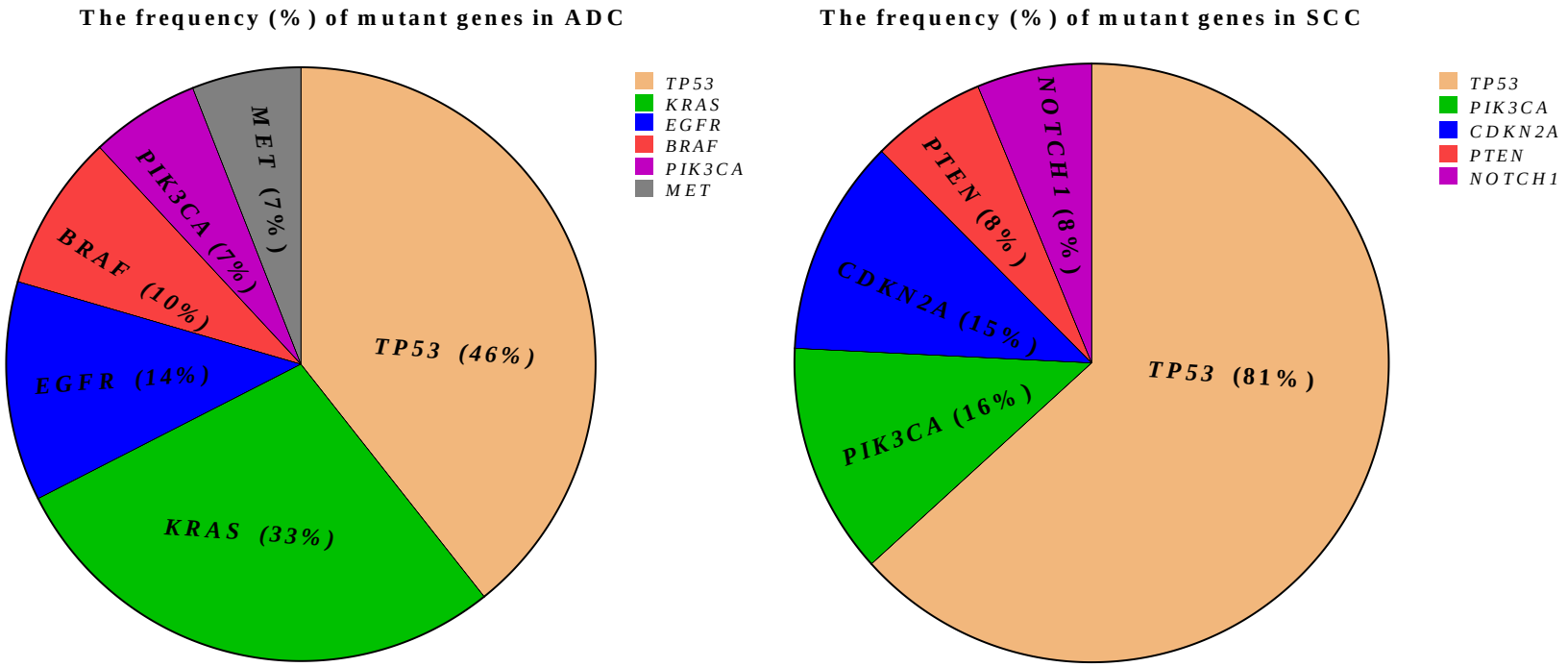

Figure 1. 5 The frequency (%) of the common genomic mutations in adenocarcinoma (ADC) and squamous cell carcinoma (SCC).

Both *TP53* and *PIK3CA* mutations were shared in ADC and SCC, whereas SCC showed a higher frequency of mutation in the genes (81% for *TP53* and 16% for *PIK3CA*), compared to the counterparts (46 and 7% respectively) in ADC. The rest of common mutations in ADC include *KRAS* (33%), *EGFR* (14%), *BRAF* (10%) and *MET* (7%), whereas in SCC, the mutant genes such as *CDKN2A* (15%), *PTEN* (8%) and *NOTCH1* (8%) are more commonly diagnosed (The Cancer Genome Atlas Research Network, 2014) (The Cancer Genome Atlas Research Network, 2012).

1.4.3. ONCOGENE ACTIVATION, TUMOR SUPPRESSOR SILENCING AND DEVELOPMENT OF POTENTIAL TARGETED TREATMENTS

The abnormalities, primarily in proto-oncogenes are highly associated with oncogenesis and subsequent disease progression, as development of cancer tends to rely on activation of mutations that enhance cellular longevity. Oncogene activation is mainly attributed to genetic alterations but can also be caused by extracellular signal stimuli. The increase in the concentration of extracellular growth factors is associated with activation of cellular receptors (e.g. EGFR) causing stimulation of receptor tyrosine kinase (RTK) activity. This initiates signal transduction to downstream signaling pathways mediated by a variety of signaling effectors, such as KRAS, PIK3CA and Akt (or called protein kinase B (PKB), encoded by v-akt murine thymoma viral oncogene homolog (*AKT)*). The PI3K/Akt signaling pathway and RAS/RAF/MEK/ mitogen-activated protein kinase (MAPK) (also known as ERK) signaling pathway are the mostly studied in NSCLC. In addition, tumor suppressor genes, such as *TP53* and *PTEN* and their transcriptionally expressed protein products play a critical role in regulating cell growth and death. Expression of these tumor suppressors also correlates to the effectiveness of cancer treatments, such as platinum agent-based chemotherapy. Within the cancer environment, tumor suppressor genes tend to be deactivated or downregulated through dysregulation of gene expression and this often leads to a reduction in sensitivity to treatments.

The KRAS/RAF/MEK/ERK- and PI3K/Akt cell signaling pathways play critical roles in NSCLC initiation and progression, and are discussed in greater detail below.

1.4.3.1. *KRAS* oncogene

The main associated *RAS* oncogene in NSCLC is the *KRAS* oncogene, although the mutations in other two isoforms of *RAS* (*HRAS* or *NRAS*) have also been reported to rarely exist in lung cancer (mainly NSCLC) (Suda , et al., 2010). *KRAS* is considered as an important oncogenic driver mutation for NSCLC (Riely, et al., 2009) and is primarily found in adenocarcinoma, rarely in squamous cell carcinoma and never in small cell carcinoma (Suda , et al., 2010). The activation of *KRAS* is through genetic mutations primarily occurred in three codons that respectively encode 12, 13 and 61 amino acid positions, amongst which mutations in codons 12 and 13 constitute the majority compared to the codon 61 mutations in *KRAS* found in NSCLC (Suda , et al., 2010) (Riely, et al.,

2009). Mutations in the *KRAS* gene can be caused by cigarette smoking where the type of transversion mutation (G→T or G→C) is commonly discovered (Porta, et al., 2009) (Riely, et al., 2009) whereas the common type of *KRAS* mutations found in non-smokers is the transition mutation (G→A) (Carpeño & Belda-Iniesta, 2013) (Riely, et al., 2009).

1.4.3.2. KRAS/RAF/MEK/ERK MAPK Cell Signaling Pathway

The main signaling pathway mediated by KRAS is the downstream MAPK signaling pathway (KRAS/RAF/MEK/ERK) (Figure 1.6) and RAF, MEK and ERK are the main pathway components. There are three isoforms of RAF kinase that are ARAF, BRAF and CRAF. The mutations in these three isoforms have been reported in lung cancer, although the BRAF mutations are the commonest (Holderfield, et al., 2014). MEK1/2 kinase is the main substrate of RAF kinase, and MEK1 mutations are found in NSCLC accounting for about 1% (Lovly, et al., 2016) that are more frequently discovered in adenocarcinoma than squamous cell carcinoma (The Cancer Genome Atlas Research Network, 2014); ERK (1/2) is the only downstream substrate of MEK (1/2) and this kinase has so far not reported with any mutations (McArthur, 2015). The downstream signaling network for ERK is complex, and the ERK activation correlates with many cellular activities including cell cycle progression, protein synthesis and cell survival (McArthur, 2015). ERK activation is commonly found in both cancer cell lines and patient tumors (Roberts & Der, 2007). It has been reported that activation of MEK/ERK has been detected in 30-60% of primary lung cancers which was shown to be linked to a poor prognosis (Meng, et al., 2009).

The ERK MAPK signaling pathway can also be activated by the upstream receptors such as EGFR and HER2 via aberrant overexpression or mutational activation in RTKs (Roberts & Der, 2007). In addition, PI3K interacts with RAS (Figure 1.6) and so targeting PI3K signaling may have potential in treating RAS-mutant tumors (Downward, 2008). In addition, *KRAS* mutation is thought to be mutually exclusive with *EGFR* mutation, but are often concurrently found with *PIK3CA* mutation (Lovly, et al., 2015) (Yip, 2015).

1.4.3.3. Targeted Treatments by Blocking ERK MAPK Signaling Pathway

KRAS has been previously considered undruggable and there have been failures in the attempt to develop specific anti-RAS agents (Goldman & Garon, 2012) (Acquaviva, et al., 2012). Nevertheless, there has been a recent breakthrough in the development of RAS-

targeted agents, which are the specific inhibitors of *KRAS* mutation hotspot *G12C* (Helwick, 2014). Targeting the main downstream effectors of KRAS can also block KRAS-mediated activities and may ultimately result in improved outcomes for a proportion of patients exhibiting the *KRAS* mutation.

KRAS/BRAF/MEK/ERK MAPK signaling pathway is one of the main KRAS mediated signaling pathways. BRAF and MEK inhibition has been the main therapeutic targets for blocking ERK signaling pathway (Roberts & Der, 2007). As MEK is the main upstream activator of ERK, MEK inhibition is more straightforward to block ERK activation compared with BRAF inhibition (Roberts & Der, 2007).

1.4.3.4. *PIK3CA* and *AKT* oncogene

PIK3CA mutations are equally found in both squamous cell carcinoma and adenocarcinoma of lung cancer (Pao & Girard, 2011), whereas *PIK3CA* amplifications tend to be found in the subtype of lung squamous cell carcinoma (Yip, 2015) (Pao & Girard, 2011) and are often found to be exclusive to *PIK3CA* mutations implying that both genetic alterations may have oncogenic potential to promote carcinogenesis in the lung (Wang, et al., 2014). In NSCLC, the *PIK3CA* mutations frequently affect the residues Glu542 and Glu545 in exon 9 encoding the catalytic domain (Pao & Girard, 2011). The encoded protein p110α, is one isoform of the p110 catalytic subunit of class IA PI3Ks that correlates with the main function of PI3K kinase, allowing it to act as a key mediator between growth factor receptors and intracellular downstream signaling pathways (Pao & Girard, 2011). *AKT*1 mutations are found in 1% of NSCLC and exist in both squamous cell carcinoma and adenocarcinoma of lung cancer; The role of *AKT1* mutations is suggested to be associated with cellular transformation *in vitro* and *in vivo* but the specific clinical characteristic of patients with this mutation has not been described yet (Lovly, et al., 2015).

1.4.3.5. PI3K/Akt signaling pathway

PI3K/Akt pathway activation has been well documented to be involved in oncogenesis of many cancers, including NSCLC and it has been shown to be mediated via many genetic alterations. These include *PIK3CA* mutations or amplifications (Pao & Girard, 2011), *PTEN* mutations or deletions and *EGFR* or *HER2* mutations (Yip, 2015) (Zhang, et al., 2014) (Heavey, et al., 2014) (Niederst & Engelman, 2013). The activation of Akt is

mainly mediated by PI3K through recruitment of Akt to membrane-bound phosphatidylinositol (3,4,5)-trisphosphate (PIP3), which is derived from the PI3K-mediated conversion of Phosphatidylinositol 4,5-bisphosphate (PIP2) (Toulany & Rodemann, 2015) (Pal, et al., 2010). Upon reaching to the membrane, Akt is phosphorylated at Thr^{308} by 3-phosphoinositide-dependent protein kinase (PDK1) and mammalian target of rapamycin complex 2 (mTORC2 or PDK2) at Ser^{473} (Ersahin, et al., 2015) (Toulany & Rodemann, 2015). In addition, Akt activation can be caused by *PIK3CA* and *PTEN* mutations (Wang, et al., 2014) (Morrow, et al., 2011) (Hirai, et al., 2010) and also can be induced in an EGFR/PI3K/Akt-independent manner (Mccubrey, et al., 2007). The PTEN, encoded by the gene *PTEN* is a dual protein/lipid phosphatase, known as the central negative regulator of PI3K pathway by dephosphorylating PIP_3 into PIP2 to antagonize PI3K activity (Figure 1.6). Therefore, loss of the negative regulation by PTEN can lead to activation of PI3K/Akt signaling (Fumarola , et al., 2014) (Chalhoub & Baker, 2009). *PTEN* loss of function is mainly attributable to PTEN mutations, which as shown above (Figure 1.5) are more common in squamous cell carcinoma than in adenocarcinoma (The Cancer Genome Atlas Research Network, 2012) and the proportion of PTEN mutations in NSCLC is about 4-8% (Lovly, et al., 2016) and can occur in multiple exons within the gene, although few studies have reported the common mutant hotspots in *PTEN* (Lovly, et al., 2015).

The function of Akt activation is to mediate cell growth and survival by phosphorylating various cytoplasmic proteins. The major downstream effector of Akt is the serine/threonine kinase-mTOR (Ersahin, et al., 2015). The activation of PI3K/Akt/mTOR signaling is often deregulated in NSCLC and associated with genetic aberrations in the cascade components (Yip, 2015). Other downstream effectors activated by Akt include mouse double minute-2 (MDM2) and ikappaB kinase alpha (IKKα) (the regulator of nuclear factor kappa B (NF-κB)), whereas the effectors inactivated by Akt include B-cell lymphoma 2 (Bcl-2)-associated death promoter (BAD) and caspase-9 (Ersahin, et al., 2015). In addition, many Akt downstream effectors are co-regulated by ERK; Akt and ERK signaling can compensate each other in the activation of cell survival processes (Ersahin, et al., 2015) (Figure 1.6).

1.4.3.6. PI3K/Akt Signaling Pathway Blockade

The downstream phosphorylation and activity of Akt acts as an indicator of the cascade activity and also as a determinant of sensitivity to the targeted therapy of PI3K signaling (Cheng, et al., 2014). Inhibitors that target the key components of PI3K/Akt/mTOR pathway have been developed and advanced to phase I or II clinical trials for NSCLC. Such targeted treatments include PI3K, Akt, mTOR, dual mTOR1/2 and dual PI3K-mTOR inhibitors (Yip, 2015) (Cheng, et al., 2014). In addition, PI3K pathway inhibitors combined with other therapies, such as targeted therapy (EGFR and MEK inhibitors) and chemotherapy seem to be more successful than the single PI3K signaling (Yip, 2015), which highlights the role of PI3K signaling in crosstalk with other pathways. Tank binding kinase 1 (TBK1) can also directly activate Akt by phosphorylating T308 and S473 residues. Although IKKε also plays a role in Akt activation, there remains some ambiguity regarding this function (Mahajan & Mahajan, 2012) (Ou, et al., 2011). Both TBK1 and IKKε are non-canonical IKKs that are structurally and functionally distinct from canonical IKKs (IKKα and IKKβ) (Kim, et al., 2013) (Shen & Hahn, 2011). TBK1 activation is required for KRAS-mediated/dependent tumor cell survival (including NSCLC) via a signaling cascade of KRAS/RALB/TBK1 (RALB encoded by RAS like proto-oncogene B (*RALB*)) (Ou, et al., 2011) (Barbie, et al., 2009) (Kim, et al., 2013), which is also one of the main KRAS-dependent signaling pathways. Furthermore, PI3K and the guanine nucleotide exchange factors of the RAS-like small guanosine-5'-triphosphate (GTP)-binding protein regulators (GTPases) (RAL-GEF) that is the upstream activator of RAL and TBK1 was identified as the proximal mediators in RAS-dependent cell transformation in lung cancer (Zhu & Golay, 2014). Moreover, TBK1 has been recognized as a novel therapeutic target in lung cancer (Kim, et al., 2013) (Barbie, et al., 2009). The ability of TBK1 to mediate KRAS-mediated tumorigenesis and regulate Akt phosphorylation and activity, suggests that a crosstalk between PI3K/Akt- and KRAS/RALB/TBK1 signaling may exist.

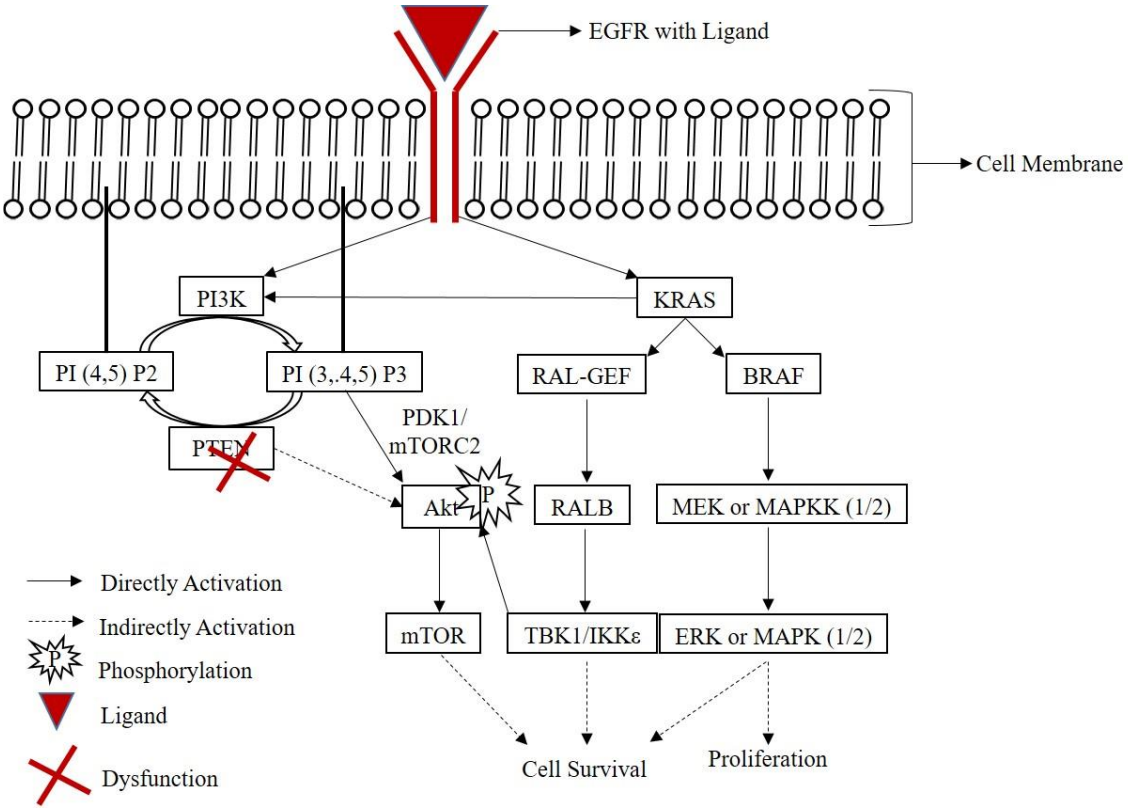

Figure 1. 6 Direct activation and indirect activation of PI3K/Akt signaling pathway

Akt can be directly activated by the upstream EGFR and KRAS via PI3K activation, and KRAS/RALB/TBK1 signaling pathway can also activate Akt via phosphorylation at S^{473} and T^{308}. KRAS mediated downstream signaling pathways include the PI3K/Akt-, RALB/TBK1- and BRAF/MEK/ERK signaling pathways, which are all able to promote cell survival. Akt can be indirectly activated by the crosstalk among these pro-survival signaling pathways. PTEN is a negative regulator of PI3K and dysfunctional PTEN (mainly results from either genetic mutation or deletion) can also indirectly activate PI3K/Akt signaling pathway.

1.4.3.7. Dysregulation of *P53* Tumor Suppression Gene

In NSCLC, the frequency of *P53* mutations is the highest with 81% compared with other genomic mutations, which are commonly found in both main subtypes of NSCLC (Figure 1.5). *P53* mutations in NSCLC usually occur within the DNA-binding domain (V157, R 158, R175, G245, R248, R249, R273) with or without allele loss at chromosome 17p13 and are associated with carcinogens in tobacco smoking (Gibbons, et al., 2014) (Mogi & Kuwano, 2011). *P53* mutations are associated with tumorigenesis of lung cancer and most clinical studies showed that *P53* mutations are responsible for a worse prognosis of NSCLC and correlate with resistance to chemotherapy and radiation (Mogi & Kuwano, 2011). The functional P53 is an important transcription factor that stands out as a key tumor suppressor and a master regulator of various signaling pathways involved in the

tumorigenic process. The many roles of P53 as a tumor suppressor include cell cycle arrest, DNA repair, senescence and apoptosis (Rivlin, et al., 2011). P53 mediates cell cycle arrest and apoptosis in response to many DNA damage stimuli, such as cytotoxic chemotherapy by which P53 is activated by the key regulators of DNA damage response (DDR) such as ataxia-telangiectasia mutated protein kinase (ATM) (Jiang , et al., 2009). Targeting DDR by restoring P53 function has been shown to sensitize cells to chemotherapy (Bouwman & Jonkers, 2012)

1.4.3.8. Cross-talk between P53 and PTEN/PI3K/Akt Signaling Pathway

The function of P53 in regulating cell survival has been shown to interrelate with PI3K/Akt signaling pathway. In the study of epithelial tumors (including lung) it was found that P53 could regulate cell survival by inhibiting PI3K/Akt signaling, and that such inhibition was required for P53-mediated apoptosis (Singh, et al., 2002). It was also shown that downregulation of Akt plays a role in accelerating P53-mediated apoptosis. Conversely, Akt-mediated activation of MDM2 can lead to P53 inactivation and eventual inhibition of P53-dependent apoptosis (Gottlieb, et al., 2002) (Figure 1.7). In addition, crosstalk exists between PTEN and P53 (Figure 1.7), by which P53 can transcriptionally activate PTEN which functions to downregulate Akt phosphorylation leading to MDM2 inhibition (Singh, et al., 2002). PTEN can also activate P53 through direct and indirect protein-protein interactions. PTEN loss in function is associated with decreased P53 function, with this relationship likely to depend on cell-type and tumor type context (Chalhoub & Baker, 2009).

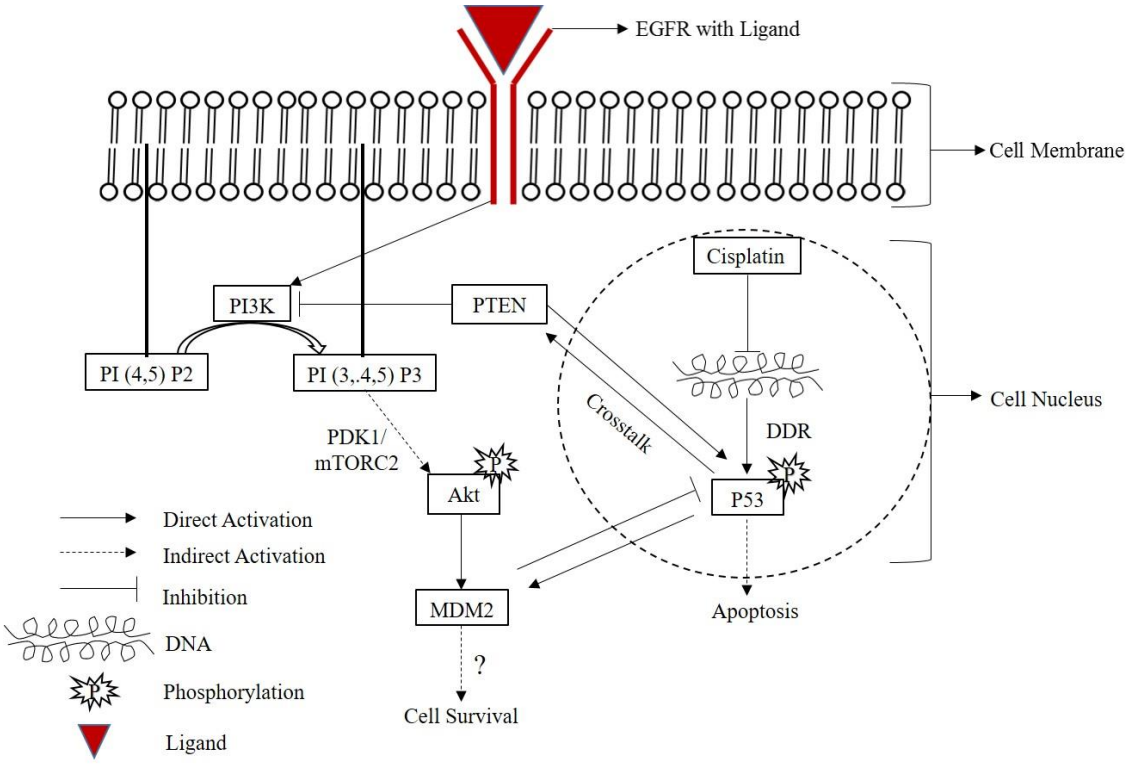

Figure 1. 7 P53-mediated cisplatin-induced DNA damage and crosstalk between P53 and PTEN/PI3K/Akt signaling pathway

P53 mediated apoptotic pathways in response to cisplatin-induced DNA damage and PTEN/PI3K/Akt signaling pathway are important to determine cell survival of tumor cells. Cisplatin-induced DNA damage activates DDR and then subsequently P53 activities including induction of apoptosis in cytoplasm. The crosstalk between P53 and PTEN is that P53 can regulate and inhibit PI3K signaling in conjunction with PTEN to promote P53 activity by inhibiting the Akt downstream effector-MDM2, which can regulate P53 degradation; whereas PTEN can activate P53 through direct and indirect protein-protein interactions.

1.5TREATMENT OF LUNG CANCER

1.5.1 TREATMENT OF LUNG CANCER BY SUBTYPES

Generally, the options available for lung cancer treatment can be classified based on whether they fall into the category of NSCLC or SCLC. Surgery is the most commonly recommended option for NSCLC treatment (Sankaranarayanan , et al., 2011) but also can be used for treating SCLC only if the cancer is found in one lung and in nearby lymph nodes (National Cancer Institute, 2016). The other currently used treatments for NSCLC include radiotherapy, chemotherapy and targeted therapy. Radiotherapy or chemotherapy can be given after surgery to help to lower the risk of recurrence of cancer and such regimens are called adjuvant therapy (National Cancer Institute, 2016). The combination regimen of radiotherapy and chemotherapy for NSCLC was shown to be able to cure a small portion of patients and to produce palliation in most patients (Sankaranarayanan , et al., 2011). SCLC is more responsive to chemotherapy and radiotherapy, but the long-term survival and cure is difficult to achieve due to its tendency to disseminate early and widely (Sankaranarayanan , et al., 2011). Targeted therapy is only available for NSCLC and the currently used drugs for NSCLC are monoclonal antibodies and RTKs inhibitors (National Cancer Institute, 2016).

1.5.2 TREATMENT OF LUNG CANCER BY STAGE AT DIAGNOSIS

Different treatment options for lung cancer are usually classified by stage. For NSCLC, occult NSCLC can be cured by surgery and all non-extensive stages of lung cancer (stage 0, I, II and IIIa) have the option of surgical resection either alone or combined with other therapies. The late stages of NSCLC are not considered suitable for surgery. Either chemotherapy or radiotherapy are more likely to be given to lung cancer patients at early stages, whereas the combination regimen of these two therapies is commonly used for treatment of later stages of NSCLC (stage IIIa and IIIb). Chemotherapy combinations and the combined regimens of combination chemotherapy with targeted drugs are the major therapeutic options for treatment of advanced stage NSCLC (stage IV) (National Cancer Institute, 2016).

For SCLC, only at stage I where tumors have not yet spread to lymph nodes or elsewhere, is surgery an option. Patients at other early limited stages of disease are mostly given the combination regimen of chemotherapy and radiotherapy (concurrent chemoradiation) or

just chemotherapy. For extensive and more advanced stages, combination chemotherapy may also combine with radiation therapy or laser surgery as the main treatment option of SCLC (American Cancer Society, 2016).

Palliative or supportive treatment is often given to patients with lung cancers of all stages with the purpose to relieve adverse effects caused by cancer and help to improve qualit of life (American Cancer Society, 2014).

1.5.3 TREATMENT FOR RECURRENT LUNG CANCER

For NSCLC, there are fewer therapeutic options for patients with recurrent cancers than those with initial cancers. Surgery is no longer recommended for treating recurrent NSCLC unless it has spread to the brain, and radiosurgery (stereotactic radiotherapy) is applied for patients that are unsuitable for surgery. Laser, radio and chemo therapies or combined with targeted therapy are used for treatment of recurrent cancers (National Cancer Institute, 2016).

1.5.4 CHEMOTHERAPY FOR NSCLC

As the main forcus of this thesis will be on NSCLC, the chemotherapeutic strategies only will be discussed herein. For patients with NSCLC, cisplatin (Platinol) or carboplatin (Paraplatin)-based combination treatments are mostly used as the main treatment option for all stages of NSCLC (Cancer Research UK, 2014). Non-platinum chemotherapeutic drugs that are usually combined with platinum agents (e.g. cisplatin or carboplatin) include paclitaxel (Taxol), docetaxel (Taxotere), gemcitabine (Gemzar), vinorelbine (Navelbine) and pemetrexed (Alimta) (American Cancer Society, 2016). The combination of two non-platinum drugs (e.g. gemcitabine combined with vinorelbine or paclitaxel (American Cancer Society, 2016)) can also be used for treating NSCLC and suggested for patients who are unable to tolerate platinum-containing regimens (A.D.A.M., 2013).

Following routine chemotherapy, pemetrexed (Alimta)-driven maintenance therapy, (sometimes containing targeted therapy such as bevacizumab (Avastin)) is preferred for treating non-squamous type NSCLC (American Cancer Society, 2016) (Spira, et al., 2015). Pemetrexed is usually combined with cisplatin or carboplatin as the regimen for treatment of advanced stage NSCLC, whilst other chemotherapy treatments including the combination of cisplatin and docetaxel (if patients have not been given with this regimen

before), are recommended for patients who are resistant to the current platinum-based chemotherapy treatments (Cancer Research UK, 2014). Chemotherapy can be combined with other non-operative therapies, including radiotherapy and molecularly targeted treatments. Adding a third chemotherapeutic agent into platinum-based chemotherapy regimens was not shown to further improve the efficacy of chemotherapy (Bonomi, 2010) (American Cancer Society, 2016). The combination of chemotherapeutic drugs and molecularly targeted agents were found to be effective in treatment of some advanced lung cancers and such targeted agents that have recently approved by the US food and drug administration (FDA) include bevacizumab, ramucirumab (Cyramza) and necitumumab (Portrazza) (American Cancer Society, 2016).

1.5.4.1. Cisplatin-based Chemotherapeutic Agents

Cisplatin (cisplatinum, or cis-diamminedichloroplatinum (II)) has been the mainline treatment for cancers, including NSCLC since it was discovered to have anticancer activity back to 1960s. The functions of cisplatin-mediated anticancer effects include crosslinking with purine bases in DNA, interfering with DNA repair mechanisms, causing DNA damage and subsequently inducing apoptosis in cancer cells (Dasari & Tchounwou, 2014). Platinum agents are usually combined with other chemotherapeutic agents including gemcitabine and pemetrexed for treatment of all stages of lung cancer (Dasari & Tchounwou, 2014). The adjuvant therapy that is the cisplatin-based chemotherapy applied after operation is clinically used for treatment of early stages lung cancer and has been shown to have a 5% increase in five-year survival with a median five-year survival rate of 45-70% (Stevenson, 2016). For advanced stage of lung cancer, cisplatin-based chemotherapy was shown historically to have an overall survival (OS) of 8-10 months, with a one-year survival rate of 33% and progression-free survival (PFS) of 3-5 months (Polo & Besse, 2014). Cisplatin-based chemotherapy is given as a full treatment of 4-6 cycles, with 3-4 weeks per cycle. Cisplatin is given to patients at a concentration of 50-100 mg/m^2 intravenously (IV) for one cycle treatment (Stevenson, 2016). Despite an improvement in the survival of patients (10-15%), the efficacy of cisplatin-based regimens is limited, as most patients eventually exhibit resistance to the treatments. The mechanisms of cisplatin resistance include, decreased influx of cisplatin, increased detoxification by increasing levels of thiol-containing biomolecules such as glutathione and metallothioneins, enhanced DNA damage repair and blockade of apoptosis induction,

such as alterations of signal transduction pathways involved in apoptosis (Heavey, et al., 2014) (Liu, et al., 2007) (Wang , et al., 2000). Cisplatin is a cytotoxic agent and can cause several toxic effects including nephrotoxicity, hepatotoxicity and cardiotoxicity (Dasari & Tchounwou, 2014). Elderly patients have more comorbidities and tend to be less tolerant to the toxic treatments like chemotherapy than the younger counterparts (Maione, et al., 2010). In order to overcome the side effects and toxicities caused by cisplatin treatment, a large number of platinum complexes have been prepared and tested for anticancer activity, which lead to the successful discovery of two platinum-derived agents-carboplatin and oxaliplatin (Eloxatin), both of which have been approved as standard therapy for clinical use (Johnstone, et al., 2014).

1.5.5 TARGETED TREATMENT FOR ADVANCED NSCLC

Molecularly targeted therapy has recently been recommended for advanced NSCLC treatment. To date, there are three therapeutic targets that have been successfully developed into targeted treatments for advanced NSCLC, which are EGFR, ALK and vascular endothelial growth factor receptor (VEGFR) (Minguet, et al., 2016).

The approved drugs for inhibiting EGFR are gefitinib (Iressa), erlotinib (Tarceva) and afatinib (Gilotrif), all of which have been approved for use in the UK, with the first two drugs recommended for first-line targeted therapy in those patients with activated EGFR (Cancer Research UK, 2014). Afatinib is more effective than the first two drugs and is recommended for patients with resistance to gefitinib or erlotinib. There are more EGFR inhibitors that have been undergoing investigations in clinical trials, which include dacomitinib (©Pfizer), neratinib (©Puma Biotechnology) and rociletinib (©Clovis Oncology) (Minguet, et al., 2016). EGFR inhibitors are mostly used as post-chemotherapy treatment for advanced stage adenocarcinoma exhibiting EGFR expression or an activating mutation (Minguet, et al., 2016).

ALK-targeted inhibitors are recommended for advanced ALK-positive NSCLC after relapse following chemotherapy. Drugs that have been approved by the FDA, european medicines agency (EMA) are crizotinib (Xalkori) and ceritinib (Zykadia). A candidate drug called alectinib (©Roche) (which has already been approved in Japan (Spira, et al., 2015)) is under investigation for its potential to overcome crizotinib resistance (Minguet, et al., 2016).

In contrast to the above inhibitors, anti-VEGFR inhibitors are applicable for the majority of cancer patients due to the fact that angiogenesis is required for tumor growth. The approved drugs for clinical use are bevacizumab and nintedanib (Vargatef) (Minguet, et al., 2016).

1.5.6 IMMUNOTHERAPY FOR ADVANCED NSCLC

Recently, several immunotherapy drugs have been approved by the FDA for cancer treatments, although there are many drugs that are currently being assessed in early phase clinical trials. The types of immunotherapy drugs for cancer treatment include checkpoint inhibitors, monoclonal antibodies, therapeutic vaccines and adoptive cell therapies (American Cancer Society, 2016) (National Cancer Institute, 2015). Checkpoint inhibitors (i.e. anti-programmed death-1 (PD-1) antibodies) are the best studied immunotherapy drugs (Steven, et al., 2016) (González-Cao, 2015), such as nivolumab (Opdivo) (FDA, 2015), which is recommended for treatment of advanced NSCLC with progression on or after platinum-based chemotherapy (Steven, et al., 2016), and pembrolizumab (Keytruda® (FDA, 2015)) that is applied for second-line treatment for NSCLC after chemotherapy (Steven, et al., 2016). It was suggested that the combination of anti PD-1 antibodies with other targeted drugs (EGFR- or ALK-targeted drugs) can help to overcome drug resistance (González-Cao, 2015). Other immunotherapy drugs that are currently under investigations for NSCLC include anti-cytotoxic T-lymphocyte antigen-4 (CTLA-4) inhibitors, anti-toll-like receptors (TLRs) and development of specific tumor associated antigens (TAAs) vaccines (Steven, et al., 2016).

1.5.7 PROGRESSION FOR NEW THERAPY DEVELOPMENT

1.5.7.1. Targeted Therapy Candidates for Advanced NSCLC

There are a large number of novel targeted agents that have been undergoing investigations in early clinical trials for testing their potential in treatment of advanced NSCLC, including anti-PI3K, anti-Akt, anti-heat shock protein (HSP)-90 and anti-MEK inhibitors. The administration of novel drugs is either given to patients alone or in combination with other therapies, such as chemotherapeutic (e.g. cisplatin/docetaxel) and targeted agents (e.g. gefitinib/erlotinib). Anti-PI3K inhibitors mainly refer to drugs that specifically block the activities of class I PI3Ks and there have been several PI3K inhibitors currently tested in clinical trials. PI3K inhibitors can be generally classified as

pan-PI3K and PI3K-isoform specific inhibitors. The candidates for pan-PI3K inhibitors include PX-866 (Sonolisib), NVP-BKM120 (Buparlisib), GDC-0941 (Pictilisib) and XL-147 (Pilaralisib) and those for the specific PI3K inhibitors include NVP-BYL719 (Alpelisib), GSK-2636771 (©GlaxoSmithKline) and AZD8186 (©Astrazeneca) (AstraZeneca, 2017) (Fumarola , et al., 2014). There are mainly three Akt inhibitors investigated in clinical trials for NSCLC treatment that are MK-2206 (©Merck), KRX-0401 (Perifosine) (Fumarola , et al., 2014) and AZD5363 (©Astrazeneca) (University of Birmingham , 2016). The candidate MEK-targeted drugs include MEK162 (Binimetinib) (H. Lee Moffitt Cancer Center & Research Institute, 2017), AZD6244 (Selumetinib), GSK1120212 (Trametinib) and PD-0325901 (©Pfizer) (Goldman & Garon, 2012). The inhibitors targeting HSP90 that include STA-9090 (Ganetespib), IPI-504 (Retaspimycin) (Bhattacharya, et al., 2015) and AT13387 (Onalespib) (National Cancer Institute (NCI) , 2017) are undergoing progression in clinical trials.

1.5.7.2. Combined Cisplatin Treatment with Novel Targeted Agents

The combinations of cisplatin-based chemotherapy with targeted agents (e.g. EGFR and ALK inhibitors) have been the first-line treatment for advanced NSCLC for improving PFS, response rate and quality of life (QoL) (Polo & Besse, 2014). Unfortunately, many patients have developed acquired resistance to the combination regimens and this highlights the requirement for the alternative cisplatin-based combination treatments. The identification of key oncogenic driver mutations or signaling pathways has been highly linked to the poor therapeutic outcomes for patients with advanced NSCLC.

KRAS mutation is frequently associated with the resistance to EGFR inhibition (Stewart, et al., 2015), whereas correlation between *KRAS* mutation status and response to chemotherapy in patients with advanced NSCLC has not been well demonstrated. KRAS mutation has been shown to associate with a poorer prognosis and resistance to chemotherapy (Chan & Hughes, 2015) (Riely , et al., 2009). A recent study reported that both PFS and OS in *KRAS*-mutant patients with advanced NSCLC after receiving chemotherapy is significantly shorter than the counterparts in *KRAS*-WT patients (Hames, et al., 2016). In contrast Mellema et al previously reported the *KRAS* mutation was not significantly associated with poor outcomes of chemotherapy (Mellema , et al., 2013). Nevertheless, *KRAS*-driven NSCLC has been well studied for the development of targeted therapy. As reviewed above (1.4.3.3 and 1.4.3.5), MEK inhibition can effectively inhibit

downstream ERK activation and may also affect the Akt-associated downstream pro-survival signaling pathway. *KRAS* mutation is predictive for response to MEK inhibition and data from Genomics of Drug Sensitivity in Cancer Project (http://www.cancerrxgene.org/) show that *KRAS* mutation is significantly associated with the sensitivity to the MEK inhibitors-AZD6244 and GSK1120212. Several MEK inhibitors have undergone several clinical investigations for testing the combination with chemotherapeutic agents for treatment of advanced NSCLC.

PI3K/Akt signaling can be efficiently activated by the upstream KRAS and is associated with oncogenesis of *KRAS*-driven NSCLC. In addition, the activation of PI3K/Akt signaling pathway could be driven by *PIK3CA* and PTEN mutations (reviewed in 1.4.3.5). Akt activation can correlate with resistance to chemotherapy and radiotherapy (Scrima, et al., 2012) (Tsurutani , et al., 2006). In addition, the activation of PI3K/Akt signaling pathway is also linked to resistance to the EGFR/ALK-targeted agents (Stewart, et al., 2015) (Yang, et al., 2014).Akt activation via phosphorylation at S^{473}has been correlated with poor clinical outcomes in many types of tumors, such as breast and prostate cancers, whereas in NSCLC such correlation was not consistently observed in studies (Scrima, et al., 2012) (Tsurutani , et al., 2006). Inhibitors of PI3K/Akt signaling could be a potent therapy for improving clinical response. Several PI3K inhibitors have undergone assessment of combination treatments with chemotherapeutic agents in clinical trials, whereas Akt inhibitors are usually tested as single treatments or in combinations with other targeted agents, such as EGFR inhibitors (Fumarola , et al., 2014). MK-2206 was demonstrated in preclinical studies that could generate a synergistic effect in combination with cytotoxic agents, such as docetaxel and carboplatin in lung H460 cells (Fumarola , et al., 2014).

TBK1 has been discovered as a synthetic lethal gene in combination with *KRAS* mutation in *KRAS*-driven NSCLC (Vasan, et al., 2014) (Suda , et al., 2010). As reviewed in 1.4.3.6, TBK1 is essential for promoting cancer survival in *KRAS*-mutant NSCLC and hence has been selected as a novel therapeutic target for NSCLC. KRAS/RALB/TBK1 signaling can regulate downstream to lead to NF-κB activation, which plays a role in promoting lung carcinogenesis. *KRAS*-mediated NF-κB activation may correlate with cisplatin resistance (Godwin, et al., 2013). Hence, blocking TBK1 activity can attenuate NF-κB downregulation and hence may promote sensitivity to chemotherapy. In addition, IKKε

also plays a role in driving NSCLC, and IKKε inhibition can increase NSCLC cells sensitivity to chemotherapy and induces apoptosis. Moreover, IKKε, like TBK1 can also be activated by upstream KRAS to mediate downstream NF-κB activation (Li, et al., 2015). To the best of my knowledge, no any available inhibitors of TBK1/IKKε have yet undergone clinical assessment to the date. Nevertheless, there are several potent TBK1/IKKε inhibitors that have been tested in preclinical studies include 6-aminopyrazolopyrimidine derivative (Compound II) and MPI-0485520 (Mahajan & Mahajan, 2012).

HSP90 is a key molecule that acts as a molecular chaperone to aid maturation of many signal transduction (client) proteins, including mutant BRAF, mutant HER2, mutant or overexpressed MET, mutant or wildtype (WT) EGFR (Shimamura & Shapiro, 2008) and Akt (Smith , et al., 2015). HSP90 can crosstalk with PI3K/Akt signaling, interacting with Akt via intermolecular binding. Blocking Akt-HSP90 binding results in dephosphorylation and inactivation of Akt and promotes apoptosis (Sato, et al., 2000). Tumor cells are highly dependent on HSP90 for proliferation and survival (Chatterjee, et al., 2016) (Shimamura & Shapiro, 2008). HSP90 plays an important role in regulating *KRAS*-mutant NSCLC cell survival (Chan & Hughes, 2015) (Suda , et al., 2010). The combinations of HSP90 inhibition with chemotherapeutic agents have undergone investigations in clinical trials and such HSP90 inhibitors include IPI-504 and STA-9090 (Pillai & Ramalingam, 2012). The combination of HSP90 inhibition with conventional chemotherapy like docetaxel was shown not effective in improving clinical outcomes (PFS and OS) as compared with docetaxel single treatment (Synta Pharmaceuticals Corp. , 2016). A preclinical study showed HSP90 inhibition may promote cisplatin cytotoxicity by downregulating cisplatin-induced thymidine phosphorylase expression and blocking ERK1/2 and Akt activation (Weng , et al., 2012).

1.6PRECLINICAL MODELS FOR DRUG SCREENING

Due to the complexity and tissue-specificity of the TME, it is difficult to mimic tumor morphology and histology of tumors *in vitro*. Although there is a wide availability of xenograft models (animal-derived models) for the application of *in vivo* studies, they still frequently only reflect a single cell type and fail to reflect the complexity of TME. Nevertheless, simple *in vitro* models, such as 2 Dimensional (2D) cell line cultures and

animal-derived *in vivo* models are still the most applied for evaluation of the preclinical efficacies of new drugs or new drug combinations.

1.6.1 2D MONOLAYER

The simplest *in vitro* models are 2D monolayer cultures of established cell lines. Such cultures are easily established under *in vitro* conditions and have been successfully applied for testing potencies of therapeutic drugs for many years (Lama, et al., 2013). Nevertheless, 2D cultures are monoclonal models that lack structures of 3D models involving multiple cell types. The 2D model lacks of components such as ECM and the intercellular interactions which dictate many biological functions of tumors and it may not accurately predict the drug effects on physiologic functions (Matsusaki, et al., 2014).

1.6.2 3D SPHEROIDS

3D spheroid culture has been developed from 2D monolayer culture, as it involves greater cell-cell interactions and better models a 3D multicellular environment. There are many means of preparing 3D spheroid cultures. The simple way to grow spheroids is to culture 2D cells on low-cell binding materials, such as agarose (Hirschhaeuser, et al., 2010), which prevents attachment of cells to the artificial surface so that they preferentially attach to one another. Spheroids can also be constituted from two types of cells (cancer and stromal cells) and allows cell-stroma interactions. Spheroids established from human tissues (also known as tumor fragment spheroids), provide a better 3D model that is reconstituted from original tumor components and is thus more likely to reflect the original TME (Wilson, et al., 2008). The complexity of this 3D environment has been shown to greatly impair the sensitivity to drug interventions in comparison to their 2D counterparts (Barbone, et al., 2011) (Yang, et al., 2009).

1.6.3 ORGANOTYPIC CO-CULTURE MODEL

Similarly to 3D spheroid culture, the organotypic culture is composed of tumor and stromal cells in the presence of ECM components, such as collagen (type I), acting as a scaffold. Such models are advantageous for studying the progression of carcinoma *in situ* invading into the stromal phase. The model for tumor invasion needs to be developed for a longer period (around 12 days), as compared with 2D and 3D spheroid models. The organotypic model has been shown to be more reliable for the reflection of the *in vivo* cell invasion in comparison to those previously developed cell invasion assays (e.g.

modified boyden chamber assay), and is suitable for assessment of drug potencies (Nyström, et al., 2005). The Matrigel™ contains many basement membrane components such as laminin and collagen as well as a variety of growth factors, which can promote cell metastasis and acceleration of tumor growth (Fecher, et al., 2016) (Benton , et al., 2011).

1.6.4 PRIMARY TISSUES DERIVED EXPLANTS

Human tissue-derived 3D models, such as histoculture (Pirnia, et al., 2006) and organotypic culture (Vaira, et al., 2010) are more cost-effective than the animal models, and provide the advantage of maintaining the original tumor morphologies that consists of malignant cells, stroma and inflammatory cells (Vaira, et al., 2010). Whilst it cannot provide information relating to drug metabolism or pharmacokinetic data in the same way that animal models can, such cultures can be established within a short period of time and are used for high throughput screening of drug efficacy (Pirnia, et al., 2006). Immunohistochemistry (IHC) can then be applied to evaluate a multitude of markers in the tumor tissue in order to establish drug sensitivity and mechanisms of action that can be correlated to clinical parameters. The explant model used within this project was directly obtained from primary human lung tumor tissue, and was initiated and developed as part of a prior PhD project (Karekla Thsis,2014). Our expertise with this model means that we can now use it for further investigation of drug potencies.

1.6.5 XENOGRAFT MODELS

Xenograft models are widely used for studying TME *in vivo* where tumors are able to develop their own blood supply, and hence are more useful to study tumor development and progression than those *in vitro* models mentioned above. One of the major limitation for such models is that they involve different cell-stroma interactions to that observed in patient populations, which might impact on tumor growth and drug response (FLEMING, et al., 2010) (Vaira, et al., 2010). Additionally, animal models come with greater cost, can take a long time to establish and come with ethical implications which must be adequately justified (Kim, 2005).

1.7HYPOTHESIS FOR PROJECT

Addition of Akt-targeted treatments into the cisplatin-based chemotherapy regimen can improve the drug potencies of platinum-based agents for treatment of NSCLC.

1.7.1 AIMS

This project will test a number of Akt-targeted drugs in combination with cisplatin, to assess which combinations are likely to show the greatest potencies in models of NSCLC. The potent combinations will be tested in a variety of models in order to assess whether the drug sensitivity is model-dependent.

1.7.2 OBJECTIVES

- To assess cell viability in NSCLC cell lines (2D) respectively treated with cisplatin, molecularly targeted agents alone, and the combinations of cisplatin with the targeted agents. Responses to the most potent agents will then be compared between 2D and 3D cell culture and expression of key signaling molecules pertinent to known mechanisms of drug action assessed.
- To develop the air-interface organotypic co-culture model using a combination of NSCLC cells and lung fibroblasts (i.e. MRC-5), selecting appropriate cancer/fibroblast cell ratios to give optimal invasive capacity of cancer cells. These models will then be utilized to assess potencies of drug combinations, and activities on relevant signaling molecules.
- To develop primary human lung tissue-derived explants and to assess the response to cisplatin. Within this model, due to the limitation of time and tissue resources it is not possible to evaluate the drug potencies of all cisplatin-based combination regimens.

2. CHAPER TWO: MATERIALS AND METHODS

2.1 CULTURE ON 2D ADHERENT CELL LINES AND 3D SPHEROIDS

2.1.1 MATERIALS FOR 2D AND SPHEROID CULTURE MODELS

2.1.1.1. Cell Lines

Cell lines	Cell types/disease[2]	Providers	Mutations[3]
A549[1]	Epithelial/carcinoma	Prof. Karen Brown's lab[1]	*KRAS* (G12S)
H460[2]	Epithelial/large cell carcinoma	ATCC[2]	*KRAS* (Q61H) *PIK3CA* (E545K)
H596[2]	Epithelial/adenosquamous carcinoma	ATCC[2]	*PIK3CA* (E545K) *TP53* (G245C)
MRC-5[1]	Normal fibroblast	Prof. Karen Brown's lab[1]	None

1: Kindly provided by Prof. Karen Brown's lab (Dept. Cancer Studies, University of Leicester).
2: cell lines were purchased from ATCC (LGC Standards, Middlesex, UK) and all information for the Cell type/disease is taken from https://www.lgcstandards-atcc.org/
3: All mutations shown above are considered existing in the cell lines, based on data from the COSMIC cell line project (COSMIC Cell Lines Project, 2016).

2.1.1.2. Cell Culture Reagents

Cell lines	Culture medium	Supplements		
		10% FBS[4]	1% Sodium pyruvate[5]	1% Hepes buffer[5]
A549	RPMI 1640 media[1]	Yes	No	No
H460	RPMI 1640 media[1]	Yes	Yes	Yes
H596	RPMI 1640 media[2]	Yes	No	No
MRC-5	DMEM-high glucose[3]	Yes	No	No

1: Purchased from Thermo Fisher Scientific, Loughborough, UK
2: Purchased from ATCC
3: Dulbecco's Modified Eagle's Medium was purchased from Sigma Aldrich
4. Fetal bovine serum (FBS, heat inactivated, ©Thermo Fisher Scientific).
5: Both sodium pyruvate (100X) and Hepes buffer (100X) were purchased from Sigma Aldrich, Dorset, UK.

2.1.1.3. Other Associated Materials for Cell Culture:

Reagents		Plasticwares	
Names	Purpose	Names	Purpose
Typsin-EDTA1 (0.5% v/v) (Ethylenediaminetetraacetic acid)	Preparing cell trypsinization buffer	96-well microplates[2]	Adherent 2D cell culture
Phosphate buffered saline (PBS)[1], Oxoid™	Diluting typsin-EDTA/washing cells	Black-wall-with transparent-bottom 96-well microplates[2]	Fluorescence detection
		96-well ultra-low attachment[3]	3D spheroids culture

1: Purchased from Thermo Fisher Scientific
2: Purchased from Greiner Bio One International GmbH (Gloucestershire, UK)
3: Purchased from Sigma Aldrich

2.1.1.4. Investigational Drugs

Drugs	Providers
Cisplatin	Sigma-aldrich
GDC-0941, MK-2206 2HCL, AZD6244, STA-9090	Stratech (a distributor of selleck chemicals, Suffolk, UK)
TBK1/IKKε inhibitors (DMX502320-04 and DMX503433-09)	Kindly provided by Mr. Gary Newton (IKKε/TBK1 project leader from Domainex) (Essex, UK).
Drug Vehicles	**Providers**
Dimethylformamide (DMF) and dimethylsulfoxide (DMSO)	Sigma-aldrich

2.1.1.5. General Reagents and Antibodies

Reagent	Provider	
Alamarblue® cell viability reagent, Invitrogen™	Thermo fisher scientific	
Primary antibodies for the In-cell western (ICW) assay	**Providers**	
Anti-Akt (pan, C67E7 rabbit mAb)	Cell signaling technology (MA, USA)	
Anti-phospho-Akt (Ser473, (D9E) XP®, rabbit mAb)		
Anti-P53 (7F5, rabbit mAb)		
Anti-PTEN (138G6, rabbit mAb)		
Anti-cleaved caspase-3 (17/19 kDa cleaved fragment of caspase-3, Asp175, rabbit polyclonal Ab)		
Anti-actin (I-19, goat poly-clonal Ab) as loading control	Santa cruz biotechnology (Heidelberg, Germany)	
Secondary antibodies for ICW	**Provider**	
IRDye® 800CW (goat-anti-rabbit or donkey-anti-rabbilt)	LI-COR bioscience (Cambridge, UK)	
IRDye® 680RD (donkey-anti-goat)		
Other matericals associated with ICW	**Providers**	**Purpose**
Formalin (10% v/v)	Prepared in-house	Fixation of 2D adherent cells
Triton™ X-100 (diluted to 0.1% v/v in PBS)	Sigma-aldrich	Cell permeabilization prior to incubation with primary antibodies
Tween®20 (diluted to 0.1% v/v in PBS)		Washing cells
Odyssey® blocking buffer (PBS)	LI-COR bioscience	Non-specific blocking and preparation of primary and secondary antibodies
EZBlock™ T20 (PBS) blocking buffer		

2.1.1.6. Software and Equipment

Software	Providers	Purpose
Microsoft®Excel®2016 (USA)	Microsoft corporation (USA)	Analysing data
IBM® SPSS® statistics version 22 and 24	IBM (UK)	
Prism 7 (7.02 version)	Graphpad software (USA)	Analysing data and generating bar charts
Equipment	**Providers**	**Purpose**
FLUOstar® optima microplate reader	BMG LABTECH (Germany)	Fluorescence detection
Odyssey® infrared imaging system	LI-COR bioscience (USA)	
CompuSyn	http://www.combosyn.com/	Calculating combination index (CI) values

2.1.2 METHODS

2.1.2.1. 2D Adherent Cell and 3D Spheroid Cultures

Frozen cells were snap-thawed and transferred immediately into a Falcon tube, containing 10 mL of fresh medium for cell culture. The cell suspension was centrifuged at 350 x g for 5 minutes to harvest a cell pellet. The pellet was then re-suspended in fresh media, a portion of the suspension transferred into a T75 or T175 tissue culture flask and cells cultured for 3-4 days in the incubator with an atmosphere of 37 °C and 5% CO_2 (Figure 2.1). After cells reached approximately 70% confluency, they underwent subculture. Cells were washed x 2 in PBS and were detached from plasticware using trypsin-EDTA. The trypsinization was stopped by adding an equal volume of FBS-containing medium and then the cell suspension was processed for cell pelleting and resuspension as described above. For cell culture in 96-well microplate, a cell concentration of 3×10^4 cells per 200 µL was prepared from the suspended cell stock concentration and was aliquoted in the 96-well plate and incubated overnight to allow cell attachment and acclimatisation in the culture environment.

For 3D spheroid culture, the cells were trypsinized and re-suspended as described for 2D culture, and were seeded at a concentration of 8000 cells per 200 µL into a low-attachment 96-well plate. The plate was briefly centrifuged in order to accumulate cells centrally in each well and cells were cultured overnight (nearly 18 hours (hr)). This allowed formation of one single, large spheroid (Figure 2.1).

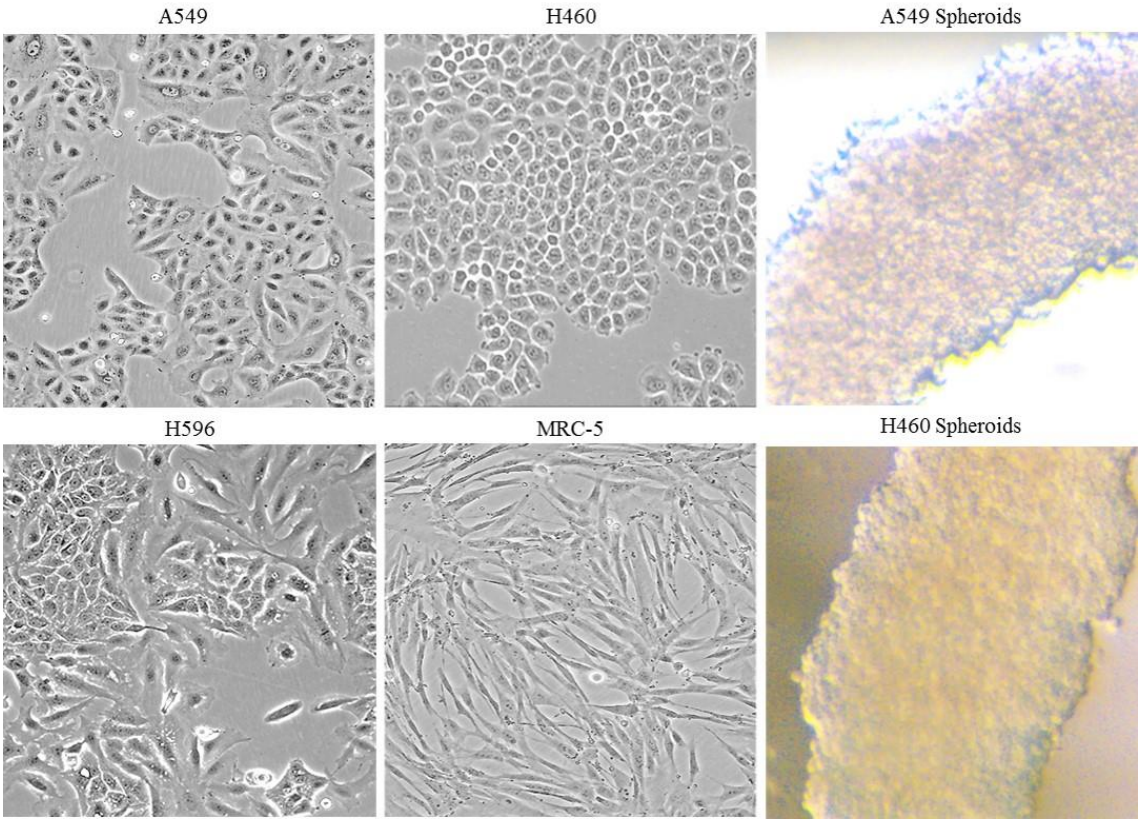

Figure 2. 1 A549, H460, H596 and MRC-5 micrographs and A549, H460 spheroids

A549, H596 and MRC-5 cell line micrographs were taken from ATCC (https://www.lgcstandards-atcc.org/); H460 graph was taken from (Amoêdo , et al., 2011). Both A549 and H460 spheroid graphs were taken from experiments (control group with drug vehicles).

2.1.2.2. Drug Treatments and Cell Viability Assay

On the next day following cell culture, media was replaced with either treatment-containing media or vehicle-containing media and cells were continuously cultured for 24, 48 or 72-hr. For single drug treatments, five or six groups were prepared and each group contained 6-7 replicates. The groups consisted of a blank group (vehicle-containing media without cells), control group (vehicle-containing media with cells) and different concentrations of drug treatments or various drug treatments including single and combination treatments that respectively incubated with the cells.

All targeted agents were prepared for stock concentration and could be preserved for a long time (up to 6 months), particularly for GDC-0941, MK-2206 and AZD6244, whereas DMX502320-04 and DMX503433-09 stock concentration, recommended by Gary Newton, need a refresh every several weeks. The stock concentration for the drugs is prepared with DMSO and is respectively 10 mM for GDC-0941, 30 Mm for MK-2206,

100 mM for AZD6244, 2 mM for STA-9090 and 10 mM for both DMX502320-04 and DMX503433-09 and the drug stock solutions were aliquoted into a 10-20 µL volume, stored in -20 °C freezer. Cisplatin stock solution was prepared with DMF according to the provider and is unable to be preserved for a long duration and hence a fresh stock concentration (20 mM) was prepared prior to treatment. For preparing treatment media, stock concentrations of drugs were prepared for a series of diluted concentration solutions (diluted doses) as reviewed below:

Drugs	Cisplatin	STA-9090	DMX502 320-04	DMX503 433-09	GDC-0941	MK-2206	AZD6244
Diluted doses	10, 5, 1 mM	200, 20, 2 µM	1, 0.6, 0.3 mM,	1, 0.6, 0.3 mM,	5,1 mM	12, 3 mM	50, 10 mM

The endpoint concentration for each drug was prepared by adding proper volume of each diluted dose or the stock concentration into the media at a 1:1000 dilution factor. Therefore, the treatment concentrations for cisplatin were 1, 5, 10 and 20 µM; for STA-9090 were 0.002, 0.02, 0.2 and 2 µM; for both DMX502320-04 and DMX503433-09 were 0.3, 0.6, 1 and 10 µM; for GDC-0941 were 1, 5 and 10 µM; for MK-2206 were 3, 12 and 21 µM; and lastly for AZD6244 were 10, 50 and 100 µM.

Each treatment contained equivocal concentrations of drug vehicle, which did not exceed 0.1%. The vehicle for Cisplatin was DMF, with DMSO used as the vehicle for all of the targeted drugs.

Following single treatments at 24, 48 or 72 hr, alamarblue® reagent was added with a 1:10-dilution factor directly into the media-containing wells and plates incubated at 37 °C for 2 hr. One hundred µL of the alamarblue-containing media from each well was transferred into black-walled 96-well plates for detection of fluorescence, which was undertaken using the Fluostar Optima plate reader at an excitation wavelength of 544 nm and emission wavelength of 580 nm.

For the data analysis of drug treatments, Excel software was applied for calculating relative viability (% of control group) for each treatment group (the control group was treated as 100%) by the formula: $\frac{F_t - F_b}{F_c - F_b} \times 100\%$ (F_t: the fluorescent intensity of each treatment replicate, F_b: the median fluorescent intensity of all blank replicates, F_c: the fluorescent intensity of each control replicate). Each experiment was repeated for 3-4

times under the same conditions and the data of each group (including the control group) was averaged to be presented as Mean ± standard deviation (M ± SD). The comparisons amongst groups between 24 and 48 or 72 hr were analyzed by univariate analysis of variance (ANOVA) using SPSS software.

The combination treatments were all cisplatin-based doublets and were prepared from selected doses of cisplatin or targeted drugs that exhibited no greater than a 30% decrease in the cell viability (exhibiting a 70% relative viability as compared to control group). As cisplatin and all targeted drugs required different solvents, the same concentrations of DMF and DMSO were added to each group.

The data analysis for comparisons between single treatments and combination therapies and those between control and treatment groups were all analyzed by one-way (ANOVA) with prism software.

The most potent cisplatin-based doublets that were observed in 2D culture were taken forward into the 3D spheroid culture model. Cells for spheroid culture were seeded as described above (2.1.2.1). After 3-days of culture, spheroids were overlaid with different treatments and cultured for a further 24 or 72 hr. Spheroids were incubated for 6 hr with alamarblue rather than 2 hr, due to the compact structure of the spheroids. The process of fluorescence detection, data analysis and presentation using the software for spheroid culture was exactly the same as that described for 2D culture.

2.1.2.3. ICW for Detection of Antigen Expression

The most potent cisplatin-based doublets observed on 2D and 3D spheroid cultures were selected for detection of antigens of interest, allowing combinations to be compared with control and corresponding single treatments. Cells were cultured (3×10^5cells per 200 µL) and treated as described for 2D culture. Following treatments, cells were washed three times in PBS and then fixed in 10% formalin for approximately 20 minutes at 4 °C. The formalin was removed and cells were washed three times in 0.1% Triton X-100 in PBS solution on a shaking platform. Odyssey® blocking buffer was added and incubated with cells for 1.5 hr on the shaking platform. Each primary antibody was prepared to a proper recommended concentration with a 1: 1000 dilution factor applied for all primary antibodies used in experiments and each dilution was prepared with the Odyssey® blocking buffer and then incubated with cells at 4 °C with shaking overnight. On the

following day, cells were gently washed x 3 in 0.1% Tween-20 in PBS on a shaking platform and then incubated with the fluorophore-bound secondary antibodies (the recommended dilution factor is 1: 5000) for simultaneous detection of both primary antibodies for 1 hour with shaking at room temperature. Cells were then washed x 3 on the shaking platform with 0.1% Tween20 in PBS, prior to fluorescence detection. Fluorescence detection for IRDye 680 RD and IRDye 800 CW fluorophores was undertaken using the Odyssey® infrared imaging system. Each antigen expression was presented as a fold increase compared to control group. The comparisons of each antigen expression between control and all other groups and those between cisplatin and combination treatments were analyzed by one-way ANOVA using SPSS.

2.2ORGANOTYPIC CULTURE

2.2.1. MATERIALS FOR ORGANOTYPIC CULTURE

2.2.1.1. Materials for Organotypic Culture Model

Gel set-up materials		**Keratinocyte growth medium (KGM)**	
		Names	Providers
Names	Providers	α Modified eagle's medium (α-MEM) (1 L)	Thermo fisher scientific
1. 10X DMEM	Prepared in-house	10% FBS	
DMEM powder (dulbecco's modified eagle's medium-high glucose)	Sigma-Aldrich	1 % GlutaMAX™ medium	
Sodium bicarbonate		Glacial acetic acid for dissolving Insulin	
2. 10% FBS	Thermo fisher scientific	10 µg human epidermal growth factor	Sigma-aldrich
3. Rat tail collagen type I	EMD millipore (Hertfordshire, UK)	400 µg hydrocortisone	
4. Coring® Matrigel® basement membrane matrix	Coring/VWR (Flintshire, UK)	5 mg insulin from bovine pancreas	
5. MRC-5 culture media with or without MRC-5)	Prepared in-house	33.12 mg adenine	
Collagen Coating Materials		2.2 g sodium bicarbonate	
Names	Providers	**Other General Materials**	
1. Rat collagen type I	Merck/EMD millipore	Names	Providers
2. 10% FBS	Thermo fisher scientific	Nylon sheets (Spectra Mesh® woven filters)	Spectrum laboratories/VWR
3. 10X DMEM	prepared in-house	Woven wire mesh for stainless steel metal grids	The mesh company (Cheshire, UK)
4. MRC-5 culture media		25% glutaraldehyde solution	Sigma-aldrich
5. Sodium hydroxide for potential of hydrogen (PH) adjustment	Sigma-aldrich	PBS, Oxoid™	Thermo fisher scientific
		Sterile bottle filters (Nalgene™ Rapid-Flow™ sterile disposable filter units with PES membrane)	
		6-well microplates	
		24-well microplates	Greiner bio one international GmbH

2.2.1.2. Cells, Drugs and Primary Antibodies

All the cells and drugs, primary antibodies associated with organotypic culture were the same as those used for 2D adherent and spheroid cultures (2.1.1). Additionally, cytokeratin detection was via the specific anti-cytokeratin primary antibody ([AE1/AE3], ©Dako, Cambridgeshire, UK) and was used to distinguish tumor cells in the organotypic culture model.

2.2.1.3. Software and Equipment

Software and Equipment	Providers	Purpose
NDP.view2	Hamamatsu Photonics K.K. (Japan)	Slide imaging and image processing
Hamamatsu slide scanner		
ImageJ	1.49v. https://imagej.nih.gov/ij/	
Adobe photoshop CS5 extended 12.0X32 version	Adobe systems Software (Ireland)	
Excel	Microsoft corporation	Analysing data
Prism 7	Graphpad software	Generating bar chart

2.2.2. METHODS

2.2.2.1. Set-up of Organotypic Co-culture

The procedure for preparation of organotypic culture is demonstrated in the diagram shown below (Figure 2.2). In brief, set-up was undertaken over three days. On day 1, gels were prepared using collagen type I (3.5 volumes), Matrigel (3.5 volumes), 10 x DMEM (sterilised, 1 volume), filter-sterilised FBS (1 volume) and 1 volume of MRC-5 medium (or medium containing MRC-5 cells suspended at a concentration of 250,000 per gel) and distributed into 24-well plates before being incubated at 37 °C for one hour to allow formation of the gels. One mL of MRC-5 medium was subsequently added to each individual gel prior to incubation overnight. On day 2, sterilised nylon sheets (approximately 2 cm x 2 cm) were overlaid with a collagen-containing mixture, prepared from 7 volumes of collagen type I, 1 volume of 10 x DMEM, 1 volume of filtered FBS and 1 volume of MRC-5 medium and incubated for 30 minutes at 37 °C. A 1% glutaraldehyde solution was prepared by diluting the stock solution (25%, 840 µL) into 20.1 mL of PBS, followed by filter sterilization. The sterilized 1% glutaraldehyde was added to the collagen-coated nylon sheets before being stored in the fridge at 4 °C for 1 hr. The glutaraldehyde solution was removed by washing x 3 with sterile PBS and the membranes were stored in MRC-5 medium at 4 °C overnight.

A mixture of cancer cells (A549, H460 or H596) and MRC-5 was then prepared, with various cell ratios between cancer and MRC-5 cells investigated in order to optimise the appropriate cell ratios necessary for cell invasion. These ratios were 1:5, 5:1, 1:2, 2:1 and 1:1 of cancer to MRC-5 cells. One mL of the mixed cell suspension solution contained a total of 750,000 cells and was used to replace the media overlaying gels in the plate. The gels were then further cultured in the incubator overnight to allow the cell mixtures to attach to the gels. On day 3, media was removed from the top of the gels; each gel was carefully transferred on to a collagen-coated nylon sheet (developed from day 2) and then placed on top of a sterilized metal grid in a 6-well plate. Appropriate volumes of KGM media was then added into each well so that it just reached the surface of the metal grid without covering the gel and then the gels were incubated for 12 days. During this time, the KGM media in wells was refreshed on every second day. Once the appropriate cell ratios had been determined for each cancer cell line, the organotypic model was ready for the application of testing combination regimens of interest.

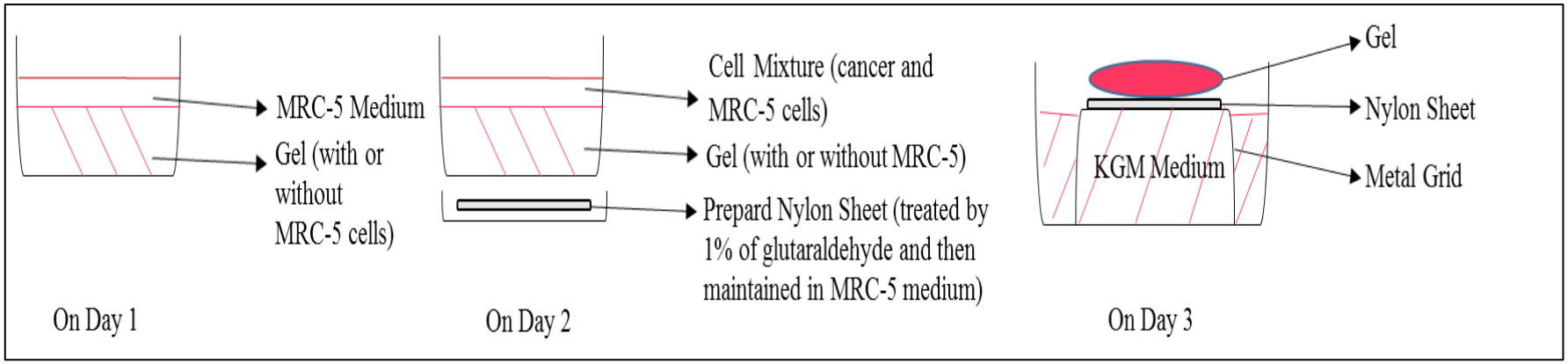

Figure 2. 2 Process for organotypic culture

Three days are required for the set-up of the culture. On day 1, the gel was prepared in a 24-well plate and then overlaid with MRC-5 medium. On day 2, the normal MRC-5 medium was replaced by the cell mixture. On day 3, the gel was transferred on to a nylon sheet, placed on a metal grid in a 6-well plate and appropriate treatment-containing media added.

2.2.2.2. Combination Therapies Using the Organotypic Model

The combination groups, along with control (drug vehicles suspended in KGM media) and associated single treatments were applied on to the organotypic models and incubated at specific time-points (24 or 72 hr) as determined by experiments from 2D and 3D spheroid cultures. Following drug treatment, media was removed and the gels were gently washed in PBS prior to fixation in 10% Formalin overnight. The gels were preserved in tissue blocks, embedded with paraffin and then were processed for sections and further IHC staining prcocesses (to be decribed later). Data processing and analysis for each antigen expression in the organotypic culture model was similar to that described for the explant culture model shown below. The data for each antigen expression summarized from all three models (A549, H460 and H596) and presented as the averaged values for control and any treatment. Statistic analysis for comparisons among groups was analyzed by one-way ANOVA using prism 7.

2.3THE EXPLANT MODEL

2.3.1. MATERIALS FOR THE EXPLANT MODEL

2.3.1.1. Culture Reagents

Materials for explant culture	
1. Plasticware	Providers
Millicell cell culture inserts	Merck millipore
6-well microplates	
2. Tissue culture medium with supplements	Providers
DMEM (4.5g/L glucose, without l-glutamine)	LONZA, UK
1% FBS	Thermo fisher scientific
1% l-glutamine (100X GlutaMAX™)	
1% penicillin/streptomycin (100X)	PAA/GE healthcare (Buckinghamshire, UK)

2.3.1.2. General Reagents for IHC

Materials for IHC	
1. Antigen retrieval solution (10 mM sodium citrate)	Providers
Citric acid monohydrate	Sigma-Aldrich
Sodium hydroxide	
2. Dilution solution for primary antibody (3% (v/v) bovine serum albumin (BSA) in 0.1% (v/v) triton-containing PBS)	Providers
Albumin bovine fraction V	MP biomedicals (Leicester, UK)
Triton™ X-100	Sigma-aldrich
PBS, Oxoid™	Thermo fisher scientific
3. Materials for immunohistochemistry staining	Providers
Adhesion slides (Polysine®Menzel Gläser®)	Thermo fisher scientific
Xylene	Genta medical (York, UK)
Industrial methylated spirits (IMS)	
DPX moutant reagent	Cell path (Powys, UK)
Novolink polymer detection systems kit	Leica biosystems (Milton Keynes, UK)
1) Peroxidase block	
2) Protein block	
3) Post primary	
4) Novolink™ polymer	
5) DAB chromogen	
6) Novolink™ DAB substrate buffer	
7) Hematoxylin	

2.3.1.3. Primary Antibodies and Drugs

Primary antibodies	**Providers**
Anti-human Ki67 antibody (clone MIB-1)	Dako (Cheshire, UK)
Anti-human P53 antibody (clone DO-7)	
Anti-Cleaved Poly (ADP-ribose) polymerase (PARP) antibody (clone E51)	Abcam (Cambridge, UK)
Anti-Akt	Cell signaling technologies
Anti-phospho-Akt (ser^{473})	
Drug	**Providers**
cisplatin	Sigma aldrich
DMF (drug vehicle)	

2.3.1.4. DNA Quantification and Genetic Mutation Detection

Materials for DNA extraction	
Names	Providers
Tris(hydroxymethyl)aminomethane (or Tris)	Sigma aldrich
Sodium dodecyl sulfate (SDS)	
Phenol/chloroform/ isoamyl alcohol (IAA) (phenol: chloroform: IAA 25:24:1)	
Chloroform/IAA (chloroform: IAA: 24:1)	
Proteinase K	QIAGEN (Manchester, UK)
Absolute ethanol	University of leicester
Materials for DNA quantification	
Names	**Providers**
Human genomic DNA (HGD)	Roche (West Sussex, UK)
TaqMan™ universal fast polymerase chain reaction (PCR) mastermix 2x	Applied biosystems/thermo fisher scientific
96-well PCR plates	
GAPDH (the gene encoding glyceraldehyde 3-phosphate dehydrogenase (GAPDH)) WT probe	Sigma aldrich
Forward primer	
Reverse primer	
Materials for *KRAS* oncogene detection	
Names	Providers
KRAS mutant hotspot (G34>A): 5'6-FAM fluorophore-bound nucleoside with 3′-minor groove binder (MGB) (6-FAM-TACGCCACDAGCTC-MGB)	Dr Almahdi Jaber (sigma aldrich)
The wild type probe for *KRAS* proto-oncogene: 5'VIC fluorophore-bound nucleoside with 3′MGB (VIC-TACGCCACCAGCTC-MGB)	
Forward primer: 5'AGGCCTGCTGAAAATGACTGA	
Reverse primer: 5'TGTATCGTCAAGGCACTCTTGC	
Genotyping master mix	Applied biosystems/thermo fisher scientific
Materials for *PIK3CA* oncogene detection	
Names	Providers
PIK3CA mutant hotspot (G1633>A): 5'6-FAM fluorophore-bound nucleoside with 3′MGB (5'6-FAM-TTCTCCTGCTTAGTGAT-MGB)	Dr Abdlrzag M. Ehdode (sigma aldrich)
The WT probe for *PIK3CA* proto-oncogene: 5'VIC fluorophore-bound nucleoside with 3′MGB (VIC-TTCTCCTGCTCAGTGAT-MGB	
Forward primer: 5'TTGAGCTGTTCTTTGTCATTTTCC	
Reverse primer + locked nucleic acid (LNA): 5'{T}CACAGGTAAGTGCTAAAATGGAGAT	
Genotyping master mix	Applied biosystems/thermo fisher scientific

2.3.1.5. Software and Equipment

Software and Equipment	Providers/websites	Purposes
NDP.view2	Hamamatsu photonics K.K.	Slide imaging and image processing
Hamamatsu slide scanner		
ImageJ	1.49v. https://imagej.nih.gov/ij/	
Adobe photoshop CS5 extended 12.0X32 version	Adobe systems software	
Prism 7	Graphpad software	Generating bar chart
The real-time PCR system (StepOnePlus™ systems	Thermo fisher scientific	Performing q-PCR reactions

2.3.2. METHODS

2.3.2.1. Primary Tissue Culture Processing for Cisplatin Treatment

Tissue culture: Human tissue explant culture is a sub-study of Molecular and Functional Mechanism of Human Lung Disease (Principle Investigator: Professor Andrew Wardlaw, Study No.: UHL10402), was approved by University hospitals of leicester (UHL) NHS Trust R&D Department and was a consented study.

Pulmonary tumor and normal surounding tissue was collected from the Glenfield General Hospital, Leicester, immediately following surgical resection and maintained on ice prior to prcocessing. Explant cultures of tissues were set up in the following manner:

On day 1, tumor tissues were finely dissected into tiny cubes (explants), each around 1 mm^3 in volume and 7-8 explants randomly grouped onto a tissue-culture insert. Excess tissue was saved, washed with PBS and then fixed immediately (prior to any culture) with 10% formalin overnight. This tissue was processed the following day and paraffin embedded ready for Hematoxylin and eosin (H&E) and IHC. Explants were placed on the inserts in a 6-well plate and then cultured overnight in the explant medium at 37 °C with 5% CO_2.

On day 2, explants with inserts were subjected to cisplatin treatments. A stock solution of cisplatin at 50 mM concentration was freshly prepared and then further diluted to 10 and 1 mM diluted doses. These three concentrations of cisplatin along with the drug vehicle (0.1% (v/v) DMF) were respectively added at a 1:1000 dilution factor into a fresh medium-containing 6-well plate. There were totally five groups, which were 1, 10 and 50 µM cisplatin treatment along with two drug vehicle-containing control groups (Figure 2.3) and 1-2 replicates were prepared for each concentration of cisplatin treatment. The cultured explants with inserts were randomly assigned into the wells of the plate. Explants

were cultured for a further 24 hr. This time-point was selected based on previous validation work by Dr Karekla.

On day 3, treatments were removed by transferring explants with inserts into a PBS-containing 6-well plate and washed x 2 in the PBS-containing plate. The explants with inserts were then transferred into a formalin-containing 6-well plate and fixed overnight. After fixation, the explants were removed from inserts and then placed into different cassettes (one cassette for each explant group) with two sponges sandwiching explants. The cassettes were submerged into a glassware containing 70% (v/v) IMS prior to further processing, by which each explant group was embedded with paraffin to be maintained in a tissue block. A series of tissue section were prepared from the block by staff in the lab and were used for staining with H&E or IHC.

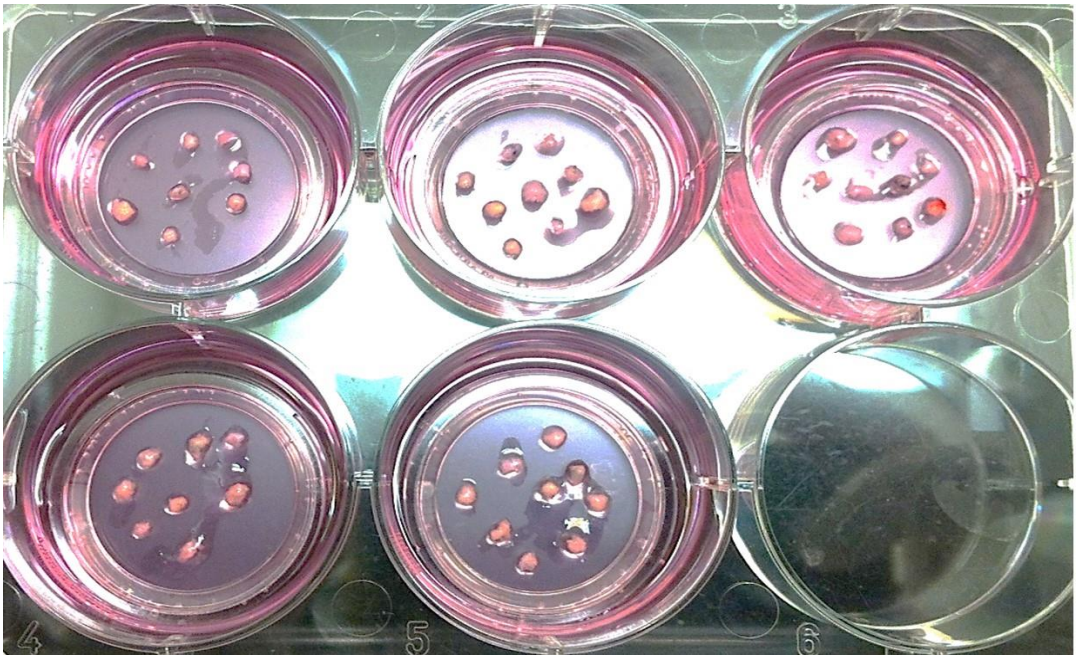

Figure 2. 3 Representative image for explant culture

The image shows randomly grouped explants cultured with inserts in a 6-well plate. The five groups were two control groups (vehicle-containing medium), 1, 10 and 50μM cisplatin treatments.

2.3.2.2. Immunohistochemistry Staining for Analysis of Antigen Expression

Tissue sections on glass slides were placed in the incubator at 65 °C for 10 minutes and sections dewaxed by placing in xylene x 2 for 3 minutes each. Tissue sections were then rehydrated by placing in 99% IMS x 2 for 3 minutes each and 95% IMS x 2 for 3 minutes, before being washed under running tap water. Antigen retrieval was undertaken by submerging slides in 10 mM sodium citrate and microwaving for 20 minutes at high power (750W), and the sections then immediately cooled in PBS ready for antigen detection using the novolink polymer detection kit. In brief, tissue sections were processed as follows: peroxidase block reagent was added for 5 minutes and slides washed x 2 with PBS prior to addition of protein block reagent for 5 minutes and further washing x 2 with PBS. Then a diluted primary antibody-containing solution was prepared with the dilution buffer (3% (v/v) BSA in PBS containing 0.1% (v/v) triton) and was added on each section and incubated with tissues at 4°C overnight. On the following day, sections were washed x 2 with PBS to remove the primary antibody and then covered with post primary block reagent for 30 minutes. Slides were washed x 2 with PBS and incubated for 30 minutes at room temperature with Novolink™ polymer reagent, before further washing x 2 with PBS. Sections were then stained using the DAB chromogen (suspended in substrate buffer) for 5 minutes with further washing (x 2, PBS) to remove excess chromogen. The final step was to counterstain the nuclei with hemotoxylin for 3 minutes and wash under running tap water. Tissue sections were then dehydrated x 2 in 95% IMS, x 2 in 99% IMS and x 2 with xylene. Following dehydration, tissue sections were mounted using cover slides and DPX mountant.

2.3.2.3. Imaging of Sections

Slides were digitally scanner using the Hamamatsu slide scanner and visualised via the NDP.viewer 2 software, allowing each explant piece present on the section to be individually exported for data collection and analysis and each antigen expression (Immunoratio (%)) was analyzed by calculating a percentage of DAB-stained cells exhibiting the protein expression within the tumor area. The whole process mentioned above was presented in Figure 2.4. The digital images of tissue pieces from each treatment group were processed to allow outlining of tumor areas with Image J software. Processed images had the background removed using photoshop software to enhance DAB (brown colour) and hemotoxylin (blue colour) staining. Finally, images were re-processed using

Image J to calculate an immunoratio (%) for the protein expression from the tumor area for each explant, which was the percentage of DAB-stained tumor cells (DAB%) expressing the antigen of interest. Each group data was summarized from all explants analyzed and calculated with the formula as follows:

$$A=\sum_{i=1} A_i, DAB_x\%=\frac{A_i \times DAB_i\%}{A} \text{ and } \sum_{x=1}^{n} DAB_x\%$$

$DAB_x\%$ is the normalized DAB%, $DAB_i\%$ is the (original) individual DAB%, A_i is the individual area, A is the total area and n is the piece number.

In brief, each piece area (A_i) was added up to A, then DAB% of the individual piece ($DAB_i\%$) was normalized to $DAB_x\%$ by multiplying with $\frac{A_i}{A}$ and all the number (n) of $DAB_x\%$ was added up together to obtain the summarized value for each group.

As the explants were tissue-specific, each case of collected tumor tissues was individually processed and analyzed. Several cases for which data will be presented included those collected by Dr E. Karekla (LT31, LT33, LT36, LT38, LT83, LT84, LT88, LT89, LT92) and the cases that were collected, treated and analyzed by the author (LT98, LT103. LT104, LT105, LT106, LT107, LT116). There were five antigens of interest undergoing immunohistochemistry staining, which are cytokeratin, Ki67, cleaved PARP (cPARP), Akt, phospho-Akt (pAkt). The data for P53 expression is only presented for P53-inducible (WT) cases.

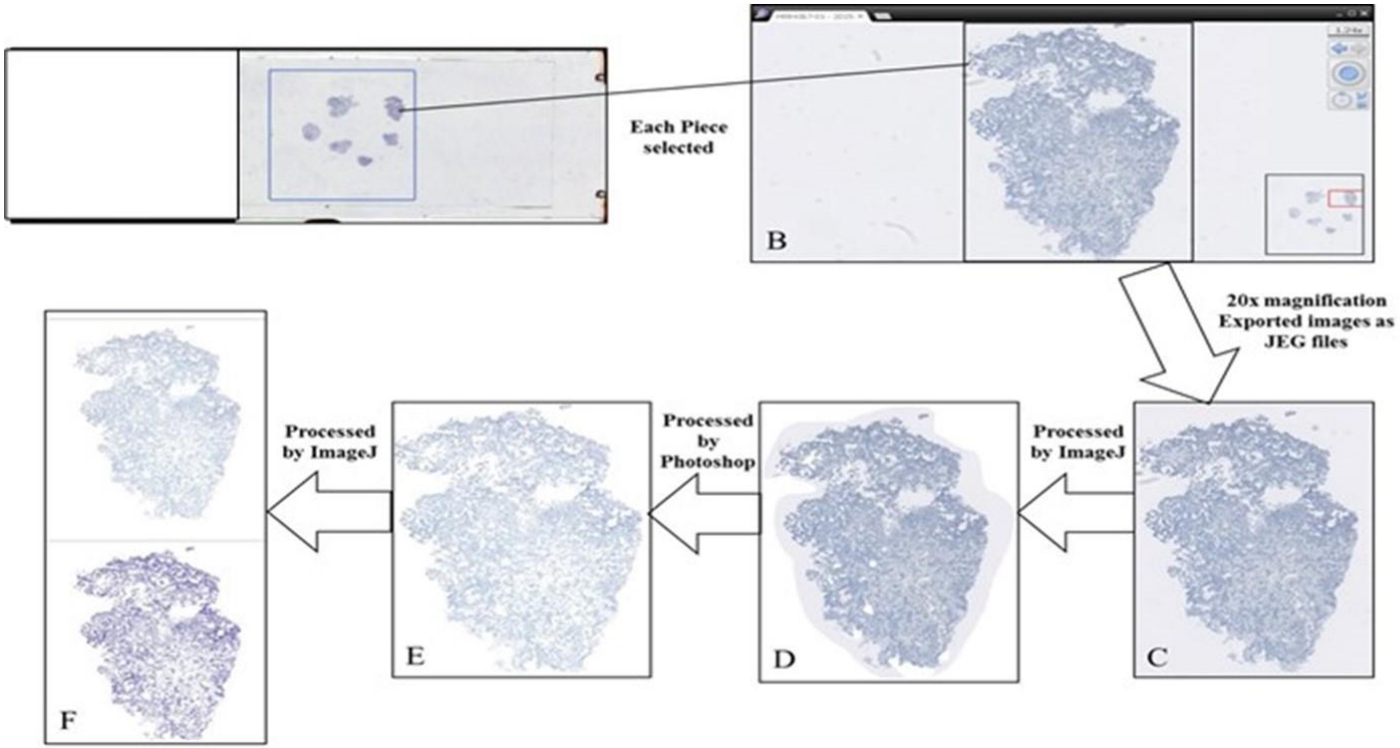

Figure 2. 4 Processing of data collected from explant tissue sections (1 treatment group)

Each piece from the section was digitally scanned by a hamamatsu slide scanner and then viewed by the DNP.viewer 2 (A→B) for export of images into ImageJ (JPEG form) at 20x magnification (B→C); image is then processed for tumor cell selection by ImageJ (C→D), followed by background removal using Photoshop (D→E) and then re-processed for analysis of immunoratio within the tumor area using ImageJ (E→F).

2.3.2.4. DNA Extration, Quantification and Genetic Mutation Detection by qPCR

Frozen tissues of all cases collected by the author were sectioned by Core Biotechnology Services and then processed for DNA extraction via the following protocol: Firstly, tissues were mixed with 0.05 M Tris-PH8.0/0.02% SDS and the mixture incubated with the appropriate amount of proteinase K solution for digestion of tissues overnight. The next day, an equal volume of phenol/chloroform/IAA was added to the mixture, followed by mixing and microfuging at a high speed (14000 rpm) for 3 minutes. The top layer of the mixture was transferred to a fresh Eppendorf, mixed with an equal volume of chloroform/IAA and then microfuged at 14000 rpm for 3 minutes. The top layer was again transferred to a fresh eppendorf, mixed with 3-times volumes of ethanol and stored in the freezer for at least 30 minutes to facilitate precipitation of DNA. The mixture with visible DNA sediment was then microfuged at 14000 rpm for 15 minutes at 4 °C. The supernatant was carefully removed and the remaining DNA pellet air dried in the ambient environment for 1 minute, prior to being dissolved in sterile ultrapure water.

The quantification of DNA samples was undertaken using a real-time PCR system (qPCR) which is described in the following protocol. A high concentrate HGD (200 µg/36 µL) was diluted into a series of 1:2 standard solutions (a range of 20-0.3125 ng per 3.6 µL) and DNA samples (extracted from tissues) were diluted at 1:10 in ultrapure water. A master mix solution (enough for all qPCR reactions) was prepared using *GAPDH* probe, forward and reverse primers and ultrapure water. A 10 µL solution was prepared for each qPCR reaction, consisting of 3.6 µL of either HGD standard solution or DNA sample, 5 µL of TaqMan™ fast mastermix and 1.4 µL of the master mix solution. The quantities of DNA in the samples were calculated via a linear regression function generated from the standard curve (shown in Figure 2.5), which was formed by a linear curve that linked all points of standard diluted solutions.

After DNA was quantified, the sample was diluted into 10 ng/3 µL concentrations using ultrapure water and then mixed with 5 µL of genotyping master mix, 0.2 µL of wild type *KRAS*/*PIK3CA* probe, 0.2 µL of mutant *KRAS*/*PIK3CA* probe, 0.6 µL of *KRAS/PIK3CA* forward primer, 0.6 µL of *KRAS/PIK3CA* reverse primer and 0.4 µL of sterile ultrapure water. Mutation detection for either *KRAS* or *PIK3CA* using the corresponding probes and primers was undertaken using with corresponding probes and primers by the qPCR

instrument. Each sample was run in triplicate in a 96-well PCR plate. An example of mutation detection results for *KRAS* and *PIK3CA* is shown in Figure 2.6.

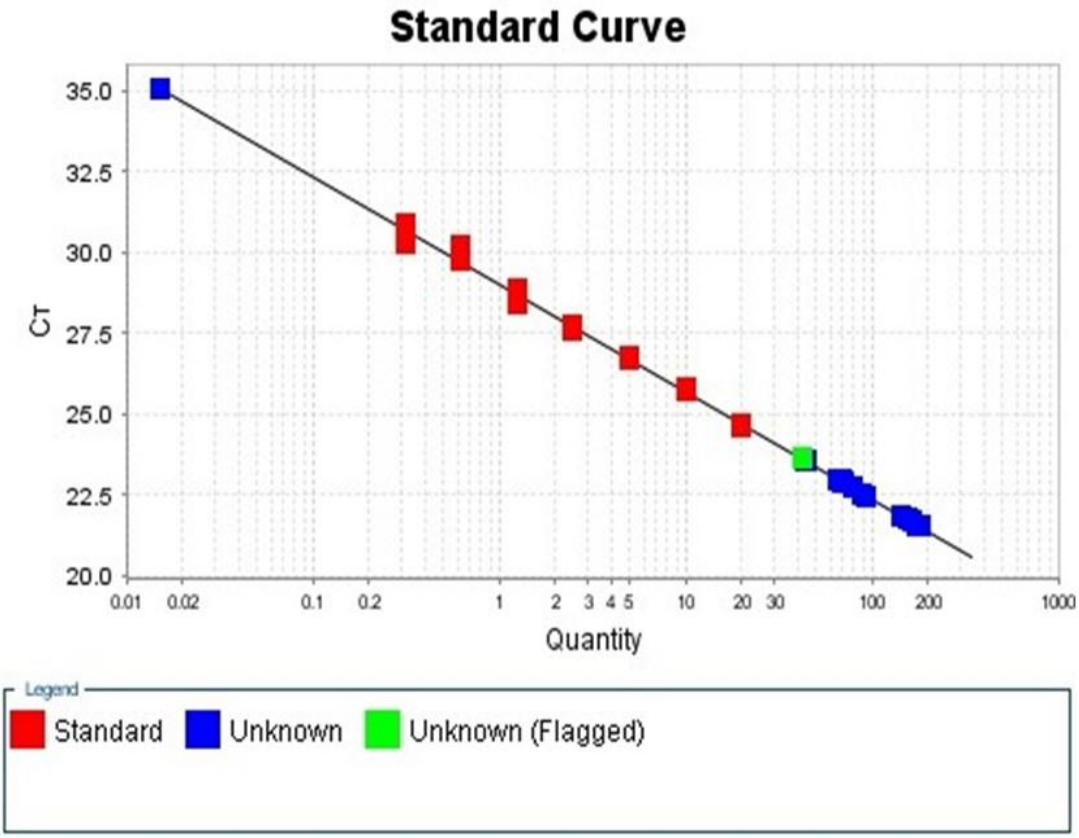

Figure 2. 5 Generation of DNA standard curve for DNA quantification using the StepOnePlus™ qPCR instrument

The figure shows the generation of linear standard curve linked through all points of HGD standard solutions (1:2 dilutions) and the concentration of unknown DNA was calculated using the curve.

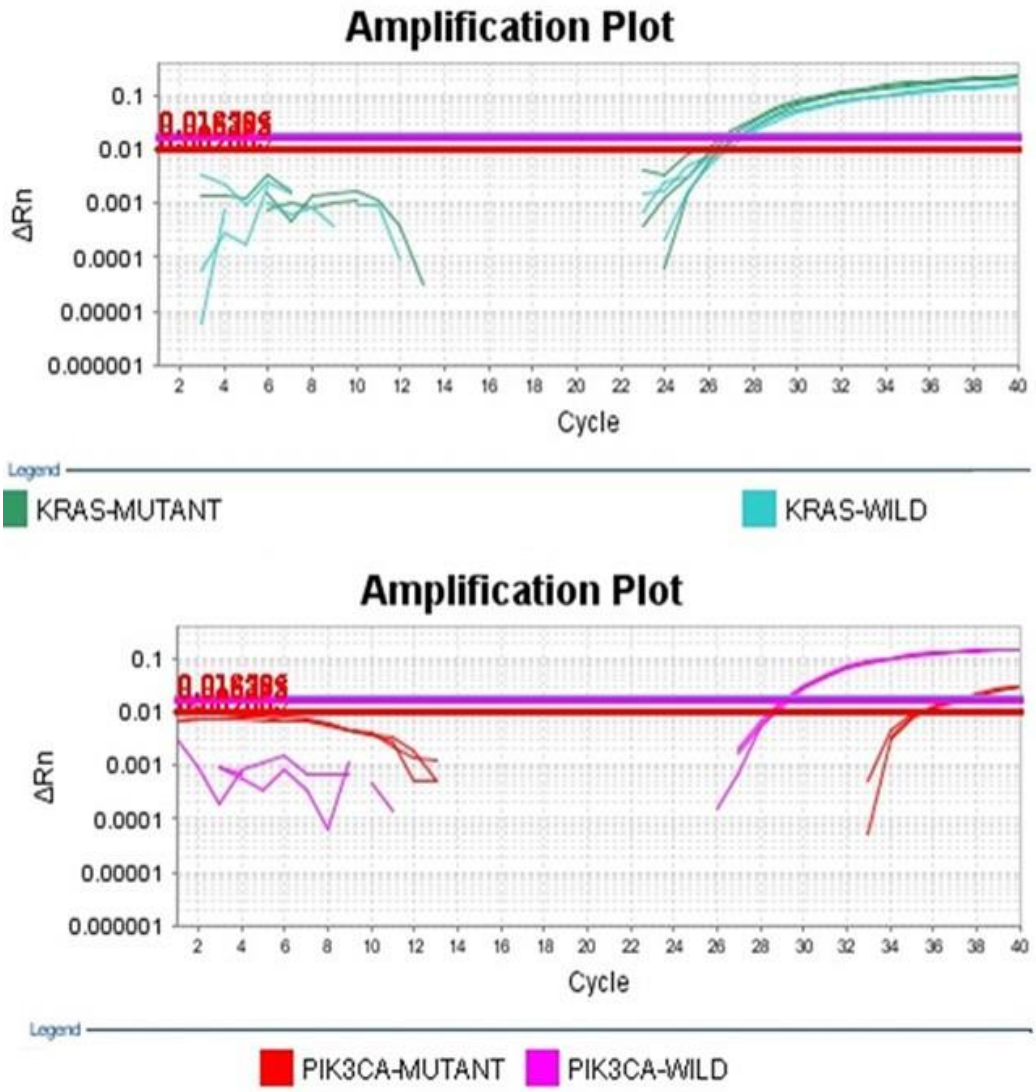

Figure 2. 6 Example of *KRAS and PIK3CA* mutation detection from qPCR analysis.

The upper plot shows that the case (T104) contained both wild type and mutant *KRAS* (G34>A), as both *KRAS* allele-labeled probes showed a similar and higher signal presenting genes amplifing from 24 to 40 cell-cycle progression. This suggested that the two copies of *KRAS* genes were heterozyous. In contrast, the lower plot is for *PIK3CA* mutation (G1633>A) detection in case of T105, which showed a stronger *PIK3CA* wild-type allele signal compared to the mutant allele signal, indicating higher abundance of the wild type *PIK3CA* allele compared to that of the mutant allele.

3. CHAPTER THREE: DRUG POTENCIES IN 2D CELL CULTURES

3.1. INTRODUCTION

Two-dimensional cell culture is standardly used for high throughput drug screening assays. Within this chapter, the alamar blue assay has been utilized to determine drug sensitivity across a panel of lung-derived cell lines exhibiting differing mutation spectra. As reviewed in 1.5.7.2, cisplatin is under clinical development for combination with a variety of targeted agents such as PI3K and Akt inhibitors, for improving the sensitivity to cisplatin treatment. So here the aim is to determine which combinations may be of interest to take forward into 3D culture models, which are less amenable to a high-throughput setting. The potency of each single targeted agent and cisplatin was assessed with cell viability assay compared to control group on a panel of cell lines (A549, H460 and H596) with PI3K/Akt signaling activation at 24, 48 and 72 hr, which would determine the optimal time-points and single drug doses for various cisplatin-based doublets. The potencies of the combination treatments were also assessed with the viability assay compared to control group and single treatments. The most potent cisplatin-based doublets would be analyzed for protein expression of Akt, pAkt, P53, PTEN and cleaved caspase-3 with ICW.

3.1.1. MOLECULARLY TARGETED AGENTS

As described in section 2.1.1.4, the drugs of interest in addition to cisplatin were as follows: GDC-0941 – pan PI3K inhibitor, MK-2206 – selective Akt 1/2/3 inhibitor, DMX502320-04 and DMX503433-09 – TBK1/IKKε inhibitors, STA-9090 – HSP90 inhibitor and AZD6244 – MEK1/2 inhibitor.

3.1.1.1. Targeted Agents Directly Block Akt Activity

GDC-0941 ($C_{23}H_{27}N_7O_3S_2$) is an oral potent pan-PI3K inhibitor that specifically target on p110 subunits of class I PI3Ks (p110 α, β, δ, γ) (Cheng, et al., 2014) (Spoerke, et al., 2012) and this drug functions to competitively bind the adenosine-5'-triphosphate (ATP) binding site of PI3K (Papadimitrakopoulou, 2012), with IC50 (half maximal inhibitory concentration) demonstrated in cell-free assay of 3 nM for p110 α/γ, 33 nM for p110 β and 75 nM for p110 γ; GDC-0941 can also moderately inhibit mTOR with IC50 of 0.58

µM (Selleck Chemicals, 2017). The preliminary study tested for the activity of this drug on H460 cell line, identified the appropriate concentration of GDC-0941 ranging from 1 µM to 10 µM.

MK-2206 ($C_{25}H_{21}N_5O.2HCl$) is an oral, highly selective, non-ATP competitive allosteric inhibitor of Akt, and is equally potent toward Akt1 (IC50:5 nM), Akt2 (IC50:12nM) and Akt3 (IC50:65nM) (Molife, et al., 2014) (Iida, et al., 2013) (Hirai, et al., 2010). This inhibitor functions to bind at a site in or near the pleckstrin-homology domain, which prevents Akt translocation to the plasma membrane (Molife, et al., 2014) (Papadimitrakopoulou, 2012). The preliminary study showed on H460 cell line that the appropriate concentration of MK-2206 ranging from 3 µM to 21 µM.

Both two TBK1/IKKε inhibitors-DMX502320-04 ($C_{19}H_{19}N_7$) and DMX503433-09 ($C_{25}H_{26}FN_9O_2$) were novel agents that were developed by the domainex incorpration. Based on the information provided by Mr. Newton, both two agents could equally target TBK1 and IKKε, and the mechanism of action was designed to reversibly bind to the target kinases. The IC50 of inhibitors was demonstrated in the assay of mouse macrophages (TBK1 in human and mouse cells is about 95% identical) that was 20 nM for DMX502320-04 whereas DMX503433-09 was 3 or 4-fold less effective. The appropriate concentration range for both two inhibitors is from 0.3 µM to 10 µM according to the provider.

3.1.1.2. Targeted Agents that Indirectly Block Akt Activity

STA-9090 ($C_{20}H_{20}N_4O_3$) is a potent, resorcinol-derived agent that selectively binds to the ATP-binding domain of HSP90 and leads to its inhibition (Pillai & Ramalingam, 2014) (Shimamura, et al., 2012). The IC50 of STA-9090 tested in 8 Osteosarcoma (OSA) cells was 4 nM (Selleck Chemicals, 2017). The previous study (Busacca, et al., 2016) has demonstrated the appropriate concentration of STA-9090 ranging from 0.02 µM to 2 µM, although 0.002 µM was used as the smallest concentration in the experiments.

AZD6244 ($C_{17}H_{15}BrClFN_4O_3$) is a potent, allosteric inhibitor of MEK1/2 that functions to inhibit the catalytic activity of kinases and prevents ERK activation (Meng, et al., 2010) AZD6244 has an IC50 of 14 nM for MEK1 (Goldman & Garon, 2012) (Garon , et al., 2010) and has a similar potency on inhibiting ERK1/2 phosphorylation (IC50:10 nM)

(Selleck Chemicals, 2017). The range of concentration for AZD6244 that was tested in the preliminary study on H460 cell line is from 10 μM to 100 μM.

3.2. SINGLE AGENT POTENCIES

3.2.1. CISPLATIN TREATMENT

The A549 cell line exhibited resistance to cisplatin across all three time points, with relative viability (% of control) decreasing by a maximum of 25% only at the highest dose of 20 μM cisplatin, which was significantly ($P<0.05$) greater at 48 and 72 hr compared to 24 hr (Figure 3.1). Table 3.1 shows that relative viability was decreased significantly compared to that observed in the control from 5 μM cisplatin at 24, 48 and 72 hr. This suggests that even though the A549 cells exhibit a degree of resistance to cisplatin, there is evidence of both a dose- and time-dependent effect.

H460 cells exhibited greater sensitivity to cisplatin than did the A549 cells, in an obvious dose- and time- dependent manner. Relative viability was decreased by up to 87% following treatment with 20 μM at 72 hr, with significant inhibition observed from 5 μM cisplatin at 24, 48 and 72 hr.

Similarly to H460 cells, H596 cells exhibited a greater sensitivity to cisplatin which was both time- and dose-dependent. A 72-hr treatment proved to be the most active, with 20 μM cisplatin decreasing viability by 98%, with significant decreases observed from the lowest dose (1 μM) across all time points (see appendix 7.1 for 48 hr data).

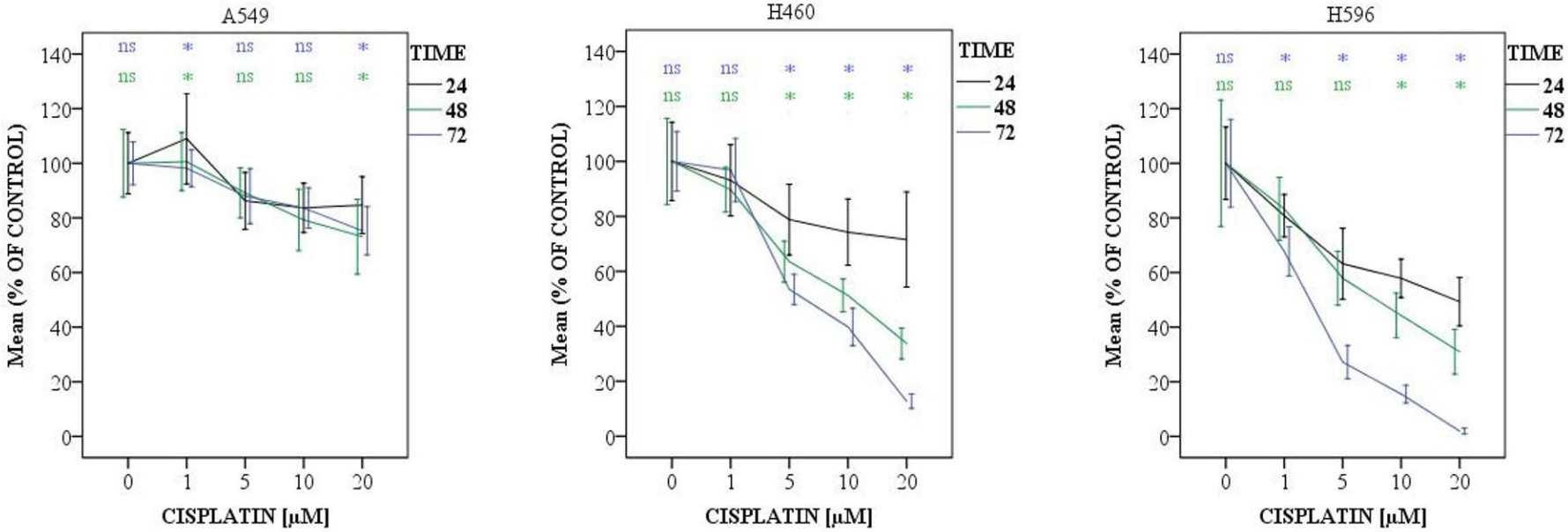

Figure 3. 1 Cisplatin treatment on A549, H460 and H596 cell lines at 24 (black), 48 (green) and 72 (blue) hr.

The doses for single agent cisplatin are 1, 5, 10 and 20 µM and the control group is expressed as zero. Data were analyzed by univariate ANOVA by SPSS and results are shown as M ± SD of over 19 replicates and '*' means P<0.05 and 'ns' means non-significant. The significant symbols stand for 24 vs 48 hr (shown in green) and 24 vs 72 hr (shown in blue).

Table 3. 1 The comparison of different concentrations of cisplatin treatments and the optimal single dose selection at 24 and 72 hr for A549, H460 and H596 cell lines.

The data were analyzed by one-way ANOVA (SPSS) and results are shown as M ± SD of over 19 replicates and '*' means P<0.05 and 'ns' means non-significant. The highlighted doses are selected for combination treatments at 24 or 72 hr.

A549											
Drugs	Doses (μM)	Time-point (hr)	M	SD	N	Drugs	Doses (μM)	Time-point (hr)	M	SD	N
Cisplatin	0	24	100	11	23	Cisplatin	0	72	100	8	30
	1		109	17	21		1		98	7	28
	5		86*	10	21		5		88*	10	28
	10		84*	9	21		10		84*	7	28
	20		85*	10	21		20		75*	9	28
H460											
	Doses (μM)	Time-point (hr)	M	SD	N	Drugs	Doses (μM)	Time-point (hr)	M	SD	N
Cisplatin	0	24	100	14	19	Cisplatin	0	72	100	11	21
	1		93	13	21		1		97	11	21
	5		79*	13	21		5		53*	6	21
	10		74*	12	21		10		40*	7	21
	20		72*	17	19		20		13*	3	20
H596											
Drugs	Doses (μM)	Time-point (hr)	M	SD	N	Drugs	Doses (μM)	Time-point (hr)	M	SD	N
Cisplatin	0	24	100	13	20	Cisplatin	0	72	100	16	21
	1		81*	8	21		1		68*	9	21
	5		63*	13	21		5		27*	6	21
	10		58*	7	21		10		15*	3	21
	20		49*	9	21		20		2*	1	21

3.2.2. STA-9090 TREATMENT

For STA-9090 treatment on A549 cells, a maximal reduction in viability of 59% was observed following a 72-hr treatment at the highest dose of 2 μM. This effect was time-dependent at 48 hr only, although the highest dose also caused a significant decrease in viability at 72 hr compared with the decrease observed at 24 hr. Significant decreases compared to the control at each time point were observed from a dose of 0.02 μM (Figure 3.2 and Table 3.2).

Response to STA-9090 was also more marked in the H460s compared with the A549s. Here, a time- and dose-dependent decrease in viability was observed at 72 hr only, with maximal inhibition of up to 64% caused by 2 μM STA-9090. The significant inhibition in relative viability compared to control started to be observed from 0.002 μM at 72hr in contrast to 0.02 μM at 24 hr and 0.2 μM at 48 hr.

Treatment with STA-9090 on H596 cells evoked a similar response to that observed for the other cell lines, only showing an obvious time- and dose- dependent effect at the 2 highest treatment concentrations (0.2 and 2 μM). Maximal inhibition of 60% was observed at 72 hr following treatment with 2 μM STA-9090. The significant inhibition in viability compared to control was seen from either 0.002 or 0.02 across all time points (see appendix 7.1 for 48 hr data).

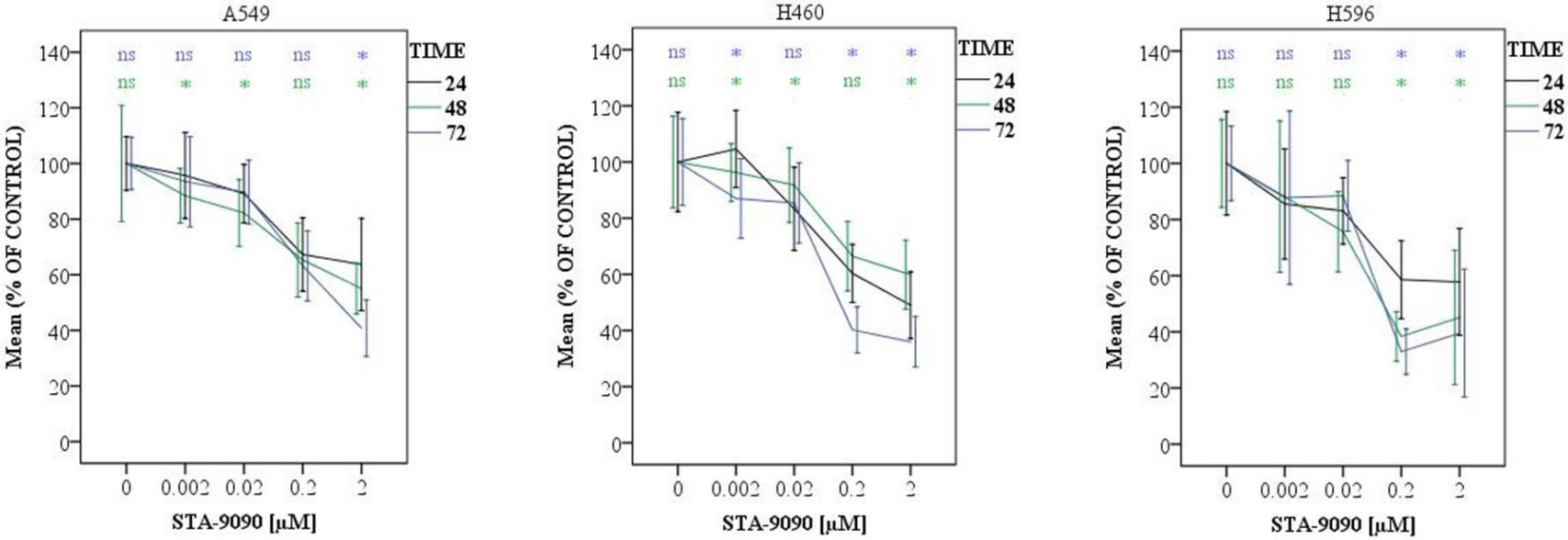

Figure 3. 2 STA-9090 treatment on A549, H460 and H596 cell lines at 24 (black line), 48 (green) and 72 (blue) hr.

The doses for single STA-9090 agent are 0.002, 0.02, 0.2 and 2 µM and control group is expressed as zero. Data were analyzed by univariate ANOVA (SPSS) and results are shown as M ± SD of over 28 replicates and '*' means P<0.05 and 'ns' means non-significant. The significant symbols stand for 24 vs 48 hr (shown in green) and 24 vs 72 hr (shown in blue).

Table 3. 2 The comparison of different concentrations of STA-9090 and the optimal dose selection at 24 and 72 hr for A549, H460 and H596 cell lines

Data were analyzed by one-way ANOVA (SPSS) and results are shown as M ± SD of over 28 replicates and '*' means P<0.05 and 'ns' means non-significant. The highlighted doses are selected for combination treatments at 24 or 72 hr.

A549											
Drugs	Doses (μM)	Time-point (hr)	M	SD	N	Drugs	Doses (μM)	Time-point (hr)	M	SD	N
STA-9090	0	24	100	10	30	STA-9090	0	72	100	9	30
	0.002		96	15	28		0.002		93	16	28
	0.02		89*	11	28		0.02		90*	11	28
	0.2		67*	13	28		0.2		63*	13	28
	2		64*	17	28		2		41*	10	28
H460											
Drugs	Doses (μM)	Time-point (hr)	M	SD	N	Drugs	Doses (μM)	Time-point (hr)	M	SD	N
STA-9090	0	24	100	18	37	STA-9090	0	72	100	15	30
	0.002		105	14	35		0.002		87*	14	28
	0.02		83*	15	35		0.02		85*	14	28
	0.2		60*	10	34		0.2		40*	8	28
	2		49*	12	35		2		36*	9	28
H596											
Drugs	Doses (μM)	Time-point (hr)	M	SD	N	Drugs	Doses (μM)	Time-point (hr)	M	SD	N
STA-9090	0	24	100	18	29	STA-9090	0	72	100	13	36
	0.002		86*	20	28		0.002		88	31	35
	0.02		83*	12	28		0.02		88*	13	35
	0.2		59*	14	28		0.2		33*	8	35
	2		58*	19	27		2		40*	23	35

3.2.3. DMX502320-04/ DMX503433-09 TREATMENT

A549 cells displayed similar sensitivity to both TBK inhibitors DMX502320-04 and DMX503433-09, with maximal inhibition in viability of 54% and 64% observed respectively at 72 hr at 10 μM dose of each drug. Response to DMX502320-04 exhibited a time-dependent effect at 72 hr compared with 24 hr, with significant reductions in viability compared to control observed from 0.6 μM across all time points. The A549 cells appeared to be slightly more sensitive to DMX503433-09, with a significant decrease in viability observed from 0.3 μM across all time points (Figure 3.3 and Table 3.3).

In contrast to the A549 cells, H460s remained relatively refractory to TBK inhibition. No dose- or time dependent decreases in cell viability were observed with DMX502320-04, although a significant decrease (40%) was observed at 10 μM which was similar across all time points. DMX503433-09 was more potent at 24 hr compared to that at 72 hr, with significant decreases in viability observed from 0.3 μM to a maximal decrease of 55% at 10 μM of the drug.

H596s were similarly sensitive to DMX502320-04 as the H460s, as viability was significantly decreased at the highest dose (10 μM) only, with a maximal reduction of 52% at 48 hr and 58% at 72 hr, compared to 40% at 24 hr. For DMX503433-09 a dose- and time-dependent effect was observed at 48 hr only with a maximal decrease of 67% at 10 μM., and significant decreases in viability observed from 0.3 μM across all time points (see appendix 7.1 for 48 hr data).

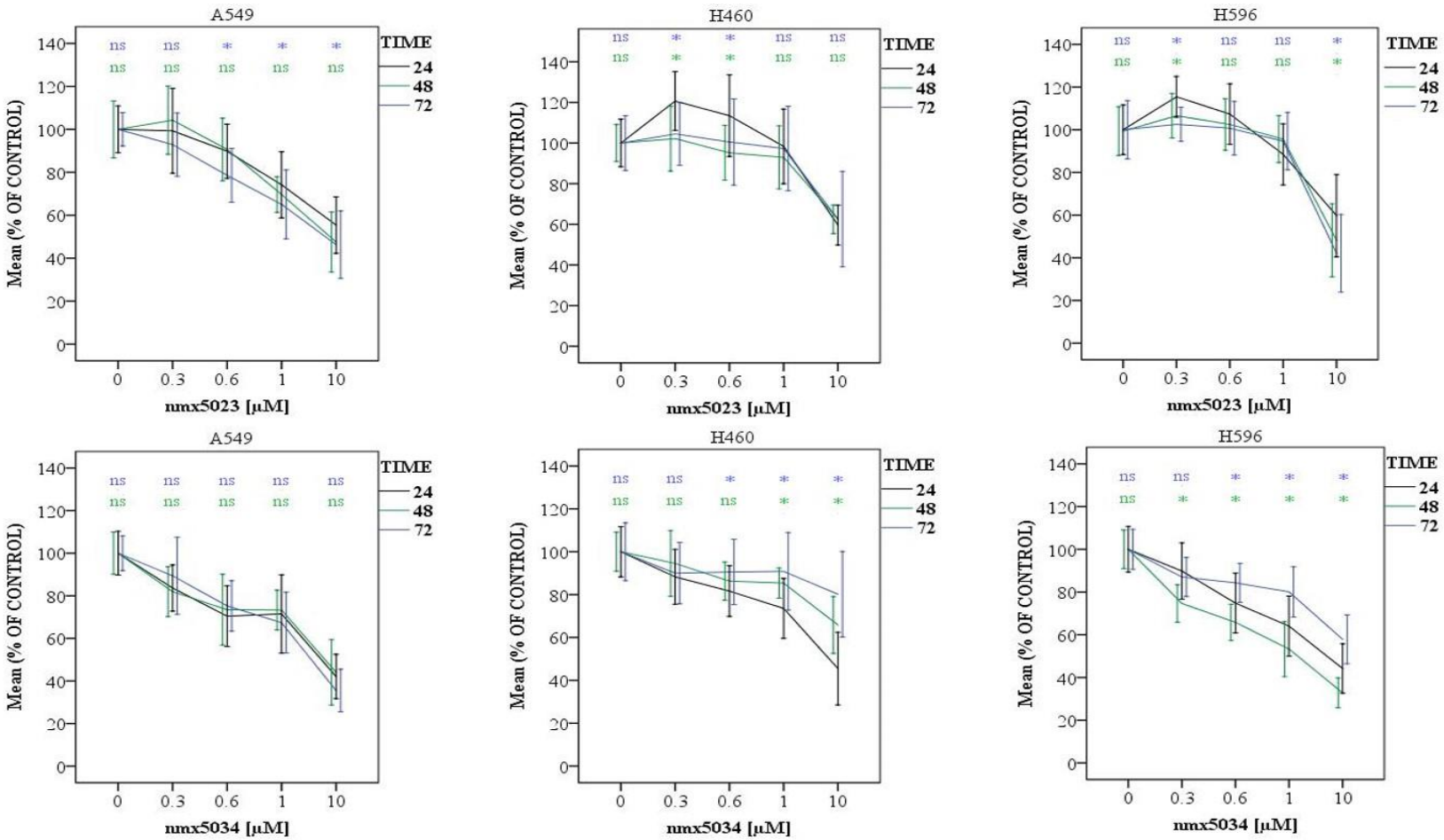

Figure 3. 3 DMX502320-04 and DMX503433-09 treatments on A549, H460 and H596 cell lines at 24 (black line), 48 (green) and 72 (blue) hr.

The doses used for both DMX502320-04 and DMX503433-09 agents are 0.3, 0.6, 1 and 10 µM and control group is expressed as zero. Data were analyzed by univariate ANOVA (SPSS) and results are shown as M ± SD of over 20 replicates and '*' means P<0.05 and 'ns' means non-significant. The significant symbols stand for 24 vs 48 hr (shown in green) and 24 vs 72 hr (shown in blue).

Table 3. 3 The comparison of different concentrations of DMX502320-04 and DMX503433-09 treatments and the optimal dose selection at 24 and 72 hr for A549, H460 and H596 cell lines

Data were analyzed by one-way ANOVA by SPSS and results are shown as M ± SD of over 20 replicates and '*' means P<0.05 and 'ns' means non-significant. The highlighted doses are selected for combination treatments at 24 or 72 hr.

A549											
Drugs	Doses (μM)	Time-point (hr)	M	SD	N	Drugs	Doses (μM)	Time-point (hr)	M	SD	N
DMX502 320-04	0	24	100	11	35	DMX502 320-04	0	72	100	8	35
	0.3		99	20	34		0.3		93	15	35
	0.6		90*	13	35		0.6		79*	13	35
	1		74*	15	34		1		65*	16	35
	10		55*	13	35		10		46*	16	34
DMX503 433-09	0	24	100	10	42	DMX503 433-09	0	72	100	8	35
	0.3		84*	11	42		0.3		89*	18	34
	0.6		70*	14	42		0.6		75*	12	35
	1		71*	18	42		1		67*	14	33
	10		42*	10	42		10		36*	10	33
H460											
Drugs	Doses (μM)	Time-point (hr)	M	SD	N	Drugs	Doses (μM)	Time-point (hr)	M	SD	N
DMX502 320-04	0	24	100	12	28	DMX502 320-04	0	72	100	13	35
	0.3		121*	14	28		0.3		105	15	34
	0.6		113*	20	28		0.6		101	21	34
	1		98	18	28		1		97	21	35
	10		60*	10	28		10		63*	23	34
DMX503 433-09	0	24	100	12	28	DMX503 433-09	0	72	100	13	35
	0.3		88*	13	28		0.3		90	14	34
	0.6		82*	12	28		0.6		91	15	34
	1		74*	14	28		1		91	18	35
	10		45*	17	28		10		80*	20	35
H596											
Drugs	Doses (μM)	Time-point (hr)	M	SD	N	Drugs	Doses (μM)	Time-point (hr)	M	SD	N
DMX502 320-04	0	24	100	12	35	DMX502 320-04	0	72	100	14	28
	0.3		115*	10	35		0.3		103	8	26
	0.6		107	14	35		0.6		101	13	26
	1		88*	14	35		1		95	13	27
	10		60*	19	35		10		42*	18	26
DMX503 433-09	0	24	100	11	42	DMX503 433-09	0	72	100	9	21
	0.3		90*	13	42		0.3		87*	9	21
	0.6		75*	14	41		0.6		84*	9	20
	1		64*	14	42		1		80*	12	20
	10		44*	12	42		10		58*	11	20

3.2.4. GDC-0941 AND MK-2206 TREATMENTS

GDC-0941 exhibited a good potency in the A549 cells, with cell viability being decreased by up to 75% following a 48-hr treatment. A significant decrease in viability compared to control was observed from 1 μM GDC-0941 at 24 and 48 hr, and from 5 μM at 72 hr. Inhibition of Akt by MK-2206 elicited similar results to that observed with the PI3K inhibitor in that a dose- and time-dependant decrease was observed at 48 hr only. Significant dose-dependent reductions were observed from 3 μM at 24 and 48 hr and from 12 μM at 72 hr (Figure 3.4 and Table 3.4).

For H460s, PI3K inhibition by GDC-0941 decreased viability to a slightly greater extent than that observed for A549 cells, and both 24- and 72 hr treatments were more active than that observed at 48 hr. However, the potency was very similar at both 24 and 72 hr in the H460 cell line, with a significant inhibition in viability occurring from 1 μM. A maximal reduction in viability was observed following 10 μM treatment at 72 hr (73% decrease in cell viability). Similarly to PI3K inhibition, H460 cells showed greater sensitivity to MK-2206 at 24 and 72 hr in contrast to 48 hr, with significant decreases occurring from 3 μM, and a maximal inhibition of 63% occurring at 21 μM.

For H596, both the PI3K and Akt inhibitors were significantly more active at the shorter time point of 24 hr compared to 72 hr, with inhibition in viability of up to 60% and 45% for GDC-0941 and MK-2206 respectively at 24 hr. Sensitivity to both compounds at 24 hr was similar to that observed in A549 cells. Significant decreases in viability were elicited from a 1 μM dose of GDC-0941 across all time points, and a 3 μM MK-2206 dose across all time points (see appendix 7.1 for 48 hr data).

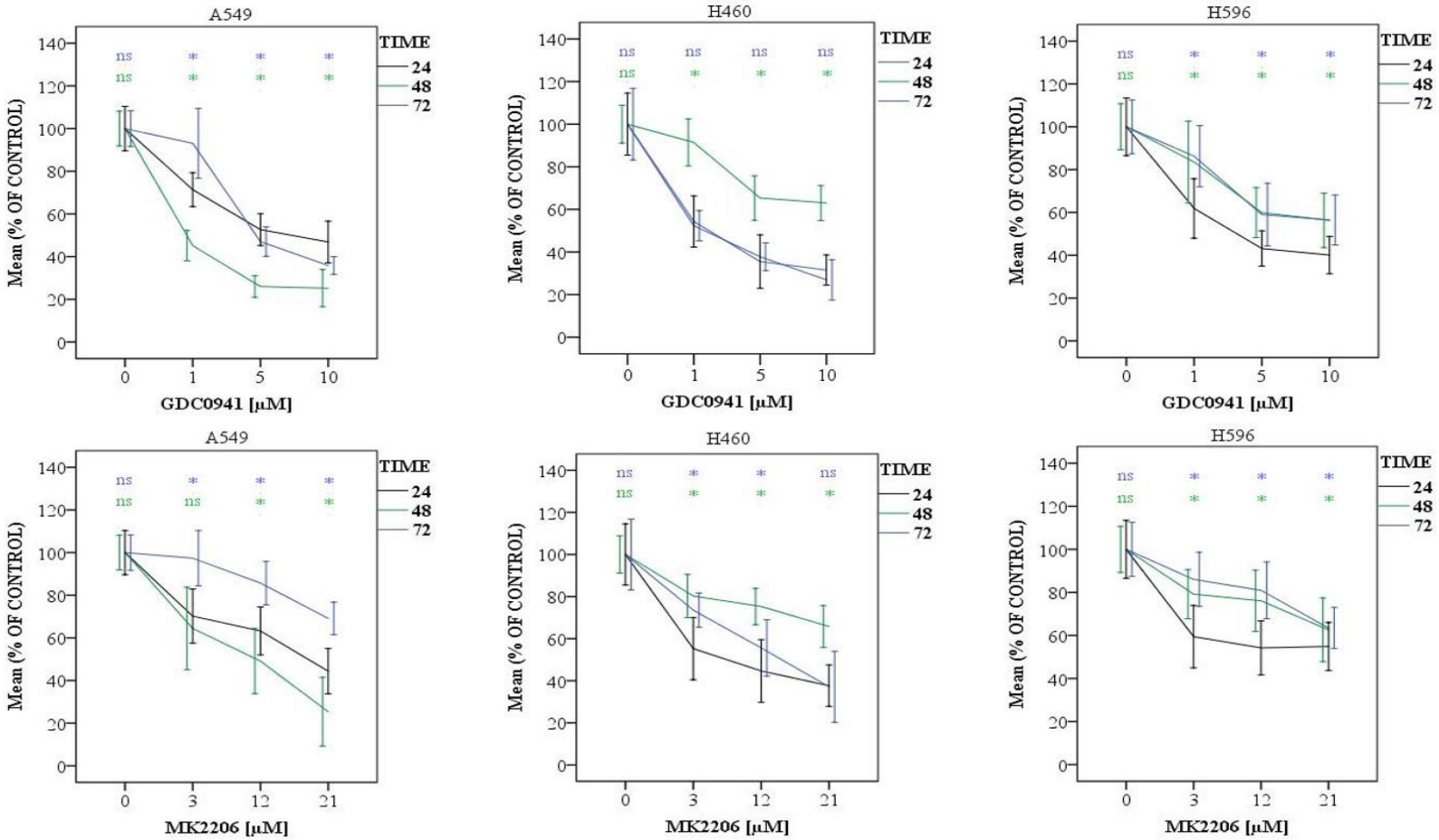

Figure 3. 4 GDC-0941 and MK-2206 treatments on A549, H460 and H596 cell lines at 24 (black line), 48 (green) and 72 (blue) hr.

The doses used for GDC-0941 are 1, 5 and 10 µM and for MK-2206 are 3, 12 and 21 µM. The control group is expressed as zero. Data were analyzed by univariate ANOVA (SPSS) and results are shown as M ± SD of over 19 replicates and '*' means P<0.05 and 'ns' means non-significant. The significant symbols stand for 24 vs 48 hr (shown in green) and 24 vs 72 hr (shown in blue).

Table 3. 4 The comparison of different concentrations of GDC-0941 and MK-2206 treatments and dose selection at 24 and 72 hr for A549, H460 and H596 cell lines Data were analyzed by one-way ANOVA (SPSS) and results are shown as M ± SD of over 19 replicates and '*' means P<0.05 and 'ns' means non-significant. The highlighted doses are selected for combination treatments at 24 or 72 hr.

A549											
Drugs	Doses (μM)	Time-point (hr)	M	SD	N	Drugs	Doses (μM)	Time-point (hr)	M	SD	N
GDC-0941	0	24	100	10	21	GDC-0941	0	72	100	8	21
	1		71*	8	20		1		93	16	21
	5		53*	7	21		5		47*	7	20
	10		47*	10	21		10		36*	4	21
MK-2206	0	24	100	10	21	MK-2206	0	72	100	8	21
	3		70*	13	20		3		97	13	21
	12		63*	11	21		12		86*	10	21
	21		44*	11	21		21		69*	8	21
H460											
Drugs	Doses (μM)	Time-point (hr)	M	SD	N	Drugs	Doses (μM)	Time-point (hr)	M	SD	N
GDC-0941	0	24	100	15	19	GDC-0941	0	72	100	17	19
	1		54*	12	21		1		52*	7	20
	5		36*	12	21		5		38*	7	19
	10		32*	7	21		10		27*	9	20
MK-2206	0	24	100	15	19	MK-2206	0	72	100	17	19
	3		55*	15	21		3		74*	8	19
	12		45*	15	21		12		56*	13	19
	21		38*	10	21		21		37*	17	19
H596											
Drugs	Doses (μM)	Time-point (hr)	M	SD	N	Drugs	Doses (μM)	Time-point (hr)	M	SD	N
GDC-0941	0	24	100	13	21	GDC-0941	0	72	100	13	21
	1		62*	14	20		1		86*	14	20
	5		43*	8	20		5		59*	15	20
	10		40*	9	21		10		56*	12	20
MK-2206	0	24	100	13	21	MK-2206	0	72	100	13	21
	3		59*	14	20		3		86*	13	21
	12		54*	13	21		12		81*	13	20
	21		55*	11	21		21		63*	10	20

3.2.5. AZD6244 TREATMENT

The MEK inhibitor showed little effect on A549 cells following a 24-hr treatment, but effects were enhanced over time. A significant decrease in cell viability was observed from 10 μM (all time points), with viability decreasing to 57% of control at the highest dose (100 μM) at 72 hr (Figure 3.5 and Table 3.5).

For AZD6244 on H460s, a time-dependent effect was observed for the higher doses only (50 and 100 μM). Significant decreases in viability were observed from 10 μM at 48 and 72 hr (a maximal decrease of 28% at 72 hr), but there appeared to be little additional benefit from increasing the dose beyond this.

The response to AZD6244 was very similar for H596s as for H460s. The maximum decrease in cell viability was observed at 72 hr (31%), but this was observed at the lowest concentration of 10 μM, and did not change even when the dose was increased to 100 μM. Significant decreases in viability were observed from 10 μM at 48 (see appendix 7.1) and 72 hr.

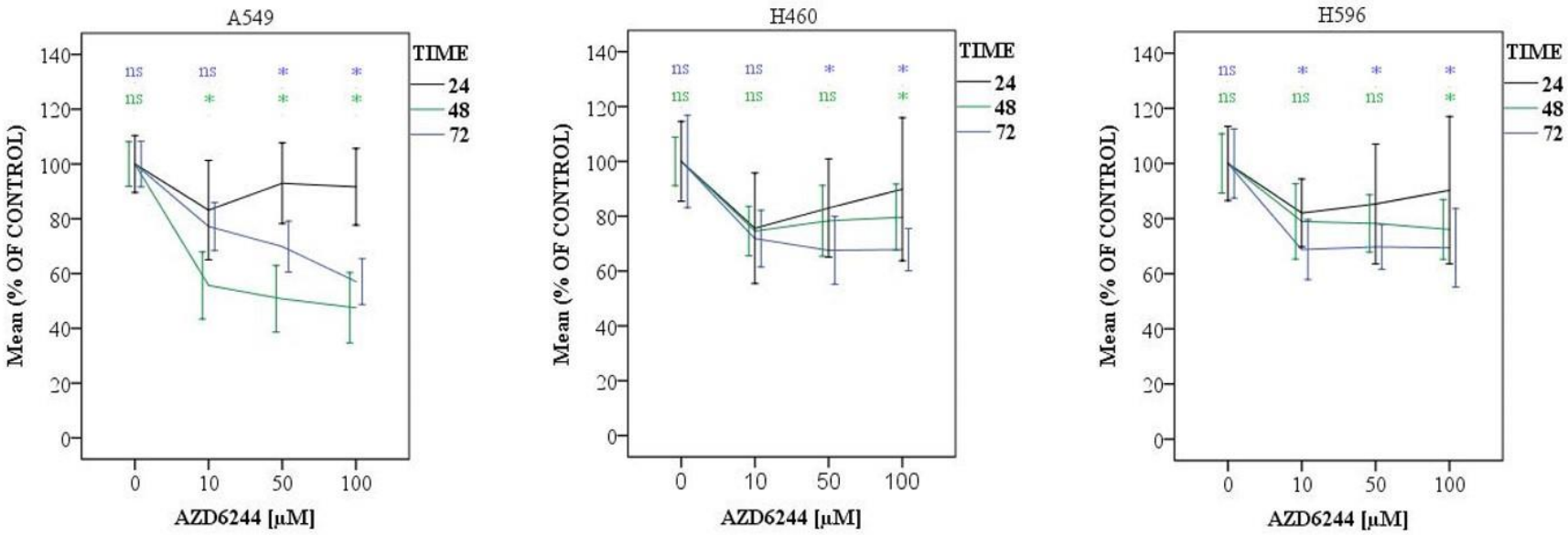

Figure 3. 5 AZD6244 treatment on A549, H460 and H596 cell lines at 24 (black line), 48 (green) and 72 (blue) hr.

The doses used for AZD6244 are 10, 50 and 100 µM and control group is expressed as zero. Data were analyzed by univariate ANOVA (SPSS) and results are shown as M ± SD of over 19 replicates and '*' means P<0.05 and 'ns' means non-significant. The significant symbols stand for 24 vs 48 hr (shown in green) and 24 vs 72 hr (shown in blue).

Table 3. 5 The comparison of different concentrations of AZD6244 treatments and dose selection at 24 and 72 hr for A549, H460 and H596 cell lines

Data were analyzed by one-way ANOVA (SPSS) and results are shown as M ± SD. of over 19 replicates and '*' means P<0.05 and 'ns' means non-significant. The highlighted doses are selected for combination treatments at 24 or 72 hr.

A549											
Drugs	Doses (μM)	Time-point (hr)	M	SD	N	Drugs	Doses (μM)	Time-point (hr)	M	SD	N
AZD6244	0	24	100	10	21	AZD6244	0	72	100	8	21
	10		83*	18	21		10		77*	9	21
	50		93	15	21		50		70*	9	21
	100		92	14	21		100		57*	8	21
H460											
Drugs	Doses (μM)	Time-point (hr)	M	SD	N	Drugs	Doses (μM)	Time-point (hr)	M	SD	N
AZD6244	0	24	100	15	19	AZD6244	0	72	100	17	19
	10		76*	20	21		10		72*	10	19
	50		83	18	20		50		68*	12	19
	100		90	26	21		100		68*	8	19
H596											
Drugs	Doses (μM)	Time-point (hr)	M	SD	N	Drugs	Doses (μM)	Time-point (hr)	M	SD	N
MK2206	21	24	55*	11	21	MK2206	21	72	63*	10	20
AZD6244	0	24	100	13	21	AZD6244	0	72	100	13	21
	10		82*	12	21		10		69*	11	20
	50		85	22	21		50		70*	8	20
	100		90	27	21		100		69*	14	20

To summarize, cisplatin treatment exhibited potency in a time- and dose dependent manner on nearly all cell lines, with H596 cells showing the greatest and A549 showing the least sensitivity. Similarly to cisplatin treatment, HSP90 inhibition (STA-9090) reduced viability in all cell lines, which was enhanced at the longer incubation times and higher doses of the drug. All cell types were similarly sensitive to STA-9090 treatment. For TBK1 inhibition, DMX503433-09 appeared to be more active in reduction of viability than did DMX502320-04. Both H460 and H596 cells were refractory to DMX502320-04 with the maximal and significant inhibition observed at the highest dose across all time points. DMX503433-09 had a similar effect on A549s as did DMX502320-04; for H460, the shorter incubation with either TBK1/IKKε inhibitor was more active in reduction of cell viability than was the longer one; for H596, only the 48-hr treatment with TBK1/IKKε inhibition had a time- and dose-dependent effect on reduction of viability compared to the 24-hr treatment. PI3K and Akt inhibitions were similarly active to reduce cell viability of all types of cells at shorter incubation times, amongst which H460s were more sensitive than the other two cells in response to these two treatments at 24 and 72 hr. Lastly, all cell lines were insensitive to AZD6244 treatment and only A549 cells saw a time- and dose dependent effect with this treatment whereas the other two cell lines were refractory to MEK inhibition across all time points, with the lowest dose appearing to be more active than the highest dose.

The data for single drug treatments across the cell lines can be broadly summarized (averaged from all time point effects) with respect to drug sensitivity:

Order of sensitivity for cisplatin: H596>H460>A549.

Order of sensitivity for STA-9090: H460>H596>A549

Order of sensitivity for DMX502320-04: A549≥H596≥H460.

Order of sensitivity for DMX503433-09: A549>H596>H460.

Order of sensitivity for GDC-0941: H460>A549≥H596

Order of sensitivity for MK-2206: H460>H596≥A549.

Order of sensitivity for AZD6244: A549>H596=H460.

3.2.6. RATIONALISING DOSE SELECTION FOR COMBINATION TREATMENTS

From the previous section, not only were dose- and time-dependant effects observed, but these effects were often cell-line specific. For example, the 72-hr treatment with cisplatin typically exhibited increasing potency when compared to earlier treatments, whereas the targeted agents generally displayed equivocal activities or were more potent at 24 hr. In light of this, future experiments with combinations would be tested at 24 and 72 hr respectively.

Selection of dose was based on the effect on cell viability reduction by each drug. As we wished to be able to determine whether the drugs could have an additive or greater-than-additive effect when in combination with cisplatin, it was important to choose a dose for each drug at which cell viability was decreased by less than 30% in each cell line at the selected time points. All dose selections are highlighted in Tables 3.1, 3.2, 3.3, 3.4 and 3.5 for each cell line, and are as follows:

- Cisplatin Treatment

Cisplatin doses for 24-hr treatment on both A549 and H460 cell lines covered the entire range from 1 – 20 μM, and for H596, only 1 μM was selected; for 72 hr treatments, A549 cell line doses covered the entire range from 1 – 20 μM and for both H460 and H596 cell lines only 1 μM was selected.

- STA-9090 Treatment

STA-9090 was used at 0.002 and 0.02 μM for all cell lines at 24 and 72 h.

- DMX502320-04 and DMX503433-09 Treatments

DMX502320-04 was used at 0.3, 0.6 and 1 μM for all cell lines at 24 hr and for H460 and H596 at 72 hr. For A549, 0.3 and 0.6 μM of DMX502320-04 were used at 72 hr. DMX503433-09 was used at 0.3, 0.6 and 1 μM for A549 and H460 at 24 hr and for H596, only the first two doses were used at 24 hr. For 72 hr treatments, A549 cells were the most sensitive with only 0.3, 0.6 selected, followed by H460 with 0.3, 0.6 and 1 μM selected and H596 showed the least sensitivity with all four doses selected.

- GDC-0941and MK22-06 Treatments

GDC-0941 was used at 1 µM only for all cell lines at 24 and 72 hr. The doses selected for MK-2206 included 3 µM for all cell lines at 24 hr and for H460 at 72 hr, 12 µM for A549 and H596 at 72 hr and lastly 21 µM for A549 at 72 hr.

- AZD6244 Treatment

AZD6244 was used at 10, 50 and 100 µM for all cell lines at 24 hr and for H460 and H596 cell lines at 72 hr. For A549, only the first two doses were selected for 72 hr.

3.3. POTENCIES OF CISPLATIN-BASED DOUBLETS

3.3.1. CISPLATIN-STA-9090 COMBINATION TREATMENTS

As reviewed in 3.2.6, the doses of cisplatin and STA-9090 used for combinations at 24 and 72 hr are shown below:

Doses	A549		H460		H596	
	24 hr	72 hr	24 hr	72 hr	24 hr	72hr
Cisplatin (µM)	1-20	1-20	1-20	1	1	1
STA-9090 (µM)	0.002-0.02	0.002-0.02	0.002-0.02	0.002-0.02	0.002-0.02	0.002-0.02

3.3.3.1. A549 Treatment

For single cisplatin treatments (Table 3.6), both 24 hr- and 72 hr-treatments saw a significant ($P<0.05$) reduction in cell viability of A549 cells compared to control, decreasing from 10-20% at 5 µM to up to 30-40% at 20 µM cisplatin. Single STA-9090 treatment at 24 hr seemed to be potent than that at 72 hr with both doses significantly decreasing the viability up to 25% compared to control. The combination of cisplatin with STA-9090 at 24 and 72 hr was more active to affect the viability than those single agents, particularly at 0.02 µM STA-9090-containing combination groups, in which the combination of 20 µM cisplatin with STA-9090 decreased the viability by up to 80% at 72 hr. The combination index (CI) analysis (CI>1 antagonism, CI=1 summation, CI<1 synergism) for combination effects between cisplatin and STA-9090 showed that 72 hr treatment with all cisplatin-STA-9090 combination groups were more synergistic (CI<0.5)

particularly at higher doses of cisplatin (10 and 20 µM)-containing combination groups, although 0.02 µM STA-9090-cisplatin (1 µM) combination group was synergistic (CI=0.07) as much as those high concentrations of cisplatin-STA-9090 combination treatments. In contrast, the combination treatments at 24 hr were less synergistic (CI>0.5) with the combination of 1 µM cisplatin with 0.02 µM STA-9090 having the maximal synergism with a CI of 0.40. Therefore, 1µM cisplatin combined with 0.02 µM STA-9090 seems to be the optimal combination regimen for generating the maximal synergism.

As for the comparison of cisplatin treatment with cisplatin-STA-9090 combination treatment (Figure 3.6), 0.02 µM STA-9090-containing combination treatments at 24 and 72 hr were more potent to reduce the viability compared to cisplatin single treatments, and 72 hr treatments were more active to affect the viability than the 24 hr treatments, with the biggest difference in the reduction of viability (37%) at 20 µM cisplatin combined with 0.02 µM STA-9090, significantly different from that of cisplatin treatment. Whereas 1 µM cisplatin combined with 0.02 µM also significantly reduced the viability by 30% compared to cisplatin treatment. Therefore, the 1 µM cisplatin combined with 0.02 µM STA-9090 at 72 hr will be the selected regimen for testing cisplatin-STA-9090 on A549 in further experiments.

Table 3. 6 Comparison of control vs each treatment and CI analysis for A549 treated with cisplatin-STA-9090 combination at 24 and 72 hr

The significant reduction in the viability (M ± SD) between control and treatment group at 24 and 72 hr was analyzed by one-way ANOVA (prism) and is labelled with '*', which means P<0.05. The CI value for each single dose combination at 24 or 72 hr was analyzed by CompuSyn software. Those combination groups at 24 or 72 hr showing synergic effects (CI<1) are highlighted. Fa means fraction affected by dose.

	Cisplatin-STA-9090-24 hr																																	
Doses (μM)	Control-0			STA-9090-0.002			STA-9090-0.02			Cisplatin-1			1+0.002			1+0.02			Cisplatin-5			5+0.002			5+0.02			Cisplatin dose (μM)	STA-9090 dose (μM)	Combination Fa values	CI value
	M	SD	N	M	SD	N	M	SD	N	M	SD	N	M	SD	N	M	SD	N	M	SD	N	M	SD	N	M	SD	M				
Relative viability (% of control)	100	13	59	89*	16	56	75*	19	59	109	11	21	95	16	23	70*	19	24	73*	14	25	76*	17	30	67*	17	29	1	0.002	0.05	0.90
																												1	0.02	0.3	0.40
																												5	0.002	0.24	0.61
																												5	0.02	0.33	0.67
Doses (μM)	Cisplatin-10			10+0.002			10+0.02			Cisplatin-20			20+0.002			20+0.02												10	0.002	0.23	1.22
	M	SD	N	M	SD	N	M	SD	N	M	SD	N	M	SD	N	M	SD	N										10	0.02	0.42	0.78
Relative viability (% of control)	75*	11	19	77*	18	24	58*	15	21	61*	18	24	52*	20	23	57*	23	23										20	0.002	0.48	1.05
																												20	0.02	0.43	1.35
	Cisplatin-STA-9090-72 hr																											Cisplatin dose (μM)	STA-9090 dose (μM)	Combination Fa values	CI value
Doses (μM)	Control-0			STA-9090-0.002			STA-9090-0.02			Cisplatin-1			1+0.002			1+0.02			Cisplatin-5			5+0.002			5+0.02						
	M	SD	N	M	SD	N	M	SD	N	M	SD	N	M	SD	N	M	SD	N	M	SD	N	M	SD	N	M	SD	M				
Relative viability (% of control)	100	6	48	97	10	29	85*	9	34	91	13	18	98	10	18	61*	13	18	82*	9	18	84*	18	18	50*	10	18	1	0.002	0.02	2.32
																												1	0.02	0.39	0.07
																												5	0.002	0.16	1.89
																												5	0.02	0.50	0.19
Doses (μM)	Cisplatin-10			10+0.002			10+0.02			Cisplatin-20			20+0.002			20+0.02												10	0.002	0.53	0.32
	M	SD	N	M	SD	N	M	SD	N	M	SD	N	M	SD	N	M	SD	N										10	0.02	0.74	0.09
Relative viability (% of control)	60*	20	17	47*	12	18	26*	6	18	57*	16	18	36*	9	18	20*	6	18										20	0.002	0.64	0.34
																												20	0.02	0.80	0.11

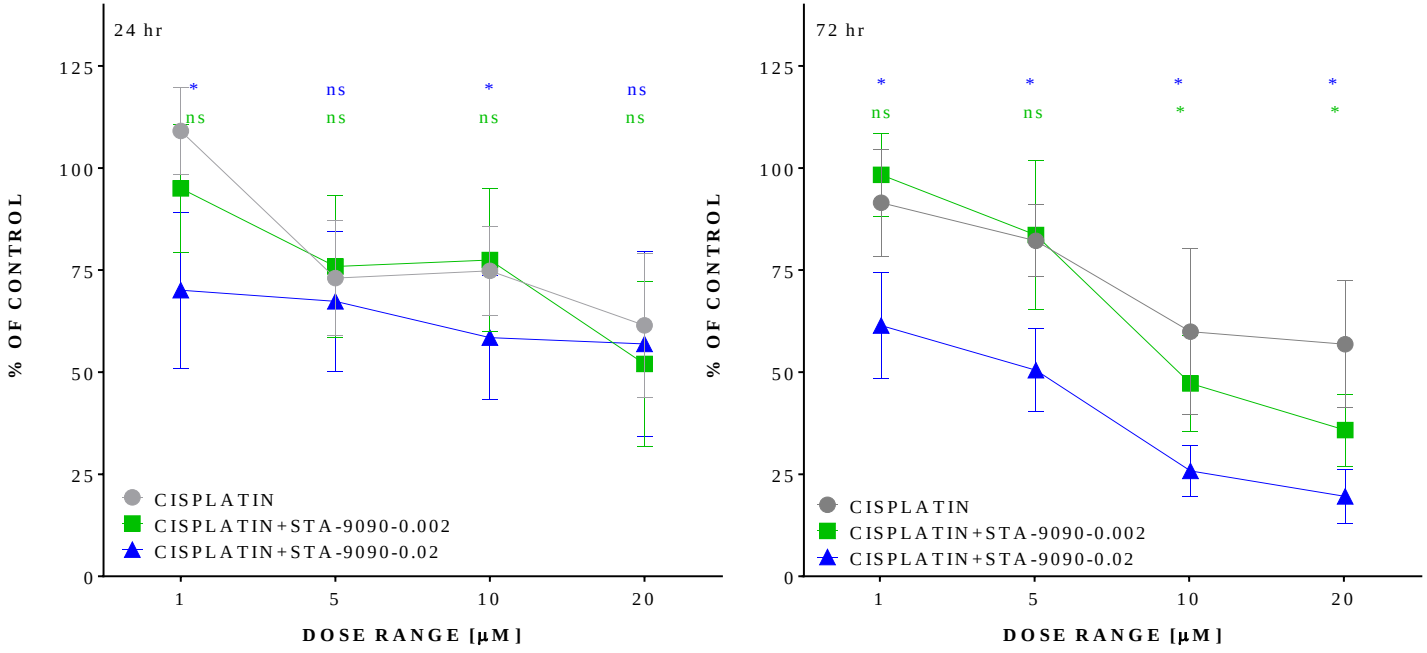

Figure 3. 6 Comparison of cisplatin (1-20 µM) and various cisplatin-STA-9090 combination treatments on A549 at 24 and 72 hr

Data were analyzed by two-way ANOVA by prism and results are shown as M ± SD with N over 18. '*' means P<0.05 and 'ns' means non-significant. The significance for cisplatin treatments (1-20) compared with 0.002 µM STA-9090-based combination treatments is shown in green and the significant comparison of cisplatin with 0.02 µM STA-9090-cisplatin combination treatments is shown in blue.

3.3.3.2. H460 Treatment

Similarly as A549 cells at 24 hr, H460 cells showed a significant reduction in cell viability compared to control when the dose of cisplatin increased from 5 to 20 µM. The maximal reduction in the viability compared to control at 24 hr was observed at 5 µM cisplatin with viability decreased by 44%. Similarly shown in CI analysis, all 5 µM cisplatin-containing groups showed a higher synergistic effect compared to the rest of cisplatin-STA-9090 combination treatments with a median CI of 0.07. The combination of 1 µM cisplatin with 0.02 µM STA-9090 also showed a high level of synergistic effect with CI decreasing to 0.01 (Table 3.7).

For 72-hr treatment, H460 was demonstrated to be sensitive to cisplatin treatments at the singlet treatment experiments (reviewed in 3.2.1) and hence only 1 µM cisplatin was selected for combination treatments on H460 at 72 hr, which is not appropriate to analyze CI with only one dose selected for cisplatin treatment. The 72-hr treatment had a reduction in viability by up to approximately 60% at 1 µM cisplatin combined with 0.02 µM STA-9090, which was significantly different from that of control group. Moreover, the difference in viability between 1 µM cisplatin and 1 µM cisplatin combined with 0.02 µM STA-9090 was significant at 39% (Figure 3.7). Therefore, the 1 µM cisplatin-STA-9090 (1 µM) combination was also selected for H460 at 72 hr.

Table 3. 7 Comparison of control vs each treatment and CI analysis for H460 treated with cisplatin-STA-9090 combination at 24 and 72 hr.

The significant reduction in the viability (M ± SD) between control and treatment group at 24 and 72 hr was analyzed by one-way ANOVA (prism) and is labelled with '*', which means P<0.05. The CI value for each single dose combination at 24 hr was analyzed by CompuSyn software. Those combination groups at 24 hr showing synergic effects (CI<1) are highlighted.

	Cisplatin-STA-9090-24 hr																										
Doses (μM)	Control-0			STA-9090-0.002			STA-9090-0.02			Cisplatin-1			1+0.002			1+0.02			Cisplatin-5			5+0.002			5+0.02		
	M	SD	N	M	SD	N	M	SD	N	M	SD	N	M	SD	N	M	SD	N	M	SD	N	M	SD	N	M	SD	M
Relative viability (% of control)	100	15	36	81*	21	36	77*	10	36	76*	13	18	70*	13	18	63*	10	18	56*	14	18	65*	14	18	58*	11	18
Doses (μM)	Cisplatin-10			10+0.002			10+0.02			Cisplatin-20			20+0.002			20+0.02											
	M	SD	N	M	SD	N	M	SD	N	M	SD	N	M	SD	N	M	SD	N									
Relative viability (% of control)	66*	9	18	81*	15	18	71*	5	18	73*	14	18	83*	26	18	66*	13	18									

Cisplatin dose (μM)	STA-9090 dose (μM)	Fa values	CI value
1	0.002	0.30	0.54
1	0.02	0.37	0.01
5	0.002	0.35	0.13
5	0.02	0.41	0.005
10	0.002	0.19	15036.0
10	0.02	0.29	10.21
20	0.002	0.17	179182
20	0.02	0.34	0.96

	Cisplatin-STA-9090-72 hr																	
Doses (μM)	Control-0			STA-9090-0.002			STA-9090-0.02			Cisplatin-1			1+0.002			1+0.02		
	M	SD	N	M	SD	N	M	SD	N	M	SD	N	M	SD	N	M	SD	N
Relative viability (% of control)	100	11	18	88	13	18	48*	20	18	78*	15	18	69*	19	18	39*	17	18

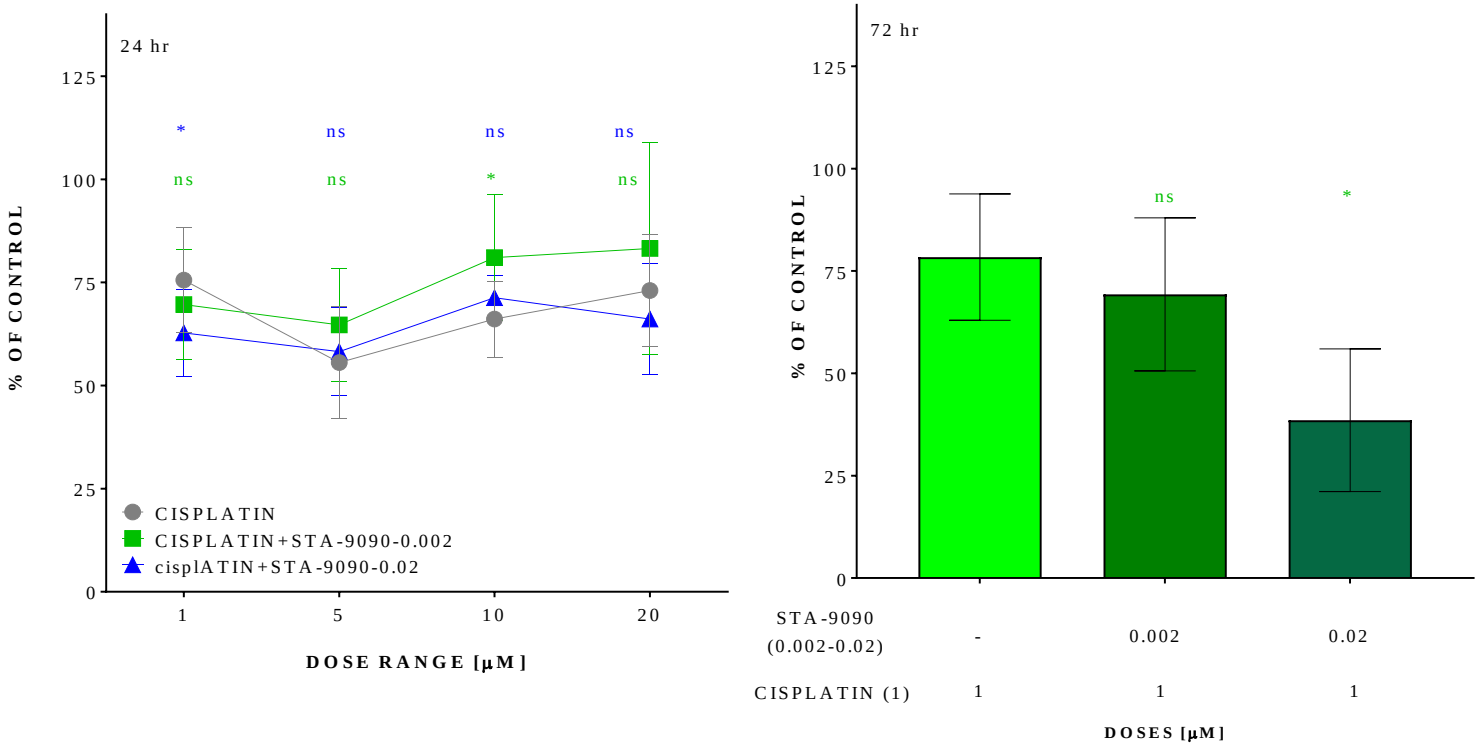

Figure 3. 7 Comparison of cisplatin and various cisplatin-STA-9090 combination treatments on H460 at 24 and 72 hr

Data were analyzed by two-way (24 hr) or one-way (72 hr) ANOVA by prism and results are shown as M ± SD with N over 18. '*' means P<0.05 and 'ns' means non-significant. For 24 hr-treatment, the significance for cisplatin treatments (1-20) compared with 0.002 µM STA-9090-based combination treatments is shown in green and that for cisplatin vs 0.02 µM STA-9090-cisplatin combination in blue. Whereas the 72 hr treatment only contain comparison of 1 µM cisplatin with all cisplatin-STA-9090 combination treatments, which is shown in green.

3.3.3.3. H596 Treatment

Similarly to H460 cells, H596 showed the most sensitivity to cisplatin treatments at both 24 and 72 hr (reviewed in 3.2.1) compared to A549 and H460, and only 1 µM cisplatin had been selected for testing cisplatin-based combination treatments on H596.

The cisplatin-STA-9090 combination treatments were less potent on H596 compared to the other two cell lines. The biggest decrease in cell viability compared to control group by any treatment was observed at 0.02 µM STA-9090 alone (39% decrease) (Figure 3.8). As for the comparison of cisplatin with cisplatin-STA-9090 combination treatments, 72 hr-treatments were more potent with the viability decreasing by up to 28% at 1 µM cisplatin combined with 0.02 µM STA-9090, which was significantly different from single cisplatin treatment. In contrast, none of cisplatin-STA-9090 combination treatments at 24 hr significantly decreased the viability compared to single cisplatin treatment. Therefore, the combination of cisplatin with STA-9090 would not be selected in further experiments for H596.

In summary, both A549 and H460 cell lines would be treated with 1 µM cisplatin combined with 0.02 µM STA-9090 at 72 hr in further experiments.

	Cisplatin-STA-9090-24 hr																	
Doses (µM)	Control-0			STA-9090-0.002			STA-9090-0.02			Cisplatin-1			1+0.002			1+0.02		
	M	SD	N	M	SD	N	M	SD	N	M	SD	N	M	SD	N	M	SD	N
Relative viability (% of control)	100	9	18	83*	13	18	61*	11	18	77*	12	18	78*	16	18	65*	21	18

	Cisplatin-STA-9090-72 hr																	
Doses (µM)	Control-0			STA-9090-0.002			STA-9090-0.02			Cisplatin-1			1+0.002			1+0.02		
	M	SD	N	M	SD	N	M	SD	N	M	SD	N	M	SD	N	M	SD	N
Relative viability (% of control)	100	6	24	101	15	24	81*	21	24	96	7	24	78*	23	24	68*	18	24

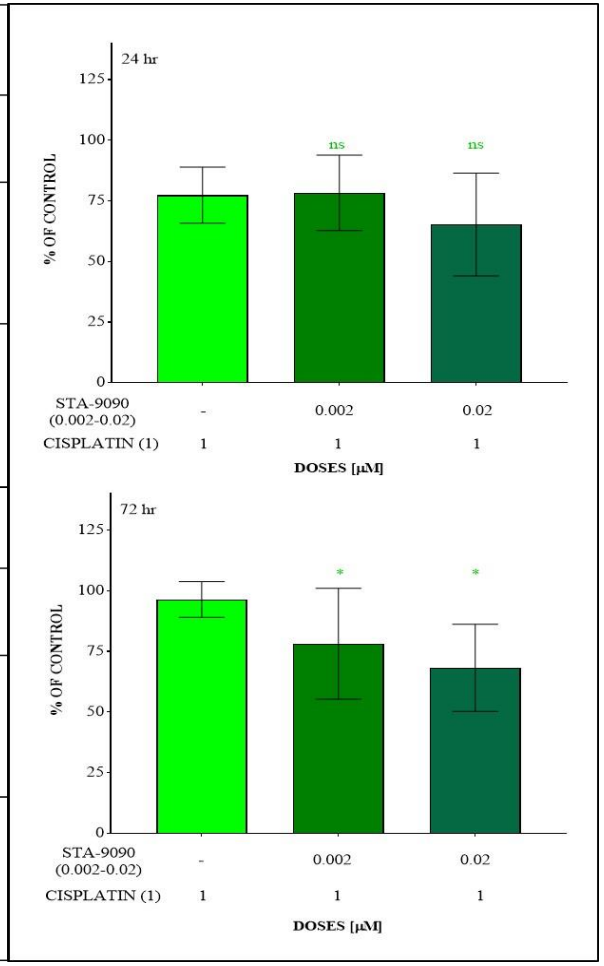

Figure 3. 8 The cisplatin-STA-9090 combinations on H596 at 24 and 72 hr

The table above compares each treatment vs control group at 24 and 72 hr and the significance is labelled with '*', which means P<0.05. The significant comparison is shown in green and '*' means P<0.05 and ns denotes non-significant. The figure shows the comparison of 1 µM cisplatin treatment with 0.002 or 0.02 µM STA-9090-cisplatin combination treatment at 24 and 72 hr. Data were analyzed by one-way ANOVA by prism and the results are shown as M ± SD with N over 18.

3.3.2. CISPLATIN- DMX502320-04 COMBINATION THERAPY

As reviewed in 3.2.6, the doses of cisplatin and DMX502320-04 used for combinations at 24 and 72 hr are shown below:

Doses	A549		H460		H596	
	24 hr	72 hr	24 hr	72 hr	24 hr	72hr
Cisplatin (µM)	1-20	1-20	1-20	1	1	1
DMX502320 -04 (µM)	0.3-1	0.3-0.6	03-1	0.3-1	0.3-1	0.3-1

3.3.2.1. A549 Treatment

Single DMX502320-04 treatments were more active to reduce the cell viability of A549 cells at 24 than 72 hr, with cell viability significantly decreased by up to 29% at 1 µM DMX502320-04 compared to control group. Single treatments with cisplatin appeared to be more active at 72 hr with the maximal significant reduction in viability by up to 79% at 20 µM cisplatin. The cisplatin-DMX502320-04 combination treatments were more active to reduce the viability than those single treatments and all showed a significant reduction in the viability compared to control group (Table 3.8). The combination treatments at 72 hr emerged to be more active than those at 24 hr with a reduction in viability by up to 90% at 20 µM cisplatin combined with 0.6 µM DMX502320-04. The CI analysis showed that all 1 µM cisplatin-containing combination treatments at 24 and 72 hr showed a synergistic effect compared to the rest of cisplatin-DMX502320-04 combination treatments with the minimal decrease in CI by up to 0.33 at 1 µM cisplatin combined with 0.6 µM DMX502320-04 at 72 hr. However, the difference in viability between 1 µM cisplatin and 1 µM cisplatin combined with 0.6 µM DMX502320-04 at 72 hr was only 19% significantly (Figure 3.9). By comparison, 1 µM cisplatin combined with 1 µM DMX502320-04 at 24 hr significantly decreased the viability by 40% compared to cisplatin treatment and showed a synergistic effect with CI of 0.69. Therefore, 1 µM cisplatin combined with 1 µM DMX502320-04 would be selected for A549 at 24 hr.

Table 3. 8 Comparison of control vs each treatment and CI analysis for A549 treated with cisplatin-DMX502320-04 combination at 24 and 72 hr

The significant reduction in the viability (M ± SD) between control and treatment group at 24 and 72 hr was analyzed by one-way ANOVA (prism) and is labelled with '*', which means P<0.05. The CI value for each single dose combination at 24 or 72 hr was analyzed by CompuSyn software. Those combination groups at 24 or 72 hr showing synergic effects (CI<1) are highlighted.

	Cisplatin-DMX502320-04-24 hr																							
Doses (μM)	Control-0			DMX502320-04-0.3			DMX502320-04-0.6			DMX502320-04-1			Cisplatin-1			1+0.3			1+0.6			1+1		
	M	SD	N	M	SD	N	M	SD	N	M	SD	N	M	SD	N	M	SD	N	M	SD	N	M	SD	N
Relative viability (% of control)	100	11	60	93	16	59	85*	19	59	71*	18	59	99	19	18	80*	12	18	81*	19	15	59*	17	17
Doses (μM)	Cisplatin-5			5+0.3			5+0.6			5+1			Cisplatin-10			10+0.3			10+0.6			10+1		
	M	SD	N	M	SD	N	M	SD	N	M	SD	N	M	SD	N	M	SD	N	M	SD	N	M	SD	N
Relative viability (% of control)	83*	14	18	72*	13	18	78*	19	18	59*	17	18	85*	15	18	73*	19	18	73*	23	18	62*	12	17
Doses (μM)	Cisplatin-20			20+0.3			20+0.6			20+1														
	M	SD	N	M	SD	N	M	SD	N	M	SD	N												
Relative viability (% of control)	79*	20*	18*	61*	14	17	62*	22	18	58*	20	18												

Cisplatin dose (μM)	DMX502320-04 dose (μM)	Combination Fa values	CI value
1	0.3	0.2	0.49
1	0.6	0.19	0.94
1	1	0.41	0.69
5	0.3	0.28	0.56
5	0.6	0.22	1.10
5	1	0.41	0.81
10	0.3	0.27	0.85
10	0.6	.0.27	1.16
10	1	0.38	1.06
20	0.3	0.39	0.87
20	0.6	0.38	1.12
20	1	0.42	1.23

	Cisplatin-DMX502320-04-72 hr																										
Doses (μM)	Control-0			DMX502320-04-0.3			DMX502320-04-0.6			Cisplatin-1			1+0.3			1+0.6			Cisplatin-5			5+0.3			5+0.6		
	M	SD	N	M	SD	N	M	SD	N	M	SD	N	M	SD	N	M	SD	N	M	SD	N	M	SD	N	M	SD	N
Relative viability (% of control)	100	8	60	97	16	60	95	20	60	95	10	24	87*	10	24	76*	10	24	79*	9	18	78*	9	18	72*	15	18
Doses (μM)	Cisplatin-10			10+0.3			10+0.6			Cisplatin-20			20+0.3			20+0.6											
	M	SD	N	M	SD	N	M	SD	N	M	SD	N	M	SD	N	M	SD	N									
Relative viability (% of control)	56*	16	18	48*	20	18	45*	19	18	21*	19	18	11*	7	18	10*	6	18									

Cisplatin dose (μM)	DMX502320-04 dose (μM)	Combination Fa values	CI value
1	0.3	0.13	0.53
1	0.6	0.24	0.33
5	0.3	0.22	1.31
5	0.6	0.28	1.06
10	0.3	0.52	0.95
10	0.6	0.55	0.88
20	0.3	0.89	0.44
20	0.6	0.90	0.40

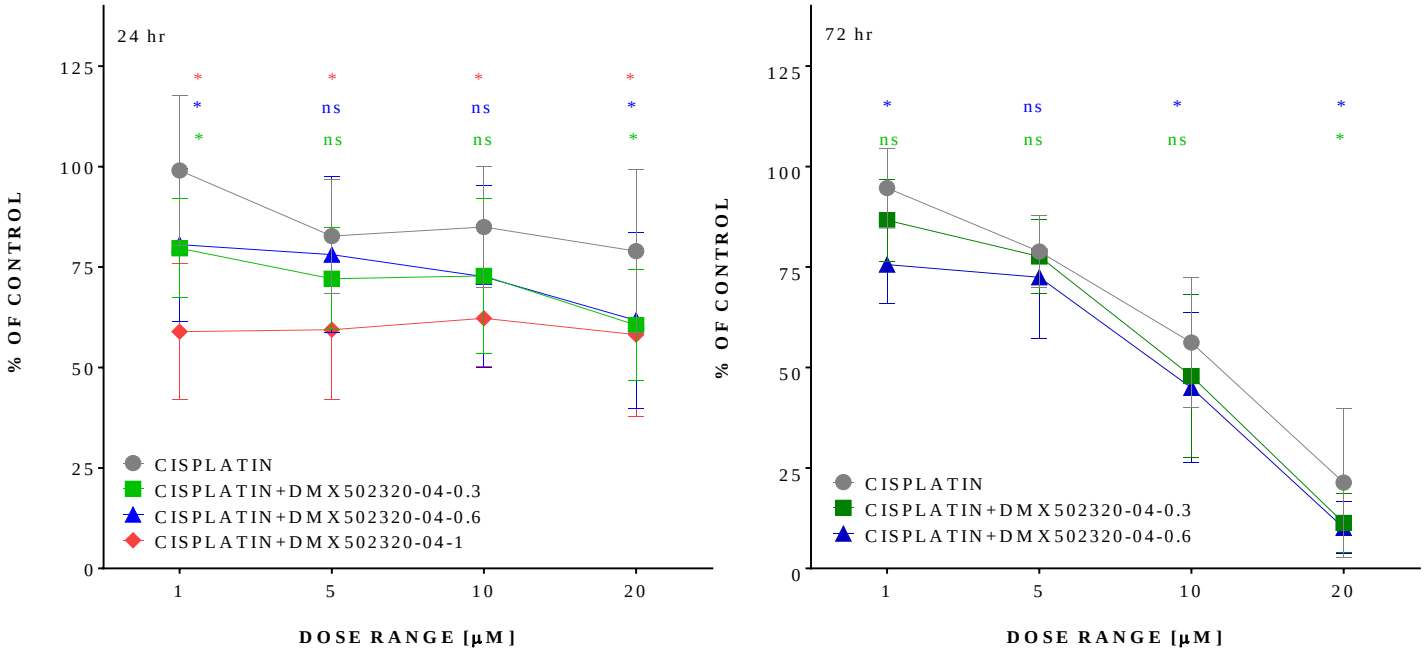

Figure 3. 9 Comparison of cisplatin (1-20 µM) treatments with cisplatin-DMX502320-04 combination treatments on A549 at 24 and 72 hr

Data were analyzed by two-way ANOVA by prism and results are shown as M ± SD with N over 18. '*' means P<0.05 and 'ns' means non-significant. The significance for cisplatin treatments (1-20) compared with 0.3 µM DMX502320-04-based combination treatments is shown in green and the significant comparison of cisplatin with 0.6 µM DMX502320-04-cisplatin combination treatments is shown in blue and lastly the red denotes the significant comparison between cisplatin and 1 µM DMX502320-4 containing combination treatments.

3.3.2.2. H460 Treatment

In contrast to A549 cells, H460 cells were not sensitive to the cisplatin-DMX502320-04 combination treatments with the maximal reduction in viability by up to 45% at 20 µM cisplatin combined with 0.3 µM DMX502320-04, which showed a synergistic effect with a CI value of 0.73. Similarly, the combination of 1 cisplatin combined with 0.3 DMX502320-04 showed a CI value of 0.72 that is synergistic (Table 3.9). As for the comparison of cisplatin treatments with cisplatin-DMX502320-04 combinations (Figure 3.10), the 1 or 20 µM cisplatin combined with 0.3 µM DMX502320-04 at 24 hr showed a slight significant decrease in the viability compared to cisplatin treatments with viability decreased by about 10%. By comparison, the combination of 1 µM cisplatin with 0.6 or 1 µM DMX502320-04 showed a significant reduction of viability by approximate 30% compared to cisplatin alone. Therefore, 0.6 and 1 µM DMX502320-04 would be selected for testing this cisplatin-based combination at 72 hr in the further experiments.

Table 3. 9 Comparison of control vs each treatment and CI analysis for H460 treated with cisplatin-DMX502320-04 combination at 24 and 72 hr

The significant reduction in the viability (M ± SD) between control and treatment group at 24 and 72 hr was analyzed by one-way ANOVA (prism) and is labelled with '*', which means P<0.05. The CI value for each single dose combination at 24 hr was analyzed by CompuSyn software. Those combination groups at 24 hr showing synergic effects (CI<1) are highlighted.

	Cisplatin-DMX502320-04-24 hr																							
Doses (μM)	Control-0			DMX502320-04-0.3			DMX502320-04-0.6			DMX502320-04-1			Cisplatin-1			1+0.3			1+0.6			1+1		
	M	SD	N	M	SD	N	M	SD	N	M	SD	N	M	SD	N	M	SD	N	M	SD	N	M	SD	N
Relative viability (% of control)	100	11	60	101	15	54	90*	13	51	77*	12	54	94	16	18	87*	12	18	89	14	13	80*	9	18
Doses (μM)	Cisplatin-5			5+0.3			5+0.6			5+1			Cisplatin-10			10+0.3			10+0.6			10+1		
	M	SD	N	M	SD	N	M	SD	N	M	SD	N	M	SD	N	M	SD	N	M	SD	N	M	SD	N
Relative viability (% of control)	80*	11	18	77*	14	18	75*	15	18	68*	13	18	78*	14	18	87*	10	18	83*	13	18	72*	10	18
Doses (μM)	Cisplatin-20			20+0.3			20+0.6			20+1														
	M	SD	N	M	SD	N	M	SD	N	M	SD	N												
Relative viability (% of control)	66*	8	18	55*	12	18	57*	15	18	61*	15	18												
	Cisplatin-DMX502320-04-72 hr																							
Doses (μM)	Control-0			DMX502320-04-0.3			DMX502320-04-0.6			DMX502320-04-1			Cisplatin-1			1+0.3			1+0.6			1+1		
	M	SD	N	M	SD	N	M	SD	N	M	SD	N	M	SD	N	M	SD	N	M	SD	N	M	SD	N
Relative viability (% of control)	100	12	18	106	20	18	102	20	18	98	27	18	106	33	18	78*	11	17	78*	9	18	72*	17	18

Cisplatin dose (μM)	DMX502320-04 dose (μM)	Combination Fa values	CI value
1	0.3	0.13	0.72
1	0.6	0.11	1.28
1	1	0.2	1.28
5	0.3	0.23	0.88
5	0.6	0.25	1.09
5	1	0.32	1.19
10	0.3	0.13	3.54
10	0.6	0.17	2.70
10	1	0.28	1.73
20	0.3	0.45	0.73
20	0.6	0.43	1.03
20	1	0.39	1.55

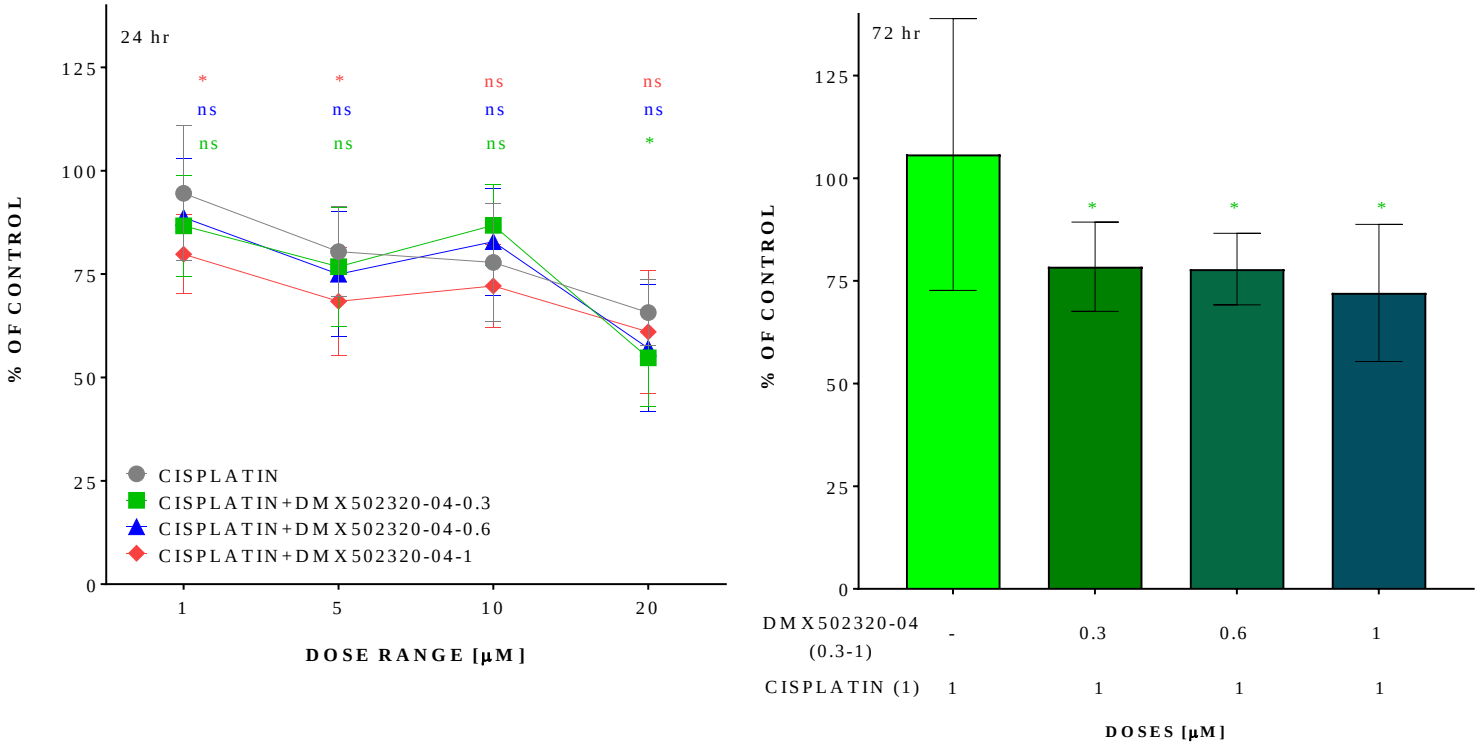

Figure 3. 10 Comparison of cisplatin and various cisplatin-DMX502320-04 combination treatments on H460 at 24 and 72 hr

For 24 hr-treatment, the significance for cisplatin treatments (1-20) compared with 0.3 µM DMX502320-04-based combination treatments is shown in green and that for cisplatin vs 0.6 µM DMX502320-04-cisplatin combination in blue and lastly red represent cisplatin vs 1 µM DMX502320-04-cisplatin combination treatments. Whereas the 72 hr treatment only contain comparison of 1 µM cisplatin with all cisplatin-DMX502320-04 combination treatments, which is shown in green. Data were analyzed by two-way (24 hr) or one-way (72 hr) ANOVA by prism and results are shown as M ± SD with N over 18. '*' means P<0.05 and 'ns' means non-significant.

3.3.2.3. H596 Treatment

In contrast to the cell lines above, this cisplatin-based combination treatment was shown less potent on H596 cell line with the maximal decrease in the viability by 35% at 1 µM cisplatin combined with 0.6 µM DMX502320-04 at 72 hr (Figure 3.11). Moreover, there were no significant changes in the viability observed at the combination of cisplatin with DMX502320-04 at 24 hr when compared to cisplatin alone. Although the difference between combination treatments and cisplatin single treatments was significant across all cisplatin-DMX502320-04 combination treatments at 72 hr, the maximal reduction in viability compared to cisplatin treatment was only 18%. Therefore, DMX502320-04 would not be selected for testing cisplatin-based combination treatments on H596.

In summary, A549 will be treated with cisplatin-DMX502320-04 (1 µM dose for each drug) at 24 hr and H460 treated with 1 µM cisplatin combined with 0.6 and 1 µM DMX502320-04 at 72 hr.

	Cisplatin-DMX502320-04-24 hr																							
Doses (µM)	Control-0			DMX502320-04-0.3			DMX502320-04-0.6			DMX502320-04-1			Cisplatin-1			1+0.3			1+0.6			1+1		
	M	SD	N	M	SD	N	M	SD	N	M	SD	N	M	SD	N	M	SD	N	M	SD	N	M	SD	N
Relative viability (% of control)	103	11	18	97	14	18	82*	16	18	83*	17	18	85*	14	18	90	21	18	92	14	18	85*	13	18

	Cisplatin-DMX502320-04-72 hr																							
Doses (µM)	Control-0			DMX502320-04-0.3			DMX502320-04-0.6			DMX502320-04-1			Cisplatin-1			1+0.3			1+0.6			1+1		
	M	SD	N	M	SD	N	M	SD	N	M	SD	N	M	SD	N	M	SD	N	M	SD	N	M	SD	N
Relative viability (% of control)	100	9	18	94	12	18	85*	13	18	86*	10	18	83*	12	18	71*	14	18	65*	11	18	66*	12	18

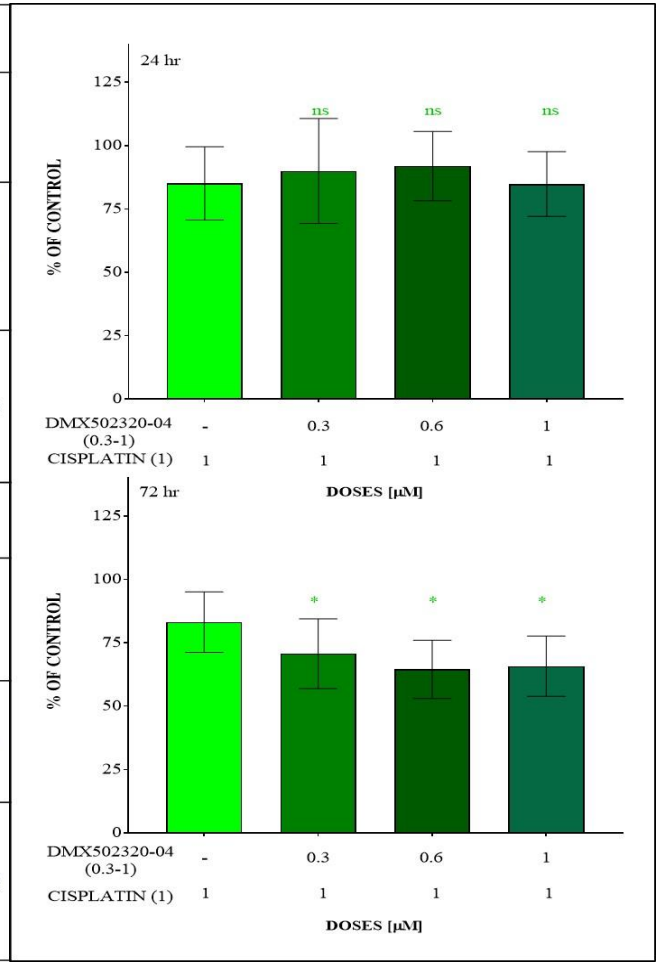

Figure 3. 11 The Cisplatin-DMX502320-04 combination treatments on H596 cell line at 24 and 72 hr

The table left compares each treatment vs control group at 24 and 72 hr and the significance is labelled with '*', which means P<0.05. The figures show the comparison of 1 µM cisplatin treatment with 0.3, 0.6 or 1 µM DMX502320-04-cisplatin combination treatment at 24 and 72 hr. Data were analyzed by one-way ANOVA by prism and results are shown as M ± SD with N over 18. The significant comparison is shown in green and '*' means P<0.05 and 'ns' denotes non-significant.

3.3.3. CISPLATIN- DMX503433-09 COMBINATION THERAPY

As reviewed in 3.2.6, the doses of cisplatin and DMX503433-09 used for combinations at 24 and 72 hr are shown below:

Doses	A549		H460		H596	
	24 hr	72 hr	24 hr	72 hr	24 hr	72hr
Cisplatin (µM)	1-20	1-20	1-20	1	1	1
DMX503433 -09 (µM)	0.3-1	0.3-0.6	0.3-1	0.3-10	0.3-0.6	0.3-1

3.3.3.1. A549 Treatment

Similarly as DMX502320-04 at 24 hr, DMX503433-09 single treatments also showed a significant reduction in cell viability at 24 hr compared to control group, with viability decreasing up to 34% at 1 µM DMX503433-09. The combination of cisplatin with DMX503433-09 further enhanced the potency of single cisplatin and DMX503433-09 treatments, with viability significantly dropping to up to 76% at 20 µM cisplatin combined with 0.6 µM DMX503433-09 at 72 hr. The combination treatments were less potent at 24 hr, with a maximal reduction in the viability by approximately 52% at 20 µM cisplatin combined with 1 µM DMX503433-09. Whereas the combination effects analysis showed that the combination of cisplatin with DMX503433-09 was more synergistic at 24 hr than at 72 hr, with a minimal CI value of 0.42 at 1 µM cisplatin combined with 0.3 µM DMX503433-09. Similarly, this combination at 72 hr also a synergistic effect with a CI value of 0.86 (Table 3.10). The rest of 1 µM cisplatin-combination treatments as well as all 20 µM cisplatin-containing combination treatments all showed a synergistic effect at 24 hr, with CI ranging from 0.4 to 0.8.

To compare the potency of cisplatin-DMX503433-09 combination with cisplatin alone, the Figure 3.12 showed that 24 hr-treatment with the doublet emerged to be more potent in significantly reducing the viability compared to cisplatin treatment, with a maximal alteration in viability of 35% at 1 µM cisplatin combined with 0.6 or 1 µM DMX503433-09. In contrast, the rest of cisplatin-DMX503433-09 combination treatments at 24 hr showed a less potency with the viability decreasing by up to 21% at 20 µM cisplatin

combined with 1 μM DMX503433-09. Therefore, 0.6 and 1 μM DMX503433-09 would be selected to combine with 1 μM cisplatin on A549 at 24 hr in further experiments.

Table 3. 10 Comparison of control vs each treatment and CI analysis for A549 treated with cisplatin-DMX503433-09 combination at 24 and 72 hr

The significant reduction in the viability (M ± SD) between control and treatment group at 24 and 72 hr was analyzed by one-way ANOVA (prism) and is labelled with '*', which means P<0.05. The CI value for each single dose combination at 24 or 72 hr was analyzed by CompuSyn software. Those combination groups at 24 or 72 hr showing synergic effects (CI<1) are highlighted.

	Cisplatin-DMX503433-09-24 hr																							
Doses (μM)	Control-0			DMX503433-09-0.3			DMX503433-09-0.6			DMX503433-09-1			Cisplatin-1			1+0.3			1+0.6			1+1		
	M	SD	N	M	SD	N	M	SD	N	M	SD	N	M	SD	N	M	SD	N	M	SD	N	M	SD	N
Relative viability (% of control)	100	10	60	92*	16	58	85*	15	58	66*	15	57	98	14	18	75*	20	17	63*	18	18	63*	13	18
Doses (μM)	Cisplatin-5			5+0.3			5+0.6			5+1			Cisplatin-10			10+0.3			10+0.6			10+1		
	M	SD	N	M	SD	N	M	SD	N	M	SD	N	M	SD	N	M	SD	N	M	SD	N	M	SD	N
Relative viability (% of control)	86*	13	18	74*	19	18	64*	21	17	69*	13	18	80*	12	15	74*	18	18	71*	16	17	63*	13	16
Doses (μM)	Cisplatin-20			20+0.3			20+0.6			20+1														
	M	SD	N	M	SD	N	M	SD	N	M	SD	N												
Relative viability (% of control)	69*	9	14	50*	11	18	50*	9	18	48*	10	17												

Cisplatin dose (μM)	DMX503433-09 dose (μM)	Combination Fa values	CI value
1	0.3	0.25	0.42
1	0.6	0.37	0.53
1	1	0.37	0.86
5	0.3	0.26	0.58
5	0.6	0.36	0.64
5	1	0.31	1.17
10	0.3	0.26	0.79
10	0.6	0.29	1.01
10	1	0.37	1.08
20	0.3	0.5	0.43
20	0.6	0.5	0.60
20	1	0.52	0.78

	Cisplatin-DMX503433-09-72 hr																										
Doses (μM)	Control-0			DMX503433-09-0.3			DMX503433-09-0.6			Cisplatin-1			1+0.3			1+0.6			Cisplatin-5			5+0.3			5+0.6		
	M	SD	N	M	SD	N	M	SD	N	M	SD	N	M	SD	N	M	SD	N	M	SD	N	M	SD	N	M	SD	N
Relative viability (% of control)	100	9	59	94*	13	58	95	17	57	97	13	19	97	18	24	90*	10	17	90*	9	18	67*	8	18	73*	7	18
Doses (μM)	Cisplatin-10			10+0.3			10+0.6			Cisplatin-20			20+0.3			20+0.6											
	M	SD	N	M	SD	N	M	SD	N	M	SD	N	M	SD	N	M	SD	N									
Relative viability (% of control)	81*	10	18	69*	11	18	65*	10	18	39*	17	18	26*	11	18	24*	7	18									

Cisplatin dose (μM)	DMX503433-09 dose (μM)	Combination Fa values	CI value
1	0.3	0.03	0.86
1	0.6	0.1	14.93
5	0.3	0.33	1544.6
5	0.6	0.27	1103.9
10	0.3	0.31	1110.6
10	0.6	0.35	4255.1
20	0.3	0.74	843491
20	0.6	0.76	2475339

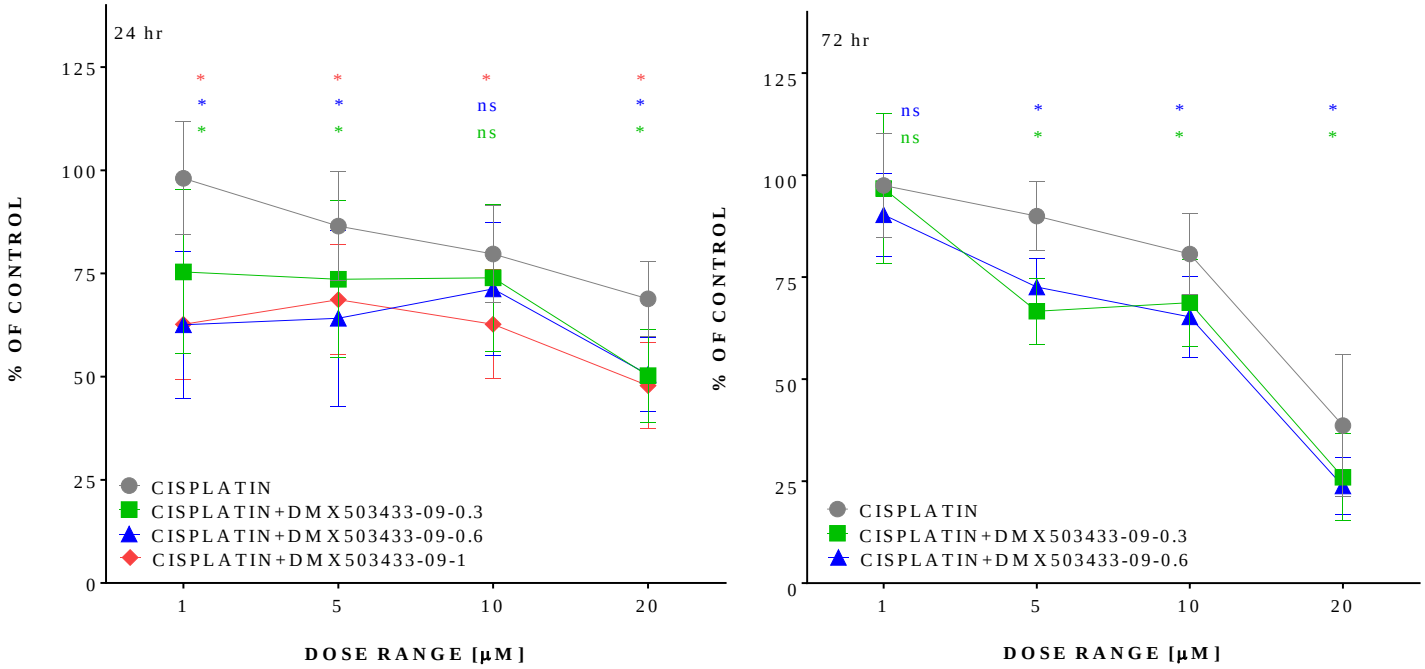

Figure 3. 12 Comparison of cisplatin (1-20 µM) treatments with cisplatin-DMX503433-09 combination treatments on A549 at 24 and 72 hr

The significance for cisplatin treatments (1-20) compared with 0.3 µM DMX503433-09-based combination treatments is shown in green and the significant comparison of cisplatin with 0.6 µM DMX503433-09-cisplatin combination treatments is shown in blue and lastly the red denotes the significant comparison between cisplatin and 1 µM DMX503433-09 containing combination treatments. Data were analyzed by two-way ANOVA by prism and results are shown as M ± SD with N over 18. '*' means P<0.05 and 'ns' means non-significant.

3.3.3.2. H460 Treatment

Similarly as A549 cells, H460 cells exhibited the most sensitivity to cisplatin-DMX503433-09 combination treatment at 72 hr with the viability significantly reduced by 58% at 10 µM DMX503433-09 combined with cisplatin. Whereas the 24 hr-treatment with this combination showed a maximal reduction in the viability by 45% at 20 µM cisplatin combined with 1 µM DMX503433-09. The CI analysis on cisplatin-DMX503433-09 combination treatments at 24 hr showed nearly all combination groups with the exception for 5 µM cisplatin combined with 1 µM DMX503433-09 and 10µM cisplatin combined with 0.6 µM of the agent, exhibited a synergism with CI altering from 0.2-0.8 (Table 3.11). The difference in the viability between cisplatin and combination treatments at 24 hr (Figure 3.13) was significantly up to 24% at 1 µM cisplatin combined with 1 µM DMX503433-09 compared to cisplatin alone. By contrast the combination was more potent at 72 hr with the viability decreased by up to 45% at 10 µM DMX503433-09-cisplatin combination compared to cisplatin. Therefore, 10 µM DMX5034-cisplatin combination would be further tested on H460 at 72 hr.

Table 3. 11 Comparison of control vs each treatment and CI analysis for H460 treated with cisplatin-DMX503433-09 combination at 24 and 72 hr

The significant reduction in the viability (M ± SD) between control and treatment group at 24 and 72 hr was analyzed by one-way ANOVA (prism) and is labelled with '*', which means P<0.05. The CI value for each single dose combination at 24 hr was analyzed by CompuSyn software. Those combination groups at 24 hr showing synergic effects (CI<1) are highlighted.

	Cisplatin-DMX503433-09-24 hr																							
Doses (μM)	Control-0			DMX503433-09-0.3			DMX503433-09-0.6			DMX503433-09-1			Cisplatin-1			1+0.3			1+0.6			1+1		
	M	SD	N	M	SD	N	M	SD	N	M	SD	N	M	SD	N	M	SD	N	M	SD	N	M	SD	N
Relative viability (% of control)	99	9	52	91*	14	51	86*	14	49	74*	13	52	85*	11	15	70*	17	18	65*	15	18	61*	14	17
Doses (μM)	Cisplatin-5			5+0.3			5+0.6			5+1			Cisplatin-10			10+0.3			10+0.6			10+1		
	M	SD	N	M	SD	N	M	SD	N	M	SD	N	M	SD	N	M	SD	N	M	SD	N	M	SD	N
Relative viability (% of control)	78*	9	17	69*	10	18	65*	8	18	71*	10	18	82*	9	17	71*	12	18	73*	12	18	67*	8	18
Doses (μM)	Cisplatin-20			20+0.3			20+0.6			20+1														
	M	SD	N	M	SD	N	M	SD	N	M	SD	N												
Relative viability (% of control)	67*	6	18	64*	16	18	58*	12	18	55*	7	18												

Cisplatin dose (μM)	DMX503433-09 dose (μM)	Combination Fa values	CI value
1	0.3	0.3	0.26
1	0.6	0.35	0.38
1	1	0.39	0.52
5	0.3	0.31	0.36
5	0.6	0.35	0.44
5	1	0.29	1.00
10	0.3	0.29	0.64
10	0.6	0.27	1.10
10	1	0.33	0.87
20	0.3	0.36	0.43
20	0.6	0.42	0.38
20	1	0.45	0.47

	Cisplatin-DMX503433-09-72 hr																													
Doses (μM)	Control-0			DMX503433-09-0.3			DMX503433-09-0.6			DMX503433-09-1			DMX503433-09-10			Cisplatin-1			1+0.3			1+0.6			1+1			1+10		
	M	SD	N	M	SD	N	M	SD	N	M	SD	N	M	SD	N	M	SD	N	M	SD	N	M	SD	N	M	SD	N	M	SD	N
Relative viability (% of control)	100	9	18	96	8	18	89	14	18	89	14	18	49*	21	18	87*	14	18	79*	19	18	68*	18	18	59*	20	18	42*	22	18

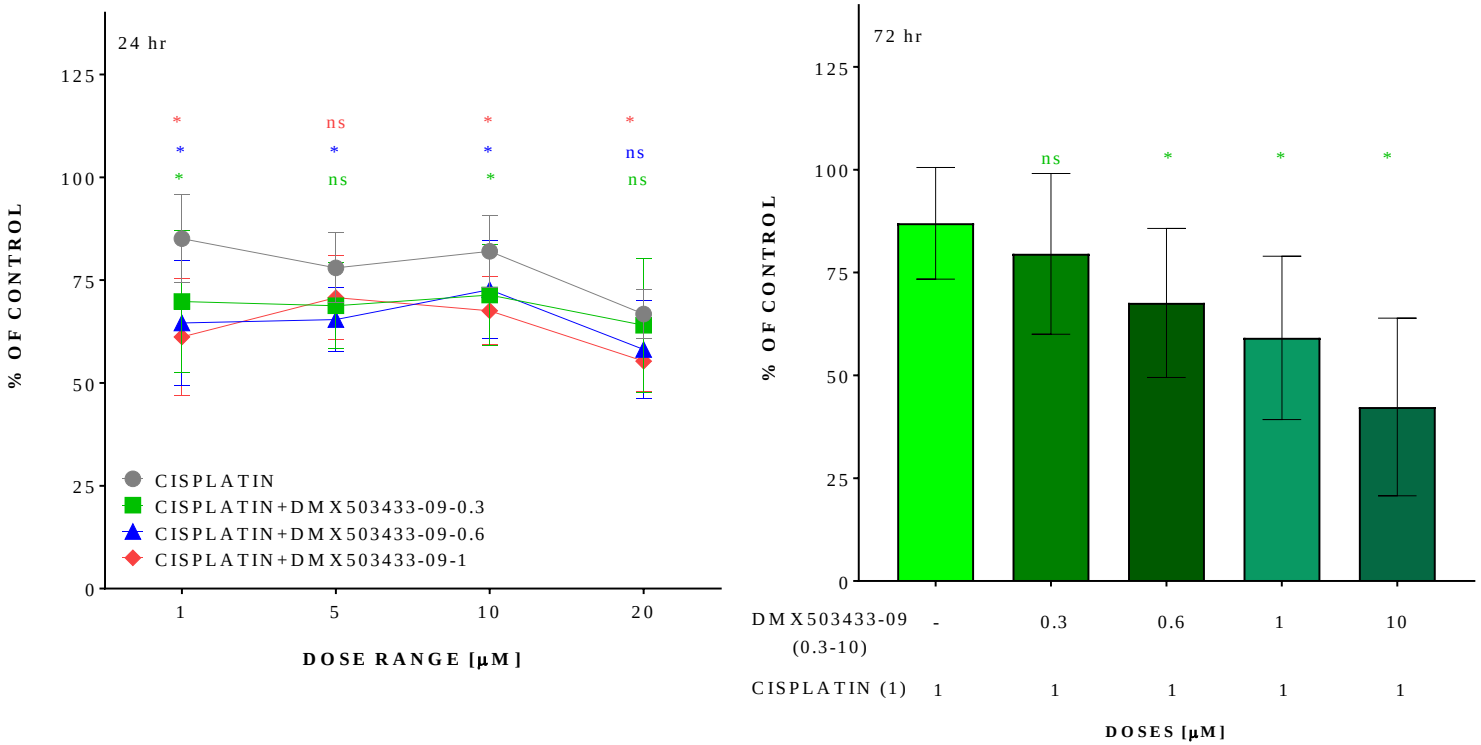

Figure 3. 13 Comparison of cisplatin and various cisplatin-DMX503433-09 combination treatments on H460 at 24 and 72 hr

For 24 hr-treatment, the significance for cisplatin treatments (1-20) compared with 0.3 µM DMX503433-09-based combination treatments is shown in green and that for cisplatin vs 0.6 µM DMX503433-09-cisplatin combination in blue and lastly red represent cisplatin vs 1 µM DMX503433-09-cisplatin combination treatments. Whereas 72 hr treatment only contain comparison of 1 µM cisplatin with all cisplatin-DMX503433-09 combination treatments, which is shown in green. Data were analyzed by two-way (24 hr) or one-way (72 hr) ANOVA by prism Results are shown as M ± SD with N over 15. '*' means P<0.05 and 'ns' means non-significant

3.3.3.3. H596 Treatment

Similarly to the potency of cisplatin-DMX502320-04 combination, cisplatin-DMX503433-09 combination was less active on H596 at 24 hr, where none of combination treatments exhibited a significant reduction in the viability compared to control or cisplatin treatment. although the 72 hr-treatment with the combination showed a maximal reduction in the viability by 29% at 0.6 µM DMX503433-09 combined with cisplatin, the difference in the viability between this regimen and cisplatin was significantly at 11% (Figure 3.14). Therefore, the combination of cisplatin-DMX503433-09 would not be tested on H596 in further experiments.

In summary, A549 would be treated with cisplatin-DMX503433-09 (0.6 and 1 µM) combination at 24 hr and H460 treated with 10 µM DMX503433-09-cisplatin at 72 hr in the further work.

	Cisplatin-DMX503433-09-24 hr																	
Doses (µM)	Control-0			DMX503433-09-0.3			DMX503433-09-0.6			Cisplatin-1			1+0.3			1+0.6		
	M	SD	N	M	SD	N	M	SD	N	M	SD	N	M	SD	N	M	SD	N
Relative viability (% of control)	100	16	18	105	13	17	95	13	17	101	18	15	97	14	15	101	17	17

	Cisplatin-DMX503433-09-72 hr																							
Doses (µM)	Control-0			DMX503433-09-0.3			DMX503433-09-0.6			DMX503433-09-1			Cisplatin-1			1+0.3			1+0.6			1+1		
	M	SD	N	M	SD	N	M	SD	N	M	SD	N	M	SD	N	M	SD	N	M	SD	N	M	SD	N
Relative viability (% of control)	100	7	18	92	9	18	99	13	18	81*	9	18	82*	9	18	73*	9	18	71*	10	18	72*	19	17

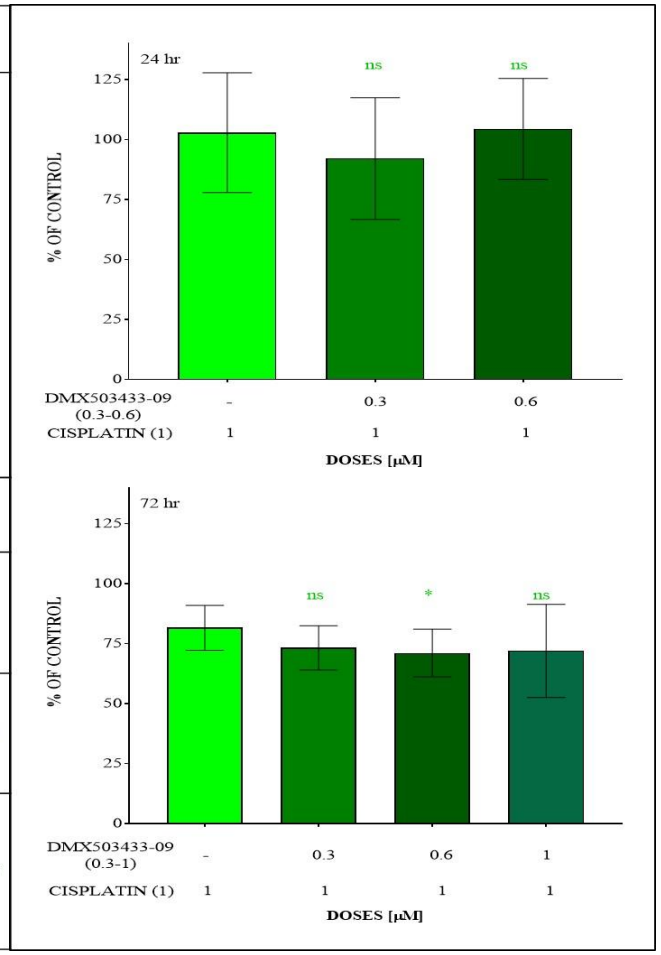

Figure 3. 14 The Cisplatin-DMX503433-09 combination treatments on H596 at 24 and 72 hr

The table left compares each treatment vs control group at 24 and 72 hr and the significance is labelled with '*', which means P<0.05. The figures show the comparison of 1 µM cisplatin treatment with 0.3, 0.6 or 1 µM DMX503433-09-cisplatin combination treatment at 24 and 72 hr. Data were analyzed by one-way ANOVA by prism and the results are shown as M ± SD with N over 17. The significant comparison is shown in green and '*' means P<0.05 and ns denotes non-significant.

3.3.4. CISPLATIN-GDC-0941 COMBINATION THERAPY

As reviewed in 3.2.6, the doses of cisplatin and GDC-0941 used for combinations at 24 and 72 hr are shown below:

Doses	A549		H460		H596	
	24 hr	72 hr	24 hr	72 hr	24 hr	72hr
Cisplatin (µM)	1-20	1-20	1-20	1	1	1
GDC-0941 (µM)	1	1	1	1	1	1

3.3.4.1. A549 Treatment

1 µM GDC-0941 single treatment exhibited an equivalent effect on reducing cell viability of A549 cells at 24 and 72 hr with a significant change of 28% approximately compared to control group. Whereas the combination with cisplatin exhibited a high potency at 72 hr compared to that at 24 hr, with the viability significantly altered by 90% at 20 µM cisplatin combined with GDC-0941 compared to control group (figure 3.15). In contrast, the maximal reduction in viability compared to control at 24 hr was nearly 40% at 1 µM cisplatin combined with GDC-0941, which was similarly to that (37%) altered by 20 µM cisplatin-GDC-0941 combination compared to control.

As for the comparison of cisplatin with this cisplatin-based doublet, the 72 hr-treatment appeared to be more potent with the viability significantly reduced by up to 48% at 20 µM cisplatin-GDC-0941 combination compared to cisplatin alone. The other cisplatin-based doublets also showed a high activity in reducing cell viability at 72 hr, with the alteration in viability compared to cisplatin single treatments was respectively 34% at 1 µM cisplatin-GDC-0941, 27% at 5 µM cisplatin containing doublet and 45% at 10 µM cisplatin-based doublet. As the previous cisplatin-based combination treatments all selected the lowest dose of cisplatin for testing the potencies of cisplatin-based doublets, the one µM cisplatin would be used to combine with cisplatin at 72 hr for A549.

	Cisplatin- GDC-0941-24 hr																	
Doses (μM)	Control-0			GDC-0941-1			Cisplatin-1			1+1								
	M	SD	N	M	SD	N	M	SD	N	M	SD	N						
Relative viability (% of control)	99	12	65	72*	12	61	81*	17	21	60*	13	23						
	Cisplatin-5			5+1			Cisplatin-10			10+1			Cisplatin-20			20+1		
	M	SD	N	M	SD	N	M	SD	N	M	SD	N	M	SD	N	M	SD	N
	93	17	23	59*	11	24	84*	14	18	66*	9	17	72*	12	18	62*	10	22
	Cisplatin- GDC-0941-72 hr																	
Doses (μM)	Control-0			GDC-0941-1			Cisplatin-1			1+1								
	M	SD	N	M	SD	N	M	SD	N	M	SD	N						
Relative viability (% of control)	99	10	70	69*	13	69	96	11	24	62*	14	24						
	Cisplatin-5			5+1			Cisplatin-10			10+1			Cisplatin-20			20+1		
	M	SD	N	M	SD	N	M	SD	N	M	SD	N	M	SD	N	M	SD	N
	60*	14	22	33*	10	24	75*	18	24	30*	14	24	57*	11	18	9*	7	24

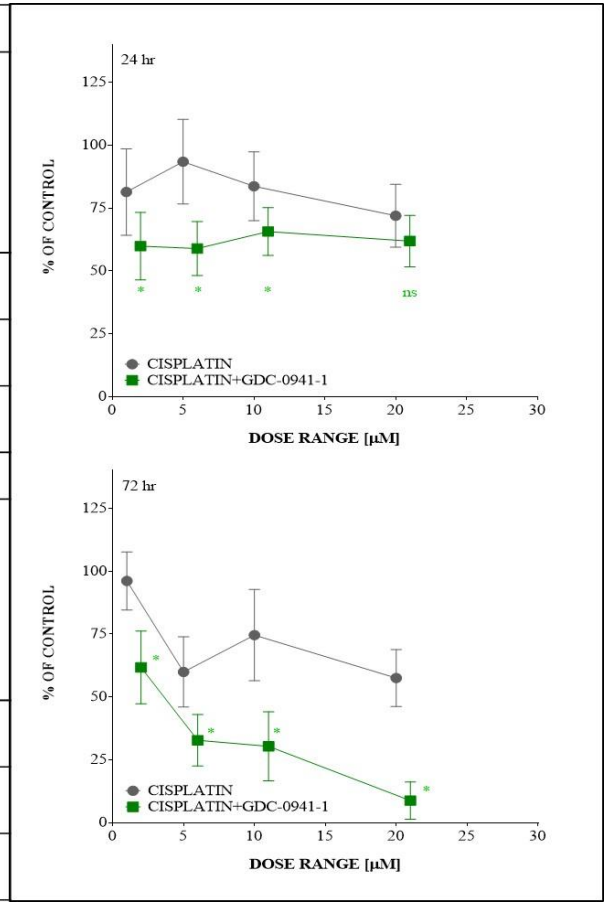

Figure 3. 15 The Cisplatin-GDC-0941 combination treatments on A549 at 24 and 72 hr

The table left compares each treatment vs control group at 24 and 72 hr (one-way ANOVA by prism) and the significance is labelled with '*', which means P<0.05. The figures show the comparison of cisplatin treatments (1-20 μM) with 1 μM GDC-0941-cisplatin combination treatments (two-way ANOVA) at 24 and 72 hr. The results are shown as M ± SD with over 17. The significant comparison is shown in green and '*' means P<0.05.

3.3.4.2. H460 Treatment

In contrast to A549 cells, H460 cells exhibited a greater sensitivity to GDC-0941 single treatment at 24 and 72 hr with the viability significantly reduced by nearly 50% compared to control group. The combination with cisplatin was more potent at 72 hr compared to that at 24 hr, with the viability reduced by 76% significantly different from that of control group. In contrast, the 24 hr-treatment exhibited a maximal significant reduction in viability by 56% at 10 µM cisplatin-GDC-0941 combination compared to control group (Figure 3.16).

Although all 24-hr treatment with cisplatin-GDC-0941 combination exhibited a significant reduction in the viability compared to cisplatin treatments, the maximal alteration in viability was observed at 1 µM cisplatin-GDC-0941 combination with a change of 32% whereas the rest of cisplatin-based doublets showed a less than 25% in the alteration of viability compared to cisplatin treatments. In contrast to 24 hr, 72 hr-treatment was more potent with a significant change of 42% at the combination treatment compared to cisplatin alone. Therefore, 72 hr-treatment with cisplatin-GDC-0941 combination would be tested on H460 in further experiments.

	Cisplatin- GDC-0941-24 hr											
Doses (µM)	Control-0			GDC-0941-1			Cisplatin-1			1+1		
	M	SD	N	M	SD	N	M	SD	N	M	SD	N
Relative viability (% of control)	99	11	52	52*	13	53	86*	11	18	54*	12	18

	Cisplatin-5			5+1			Cisplatin-10			10+1			Cisplatin-20			20+1		
	M	SD	N	M	SD	N	M	SD	N	M	SD	N	M	SD	N	M	SD	N
	73*	11	18	49*	10	18	64*	12	17	43*	10	18	82*	12	17	60*	14	18

	Cisplatin- GDC-0941-72 hr											
Doses (µM)	Control-0			GDC-0941-1			Cisplatin-1			1+1		
	M	SD	N	M	SD	N	M	SD	N	M	SD	N
Relative viability (% of control)	100	10	18	51*	6	18	66*	18	18	24*	6	18

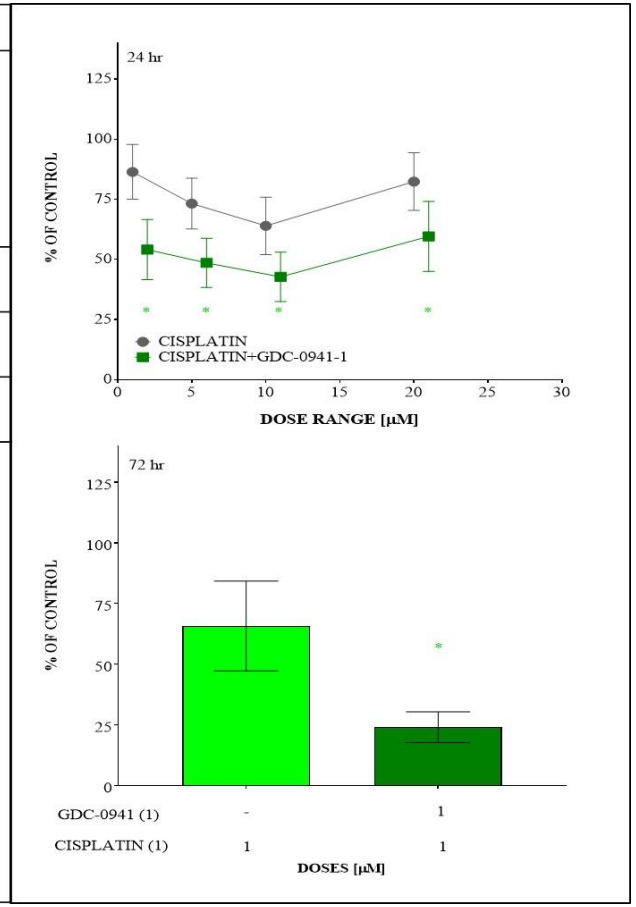

Figure 3. 16 The Cisplatin-GDC-0941 combination treatments on H460 at 24 and 72 hr

The table left compares each treatment vs control group at 24 and 72 hr (one-way-ANOVA by prism) and the significance is labelled with '*', which means P<0.05. The figures show the comparison of various doses of cisplatin treatment (1 or 1-20 µM) with 1 µM GDC-0941-cisplatin combination treatments at 24 (two-way ANOVA) and 72 (t-test) hr. The results are shown as M ± SD with over 17. The significant comparison is shown in green and '*' means P<0.05.

3.3.4.3. H596 Treatment

The combination of cisplatin-GDC-0941 was also potent on H596 cells with the viability significantly reduced by 33% at 24 hr and 60% at 72 hr respectively compared to control group (Figure 3.17). Moreover, the 72-hr treatment with this cisplatin-based doublet exhibited a significant alteration in the viability by nearly 40% compared to cisplatin alone, in contrast to 35% observed at 24 hr between cisplatin and the doublet. Therefore, 72 hr-treatment with cisplatin-GDC-0941 combination would be tested on H596 in further experiments.

In summary, the combination of cisplatin with GDC-0941 would be tested on all cell lines at 72 hr in the further work.

	Cisplatin- GDC-0941-24 hr											
Doses (µM)	Control-0			GDC-0941-1			Cisplatin-1			1+1		
	M	SD	N	M	SD	N	M	SD	N	M	SD	N
Relative viability (% of control)	100	12	18	76	7	18	102	11	18	67	13	18
	Cisplatin- GDC-0941-72 hr											
Doses (µM)	Control-0			GDC-0941-1			Cisplatin-1			1+1		
	M	SD	N	M	SD	N	M	SD	N	M	SD	N
Relative viability (% of control)	100	25	18	71	8	18	79	17	18	40	13	18

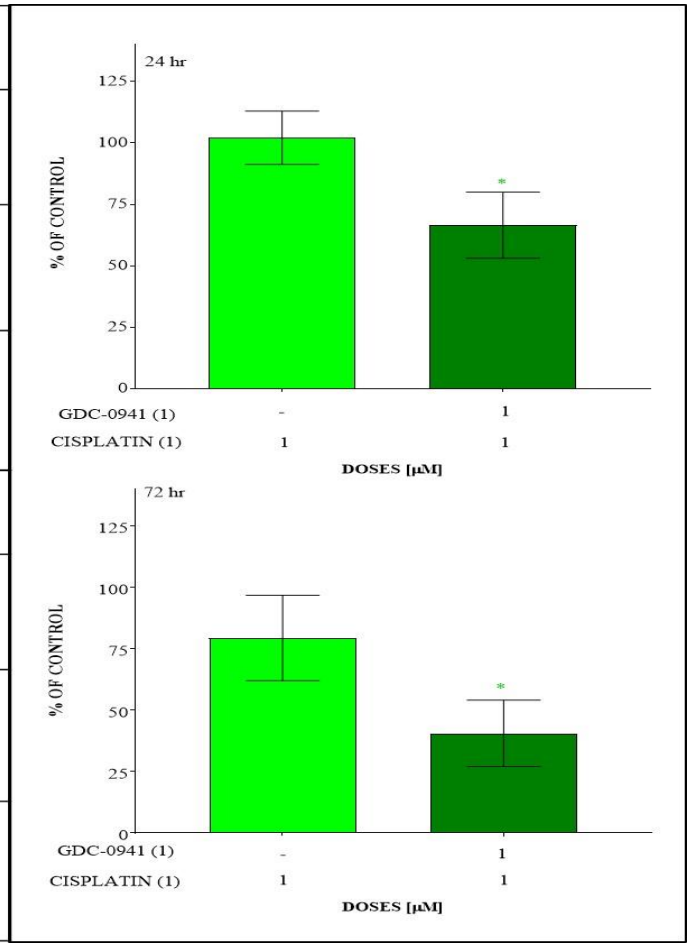

Figure 3. 17 The Cisplatin-GDC-0941 combination treatments on H596 at 24 and 72 hr

The table left compares each treatment vs control group at 24 and 72 hr (one-way ANOVA by prism) and the significance is labelled with '*', which means P<0.05. The figures show the comparison of 1 µM cisplatin treatment with 1 µM GDC-0941-cisplatin combination treatment (t-test) at 24 and 72 hr. Results are shown as M ± SD with 18 replicates. The significant comparison is shown in green and '*' means P<0.05.

3.3.5. CISPLATIN-MK-2206 COMBINATION THERAPY

As reviewed in 3.2.6, the doses of cisplatin and MK-2206 used for combinations at 24 and 72 hr are shown below:

Doses	A549		H460		H596	
	24 hr	72 hr	24 hr	72 hr	24 hr	72hr
Cisplatin (µM)	1-20	1-20	1-20	1	1	1
MK-2206 (µM)	3	3-21	3	3	3	3-12

3.3.5.1. A549 Treatment

Similarly as GDC-0941, MK-2206 single treatment was also potent in reducing the viability of A549 cells with a maximal reduction in viability by nearly 60% at 21 µM MK-2206 at 72 hr. The combination with cisplatin further enhanced the potency of cisplatin treatment. The 24 hr-treatment with cisplatin-MK-2206 combination exhibited a significant decrease in the viability by up to 50% at 1 µM cisplatin combined with 3 µM MK-2206 compared to control group (Table 3.12), whereas this combination at 72 hr showed a less potency with the viability significantly decreased by just 41% compared to control group. Nevertheless, the potency of 1 µM cisplatin-based combination treatment was further increased with a rise in the concentration of MK-2206 and the 21 µM MK-2206 containing doublet significantly reduced the viability by 90% compared to control group. Moreover, these 1 µM cisplatin-containing doublets all showed a synergism with a CI lower than 0.5. Whereas the rest of cisplatin-MK-2206 combination treatments at 72 hr also showed a significant reduction in viability compared to control, decreasing to up to 93% at 20 µM cisplatin combined with 21 µM MK-2206, and these combination treatments all exhibited synergistic effects as those 1 µM cisplatin-based doublets.

Both 24 and 72 hr treatments showed a significant reduction in viability at combinations of cisplatin with MK-2206 compared to cisplatin alone (Figure 3.18). The 24 hr-treatment showed a significant alteration in the viability with 41% at 1µM cisplatin-MK-2206 combination treatment vs cisplatin alone, whereas the rest of cisplatin-based doublets at 24 hr showed a reduction of about 10-20%, although significantly different from those of cisplatin treatments. Similarly to 24 hr-treatment, the 72-hr treatment with 1 µM cisplatin-

containing doublets showed a significant decrease in viability by 27% at 3 µM MK-2206-based combination, 47% at 12 µM MK-2206-based doublet and lastly 76% at 21 µM MK-2206-based doublet. In the further work, the combination of cisplatin with MK-2206 would be tested on A549 at 24 and 72 hr, in which all doses of MK-2206 at 24 or 72 hr would be selected to combine with 1 µM cisplatin.

Table 3. 12 Comparison of control vs each treatment and CI analysis for A549 treated with cisplatin-MK-2206 combination at 24 and 72 hr

The significant reduction in the viability (M ± SD) between control and each treatment group at 24 and 72 hr was analyzed by one-way ANOVA (prism) and is labelled with '*', which means P<0.05. The CI value for each single dose combination at 72 hr was analyzed by CompuSyn software. All combination groups at 72 hr showing a synergism (CI<1) have been highlighted.

	Cisplatin- MK-2206-24 hr																													
Doses (μM)	Control-0			MK-2206-3			Cisplatin-1			1+3			Cisplatin-5			5+3			Cisplatin-10			10+3			Cisplatin-20			20+3		
	M	SD	N	M	SD	N	M	SD	N	M	SD	N	M	SD	N	M	SD	N	M	SD	N	M	SD	N	M	SD	N	M	SD	N
Relative viability (% of control)	100	12	70	73*	15	67	91	12	16	50*	15	17	92	16	22	68*	16	23	71*	9	23	57*	15	23	68*	9	22	56*	14	24

	Cisplatin-MK-2206-72 hr																							
Doses (μM)	Control-0			MK-2206-3			MK-2206-12			MK-2206-21			Cisplatin-1			1+3			1+12			1+21		
	M	SD	N	M	SD	N	M	SD	N	M	SD	N	M	SD	N	M	SD	N	M	SD	N	M	SD	N
Relative viability (% of control)	98	10	75	81*	13	76	65*	17	71	39*	18	68	84*	14	24	57*	20	24	37*	19	24	8*	10	23
Doses (μM)	Cisplatin-5			5+3			5+12			5+21			Cisplatin-10			10+3			10+12			10+21		
	M	SD	N	M	SD	N	M	SD	N	M	SD	N	M	SD	N	M	SD	N	M	SD	N	M	SD	N
Relative viability (% of control)	74*	34	24	47*	17	24	37*	18	24	22*	11	24	83*	9	24	48*	12	23	38*	13	24	8*	7	24
Doses (μM)	Cisplatin-20			20+3			20+12			20+21														
	M	SD	N	M	SD	N	M	SD	N	M	SD	N												
Relative viability (% of control)	63*	9	24	17*	6	24	16*	6	24	5*	5	24												

Cisplatin dose (μM)	MK-2206 (μM)	Combination Fa values	CI value
1	3	0.43	0.25
1	12	0.63	0.40
1	21	0.92	0.08
5	3	0.53	0.17
5	12	0.63	0.40
5	21	0.78	0.31
10	3	0.52	0.18
10	12	0.62	0.43
10	21	0.92	0.08
20	3	0.83	0.03
20	12	0.84	0.12
20	21	0.95	0.05

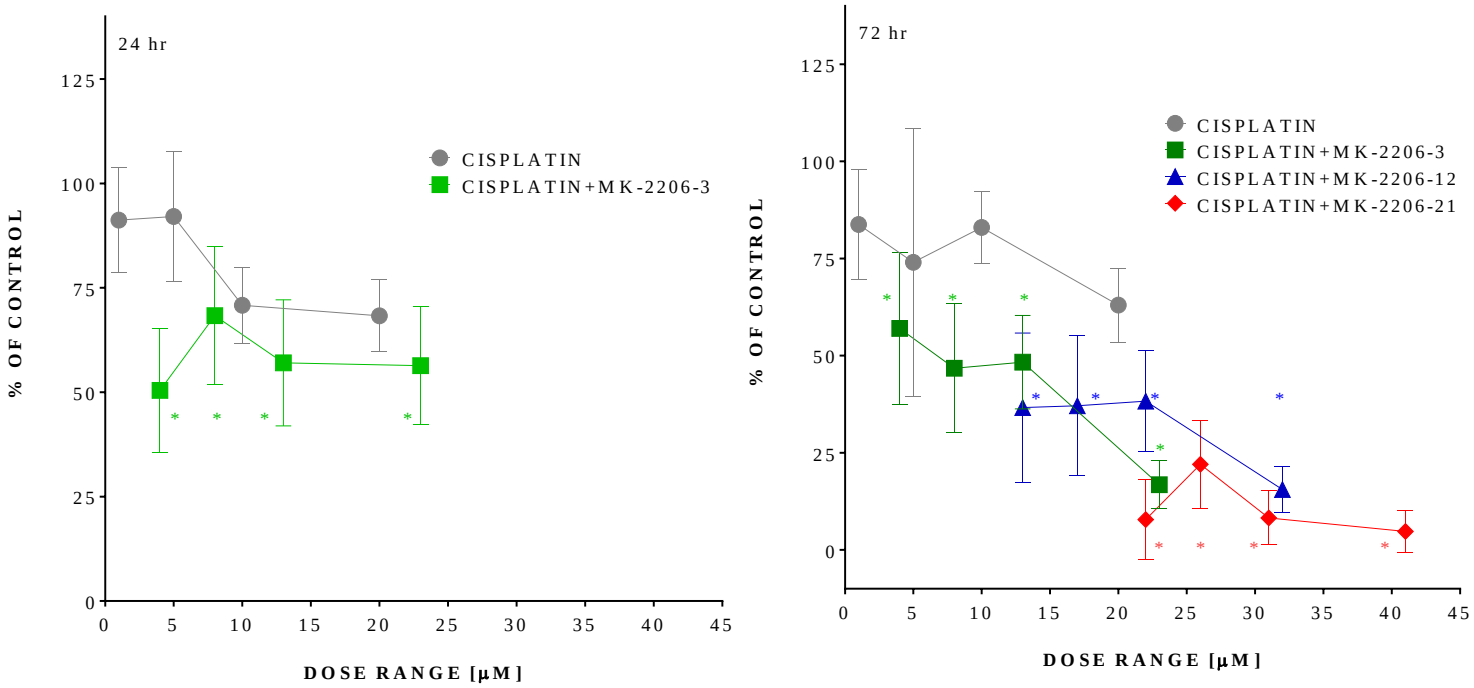

Figure 3. 18 Comparison of cisplatin (1-20 µM) treatments and various cisplatin-MK-2206 combination treatments on A549 at 24 and 72 hr

The significance for cisplatin treatments (1-20) compared with 3 µM MK-2206-based combination treatments (two-way ANOVA by prism) at 24 and 72 hr is shown in green and the significant comparison of cisplatin with 12 µM MK-2206-cisplatin combination treatments at 72 hr is shown in blue and lastly the red denotes the significant comparison between cisplatin and 21 µM MK-2206-containing combination treatments at 72 hr. Results are shown as M ± SD with N over 16. '*' means P<0.05 and 'ns' means non-significant.

3.3.5.2. H460 Treatment

In contrast to A549 cells, H460 cells exhibited less sensitivity to MK-2206 single and cisplatin-MK-2206 doublets. The maximal significant reduction in the viability compared to control group achieved at 1 µM cisplatin-MK-2206 doublet with a decrease of 64% at 72 hr (Figure 3.19). In contrast, the 24 hr-treatment with cisplatin-MK-2206 doublets showed a significant decrease in the viability by up to 43% at 10µM cisplatin-MK-2206 combination compared to control group. As for the difference in the viability compared to cisplatin treatments, the combination of cisplatin with MK-2206 was more potent at 72 hr with an alteration of 32% significantly compared to cisplatin alone. In contrast, this combination at 24 hr significantly exhibited a reduction of 14% compared to cisplatin and the rest of cisplatin-based doublets at 24 hr showed a similar potency with the viability significantly decreased by 16-17%. Therefore, 1 µM cisplatin combined with MK-2206 at 72 hr was comparably more potent and then would be tested on H460 in further experiments.

	Cisplatin- MK-2206-24 hr											
Doses (µM)	Control-0			MK-2206-3			Cisplatin-1			1+3		
	M	SD	N	M	SD	N	M	SD	N	M	SD	N
Relative viability (% of control)	99	11	52	76*	18	54	89*	13	24	75*	13	24

	Cisplatin-5			5+3			Cisplatin-10			10+3			Cisplatin-20			20+3		
	M	SD	N	M	SD	N	M	SD	N	M	SD	N	M	SD	N	M	SD	N
	74*	9	24	58*	9	24	72*	14	23	56*	11	24	78*	11	18	61*	9	18

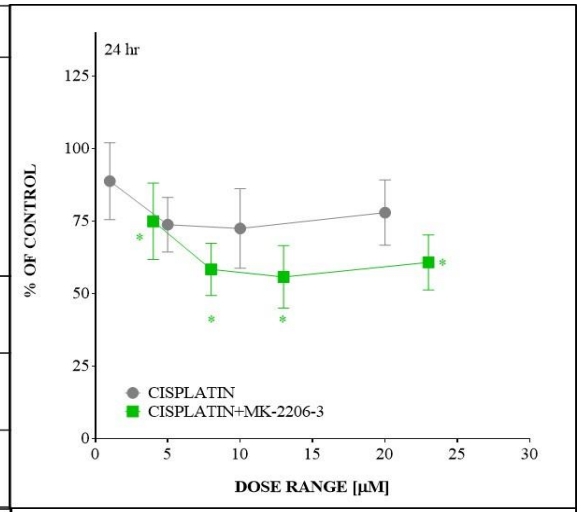

	Cisplatin- MK-2206-72 hr											
Doses (µM)	Control-0			MK-2206-3			Cisplatin-1			1+3		
	M	SD	N	M	SD	N	M	SD	N	M	SD	N
Relative viability (% of control)	100	10	18	66*	18	18	68*	7	18	36*	8	18

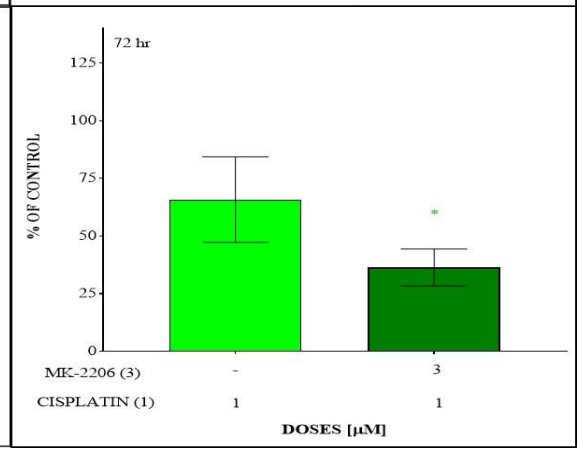

Figure 3. 19 The Cisplatin-MK-2206 combination treatments on H460 at 24 and 72 hr

The table left compares each treatment vs control group (one-way ANOVA by prism) at 24 and 72 hr and the significance is labelled with '*', which means P<0.05. The figures show the comparison of cisplatin treatments (1 µM or the whole dose range of cisplatin) with 3 µM MK-2206-cisplatin combination treatments at 24 (two-way ANOVA) and 72 hr (t-test). The results are shown as M ± SD with over 18. The significant comparison is shown in green and '*' means P<0.05.

3.3.5.3. H596 Treatment

In contrast to the cell lines above, H596 showed a less sensitivity to cisplatin-MK-2206 doublet at 72 hr, where both cisplatin-based doublets showed a non-significant effect on reducing the viability compared to control. The viability at 72 hr was only significantly reduced by 12 µM MK-2206 single treatment with a reduction of 14% compared to control (Figure 3.20). In contrast, the combination of cisplatin with MK-2206 at 24 hr was more potent in reducing the viability with a change of over 40% significantly different from that of control group. Moreover, the alteration in the viability compared to cisplatin was significantly at 33% by the doublet. Therefore, the combination of cisplatin with MK-2206 would be tested on H596 at 24 hr in further work.

In summary, A549 would be treated with cisplatin-MK-2206 at 24 and 72 hr, whereas H460 would be tested at 72 hr only and H596 tested at 24 hr only.

	Cisplatin- MK-2206-24 hr											
Doses (µM)	Control-0			MK-2206-3			Cisplatin-1			1+3		
	M	SD	N	M	SD	N	M	SD	N	M	SD	N
Relative viability (% of control)	100	8	18	77*	10	18	92	15	18	59*	11	18

	Cisplatin- MK-2206-72 hr																	
Doses (µM)	Control-0			MK-2206-3			MK-2206-12			Cisplatin-1			1+3			1+12		
	M	SD	N	M	SD	N	M	SD	N	M	SD	N	M	SD	N	M	SD	N
Relative viability (% of control)	100	8	18	92	13	18	86*	13	18	94	10	18	97	15	16	91	17	16

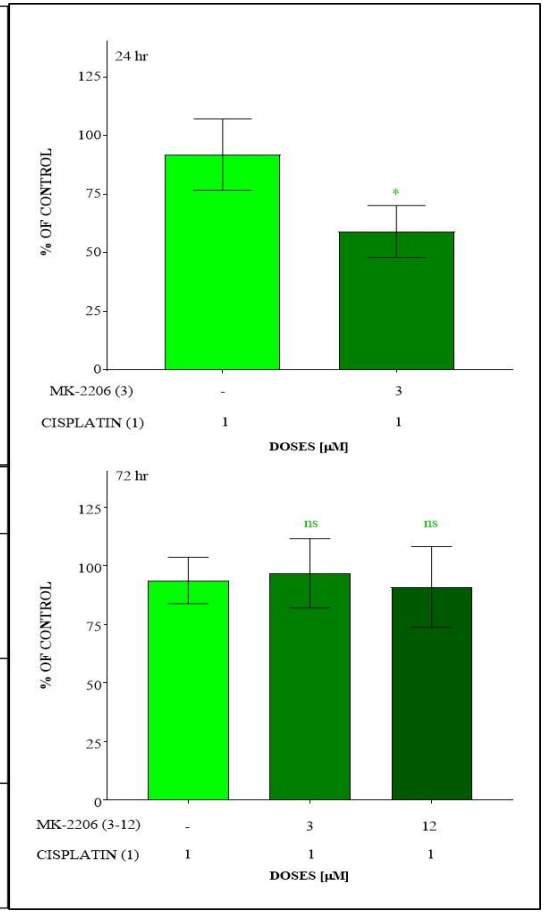

Figure 3. 20 The Cisplatin-MK-2206 combination treatments on H596 at 24 and 72 hr

The table left compares each treatment vs control group (one-way ANOVA by prism) at 24 and 72 hr and the significance is labelled with '*', which means P<0.05. The figures show the comparison of 1 µM cisplatin treatment with 3 or 3, 12 µM MK-2206-cisplatin combination treatments at 24 (t-test) and 72 hr (one-way ANOVA). The results are shown as M ± SD with N over 16. The significant comparison is shown in green and '*' means P<0.05 and ns denotes non-significant

3.3.6. CISPLATIN-AZD6244 COMBINATION THERAPY

As reviewed in 3.2.6, the doses of cisplatin and AZD6244 used for combinations at 24 and 72 hr are shown below:

Doses	A549		H460		H596	
	24 hr	72 hr	24 hr	72 hr	24 hr	72hr
Cisplatin (µM)	1-20	1-20	1-20	1	1	1
AZD6244 (µM)	10-100	10-50	10-100	10-100	10-100	10-100

3.3.6.1. A549 Treatment

AZD6244 single treatments proved to be less potent at 24 hr compared to 72 hr, which exhibited a significant reduction in cell viability of A549 cells by up to 43% at 50 µM AZD6244 compared to control group at 72 hr. In contrast, the maximal decrease in the viability at 24 hr was observed at 100 µM AZD6244 with a maximal decrease of 16%. Moreover, all cisplatin-AZD6244 doublets but 20 µM cisplatin-based doublets exhibited a drug resistance with the viability increased according to a rise in AZD6244 concentration at 24 hr. The CI analysis data showed that all AZD6244-containing doublets at 24 hr showed an antagonistic effect (Table 3.13). In contrast, the combination with AZD6244 at 72 hr exhibited a significant reduction in the viability by up to 87% at 20 µM cisplatin combined with 50 µM AZD6244 compared to control. Moreover, nearly all cisplatin-AZD6244 doublets except for 1 µM cisplatin-containing regimens showed a synergistic effect with a CI value ranging from 0.2 to 0.5.

For the comparison with cisplatin single treatments (Figure 3.21), all AZD6244-containg doublets showed a similar potency in viability reduction at 24 hr, with a maximal change of 24% in the viability at 1 µM cisplatin combined with 10 µM AZD6244 significantly compared to cisplatin alone. In contrast, the cisplatin-AZD6244 doublets at 72 hr showed a significant reduction in the viability by up to 40% at 20 µM cisplatin combined with 50 µM AZD6244 compared to cisplatin alone.

In order to compare the potency of this doublet with the rest of cisplatin-based doublets in the further work, the high dose of cisplatin-containing combination with AZD6244 was

not comparable with 1 μM cisplatin-containing doublets in the further work. Therefore, this cisplatin-AZD6244 would not selected for testing on A549 in the further work.

Table 3. 13 Comparison of control vs each treatment and CI analysis for A549 treated with cisplatin-AZD6244 combination at 24 and 72 hr

The significant reduction in the viability (M ± SD) between control and treatment group at 24 and 72 hr was analyzed by one-way ANOVA (prism) and is labelled with '*', which means P<0.05. The CI value for each single dose combination at 24 or 72 hr was analyzed by CompuSyn software. Those combination groups at 72 hr showing synergic effects (CI<1) are highlighted.

	Cisplatin-AZD6244-24 hr																							
Doses (μM)	Control-0			AZD6244-10			AZD6244-50			AZD6244-100			Cisplatin-1			1+10			1+50			1+100		
	M	SD	N	M	SD	N	M	SD	N	M	SD	N	M	SD	N	M	SD	N	M	SD	N	M	SD	N
Relative viability (% of control)	99	13	59	85*	19	51	98	16	51	83*	15	50	94	14	21	70*	26	19	75*	23	19	75*	19	20
Doses (μM)	Cisplatin-5			5+10			5+50			5+100			Cisplatin-10			10+10			10+50			10+100		
	M	SD	N	M	SD	N	M	SD	N	M	SD	N	M	SD	N	M	SD	N	M	SD	N	M	SD	N
Relative viability (% of control)	95	18	12	82	12	8	98	17	10	95	20	11	82*	17	18	65*	17	16	67*	17	18	67*	14	16
Doses (μM)	Cisplatin-20			20+10			20+50			20+100														
	M	SD	N	M	SD	N	M	SD	N	M	SD	N												
Relative viability (% of control)	63*	15	17	62*	14	16	63*	13	18	55*	11	18												

Cisplatin dose (μM)	AZD6244 (μM)	Combination Fa values	CI value
1	10	0.3	1356.8
1	50	0.25	1715.4
1	100	0.25	3430.7
5	10	0.18	35.39
5	50	0.02	13.50
5	100	0.05	3.76
10	10	0.35	4730.3
10	50	0.33	14522.1
10	100	0.33	29043.8
20	10	0.38	9606.4
20	50	0.37	38030.6
20	100	0.45	466581

	Cisplatin-AZD6244-72 hr																										
Doses (μM)	Control-0			AZD6244-10			AZD6244-50			Cisplatin-1			1+10			1+50			Cisplatin-5			5+10			5+50		
	M	SD	N	M	SD	N	M	SD	N	M	SD	N	M	SD	N	M	SD	N	M	SD	N	M	SD	N	M	SD	N
Relative viability (% of control)	99	10	70	66*	17	66	56*	18	70	100	11	18	77*	16	18	71*	16	18	57*	15	16	41*	12	16	29*	11	17
Doses (μM)	Cisplatin-10			10+10			10+50			Cisplatin-20			20+10			20+50											
	M	SD	N	M	SD	N	M	SD	N	M	SD	N	M	SD	N	M	SD	N									
Relative viability (% of control)	72*	13	18	41*	11	18	40*	8	18	52*	17	18	18*	8	22	12*	7	24									

Cisplatin dose (μM)	AZD6244 (μM)	Combination Fa values	CI value
1	10	0.23	8.14
1	50	0.29	12.23
5	10	0.59	0.28
5	50	0.71	0.19
10	10	0.59	0.53
10	50	0.60	0.58
20	10	0.82	0.47
20	50	0.88	0.34

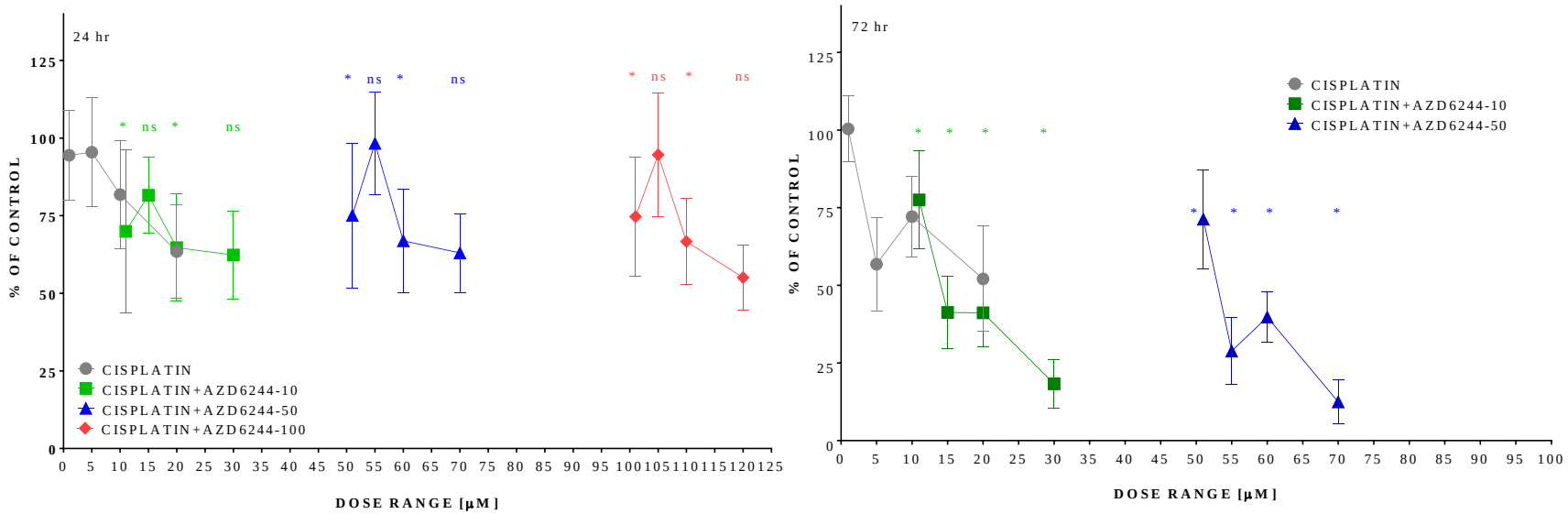

Figure 3. 21 Comparison of cisplatin (1-20 µM) treatments with cisplatin-AZD6244 combination treatments on A549 at 24 and 72 hr

The significance for cisplatin treatments (1-20) compared with 10 µM AZD6244-based combination treatments is shown in green and the significant comparison of cisplatin with 50 µM AZD6244-cisplatin combination treatments is shown in blue and lastly the red denotes the significant comparison between cisplatin and 100 µM AZD6244 containing combination treatments. Data were analyzed by two-way ANOVA and results are shown as M ± SD with N over 8. '*' means $P<0.05$ and 'ns' means non-significant.

3.3.6.2. H460 Treatment

Similarly as shown in A549 cells, H460 cells showed less sensitivity to single AZD6244 and cisplatin-AZD6244 combination treatments at 24 hr. The maximal reduction in the viability compared to control was at 10 µM cisplatin combined with 50 µM AZD6244 with a significant change of 38% (Table 3.14). The combination effect analysis showed that all cisplatin-AZD6244 doublets showed an antagonistic effect and hence the 24-hr treatment with cisplatin-AZD6244 doublet was not potent on H460. In contrast, the 72-hr treatment was more potent with the viability significantly reduced by 67% at 10 µM AZD6244-cisplatin combination treatment compared to control group. As for alteration in the viability compared to cisplatin treatment (Figure 3.22), the 24 hr-treatment showed that only the 20 µM cisplatin-containing combination treatments showed a significant change in the viability decreasing by up to 16% at 20 µM cisplatin combined with 100 µM AZD6244. In contrast, the 72-hr treatment showed a higher potency with this combination, exerting a maximal decrease in the viability by up to 33% significantly compared to cisplatin alone. Nevertheless, both 24 hr- and 72 hr treatments appeared to be refractory to the combination of cisplatin with AZD6244 on H460, with the viability slightly enhanced as the concentration of AZD6244 increased. As the 10 µM AZD6244 combined with cisplatin treatment at 72 hr proved to be more active than rest of AZD6244-containing doublets, only this regimen would be selected for H460 in the further work.

Table 3. 14 Comparison of control vs each treatment and CI analysis for H460 treated with cisplatin-AZD6244 combination at 24 and 72 hr

The significant reduction in the viability (M ± SD) between control and treatment group at 24 and 72 hr was analyzed by one-way ANOVA (prism) and is labelled with '*', which means P<0.05. The CI value for each single dose combination at 24 hr was analyzed by CompuSyn software. None of combination groups at 24 hr showed a synergic effect (CI<1).

	Cisplatin-AZD6244-24 hr																							
Doses (μM)	Control-0			AZD6244-10			AZD6244-50			AZD6244-100			Cisplatin-1			1+10			1+50			1+100		
	M	SD	N	M	SD	N	M	SD	N	M	SD	N	M	SD	N	M	SD	N	M	SD	N	M	SD	N
Relative viability (% of control)	100	11	36	89*	11	33	94	15	34	92	12	33	80*	16	17	88*	13	17	85*	15	17	84*	14	18
Doses (μM)	Cisplatin-5			5+10			5+50			5+100			Cisplatin-10			10+10			10+50			10+100		
	M	SD	N	M	SD	N	M	SD	N	M	SD	N	M	SD	N	M	SD	N	M	SD	N	M	SD	N
Relative viability (% of control)	64*	14	18	64*	9	18	74*	9	17	71*	12	17	63*	15	12	64*	17	12	62*	16	12	69*	11	12
Doses (μM)	Cisplatin-20			20+10			20+50			20+100														
	M	SD	N	M	SD	N	M	SD	N	M	SD	N												
Relative viability (% of control)	83*	8	17	72*	16	18	72*	13	18	67*	12	17												

	Cisplatin-AZD6244-72 hr																							
Doses (μM)	Control-0			AZD6244-10			AZD6244-50			AZD6244-100			Cisplatin-1			1+10			1+50			1+100		
	M	SD	N	M	SD	N	M	SD	N	M	SD	N	M	SD	N	M	SD	N	M	SD	N	M	SD	N
Relative viability (% of control)	100	10	18	64*	13	18	74*	12	18	63*	11	18	66*	18	18	33*	10	18	35*	7	18	38*	8	18

Cisplatin dose (μM)	AZD6244 (μM)	Combination Fa values	CI value
1	10	0.12	6.13
1	50	0.15	8.58
1	100	0.16	6.19
5	10	0.36	3127.8
5	50	0.26	1456.3
5	100	0.29	6219.1
10	10	0.36	3127.8
10	50	0.38	24116.6
10	100	0.31	10059
20	10	0.28	485.7
20	50	0.28	2427.5
20	100	0.33	15998.5

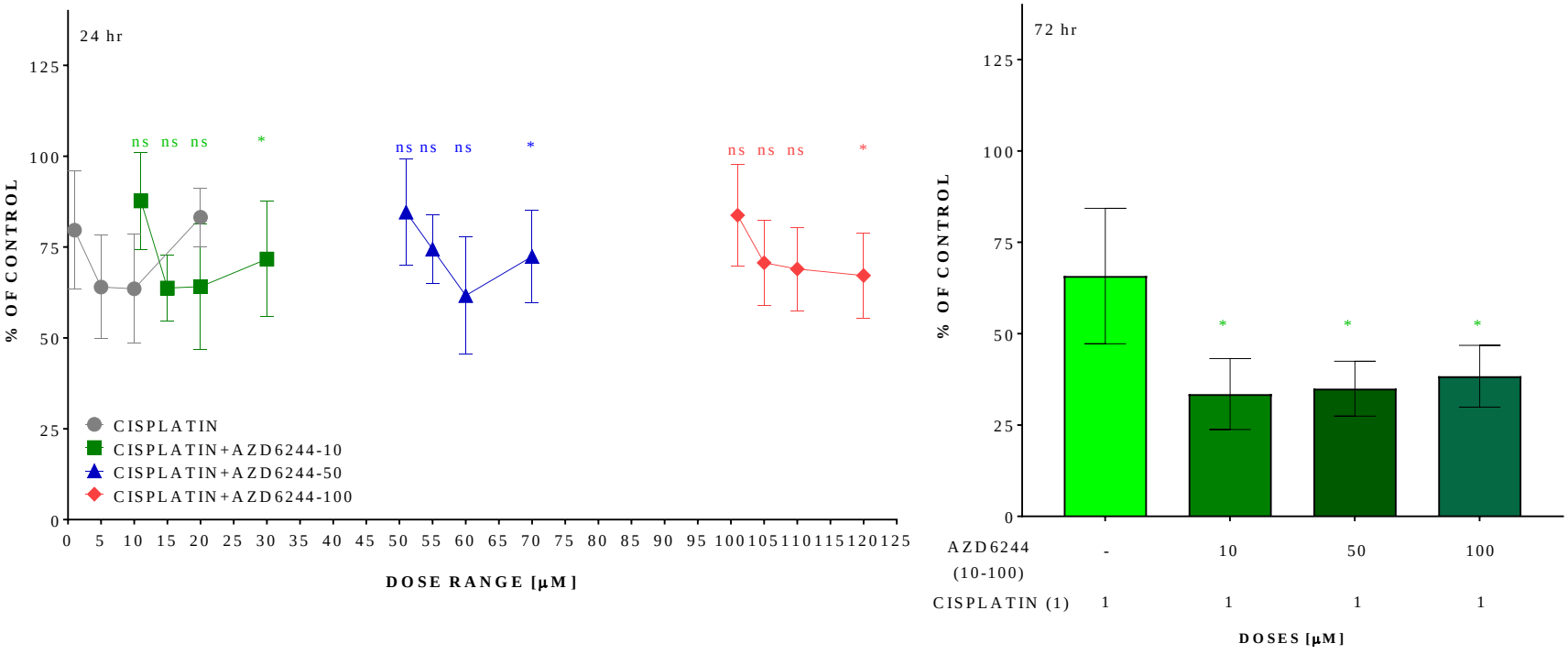

Figure 3. 22 Comparison of cisplatin and various cisplatin-AZD6244 combination treatments on H460 at 24 and 72 hr

For 24 hr-treatment, the significance for cisplatin treatments (1-20 µM) compared with 10 µM AZD6244-based combination treatments (two-way ANOVA by prism) is shown in green and that for cisplatin vs 50 µM AZD6244-cisplatin combination in blue and lastly red represent cisplatin vs 100 µM AZD6244-cisplatin combination treatments. Whereas 72 hr treatment only contain comparison of 1 µM cisplatin with all cisplatin-AZD6244 combination treatments (one-way ANOVA), which is shown in green. Results are shown as M ± SD with N over 12. '*' means P<0.05 and 'ns' means non-significant.

3.3.6.3. H596 Treatment

Similarly as H460 cells, the cisplatin-AZD6244 doublet proved to be relatively potent at 72 hr on H596 compared to that at 24 hr and the biggest change in the viability was observed at 10 µM AZD6244-cisplatin combination with a change of 59% significantly different from that of control group. In contrast, this combination at 24 hr only generated a significant decrease in the viability by 28% compared to control group (Figure 3.23). Although all cisplatin-AZD6244 doublets at 24 hr showed a significant alteration in the viability compared to cisplatin alone, the biggest gap in the viability compared to cisplatin was about 14% at 10 µM AZD6244-cisplatin combination. In opposite, the combination at 72 hr was more active in the reduction of cell viability with a significant decrease by up to 38% at cisplatin combined with 10 µM AZD6244. The cisplatin-AZD6244 combination also showed a drug-resistant trend with the increase in AZD6244 concentration. Therefore, only the 72 hr-treatment with cisplatin combined with 10 µM AZD6244 would be selected for H596 in further experiments.

In summary, only H460 and H596 cells would be treated with 1 µM cisplatin combined with 10 µM AZD6244 at 72 hr in further experiments.

	Cisplatin-AZD6244-24 hr																							
Doses (µM)	Control-0			AZD6244-10			AZD6244-50			AZD6244-100			Cisplatin-1			1+10			1+50			1+100		
	M	SD	N	M	SD	N	M	SD	N	M	SD	N	M	SD	N	M	SD	N	M	SD	N	M	SD	N
Relative viability (% of control)	100	7	18	86*	9	18	98	11	18	105	14	18	86*	9	18	72*	12	18	76*	8	18	83*	13	18

	Cisplatin-AZD6244-72 hr																							
Doses (µM)	Control-0			AZD6244-10			AZD6244-50			AZD6244-100			Cisplatin-1			1+10			1+50			1+100		
	M	SD	N	M	SD	N	M	SD	N	M	SD	N	M	SD	N	M	SD	N	M	SD	N	M	SD	N
Relative viability (% of control)	100	25	18	75*	19	18	92	22	18	72*	14	18	79*	17	18	41*	15	18	42*	12	18	47*	18	18

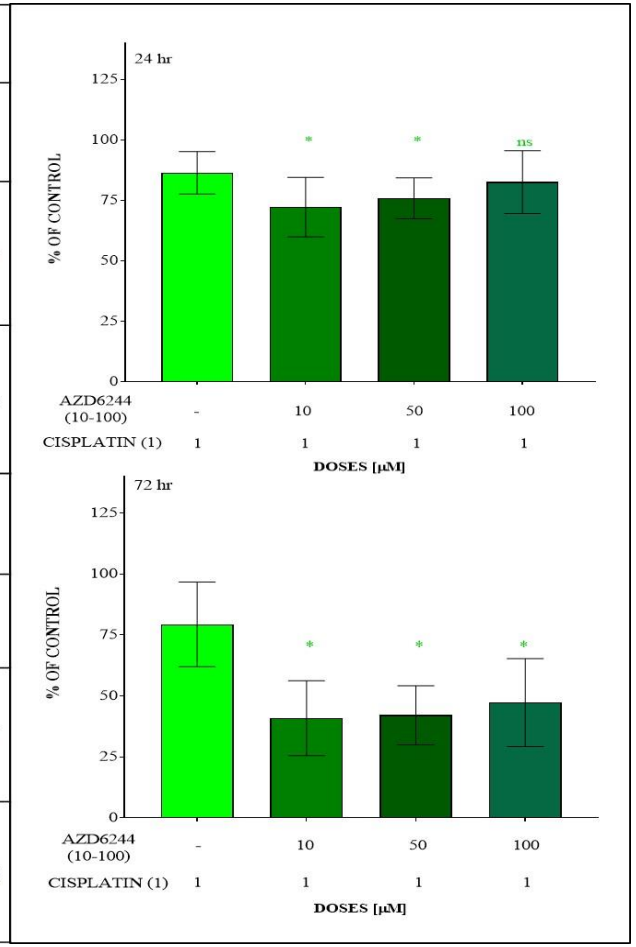

Figure 3. 23 The Cisplatin-AZD6244 combination treatments on H596 at 24 and 72 hr

The table left compares each treatment vs control group at 24 and 72 hr and the significance is labelled with '*', which means P<0.05. The figures show the comparison of 1 µM cisplatin treatment with 10, 50 or 100 µM AZD6244-cisplatin combination treatment at 24 and 72 hr. Data were analyzed by one-way ANOVA by prism and the results are shown as M ± SD with N of 18. The significant comparison is shown in green and '*' means P<0.05 and ns denotes non-significant.

3.3.7. SUMMARY

Overall, the combination of cisplatin with GDC-0941 was more potent on all cell lines compared to the rest of cisplatin-based doublets and the 72 hr treatments with this regimen on all cells were more active than the 24 hr-treatments. Cisplatin combined with MK-2206 was also potent in enhancing the cytotoxicity of cisplatin, particularly on A549 and H460. H596 exhibited resistance to the toxicity of cisplatin combined with STA-9090, DMX502320-04 or DMX503433-09 as well as the cisplatin-MK-2206 doublet at 72 hr. Whereas A549 cells emerged to be resistant to cisplatin-AZD6244 combination compared to the other cell lines.

By comparison, cisplatin combined with GDC-0941 and MK-2206 was more potent than the rest of cisplatin-based doublets and these two regimens would be tested for protein expression in all cell lines by ICW.

3.4. ICW FOR EVALUATION OF ANTIGEN EXPRESSION

The previous part of this chapter has determined the best combinations of drugs to use in 2D cell culture across a panel of lung cancer cell lines, which are cisplatin treatments combined with GDC-0941 and MK-2206 at 24 or 72 hr. Determination of whether cisplatin and the targeted agents alter consequent dysregulated protein expression provides important information regarding the mechanism of action of these drug combinations. Drugs that exhibited the greatest efficacy, both alone and in combination with cisplatin, were those that impinged upon the PI3K signaling pathway either directly or indirectly. To this end, expression of key proteins within the PI3K signaling pathway were evaluated (pAkt, Akt, PTEN) in addition to P53 and cleaved caspase-3.

Due to the number of combinations that needed to be analyzed across 3 cell lines at 2 different time points, traditional western blotting was not appropriate, and a high-throughput methodology was applied. In-cell westerns allowed for multiple analysis to be undertaken in a 96-well plate format with simultaneous detection and normalization of the antigen of interest and an appropriate loading control protein. Absolute quantification could then by undertaken fluorometrically as described in section 2.1.2.3.

3.4.1. ICW FOR CISPLATIN-GDC-0941 COMBINATION

3.4.1.1. 24 hr Treatment

As can be seen in Figure 3.24, the treatment on A549 with 1 µM cisplatin combined with 1 µM GDC-0941 showed a significant ($P<0.05$) increase in the expression of Akt with a 2-fold increase compared to control as well as cisplatin alone. Despite this increase in total Akt, p-Akt was significantly decreased to a 0.3-fold increase compared to control and was also one fifth of that observed in the 1 µM cisplatin group (1.55-fold increase). There was no significant induction of P53 following the combination treatment compared to cisplatin treatment, although 1 µM GDC-0941 significantly decreased the level of P53 expression ($P<0.05$) with a 0.3-fold increase. Similarly, no significant change in the expression of PTEN was observed for any treatment. Cleaved caspase-3 expression in the combination group was significantly increased to a 2.1-fold and nearly 5 times higher than that of single agent cisplatin treatment. In addition, the cell death at this combination was also significantly different from the rest of treatments.

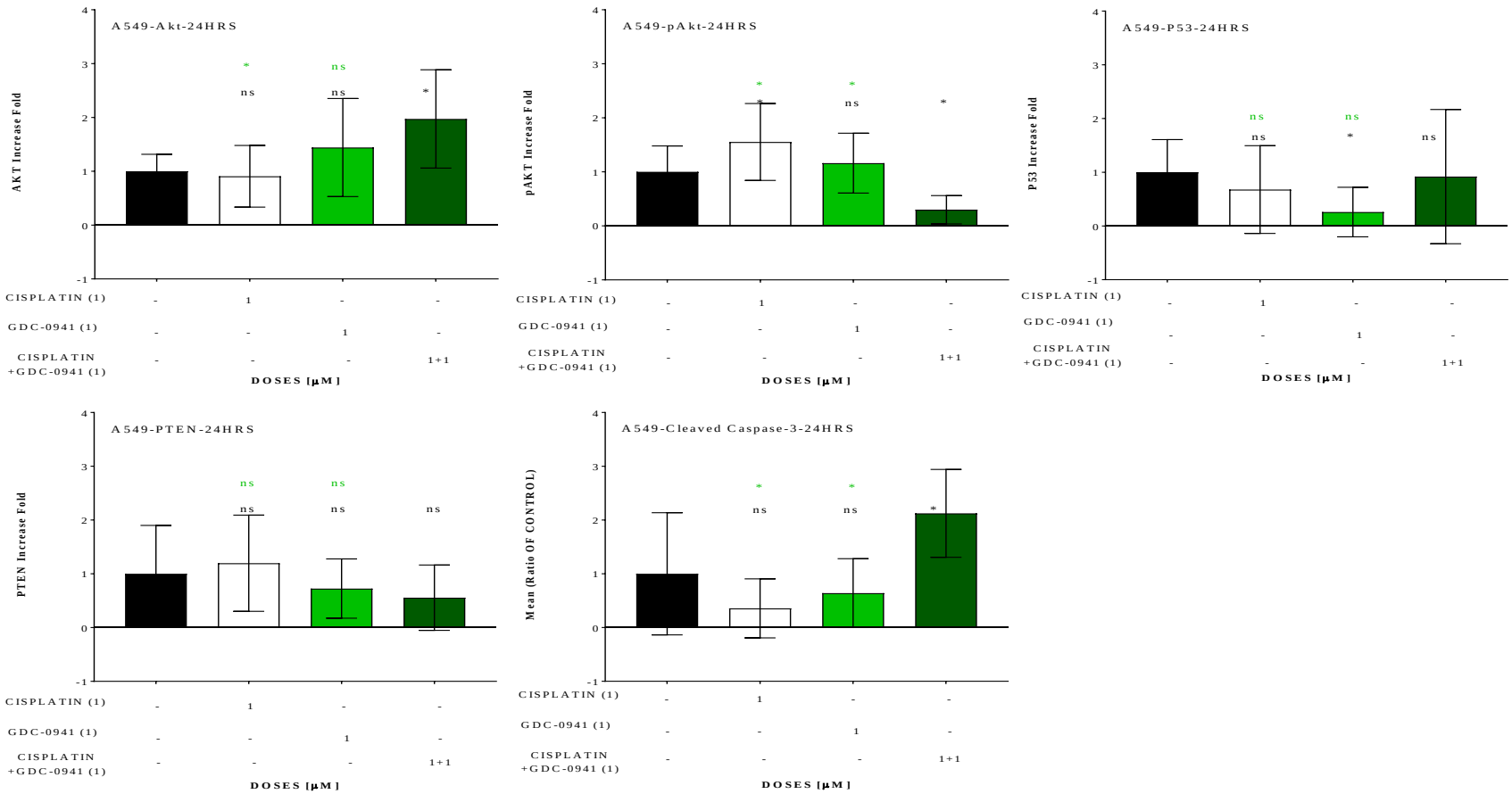

Figure 3. 24 Detection of Akt, pAkt, P53, PTEN and cleaved caspase-3 by ICW for cisplatin-GDC-0941 combination at 24 hr on A549

One µM dose was used for cisplatin and GDC-0941 at 24 hr. Results are shown as M ± SD of over 7 replicates. "*" means P<0.05 and "ns" means non-significant. The significance is shown as black between control group and each treatment group and green between cisplatin-GDC-0941 combination and corresponding single treatments and data were analyzed by one-way analysis by SPSS.

In contrast to the A549s, the combination of cisplatin with GDC-0941 elicited no significant changes to levels of Akt, p-Akt or P53 in H460s when compared to cisplatin only treatments. The combination of cisplatin with 1 μM GDC-0941 significantly affected PTEN to a 2-fold decrease (0.5) compared with cisplatin alone (1.4-fold increase compared to control). Nevertheless, the level of cleaved caspase-3 was nearly doubled at the combination group compared to control and was significantly greater than that of other treatment with 3-times more than that observed at cisplatin treatment (Figure 3.25).

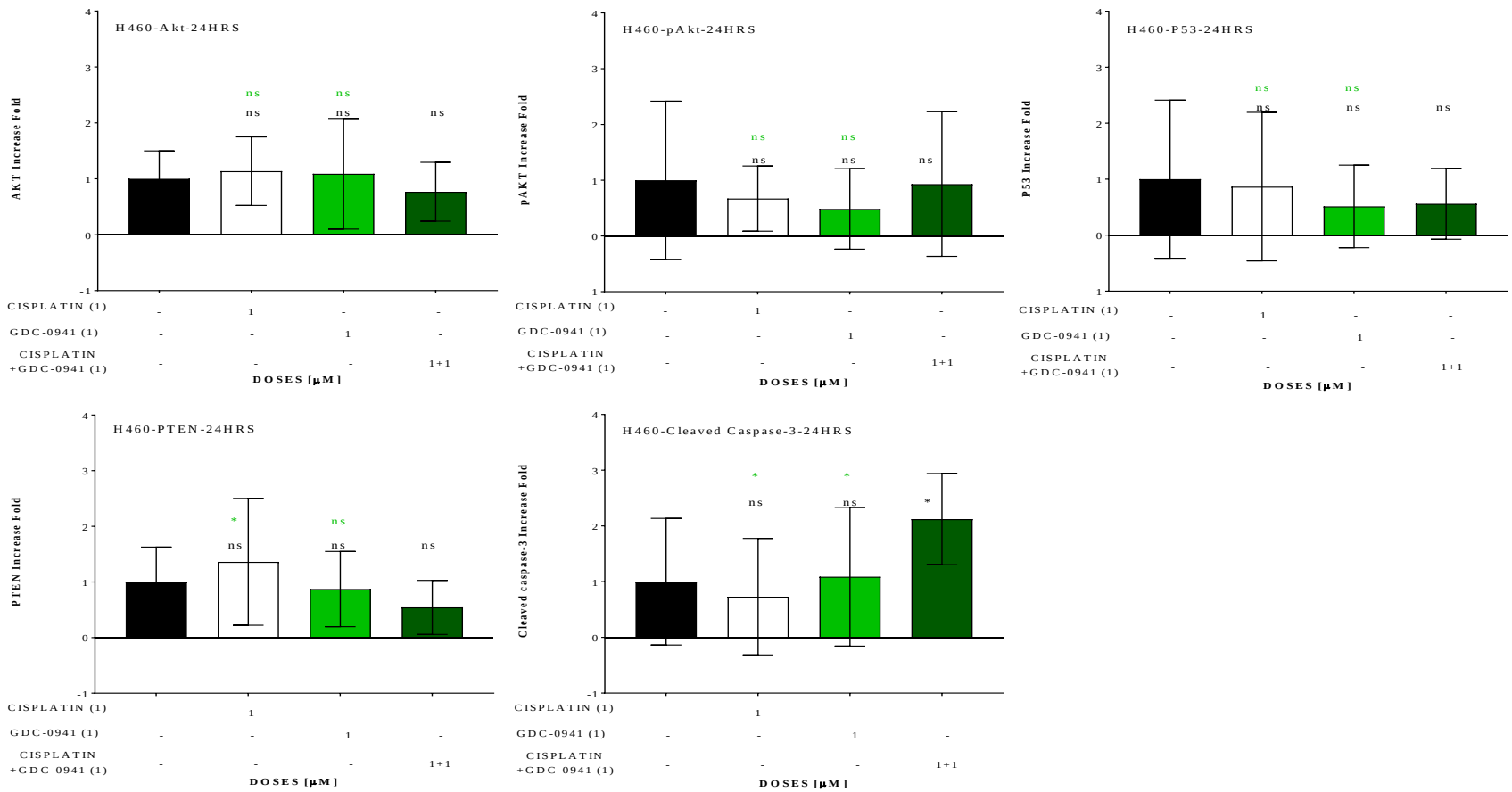

Figure 3. 25 Detection of Akt, pAkt, P53, PTEN and cleaved caspase-3 by ICW for cisplatin-GDC-0941 combination at 24 hr on H460

One µM dose was used for cisplatin and GDC-0941 at 24 hr. Results are shown as M ± SD of over 12 replicates. "*" means P<0.05 and "ns" means non-significant. The significance is shown as black between control group and each treatment group and green between cisplatin-GDC-0941 combination and corresponding single treatments. Data were analyzed by one-way ANOVA by SPSS.

Similarly as H460s, there were no significant alterations to any of the proteins of interest on H596 with the exception for cleaved caspase-3 expression at 24 hr, which was significantly increased by the treatment with 1 μM cisplatin combined with 1 μM GDC-0941 compared to any treatment and control. The cleaved caspase-3 level at 1 μM GDC-0941 combined with cisplatin was significantly increased to 2 times greater than that observed following treatment with cisplatin alone (Figure 3.26).

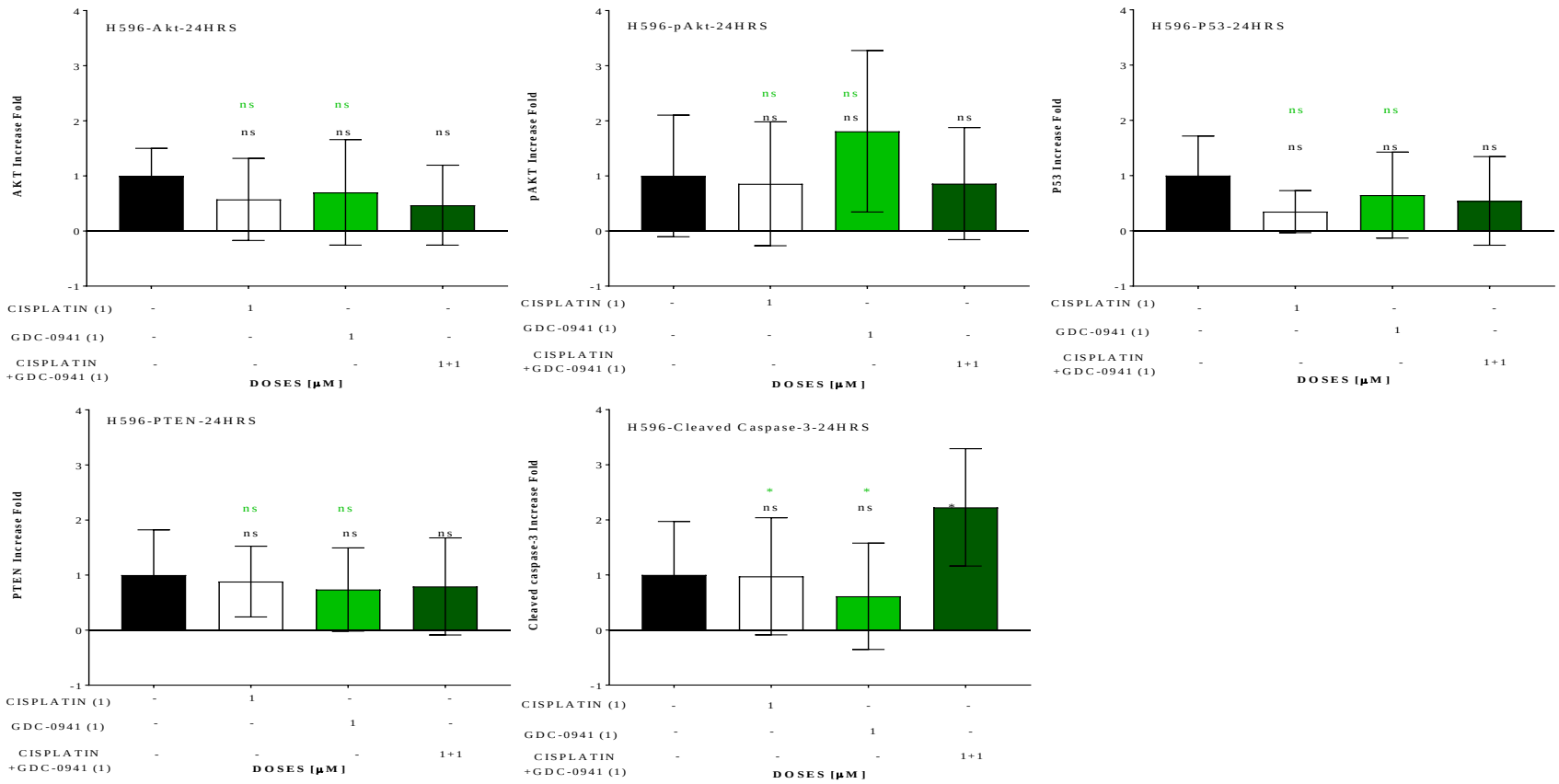

Figure 3. 26 Detection of Akt, pAkt, P53, PTEN and cleaved caspase-3 by ICW for cisplatin-GDC-0941 combination at 24 hr on H596

One µM dose was used for cisplatin and GDC-0941 at 24 hr. Results are shown as M ± SD of over 13 replicates. "*" means P<0.05 and "ns" means non-significant. The significance is shown as black between control group and each treatment group and green between cisplatin-GDC-0941 combination and corresponding single treatments. Data were analyzed by one-way ANOVA by SPSS.

3.4.1.2. 72 hr Treatment

For A549, the 72 hr treatments (Figure 3.27) with cisplatin-GDC-0941 combination revealed no significant changes in p-Akt and P53 expression compared to cisplatin alone. A significant decrease in Akt expression with the combination treatment (0.2-fold increase compared to control) compared to any treatment, which was nearly one third of the levels following treatment with cisplatin only. The combination treatment also showed a significant decrease in PTEN (0.5-fold increase) compared to cisplatin treatment, with a significant decrease in cleaved caspase-3 expression compared to control and 1 µM GDC-0941 alone.

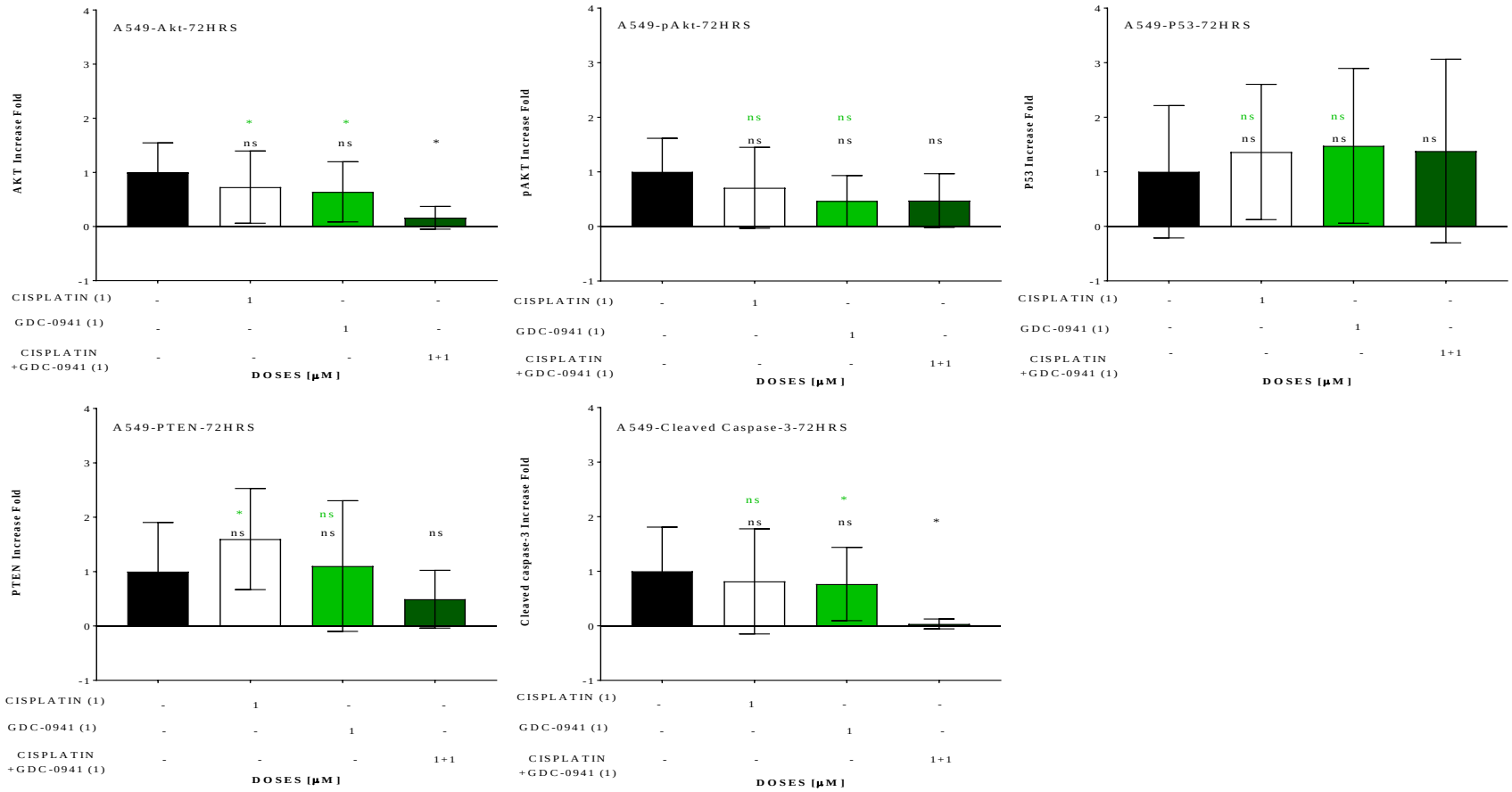

Figure 3. 27 Detection of Akt, pAkt, P53, PTEN and cleaved caspase-3 by ICW for cisplatin-GDC-0941 combination at 72 hr on A549

One µM dose was used for cisplatin and GDC-0941 at 72 hr. Results are shown as M ± SD of over 11 replicates. "*" means P<0.05 and "ns" means non-significant. The significance is shown as black between control group and each treatment group and green between cisplatin-GDC-0941 combination and corresponding single treatments. Data were analyzed by one-way ANOVA by SPSS.

There was no significant change to Akt expression in H460s, compared to that observed in A549 cells. Whereas the combination with GDC-0941 also showed a significant induction in cleaved caspase-3 (1.7-fold increase compared to control) expression compared to cisplatin treatment (0.5-fold increase), similarly observed in H460 cells. PTEN expression was also significantly increased at the combination treatment compared to control only. Both pAkt and P53 expression with the combination treatment were not significantly different from any treatment (Figure 3.28).

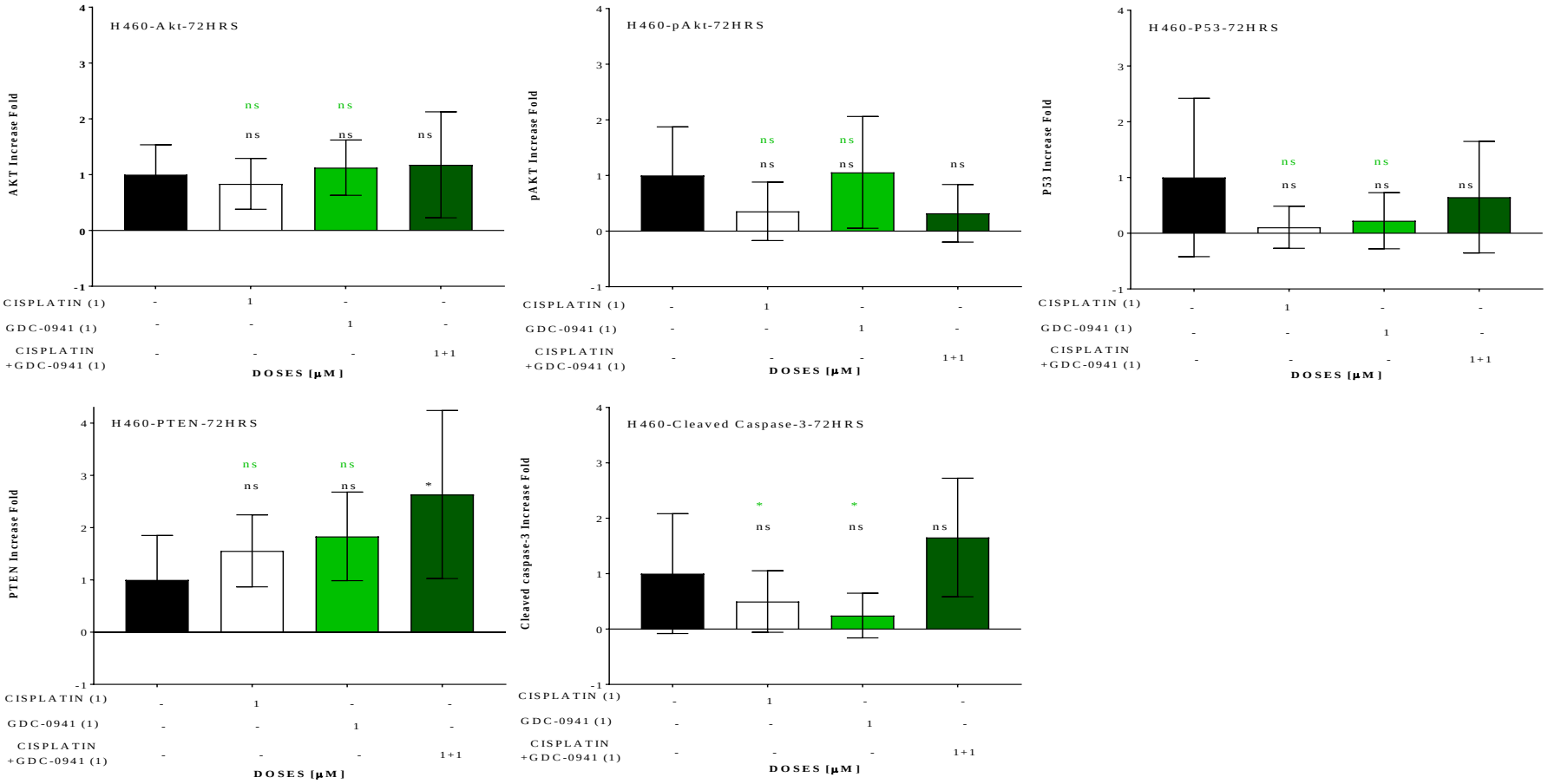

Figure 3. 28 Detection of Akt, pAkt, P53, PTEN and cleaved caspase-3 by ICW for cisplatin-GDC-0941 combination at 72 hr on H460

One µM dose was used for cisplatin and GDC-0941 at 72 hr. Results are shown as M ± SD of over 11 replicates. "*" means $P<0.05$ and "ns" means non-significant. The significance is shown as black between control group and each treatment group and green between cisplatin-GDC-0941 combination and corresponding single treatments. Data were analyzed by one-way ANOVA by SPSS.

In contrast to the cell lines above, H596 showed a significant decrease in the level of p-Akt observed at the combination of cisplatin with GDC-0941 with a 0.2-fold increase compared to control and was significantly lower than either single agent (nearly 1.8-fold increase for both). The expression of PTEN was decreased at the combination treatment compared to control only, although it was not significantly different from cisplatin treatment. Cleaved caspase-3 was decreased to zero by the cisplatin-GDC-0941 combination treatment, although it was not significantly different to any treatment (Figure 3.29).

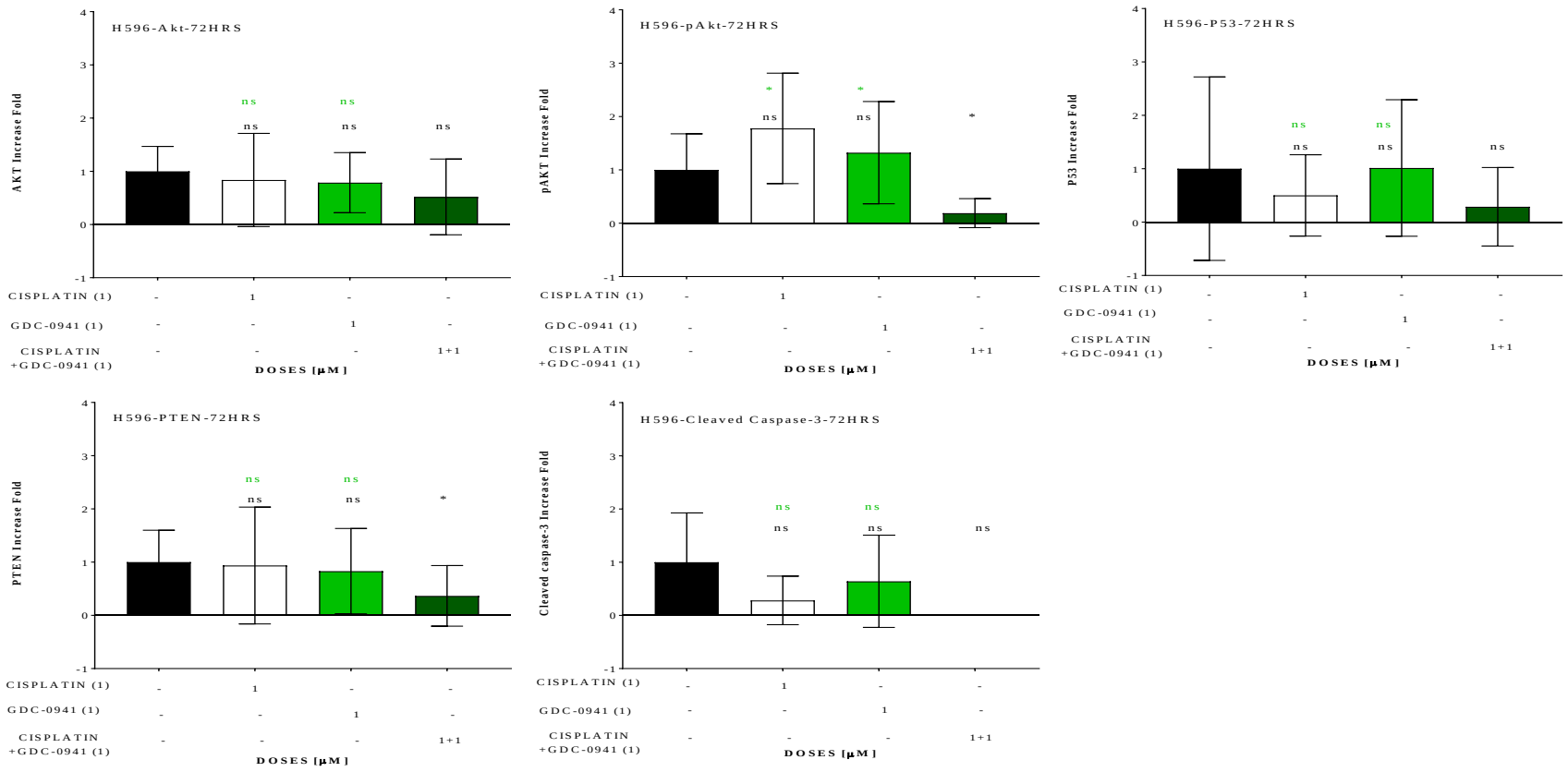

Figure 3. 29 Detection of Akt, pAkt, P53, PTEN and cleaved caspase-3 by ICW for cisplatin-GDC-0941 combination at 72 hr on H596

One µM dose was used for cisplatin and GDC-0941 at 72 hr. Results are shown as M ± SD of over 11 replicates. "*" means P<0.05 and "ns" means non-significant. The significance is shown as black between control group and each treatment group and green between cisplatin-GDC-0941 combination and corresponding single treatments. Data were analyzed by one-way ANOVA by SPSS.

3.4.2. ICW FOR CISPLATIN-MK-2206 COMBINATION

3.4.2.1. 24 hr Treatment

The combination of cisplatin with MK-2206 at 24 hr used for all cell lines consisted of 1 µM cisplatin and 3 µM MK-2206.

Following a 24-hr treatment on A549 cells, whilst there was no significant alteration to Akt expression between cisplatin and cisplatin combined with 3 µM MK-2206, pAkt expression with the combination was significantly reduced to zero, and was significantly different from either single agent and control group. Significant decreases were observed in both P53 (0.3-fold increase compared to control) and PTEN (0.5-fold increase) expressions with the combination treatment compared to cisplatin treatment (1.2- and 1.5-fold increase respectively). The combination group exhibited a similar effect on cleaved caspase-3 expression as the control group and both showed a significant increase in the cell death compared to cisplatin alone (0) (Figure 3.30).

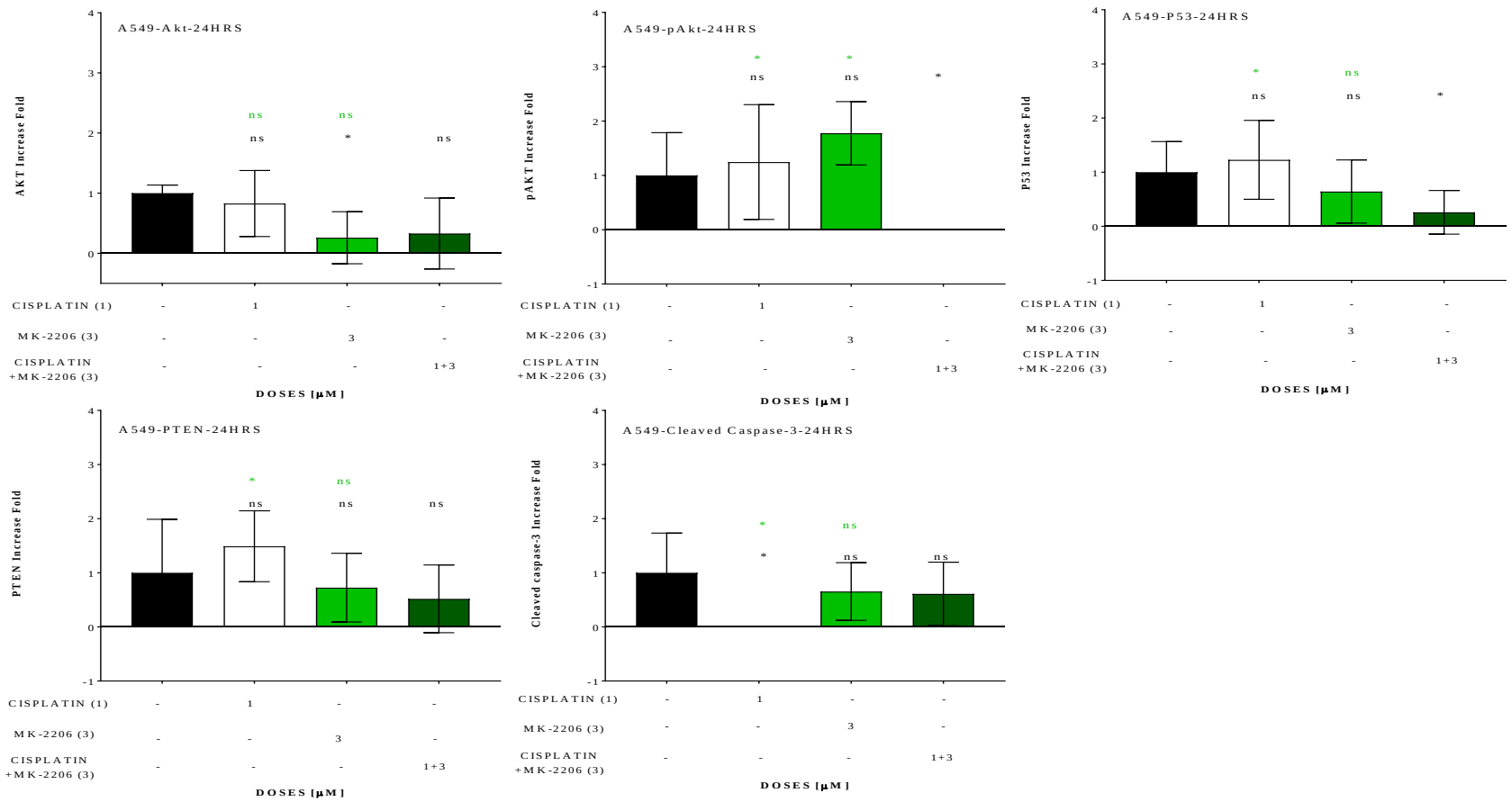

Figure 3. 30 Detection of Akt, pAkt, P53, PTEN and cleaved caspase-3 by ICW for cisplatin-MK-2206 combination at 24 hr on A549

Three µM dose was used for MK-2206 and 1 µM for cisplatin at 24 hr. Results are shown as M ± SD of over 7 replicates. "*" means P<0.05 and "ns" means non-significant. The significance is shown as black between control group and each treatment group and green between cisplatin-MK-2206 combination and corresponding single treatments. Data were analyzed by one-way ANOVA by SPSS.

For H460s, no significant changes were observed to Akt, pAkt and PTEN expression with the MK-2206-cisplatin combination treatment compared to cisplatin treatment alone. P53 expression was significantly decreased in any treatment compared to control, although no significant difference was observed between the combination group and cisplatin alone. A significant increase in cleaved caspase-3 however, was observed following combination treatment compared to 3 µM MK-2206 alone (Figure 3.31).

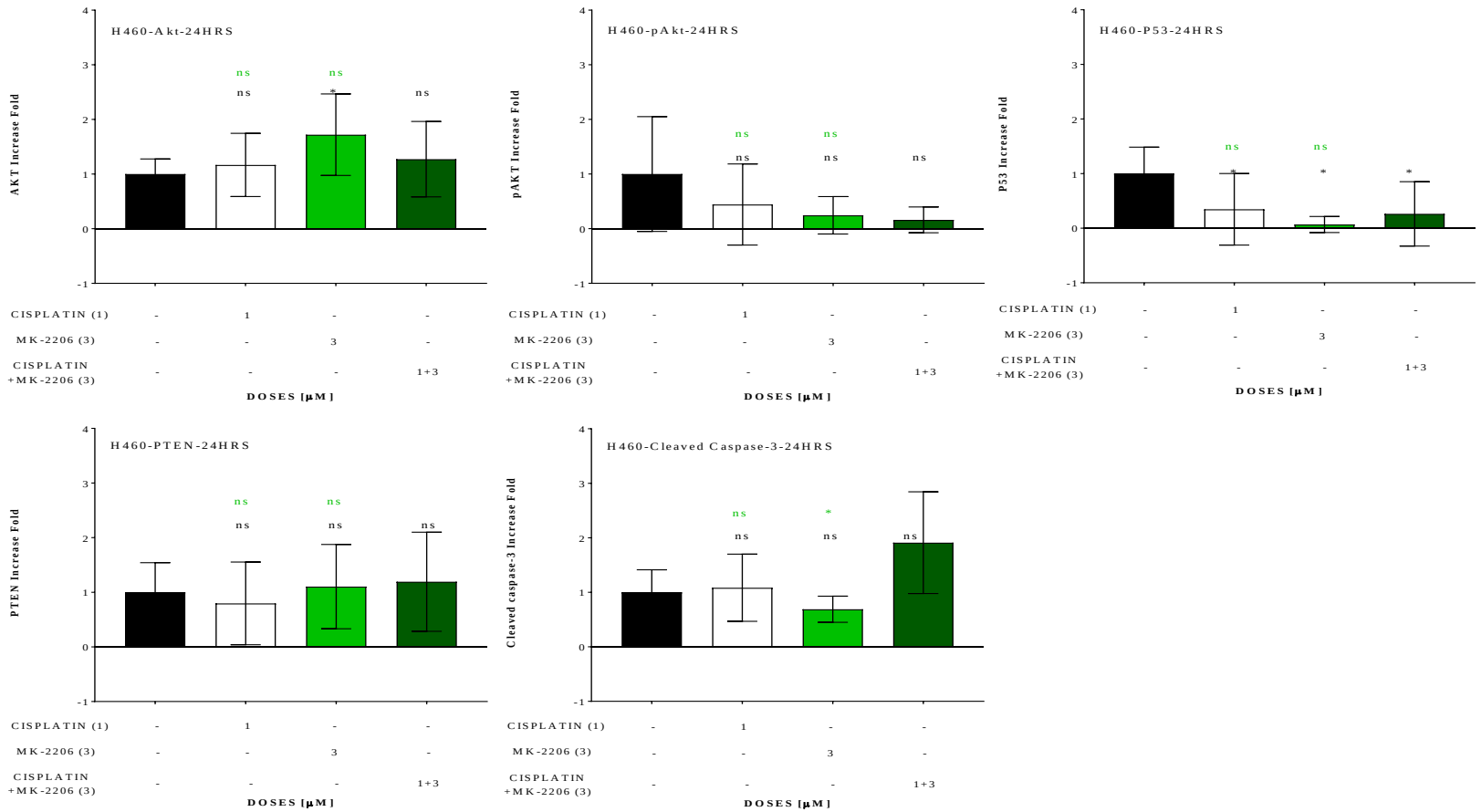

Figure 3. 31 Detection of Akt, pAkt, P53, PTEN and cleaved caspase-3 by ICW for cisplatin-MK-2206 combination at 24 hr on H460

Three µM dose was used for MK-2206 and 1 µM for cisplatin at 24 hr. Results are shown as M ± SD of over 10 replicates. "*" means P<0.05 and "ns" means non-significant. The significance is shown as black between control group and each treatment group and green between cisplatin-MK-2206 combination and corresponding single treatments. Data were analyzed by one-way ANOVA by SPSS.

Similarly to A549s, the combination of MK-2206 with cisplatin on H596s elicited a significant reduction in levels of pAkt (0.2-fold increase compared to control) compared to any treatment, being one sixth of that observed for cisplatin treatment. In conjunction with this, the cleaved caspase-3 level was significantly increased to a 1.8-fold at the combination treatment as compared to cisplatin treatment (0.5-fold increase). The levels of P53 and PTEN remained unchanged by any treatment (Figure 3.32).

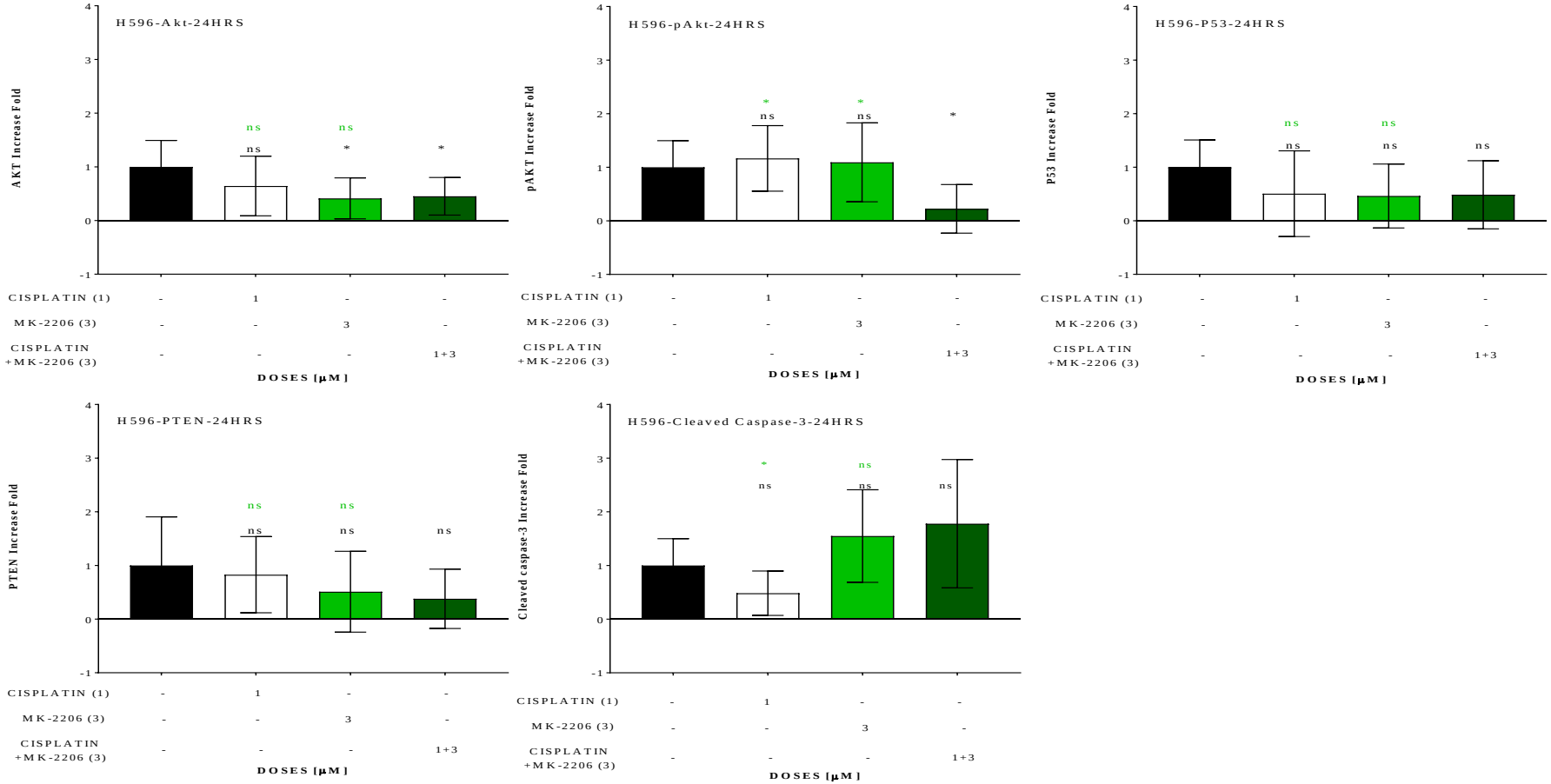

Figure 3. 32 Detection of Akt, pAkt, P53, PTEN and cleaved caspase-3 by ICW for cisplatin-MK-2206 combination at 24 hr on H596

Three µM dose was used for MK-2206 and 1 µM for cisplatin at 24 hr. Results are shown as M ± SD of over 9 replicates. "*" means P<0.05 and "ns" means non-significant. The significance is shown as black between control group and each treatment group and green between cisplatin-MK-2206 combination and corresponding single treatments. Data were analyzed by one-way ANOVA by SPSS.

3.4.2.2. 72 hr Treatment

For 72 hr treatment with the cisplatin-MK-2206 combination, MK-2206 doses for A549 cells covered the entire range and for both H460 and H596 are 3 µM. Cisplatin was used at 1 µM.

In contrast to the 24-hr treatment, 72 hr-treatment showed few significant alterations to any antigen levels between cisplatin and the MK-2206-cisplatin combinations observed in A549 cells. Nevertheless, 1 µM cisplatin in combination with 12 µM MK-2206 significantly reduced p-Akt expression compared to control group with a 0.3-fold increase. It is also notable to see that few changes in protein levels were observed with increased concentrations of MK-2206 (Figure 3.33).

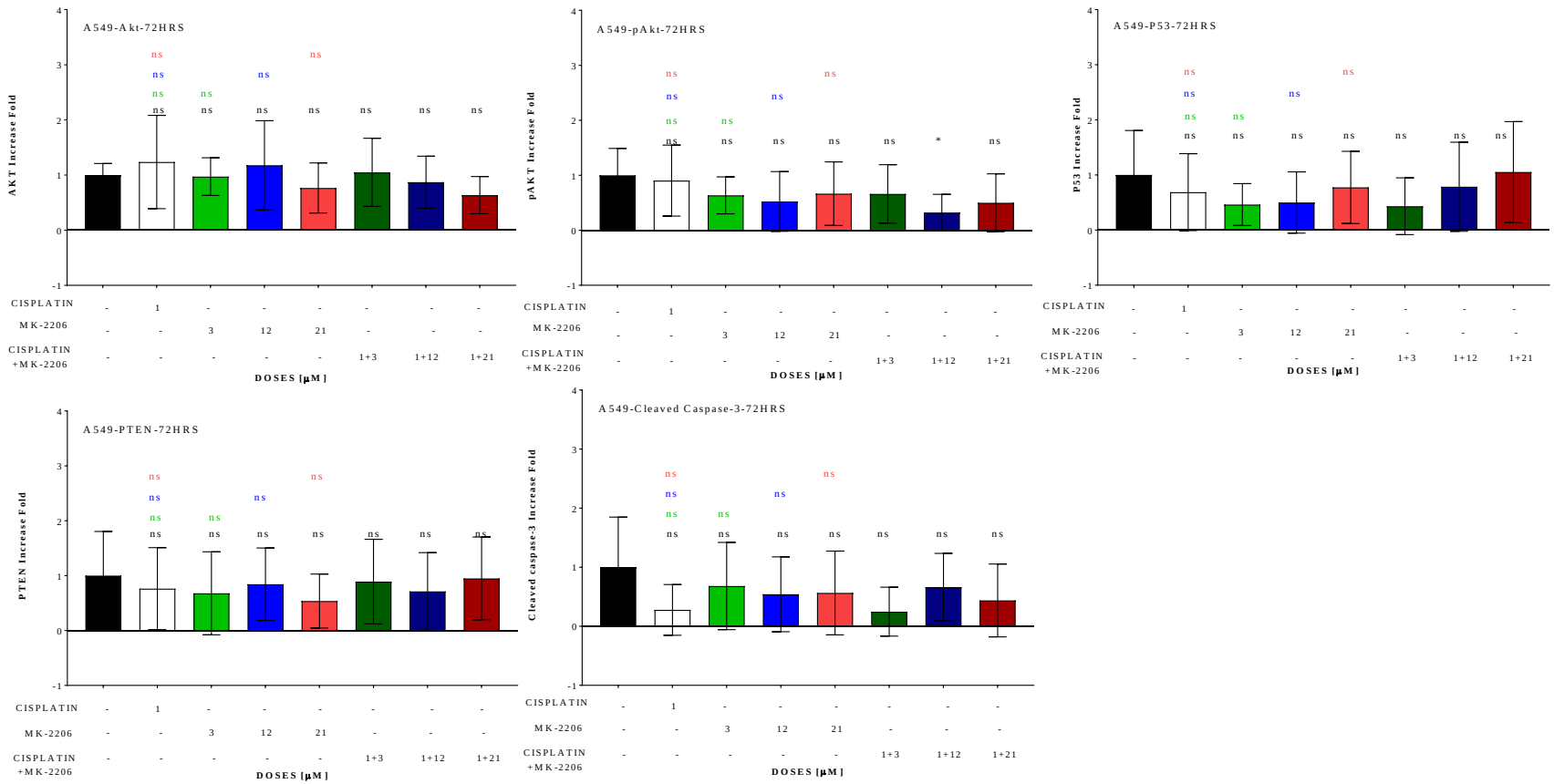

Figure 3. 33 Detection of Akt, pAkt, P53, PTEN and cleaved caspase-3 by ICW for cisplatin-MK-2206 combination at 72 hr on A549

MK-2206 doses selected at 72 hr for A549 covered the entire range. Results are shown as M ± SD of over 11 replicates. "*" means P<0.05 and "ns" means non-significant. The significance is shown as black between control group and each treatment group, green for 3 µM-, blue for 12 µM- and red for 21 µM containing combinations treatments vs corresponding single treatments. Data were analyzed by one-way ANOVA by SPSS.

Similarly as shown in A549s, no alteration to pAkt, P53, PTEN or cleaved caspase-3 expression was observed at the combination treatment compared to any groups on H460. Only Akt expression at 3 µM MK-2206 combined with cisplatin was significantly decreased compared to the control group (Figure 3.34).

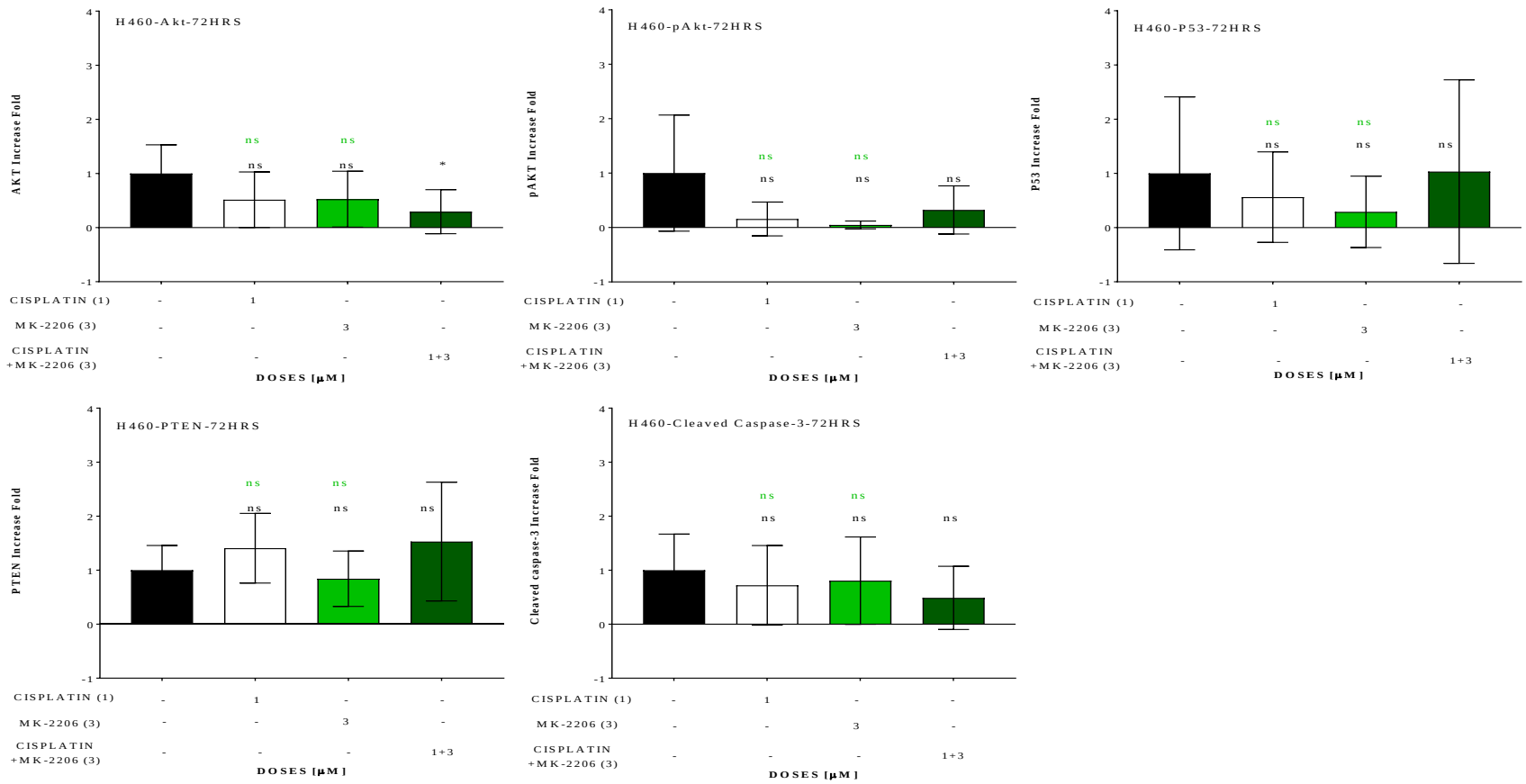

Figure 3. 34 Detection of Akt, pAkt, P53, PTEN and cleaved caspase-3 by ICW for cisplatin-MK-2206 combination at 72 hr on H460

3 µM MK-2206 dose was selected at 72 hr for H460. Results are shown as M ± SD of over 10 replicates. "*" means P<0.05 and "ns" means non-significant. The significance is shown as black between control group and each treatment group, green for 3 µM-combinations treatments vs corresponding single treatments. Data were analyzed by one-way ANOVA by SPSS.

For H596, no significant alterations were observed to any antigens of interest between cisplatin and the combination treatment. Nevertheless, the cisplatin-MK-2206 combination showed significant decreases in pAkt and PTEN levels compared to control group (Figure 3.35).

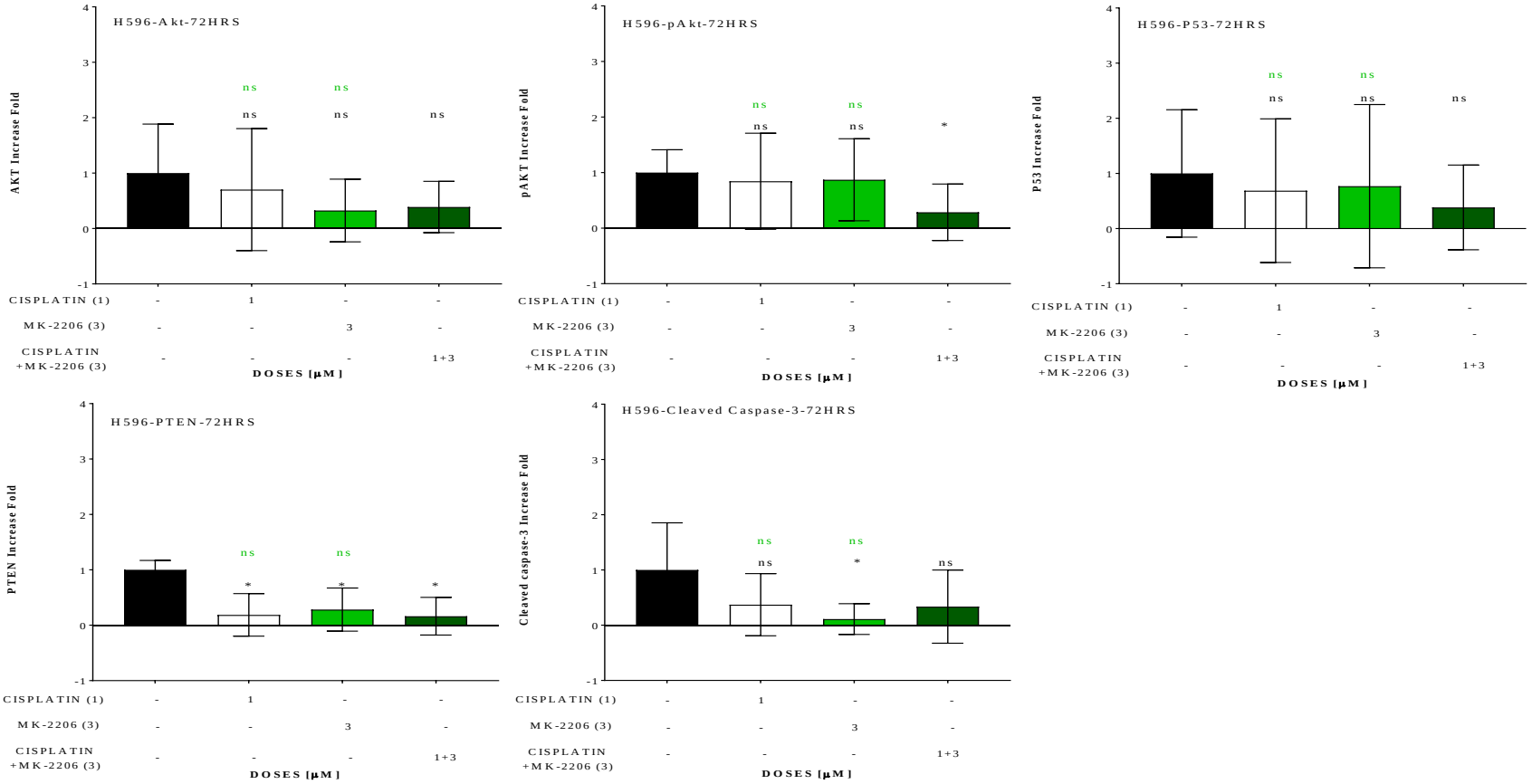

Figure 3. 35 Detection of Akt, pAkt, P53, PTEN and cleaved caspase-3 by ICW for cisplatin-MK-2206 combination at 72 hr on H596

3 µM MK-2206 dose was selected at 72 hr for H596. Results are shown as M ± SD of over 12 replicates. "*" means P<0.05 and "ns" means non-significant. The significance is shown as black between control group and each treatment group, green for 3 µM-combinations treatments vs corresponding single treatments. Data were analyzed by one-way ANOVA by SPSS.

In summary, the combination of cisplatin with GDC-0941 or MK-2206 at 24 and 72 hr across all cell lines showed few significant decreases to pAkt levels compared to cisplatin treatment. Akt inhibition seemed to be more potent at reducing pAkt than PI3K inhibition when combined with cisplatin treatment. Nevertheless, the expression of cleaved caspase-3 was observed to be significantly induced following the 24-hr treatment with both combination treatments. By comparison, GDC-0941 was more potent at inducing cell death than MK-2206 when combined with cisplatin at 24 and 72 hr. Both P53 and PTEN expression observed in all cell lines were most likely to be unaltered following treatments (both 24 and 72 hr) with cisplatin combined with GDC-0941 or MK-2206 compared to cisplatin-only treatment.

3.5. DISCUSSION

The purpose of this chapter was to perform a high-throughput screen for drug potencies in a panel of lung cancer cell lines exhibiting some of the more common mutations observed in NSCLC. The cell lines investigated exhibited *KRAS* mutation (A549); *KRAS* and *PIK3CA* mutations (H460); *PIK3CA* and *TP53* mutations (H596), and sensitivity to treatments will be discussed within this context.

3.5.1. THE ROLE OF P53 IN RESPONSE TO CISPLATIN-BASED CHEMOTHERAPY

P53 plays a role in cell response to cisplatin treatment. It can be activated by cisplatin-induced DNA damage via DDR pathways (reviewed in 1.4.3.7) and functions to transactivate genes involved in cell cycle progression, DNA repair and apoptosis (Dasari & Tchounwou, 2014). The main action of P53-mediated apoptosis is to promote pro-apoptotic protein expression, such as Bcl-2 homologous antagonist/killer (BAK), Bcl-2-like protein 4 (BAX) (Matsumoto, et al., 2016), phorbol-12-myristate-13-acetate-induced protein 1 (PMAIP1 or NOXA) and P53 upregulated modulator of apoptosis (PUMA) (Zambetti, 2005) but inhibits anti-apoptotic protein expression, such as Bcl-2 (Zambetti, 2005). P53 mutation has emerged as an important biomarker for prediction of cisplatin resistant NSCLC (Godwin, et al., 2013). Studies have shown that chemosensitivity of *P53* mutant NSCLC cell lines is restored upon transfection with the WT *P53* gene (Lai, et al., 2000) (Guntur, et al., 2010) to restore an adequate DNA damage response, leading to DNA damage-induced apoptosis and consequent increased cytotoxicity of cisplatin.

The dependence of P53 in initiating cisplatin-induced cell death is not clear-cut, as cisplatin can also induce apoptosis in P53-mutant cancer cells (Matsumoto, et al., 2016). The H596 cell line contained a *P53* mutation (G245C, missense mutation) yet still showed the greatest sensitivity to cisplatin treatments compared to A549 and H596, both of which are P53 WT. These findings relating to cisplatin sensitivities are also confirmed in other studies. H596 cells showed a greater sensitivity towards to cisplatin treatment than A549s (Shi, et al., 2014) and have also been shown to have a similar or lower IC50 than that observed in normal lung cells such as WI-38 (Shi, et al., 2014) and MRC-5 (Kong , et al., 2015). Harrington et al (Harrington , et al., 2010) showed significantly lower levels of cisplatin-induced adducts in cisplatin resistant A549 cells compared with cisplatin-sensitive H23 cells. Chen et al. also observed that H460 cells exhibited cisplatin resistance compared to other cell lines such as H23 and H520 (Chen, et al., 2011). The phenomena that cisplatin sensitivity does not correlate with WTP53 expression can also be observed in several other tumor types, as P53 mutations have been found to correlate with cisplatin sensitivity in head and neck squamous cell carcinoma (HNSCC) (Bradford, et al., 2003) and testicular cancer (di Pietro, et al., 2012).

However, there are many P53-independent factors that may affect resistance to cisplatin. Aberrant activation of cell survival pathways via mutations in *KRAS* and *PIK3CA* also represent key determinants of resistance independent from *P53* status, with *KRAS* WT H596 cells showing greatest sensitivity to cisplatin. Meta-analysis now shows more convincing evidence that *KRAS* mutations negatively predict benefit from standard-of-care chemotherapeutics and therapies directed against EGFR (Riely , et al., 2009). Emerging mechanisms of *KRAS*-mediated cisplatin resistance also include enhanced base excision repair mechanisms, leading to more efficient removal of platinum adducts and so decreasing cisplatin cytotoxicity (Caiola, et al., 2015).

3.5.2. TARGETING PI3K/AKT SIGNALING IN NSCLC

The use of targeted therapies in conjunction with standard-of-care therapeutics has become increasingly important for improving outcomes in lung cancer. Many targeted therapies are already approved, such as use of bevacizumab, crizotinib, erlotinib, gefitinib afatinib and sunitinib (Farhat & Houhou, 2013). However, as understanding of molecular profiles in lung cancer subsets improves, the number of potential molecular targets also increases.

Despite these advances and improvement to survival benefit following addition of molecularly targeted agents to the cisplatin-based chemotherapeutic regimens for NSCLC, a large proportion of patients still exhibit poor response. The resistance to EGFR inhibitors has been studied to associate with the activation of oncogenes by genetic alterations, such as *KRAS* mutations (Stewart, et al., 2015) or secondary *EGFR* mutations (e.g. T790M), *BRAF* and *PIK3CA* mutations, *MET* and *HER2* amplifications (Stewart, et al., 2015; Huang & Fu, 2015). The activation in RAS/MAPK signaling and PI3K/Akt signaling pathways is also linked to resistance to EGFR-targeted treatment (Stewart, et al., 2015). An *in vitro* study shows that Akt inhibition combined with gefitinib-mediated EGFR inhibition, could synergistically inhibit cell growth and induce apoptosis in both EGFR-mutant and WT NSCLC cell lines (Puglisi, et al., 2014). The activation of PI3K/Akt signaling was also found to correlate with the resistance to ALK-targeted therapy and blocking the PI3K pathway could enhance potency of ALK-targeted therapy in NSCLC cell lines (Yang, et al., 2014).

The PI3K signaling pathway is implicated in many processes that are critical in the regulation of tumor cell growth and survival in NSCLC, in addition to the extensive cross-talk observed between this pathway and the RAS and EGFR signaling pathways. Therefore, the PI3K/Akt signaling pathway could be a successful target for NSCLC treatment. Although the activation of Akt usually requires the concomitant phosphorylation at both S^{473} and T^{308}, the phosphorylation of Akt at S^{473} is usually applied as an indicator of Akt activity (Scrima, et al., 2012) (Brognard, et al., 2001).

3.5.3. TREATMENTS THAT DIRECTLY TARGET AKT COMBINED WITH CISPLATIN

Increase in potencies compared to single agent cisplatin or other targeted agents alone, was observed across a number of cisplatin-based doublets for the cell lines. Both A549 and H460 cells which were the most resistant to cisplatin, nearly showed benefit from all cisplatin-based doublets, whereas the H596, the most sensitive to cisplatin treatment, showed a limited effect at the cisplatin-based combination treatments. As all cell lines contain mutations that can activate the PI3K/Akt pathway (either directly or indirectly), it is unsurprising that the greatest benefit is observed with the addition of GDC-0941 or MK-2206 to cisplatin treatments.

PI3K activation is often associated with aberrant alterations in the *PIK3CA* gene (reviewed in 1.4.3.4 and 1.4.3.5) and subsequently activates downstream Akt signaling to mediate regulation of tumor cell growth and survival in NSCLC. Additionally, KRAS activation can crosstalk with the PI3K/Akt signaling pathway or mediates RALB/TBK1 signaling pathway to promote Akt activation (reviewed in 1.4.3.2 and 1.4.3.6). Akt activation is considered as a predictor of PI3K/Akt signaling pathway activity, with Akt inhibition able to actively block PI3K-mediated signaling pathway. PI3K or TBK1 inhibition is able to directly inhibit Akt phosphorylation and block consequent downstream signaling pathways. Therefore, PI3K (GDC-0941), Akt (MK-2206) and TBK1 (DMX502320-04 and DMX503433-09) inhibitors are considered as agents that directly target Akt.

3.5.3.1. Drug Response to GDC-0941 and MK-2206 Treatments

Targeting of PI3K and its downstream effector molecules such as Akt is of increasing clinical interest, with GDC-0941 already in early phase clinical trial for a number of tumor types including NSCLC (Martini, et al., 2013). H460 cells exhibiting a *PIK3CA* and *KRAS* mutation were the most sensitive to both PI3K and Akt inhibitors, compared with A549 cells possessing wild type *PIK3CA*. Zhou *et al* examined response of A549 and H460 cells to combined PI3K and MEK inhibition using GDC-0941 in combination with MEK inhibitor-UO126; A549 cells were less sensitive to GDC-0941 alone than were H460 cells (Zou , et al., 2012) in agreement with the study presented here. As sensitivity to PI3K inhibition in both cell lines was increased upon the addition UO126 (Zou , et al., 2012), it suggests that proliferative capacity in these cell lines is mediated by extensive cross-talk and that targeting of more than one signaling pathway would be of benefit. Use of the allosteric Akt inhibitor MK-2206 has also shown activity in NSCLC cell lines that exhibit resistance to EGFR inhibitors, again suggesting that combined use of inhibitors targeting multiple pathways may provide a more potent route against NSCLC cells that exhibit *KRAS* mutation (Iida, et al., 2013). Akt activation has been shown to correlate with resistance to chemotherapy and radiation (Hirai, et al., 2010) (Brognard, et al., 2001) (Lee, et al., 2008) and activated Akt can predict the response of solid tumors to chemo/radiation therapy (Toulany & Rodemann, 2015). Previous reports have suggested that cisplatin is able to induce activation of PI3K/Akt pathway in A549 and H460 cells, which further contributes to cisplatin chemoresistance. In addition, there is evidence that

MK-2206 can enhance potency of cisplatin in urothelial cancer cells due to decreased Akt signaling (Sun , et al., 2015).

Therefore, addition of PI3K/Akt-targeting agents may have the ability to restore cisplatin-based chemosensitivity. Additionally, PI3K activity was shown to play a role in Akt-associated cisplatin-resistance and PI3K inhibition could sensitize cells (particularly cisplatin-resistant cells) to cisplatin therapy via downregulating Akt activation (Liu, et al., 2007). This was similarly observed in the work presented here, as GDC-0941 was more potent than MK-2206 in promoting expression of cleaved caspase-3 when combined with cisplatin, although significant decreases to pAkt were not markedly observed when comparing combination treatments to cisplatin treatment.

As reviewed in 1.5.7.1, both GDC-0941 and MK-2206 have undergone further investigations in early phase clinical trials. GDC-0941 was assessed in combination with a MEK inhibitor-GDC-0973 in a phase Ib, which showed encouraging activity in patients with melanoma, prostate cancer and NSCLC (Papadimitrakopoulou, 2012). Another phase Ib/II tested GDC-0941 in combination with paclitaxel/carboplatin regimen with or without bevacizumab (NCT01493843) for treatment of advanced NSCLC. The phase Ib showed a good outcome with this combination regimen having a 75% overall response rate among 4 patients with squamous NSCLC and 66% showing a partial response among 9 patients with non-squamous NSCLC (Genentech clinical data (Phase I) (NSCLC), 2011) (Besse, et al., 2011). Another trial was to evaluate the efficacy of GDC-0941 in combination with erlotinib showed a poor response with only two patients showing a partial response, whereas 20 patients had a progression disease (Genentech clinical data (Phase I) (solid tumor) , 2012). MK-2206 was evaluated in phase I trial when combined with gefitinib or erlotinib for treatment of advanced NSCLC patients who had progressed after previous EGFR-targeted therapy. The result from MK-2206-erlotinb combination showed that patients with mutant and WT EGFR mutation had a poor objective response rate (ORR) less than 10%, although both two cohorts had a high disease control rate at 40-43% (National Cancer Institute (NCI) , 2016). A phase II trial (the BATTLE-2 programme) is currently evaluating MK-2206 in combination with AZD6244 or erlotinib for treatment of refractory NSCLC patients (Fumarola , et al., 2014).

3.5.3.2. Drug Response to DMX502320-04 and DMX503433-09 Treatments

A549 cells were the most sensitive cell line to TBK1 inhibition, with DMX502320-04 and DMX503433-09 exhibiting a similar effect on cell viability reduction. TBK1 blockade has been found to be active in cells harboring a *KRAS* mutation, with TBK1-mediated survival of *KRAS*-mutant cells not correlated with Akt activity, and TBK1 signaling remaining distinct from MAPK and PI3K signaling (Zhu, et al., 2014). Nevertheless, it was suggested that cell intrinsic defects in Akt-mediated signaling contributed to TBK1 regulated cell survival (Zhu, et al., 2014). The TBK1/Akt pro-survival signaling was studied to associate with selective extracellular stimuli, such as EGF, glucose and exocyst (Ou, et al., 2011). In the study, both TBK1 inhibitors were not active in treating the mutant-*PIK3CA*-containinging cell lines (H460 and H596), which contained a more active PI3K-mediated downstream signaling compared to that in A549 cells. This suggested that TBK1 inhibition-mediated Akt inactivation was not potent as compared to that by PI3K or Akt inhibition. This could explain why all cell lines were not shown sensitive to TBK1 inhibition,

3.5.4. TREATMENTS THAT INDIRECTLY TARGET AKT COMBINED WITH CISPLATIN

PI3K/Akt signaling pathway can also be indirectly activated via crosstalk with other effectors. PTEN mutation or deletion can cause indirect activation of PI3K signaling pathway (reviewed in 1.4.3.5).

3.5.4.1. Drug Response to MEK Inhibition

MEK inhibition has long been a focus for anti-cancer treatments, with *KRAS* mutations leading to sustained signaling through the MEK/ERK pathway. The data available in the genomics of drug sensitivity database (http://www.cancerrxgene.org/translation/Feature/152#t_scatter_152) that KRAS mutation significantly associates with AZD6244 sensitivity, which showed a lower IC50 of the agent in *KRAS* mutant cell lines compared to that in KRAS-WT cohorts. Nevertheless, ERK inhibition has been shown to be less active in decreasing Akt activity, with some studies showing that Akt activation was responsible for resistance to ERK inhibition (Meng, et al., 2009). Many NSCLC cells show intrinsic resistance to AZD6244 treatment, with activation of the PI3K/Akt pathway and/or weak ERK signaling thought

to correlate with this resistance (Balmanno, et al., 2009). Blockade of the PI3K pathway was demonstrated to promote the sensitivity of *KRAS* mutant cell lines to MEK inhibition (Ku, et al., 2015), with combination of AZD6244 and MK-2206 showing greater potency than either drug alone (Meng, et al., 2010). Similarly as shown in the study herein, A549 cells were the most sensitive to AZD6244, with H460 and H596 similarly resistant as one another. Similarly, inhibition of signaling through ERK has been found to increase sensitivity of cells to cisplatin treatment in squamous cell carcinoma models (Wang, et al., 2013) (Kong , et al., 2015), with activation of ERK demonstrated to play a critical role in maintaining cisplatin resistance in the lung cancer cell lines H520 and Calu-1 (Kong , et al., 2015).

AZD6244 has undergone several clinical trial studies. A phase II study showed that patients with *KRAS* mutation after given with the combination of AZD6244 with docetaxel showed a significant ($P<0.05$) improvement in PFS (median 5.3 months) and a significant ORR (37%) compared with the receiving docetaxel single treatment cohorts (PFS: 2.1 months and ORR:0%) (Stinchcombe & Johnson , 2014) (Goldman & Garon, 2012). Whereas the recent phase III study reported by ©AstraZeneca showed that the efficacy of AZD6244 combined with docetaxel shown in phase II was not demonstrated in the third trial and this combination regimen was not effective in improving the PFS of patients (AstraZeneca, 2016). Moreover, there are more clinical assessment on AZD6244 combination with cisplatin-based chemotherapy (available in https://clinicaltrials.gov/ct2/home), such as paclitaxel/carboplatin, pemetrexed/cisplatin regimen. Similarly as GDC-0941 and MK-2206, AZD6244 has also been evaluated in combination with erlotinib (the combination with gefitinib is ongoing) for treatment of advanced NSCLC in phase II. This study showed that the combination of AZD6244 with erlotinib in *KRAS* mutant patients had a higher ORR than those treated with single erlotinib, whereas the PFS was similarly observed in the two arms. This comparison has also been evaluated in *KRAS*-WT patients, which showed patients treated with either single or combination treatments had a similar PFS and ORR (Stinchcombe & Johnson , 2014).

3.5.4.2. Drug Response to HSP90 Inhibition

Evaluation of STA-9090 in a panel of *KRAS* mutant NSCLC cell lines revealed inhibition of activity for numerous signaling molecules including EGFR, Akt, MEK and STAT3

(Signal transducer and activator of transcription 3), with an associated increase in cytotoxicity (Acquaviva, et al., 2012). Additionally, HSP90 inhibition shown in a NSCLC study (Gomez-Casal, et al., 2015) and other studies (pleomorphic sarcoma (Bekki, et al., 2015), glioblastoma and colon carcinoma cells (Djuzenova, et al., 2016)), can lead to concomitant downregulation of PI3K and ERK signaling pathways to promote cell death (Djuzenova, et al., 2016) (Bekki, et al., 2015). Taken together, this alludes to the importance of HSP90 inhibition in the inactivation of Akt kinase and downregulation of Akt-associated signaling pathways (PI3K/Akt/mTOR and MAPK signaling pathways). In the study presented herein, all cell lines exhibited good sensitivity to STA-9090 treatment, although H460 cells were the most responsive.

Due to the successes of STA-9090 observed in pre-clinical models of *KRAS* mutants, there has been much interest in taking it forward to the clinic. STA-9090 has been evaluated in several clinical studies. STA-9090 as monotherapy has demonstrated objective responses or anti-tumor activity in patients with ALK-positive and with mutant BRAF or KRAS lung cancers (PiercePharma, 2012). In a phase II study, STA-9090 was effective in treatment of ALK-patients who have not been treated with a ALK inhibitor before and had experienced 50% objective response (Madrigal pharmaceuticals, 2012). STA-9090 was also tested in combination with other agents, such as crizotinib and docetaxel. A phase I/II trial at Memorial Sloan-Kettering Cancer Centre demonstrated that combination of crizotinib with STA-9090 showed activity against ALK-positive lung cancer and had potential to improve clinical outcomes (Madrigal pharmaceuticals, 2012). Although combination of STA-9090 with docetaxel in early phases showed encouraging improvements in PFS, ORR, and OS of lung cancer patients compared to the those with docetaxel alone (Ramalingam, et al., 2015) (PiercePharma, 2012), the recently completed phase III study has demonstrated that the combination of STA-9090 with docetaxel failed to enhance the toxicity of docetaxel with a similar ORR at the combination (13.7%) and docetaxel single treatment (16%) and both two arms showed a similar OS (10 months) and PFS (4 months) (Synta Pharmaceuticals Corp. , 2016).

In discussing the effects of single agent treatments on NSCLC cell lines, it should be noted that whilst the cell lines are known to have mutations in *TP53*, *PIK3CA* and *KRAS*, these cells are also subject to numerous other mutations which could have significant impact on their response to the drugs used. As previously discussed, extensive cross-talk

exists between key signaling pathways and so seemingly 'off target' effects may be observed. Furthermore, the possibility arises that downregulation of one signaling pathway may provide a compensatory upregulation of a different pro-survival/proliferation pathway. It would therefore be of interest to conduct more in-depth investigation regarding interactions between our targets of interest.

Single agent small molecule inhibitors would never be used clinically in NSCLC, and so we sought to determine their effects when in combination with the most commonly used first line chemotherapeutic agent-cisplatin.

3.5.5. PROTEIN EXPRESSION FOLLOWING COMBINATION OF CISPLATIN WITH GDC-0941 OR MK-2206

Proteins investigated here included Akt, pAkt, P53, PTEN and cleaved caspase-3. P53-mediated DNA damage response to cisplatin treatment (reviewed in 1.4.3.8) can be affected or interconnected with the PI3K/Akt signaling pathway to determine the cell survival/apoptosis. As reviewed in 1.4.3.8, Akt can activates MDM2 to promote cell survival which can inhibit the activity of P53 via degradation. Conversely, PTEN can be transcriptionally activated by P53 and then promotes downregulation of PI3K/Akt signaling. This suggests that blocking Akt may induce P53 and PTEN expression and consequently enhance sensitivity to cisplatin treatment. This was, however, not observed in the study, which showed that both cisplatin-GDC-0941 and cisplatin-MK-2206 combinations did not show a marked induction of P53 and PTEN and few cells showed significant decreases to pAkt level compared to cisplatin treatment.

3.5.6. FURTHER WORK

Further work using traditional western blotting may have been useful to help confirm key results obtained from the in-cell western assay. Results achieved from ICW showed high variance around the mean, particularly regarding cleaved caspase-3 expression. This may be due to the nature of the in-cell western assay which washes off any floating cells prior to analysis, thus removing those cells which potentially have the highest levels of cleaved caspase-3 (particularly at the longer time point). Furthermore, it must be considered that cisplatin has also been shown to cause caspase-independent apoptotic pathways via mitochondrial release and nuclear translocation of apoptosis-inducing factor (AIF) (Yang, et al., 2008).

Hyperactivation of PI3K signaling can also be caused by downregulation of the tumor suppressor PTEN which is common in lung cancers. All cell lines used within this thesis display intact PTEN function (Soria , et al., 2002). Inhibition of PI3K signaling is of increasing interest in targeting cancers that specifically exhibit PTEN loss of function, leading to deregulated PI3K signaling, and so it would be of interest to further investigate combinations of PI3K inhibitors in cell lines that also exhibit PTEN loss of function.

3.6. CONCLUSION

Cisplatin resistance was abrogated by addition of targeted therapy agents in *KRAS* mutant NSCLC cell lines. This was particularly evident with drugs that targeted the PI3K signaling pathway either directly or indirectly. Induction of apoptosis in response to the combinations (as shown by increased caspase-3 cleavage) was concurrently observed with downregulation of pAkt but not associated with P53 or PTEN function.

Whether these results translate from 2D cultures into 3D models will be further investigated in the following chapter.

4. CHAPTER FOUR: ASSESSING DRUG POTENCIES IN 3D MODELS

4.1. INTRODUCTION

The previous chapter has utilized adherent cell culture in order to assess the potencies of single drug treatments and cisplatin-based combination treatments. From this data, the range of drug combinations, appropriate concentrations and treatment times was narrowed down so that it was feasible to assess activity in cellular models of lung cancer that might show better representation of cells when in a more complex 3D environment, such as that observed in tumors. The most simplistic form of 3D model is that of the spheroid. Spheroids for A549, H460 and H596 were generated as previously described in section 2.1.2.1, and treated with drug combinations as determined in chapter 3.

As reviewed in chapter three, all cell lines with the selected cisplatin-based doublets are summarized below in the table (NA: non-applicable);

<table>
<tr><th rowspan="2">Various cisplatin-based doublets</th><th colspan="4">A549</th><th colspan="3">H460</th><th colspan="4">H596</th></tr>
<tr><th colspan="2">24 hr</th><th colspan="2">72 hr</th><th>24 hr</th><th colspan="2">72 hr</th><th colspan="2">24 hr</th><th colspan="2">72 hr</th></tr>
<tr><td>STA-9090</td><td colspan="2">NA</td><td>Yes</td><td>0.02 µM</td><td rowspan="7">NA</td><td>Yes</td><td>0.02 µM</td><td colspan="4" rowspan="3">NA</td></tr>
<tr><td>DMX502320-04</td><td>Yes</td><td>1 µM</td><td colspan="2">NA</td><td>Yes</td><td>0.6, 1 µM</td></tr>
<tr><td>DMX503433-09</td><td>Yes</td><td>0.6, 1 µM</td><td colspan="2">NA</td><td>Yes</td><td>10 µM</td></tr>
<tr><td>GDC-0941</td><td colspan="2">NA</td><td>Yes</td><td>1 µM</td><td>Yes</td><td>1 µM</td><td colspan="2">NA</td><td>Yes</td><td>1 µM</td></tr>
<tr><td>MK-2206</td><td>Yes</td><td>3 µM</td><td>Yes</td><td>3, 12, 21 µM</td><td>Yes</td><td>3 µM</td><td>Yes</td><td>3 µM</td><td colspan="2">NA</td></tr>
<tr><td>AZD6244</td><td colspan="4">NA</td><td>Yes</td><td>10 µM</td><td colspan="2">NA</td><td>Yes</td><td>10 µM</td></tr>
</table>

4.2. DRUG POTENCIES IN 3D SPHEROIDS

4.2.1. COMBINATION TREATMENTS AT 24 HR

The 24-hr treatment had only three selected cisplatin-based doublets for testing on A549 and H596 spheroids only. As showed in Figure 4.1, the single treatments showed a less potency on spheroids compared to cell line treatment. although both cisplatin combined with 0.6 or 1 µM DMX503433-09 and the combination with 3µM MK-2206 exhibited a significant reduction on the spheroid viability (averaged value for A549 and H596), with a maximal decrease of 34% at the MK-2206-cisplatin combination compared to that of control group. These two more potent doublets still showed a significant change in the viability compared to that of cisplatin alone, with a change of 19% at cisplatin-DMX503433-09 and 28% at cisplatin-MK-2206 combination. In contrast, the cisplatin-DMX502320-04 combination was less active on the spheroids with no significant alteration in the viability compared to control and cisplatin alone.

24 hr-treatment																														
Various groups	CONTROL			CISPLATIN			DMX502320-04			CISPLATIN +DMX502320-04			DMX503433-09						CISPLATIN +DMX503433-09						MK-2206			CISPLATIN +MK-2206		
Doses	0			1			1			1+1			0.6			1			0.6+1			1+1			3			1+3		
Average	101			94			76			86			77*						75*						76*			66*		
A549	M	SD	N	M	SD	N	M	SD	N	M	SD	N	M	SD	N	M	SD	N	M	SD	N	M	SD	N	M	SD	N	M	SD	N
	101	12	47	94	18	45	76	16	23	86	14	21	78	9	18	76	9	18	78	7	18	73	11	18	86	19	16	71	9	15
H460	NA																													
H596	M	SD	N	M	SD	N	NA																		M	SD	N	M	SD	N
	100	11	24	94	21	24																			66	13	24	62	13	23

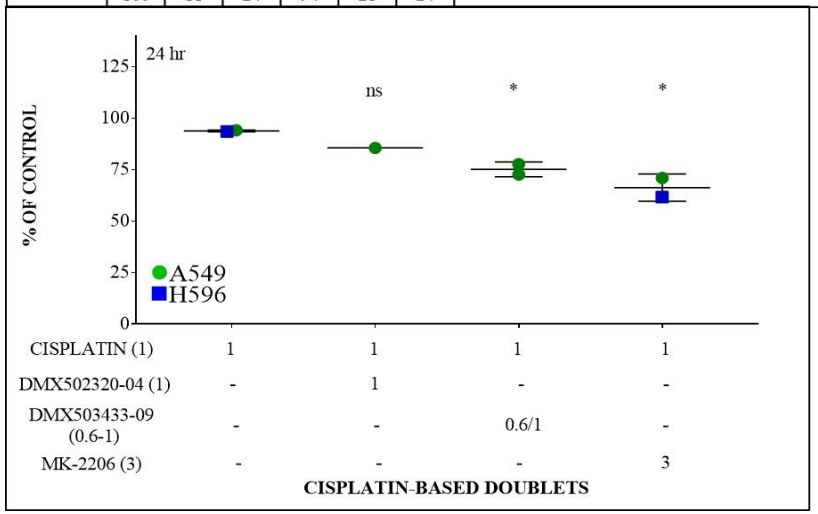

Figure 4. 1 Cisplatin-based combination treatments on A549 and H596 spheroids at 24 hr

The table above showed that only A549 and H596 were selected with cisplatin-based doublets at 24 hr. Results for each cell line are shown as M ± SD (% of control) with replicates over 15 and all cell lines were summarized as averaged values. The comparison between control in average with that of treatment (one-way ANOVA by prism) was summarized in the table with '*' to indicate significance of P<0.05. The figure below showed the comparison of 1 µM cisplatin with MK-2206, DMX502320-04 or DMX503433-09 combined with 1 µM cisplatin (average of all cell data) and the significance was marked with '*': P<0.05 and 'ns' means non-significant. NA means non-applicable.

4.2.2. COMBINATION TREATMENTS AT 72 HR

In contrast to the 24-hr treatment, there existed more cisplatin-based combination treatments tested on all spheroids. Particularly, H460 spheroids were tested with all cisplatin-based doublets mentioned in chapter three, whereas A549 tested with three and H596 with four combinations only. All selected cisplatin-based doublets for different spheroids are summarized in Table 4.1. Overview, all treatments at 72 hr exhibited a high potency, where cisplatin single treatment showed a significant reduction in the spheroid viability with an averaged change of 35% compared to control group. The maximal reduction in the viability significantly compared to control was observed at GDC-0941 single agent with viability decreased by 55%. Whereas the toxicity of the agent seemed to be limited by adding cisplatin to the regimen with a less reduced viability by 53% compared to control. The combination of cisplatin with MK-2206 was also potent in decreasing the viability with a reduction 54%, which was slightly active than the single MK-2206 agent (50% decreased in the viability compared to control). In contrast, the rest of cisplatin-based doublets were less active in affecting the viability with a drop of less than 40% compared to the control.

As for the comparison with cisplatin single agent (Figure 4.2), only cisplatin combined with GDC-0941 or MK-2206 showed a significant reduction in the viability compared to that of cisplatin alone, with a further slight decrease of 18% and 19% respectively.

.

Table 4. 1 Cisplatin-based combination treatments on A549, H460 and H596 spheroids at 72 hr

Each spheroid data are shown as M ± SD (% of control) with replicates over 16 (A549 and H460) or 22 (H596) and all cell lines were calculated as the averaged values. The comparison of control in average with that of either single or combination treatment was analyzed by one-way ANOVA by prism. '*' means P<0.05 and 'ns' means non-significant. NA means non-applicable.

72 hr-treatment																														
Various groups	CONTROL			CISPLATIN			STA-9090			CISPLATIN +STA-9090			DMX502320-04						CISPLATIN +DMX502320-04						DMX503433-09			CISPLATIN +DMX503433-09		
Doses	0			1			0.02			1+0.02			0.6			1			1+0.6			1+1			10			1+10		
Average	99			64*			67*			59*			66*						62*						77*			63*		
A549	M	SD	N	M	SD	N	M	SD	N	M	SD	N	NA																	
	99	10	35	74	14	35	71	14	17	66	12	18																		
H460	M	SD	N	M	SD	N	M	SD	N	M	SD	N	M	SD	N	M	SD	N	M	SD	N	M	SD	N	M	SD	N	M	SD	N
	98	11	61	61	12	63	64	10	18	52	8	16	71	11	17	61	14	17	61	11	16	63	8	18	77	14	17	63	13	17
H596	M	SD	N	M	SD	N							NA																	
	101	14	28	58	12	28																								

Various groups	GDC-0941			CISPLATIN +GDC-0941			MK-2206							CISPLATIN +MK-2206							AZD6244			CISPLATIN+AZD6244		
Doses	1			1+1			3			3, 12, 21				1+3			1+3/12/21				10			1+10		
Average	44*			46*			49*							45*							63*			57*		
A549	M	SD	N	M	SD	N					M	SD	N					M	SD	N						
	44	9	18	42	13	18				3	50	15	18				3	48	9	16						
										12	53	17	18				12	46	6	16						
										21	37	19	16				21	37	11	16						
H460	M	SD	N	M	SD	N	M	SD	N					M	SD	N					M	SD	N	M	SD	N
	47	11	24	50	8	24	54	13	23					49	13	24					63	18	17	59	14	16
H596	M	SD	N	M	SD	N	NA														M	SD	N	M	SD	N
	40	7	28	45	10	30															64	12	23	54	11	22

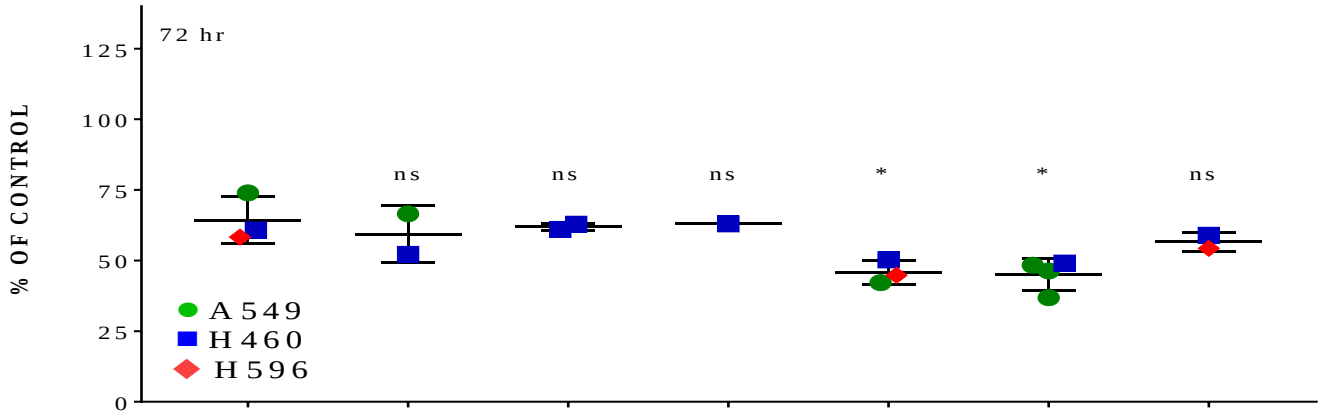

CISPLATIN (1)	1	1	1	1	1	1	1
STA-9090 (0.02)	-	0.02	-	-	-	-	-
DMX502320-04 (0.6-1)	-	-	0.6/1	-	-	-	-
DMX503433-09 (10)	-	-	-	10	-	-	-
GDC-0941 (1)	-	-	-	-	1	-	-
MK-2206 (3,12,21 or 3)	-	-	-	-	-	3,12,21/3	-
AZD6244 (10)	-	-	-	-	-	-	10

CISPLATIN-BASED DOUBLETS [μM]

Figure 4. 2 The comparison of cisplatin with the selected cisplatin-based doublets at 72 hr on A549, H460 and H596 spheroids

Results are shown as the averaged data of all cell lines in M ± SD with N=3 and were analyzed by one-way ANOVA by prism. '*' means P<0.05 and 'ns' means non-significant.

4.2.3. SUMMARY

In summary, the spheroid experiment further demonstrated that GDC-0941- or MK-2206-containing combination with cisplatin had a relatively high cytotoxicity compared to the rest of cisplatin-based doublets and a longer-duration (72 hr) emerged as the optimal time-point for enhancing potencies of these combinations compared to 24 hr treatment.

4.3. ASSESSING DRUG POTENCIES IN ORGANOTYPIC CO-CULTURES

The heterogeneous cellular composition of tumors has significant implications regarding response to therapeutic intervention. Lung tumors often exhibit a desmoplastic environment in which fibroblasts constitute a large component of the tumor mass, and play an important role in signaling events driving tumor vascularization, growth and metastasis (Bremnes , et al., 2011).

Spheroid models are able to provide a 3D tumor-like structure that can affect drug activity due to altered signaling processes (particularly in the presence of a central hypoxic core) and decreased drug penetration. However, they do not take into account whether the presence of other cell types may affect key signaling components that have implications on drug response. To this end, the MRC-5 lung fibroblast cell line was incorporated into a lung organotypic air-interface model. However, it was first important to determine drug sensitivity in this cell line.

4.3.1. DRUG POTENCY IN MRC-5 CELLS

Combinations between cisplatin and GDC-0941 or MK-2206 were demonstrated to be more potent in reducing viability of cancer cells (A549, H460 and H596). Information obtained from drug potencies observed across the different time points in conjunction with relative sensitivities between 2D and spheroid culture was taken into account when deciding on which drug combinations to further investigate in MRC-5 cells. The more potent cisplatin-based doublets-combination of cisplatin with GDC-0941 and MK-2206 were tested on MRC-5 cells.

As shown in Figure 4.3, the combination of 1 μM GDC-0941 with 1 μM cisplatin reduced viability of MRC-5 cells to a significantly greater extent (29%) than cisplatin alone at 24 hr, although there was no significant difference from single agent GDC-0941. By

comparison, the combination treatment at 72 hr was more active with the viability reduced by 41% compared to cisplatin alone, and was also significantly different from GDC-0941 alone. For cisplatin-MK-2206 combination at 24 hr, 3 μM MK-2206 combined with cisplatin significantly reduced the viability by 16% compared to cisplatin alone. MRC-5 cells were very sensitive to MK-2206 at 72 hr with a further decrease in viability of 25% for cisplatin combined with the lowest dose of MK-2206, which was further increased by 62% for the 1+12 group and 90% for the 1+21 group (100% cell kill) compared to cisplatin alone. MRC-5 cells exhibited greater sensitivity to the MK-2206 combination than the cancer cell lines in 2D and 3D cultures.

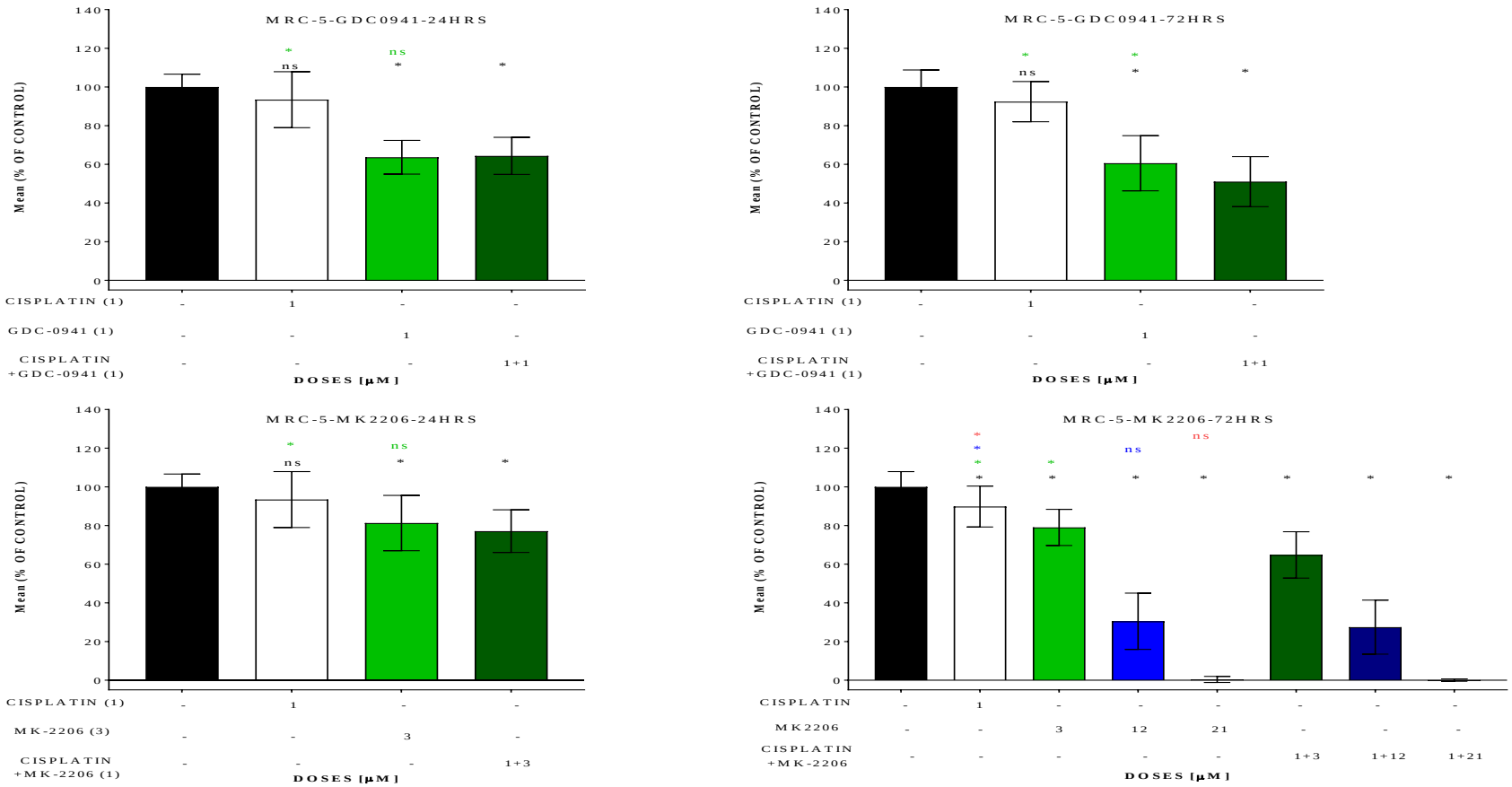

Figure 4. 3 Cisplatin-GDC-0941 and Cisplatin-MK-2206 combinations treatments on MRC-5 at 24 and 72 hr.

Results are shown as M ± SD (% of control) with replicates over 18 and analyzed by one-way ANOVA by SPSS with "*" denoting P<0.05 and "ns" means non-significant. The significant symbols (* or ns) are shown in four colours: black stands for control vs each treatment group, green for 1 µM GDC-0941 or 3 µM MK-2206-containing, blue for 12 µM MK-2206-containing and red for 21 µM MK-2206-containing combinations vs corresponding single treatments.

4.3.2. PROTEIN EXPRESSION IN MRC-5 CELLS

In keeping with previous datasets for cancer cell lines, expression of Akt-related signaling molecules was also investigated in the MRC-5 cells.

4.3.2.1. Cisplatin-GDC-0941 Combination at 24 and 72 hr

The only significant alteration observed at 24 hr was that 1 µM GDC-0941 showed a significant induction of PTEN compared to control only (Figure 4.4). In comparison, 72 hr treatment (Figure 4.5) showed a significant ($P<0.05$) decrease in the expression of Akt and p-Akt at the cisplatin-GDC-0941 combination treatment and each molecule expression showed a 0.4-fold increase compared to control, significantly different from that of cisplatin alone (1.2-and 1-fold increase respectively for Akt and pAkt expression). It is notable to see that P53 was significantly induced to a 1.8-fold increase by cisplatin alone, and this increase was abrogated by the combination treatment (significantly decreased to one tenth of control). No significant changes to PTEN and cleaved caspase-3 expression were observed following any treatment.

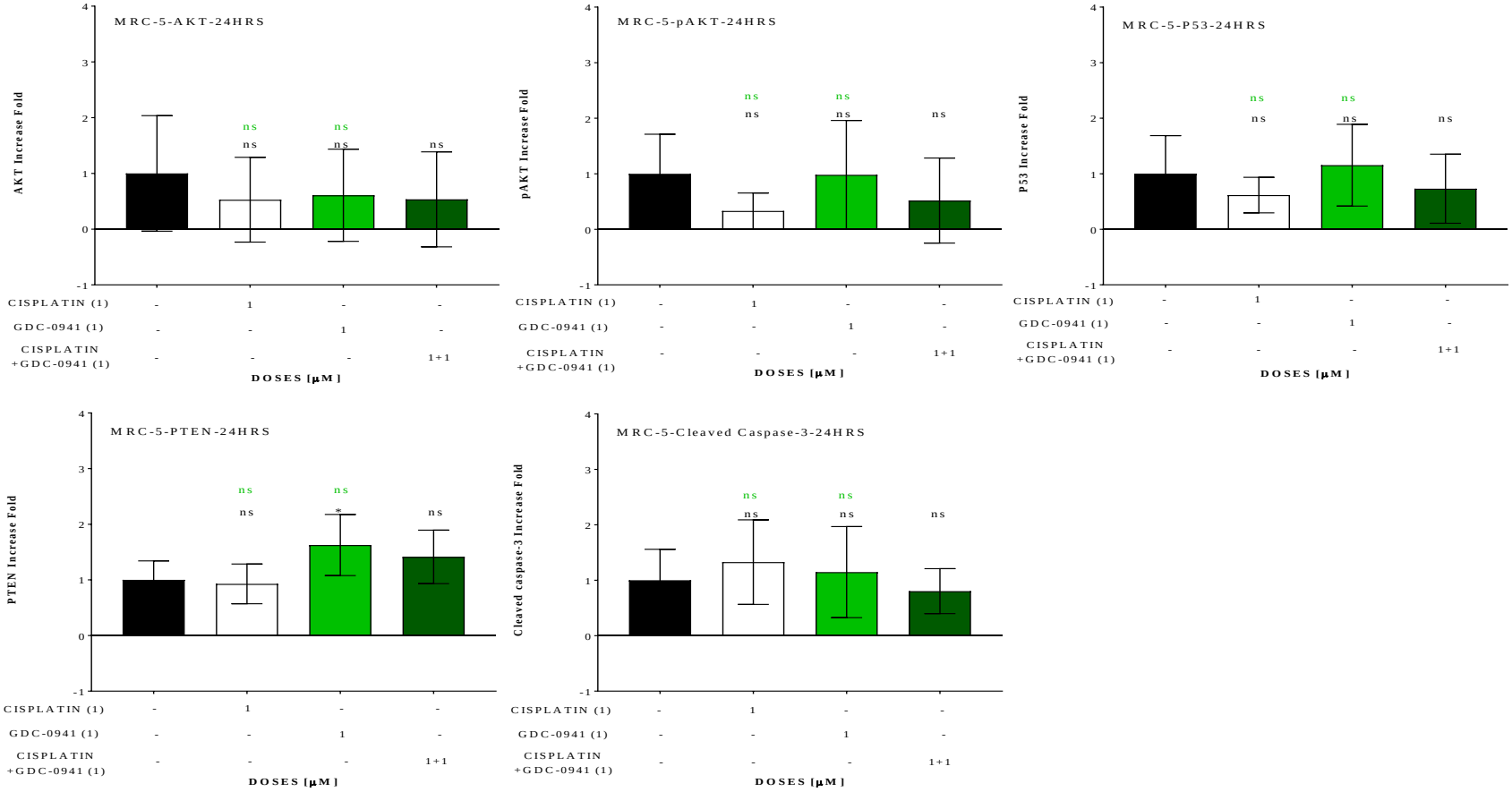

Figure 4. 4 Detection of Akt, pAkt, P53, PTEN and cleaved caspase-3 by ICW for cisplatin-GDC-0941 combination at 24 hr on MRC-5

One µM dose was used for cisplatin and GDC-0941 at 24 hr. Results (analyzed by one-way ANOVA by SPSS) are shown as M ± SD (% of control) with replicates over 8 and "*" means P<0.05 and "ns" means non-significant. The significance is shown as black between control group and each treatment group and green between cisplatin-GDC-0941 combination and corresponding single treatments.

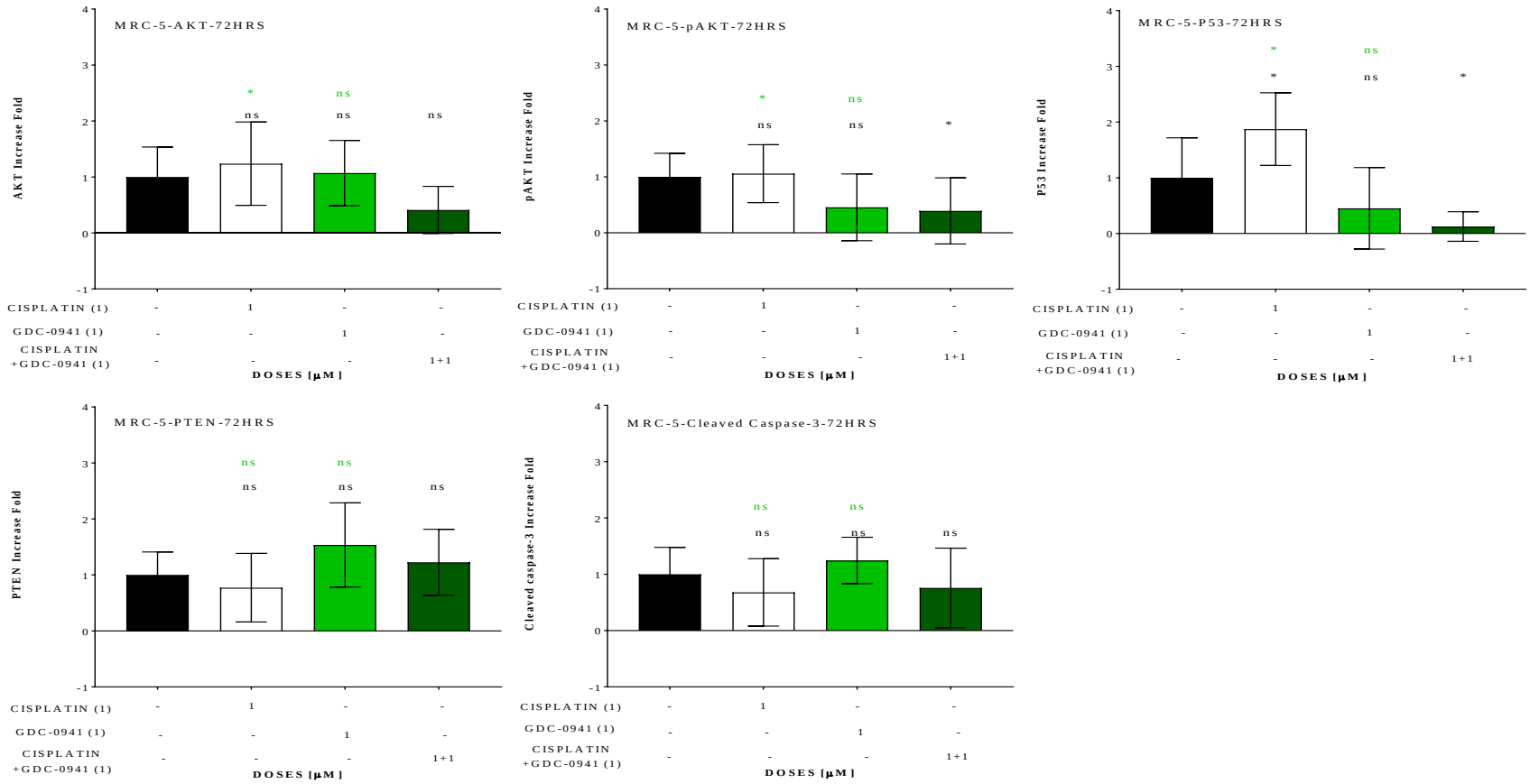

Figure 4. 5 Detection of Akt, pAkt, P53, PTEN and cleaved caspase-3 by ICW for cisplatin-GDC-0941 combination at 72 hr on MRC-5

One µM dose was used for cisplatin and GDC-0941 at 72 hr. Results (analyzed by one-way ANOVA by SPSS) are shown as M ± SD (% of control) with replicates over 8 and "*" means P<0.05 and "ns" means non-significant. The significance is shown as black between control group and each treatment group and green between cisplatin-GDC-0941 combination and corresponding single treatments.

4.3.2.2. Cisplatin-MK-2206 Combination at 24 and 72 hr

Following a 24-hr treatment (Figure 4.6), 3 µM MK-2206 (a 0.4-fold increase compared to control) or in combination with cisplatin (a 0.2-fold increase) elicited a significant decrease in Akt phosphorylation compared to control and the combination with MK-2206 also showed a significant decrease in pAkt compared to that of cisplatin alone (a 0.7-fold increase compared to control). At 72 hr (Figure 4.7), 21 µM MK-2206 alone and the combination with cisplatin showed a significant decrease in Akt expression to a 0.4- and 0.5-fold increase respectively. Moreover, the combination showed a significant downregulation in pAkt expression (0.02-fold increase) compared to either single agent (0.7 fold for both). It is also notable that 3 µM MK-2206 in combination with cisplatin significantly reduced the expression of pAkt compared to MK-2206 alone. No significant changes to either P53 or PTEN expression were caused by any treatments. The level of cleaved caspsase-3 was significantly reduced at 3 and 21 µM MK-2206 single treatments compared to control only and no significant changes to cleaved caspase-3 were observed between cisplatin and any combination treatments.

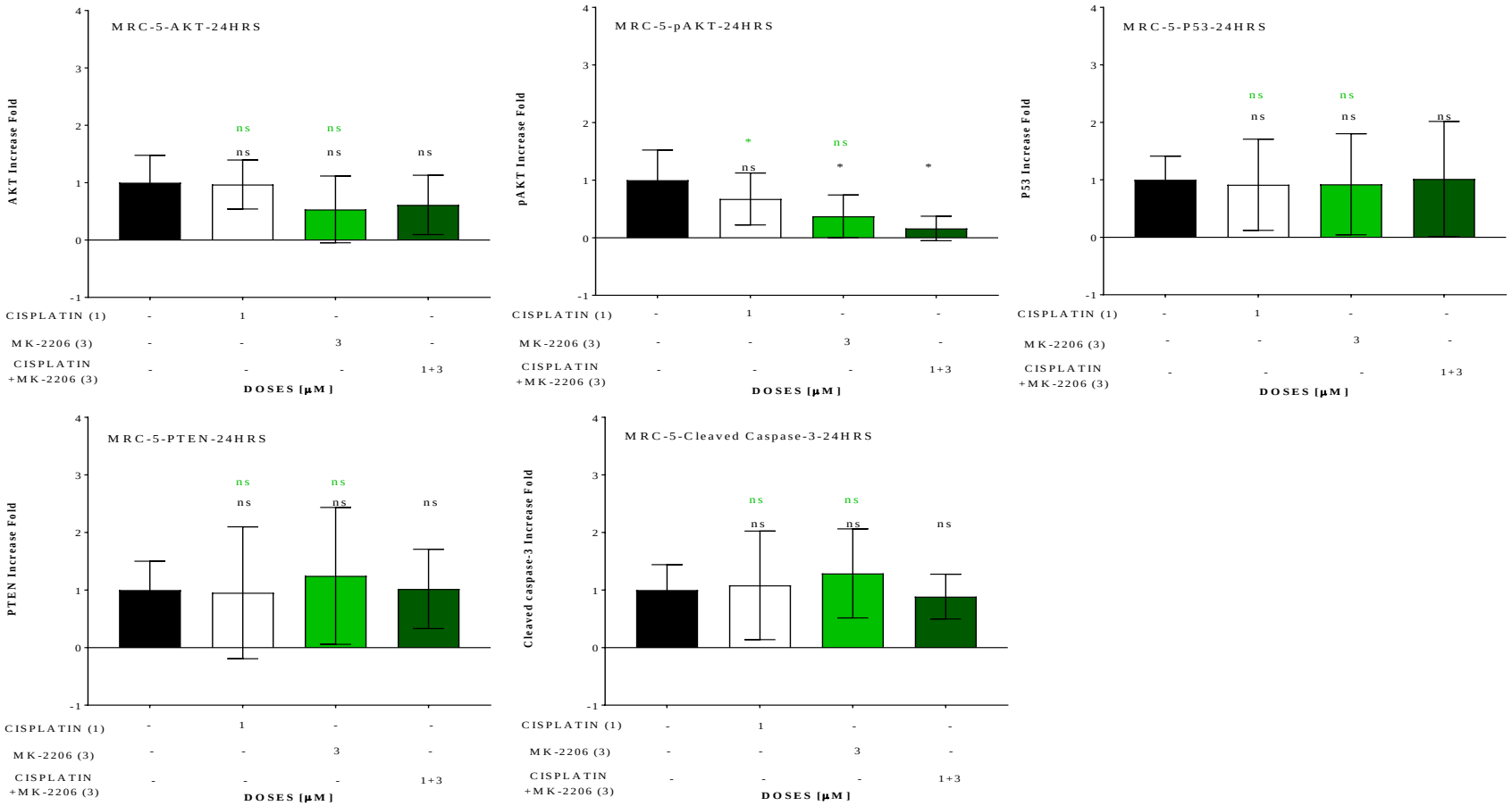

Figure 4. 6 Detection of Akt, pAkt, P53, PTEN and cleaved caspase-3 by ICW for cisplatin-MK-2206 combination at 24 hr on MRC-5

Results are shown as M ± SD (% of control) with replicates over 5 (analyzed by one-way ANOVA by SPSS) and *" means P<0.05 and "ns" means non-significant. The significance (* or ns) is shown as black between control group and each treatment group, green for 3 µM MK-2206-containing combinations vs corresponding single treatments.

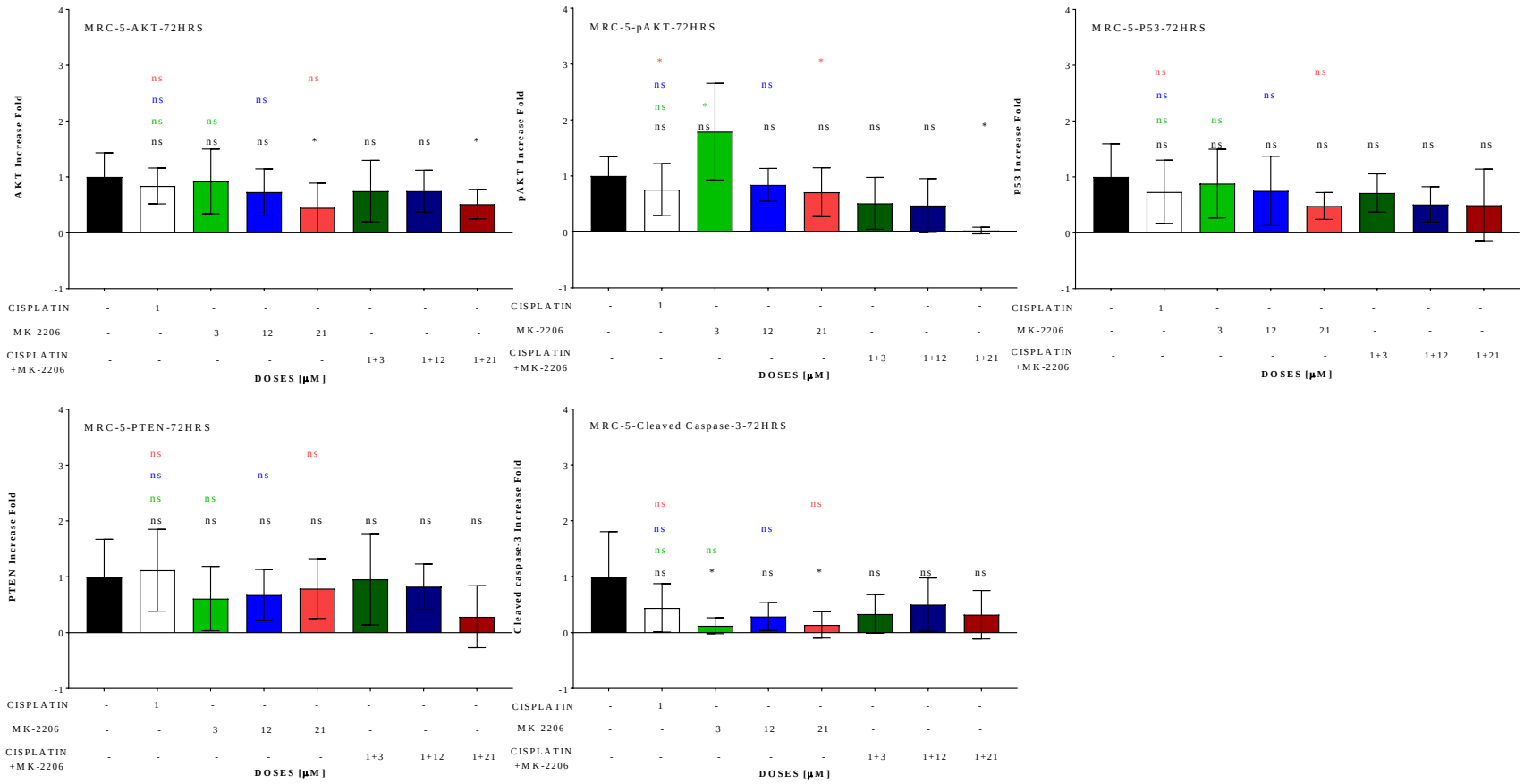

Figure 4. 7 Detection of Akt, pAkt, P53, PTEN and cleaved caspase-3 by ICW for cisplatin-MK-2206 combination at 72 hr on MRC-5

Results are shown as M ± SD (% of control) with replicates over 7 (analyzed by one-way ANOVA by SPSS) and *" means P<0.05 and "ns" means non-significant. The significance (* or ns) is shown as black between control group and each treatment group, green for 3 µM-, blue for 12 µM- and 21 µM MK-2206-containing combinations vs corresponding single treatments.

4.3.3. SUMMARY

Cisplatin combined with GDC-0941 and MK-2206 was as potent on MRC-5 as observed for cancer cells. By comparison, the 72 hr treatments generated a greater inhibition in viability than did the 24 hr treatments, with a significant reduction in Akt or Akt phosphorylation. In contrast to cancer cells, MRC-5s showed no significant increase in cleaved caspase-3 expression by any treatment at 24 or 72 hr. Moreover, cleaved caspase-3 was significantly reduced at 3 and 21 µM MK-2206 compared to cisplatin alone. A similar result as shown in cancer cells, was that few significant changes to PTEN and P53 expression were observed in MRC-5s.

4.4. DEVELOPMENT OF THE ORGANOTYPIC MODEL

The previous section has assessed MRC-5 sensitivity to the drugs of interest. It was next important to establish how co-culture of MRC-5 cells with the tumor cell lines affect tumor cell behaviour. It has previously been established in models of pancreatic cancer (cell migration through collagen-based gels), that the ratio of non-tumor to tumor cells has significant impact on tumor cell function, such as cell cycle, cell-cell signaling, cell movement, cell death and inflammatory response (Kadaba, et al., 2013). Therefore, before effects of the chosen drug combinations on PI3K and proliferation-related signaling was analyzed, we also sought to determine what ratios of tumor: fibroblast cells could potentially provide the greatest pro-invasive stimuli in the lung cancer setting.

4.4.1. DETERMINING NECESSITY OF MRC-5 CELLS FOR INVASION IN A549 ORGANOTYPIC MODEL

Previous data (Mahale, 2016) has demonstrated that the appropriate ratio of A549: MRC-5 to promote maximal invasion was 1:5. The 1:5-ratio with MRC-5 was comparatively better than other candidate ratios (5:1, 2:1, 1:1 and 1:2 – ratios also tested in presence or absence of fibroblasts embedded in the gel). For demonstration of appropriate cell invasion conditions for the A549 model, the ratio of A549: MRC-5=1:5/with MRC-5 in the gel, was shown and compared with A549/with MRC-5, A549/without MRC-5 and A549: MRC-5=1:5/without MRC-5 in the gel (Figure 4.8). H&E and cytokeratin (CK) staining is shown to compare histology among the four groups.

For the gels that contain A549 only/without MRC-5 in the gel, no invasion into the gel can be observed. For A549/with MRC-5 in the gel, the histology pattern differs with

regards to A549 localization, but no obvious invasion into the gel occurred. It is the presence of fibroblasts in direct contact with the cancer cells (shown in the 2 bottom panels of Figure 4.8) where invasion occurs to the greatest extent. Invasion appears to be independent from any extra migratory stimulus caused by the presence of fibroblasts pre-embedded in the gel. The majority of cells stained by CK were epithelial cells, which showed a better presentation of cell invasion through the collagen gel. Testing of drug combinations was therefore carried out at the 1:5-ratio of A549: MRC-5 cells, but without MRC-5 embedded in the gel.

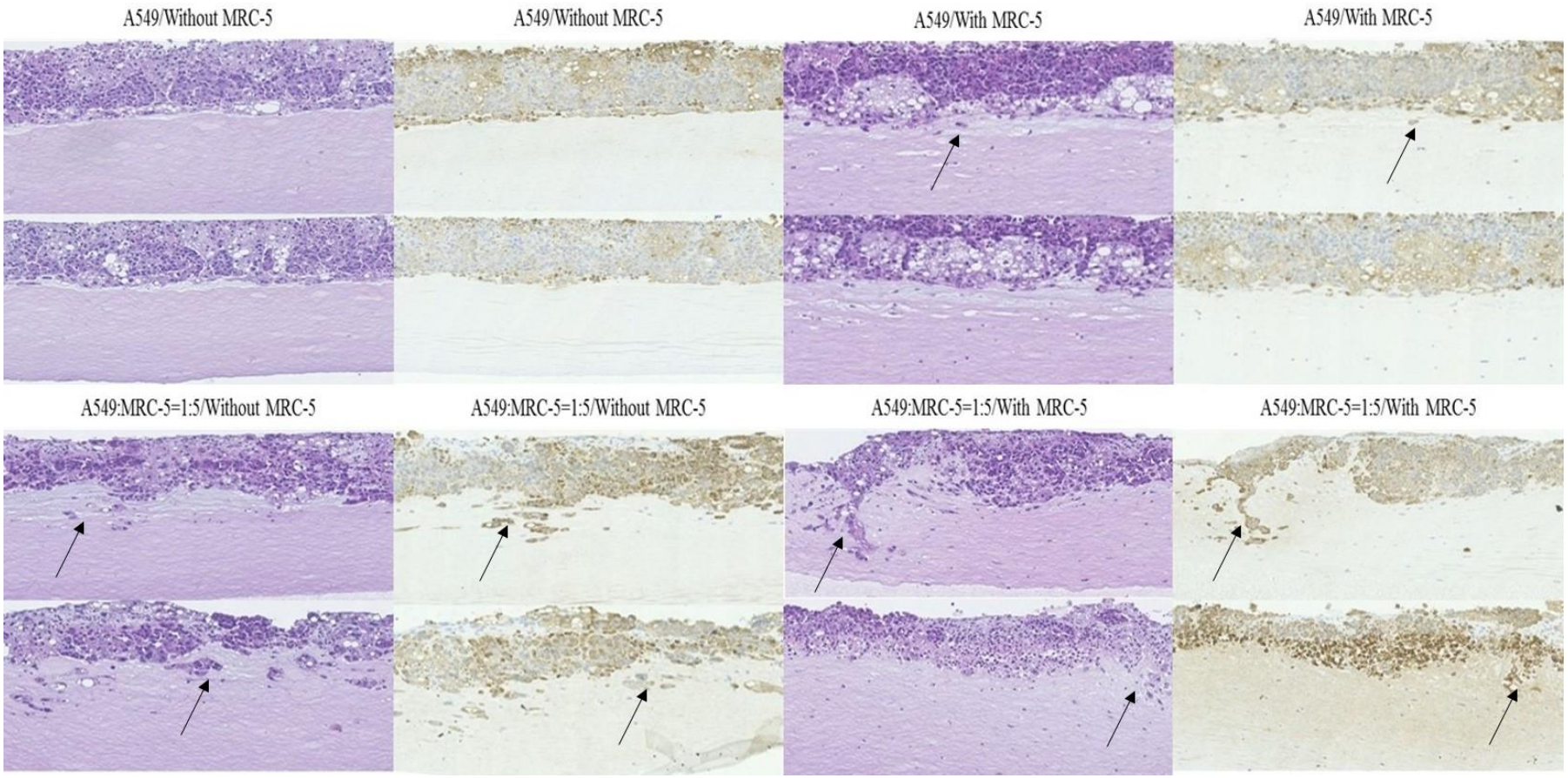

Figure 4. 8 H&E and CK staining for comparison of appropriate ratios of A549 and MRC-5 cells for setting up the cell invasion model.

The ratios combinations included the model with A549 cells on the top layer only with (A549/with MRC-5) or without MRC-5 (A549/without MRC-5) in the gel, and models with a 1:5-ratio of A549: MRC-5 with (A549: MRC-5=1:5/with MRC-5) or without MRC-5 (A549: MRC-5=1:5/without MRC-5) in the gel. Invasive cancer cells in gels are pointed out with black arrows.

4.4.2. H460: MRC-5 RATIO DETERMINATION

As there have been no previous experiments demonstrating appropriate ratios for H460 and MRC-5 cells for cancer cell invasion, several candidate ratio groups were tested for the H460 model. For each ratio, the model was assessed with and without MRC-5 cells in the gel. The ratios of H460: MRC-5 were: 5:1, 2:1, 1:1, 1:2 and 1:5. Control gels were also prepared, with only H460 cells on the top layer with or without MRC-5 in the gel (H460/with MRC-5 and H460/without MRC-5). H&E staining for controls and all candidate ratios are shown in Figure 4.9. The 2:1-ratio of H460: MRC-5 cells without MRC-5 in the gel showed greater invasion of cancer cells into the gel than any other ratio groups, and was also greater than that observed in the 2:1 ratio group with MRC-5 in the gel. This combination was therefore taken forward to assess treatment potencies.

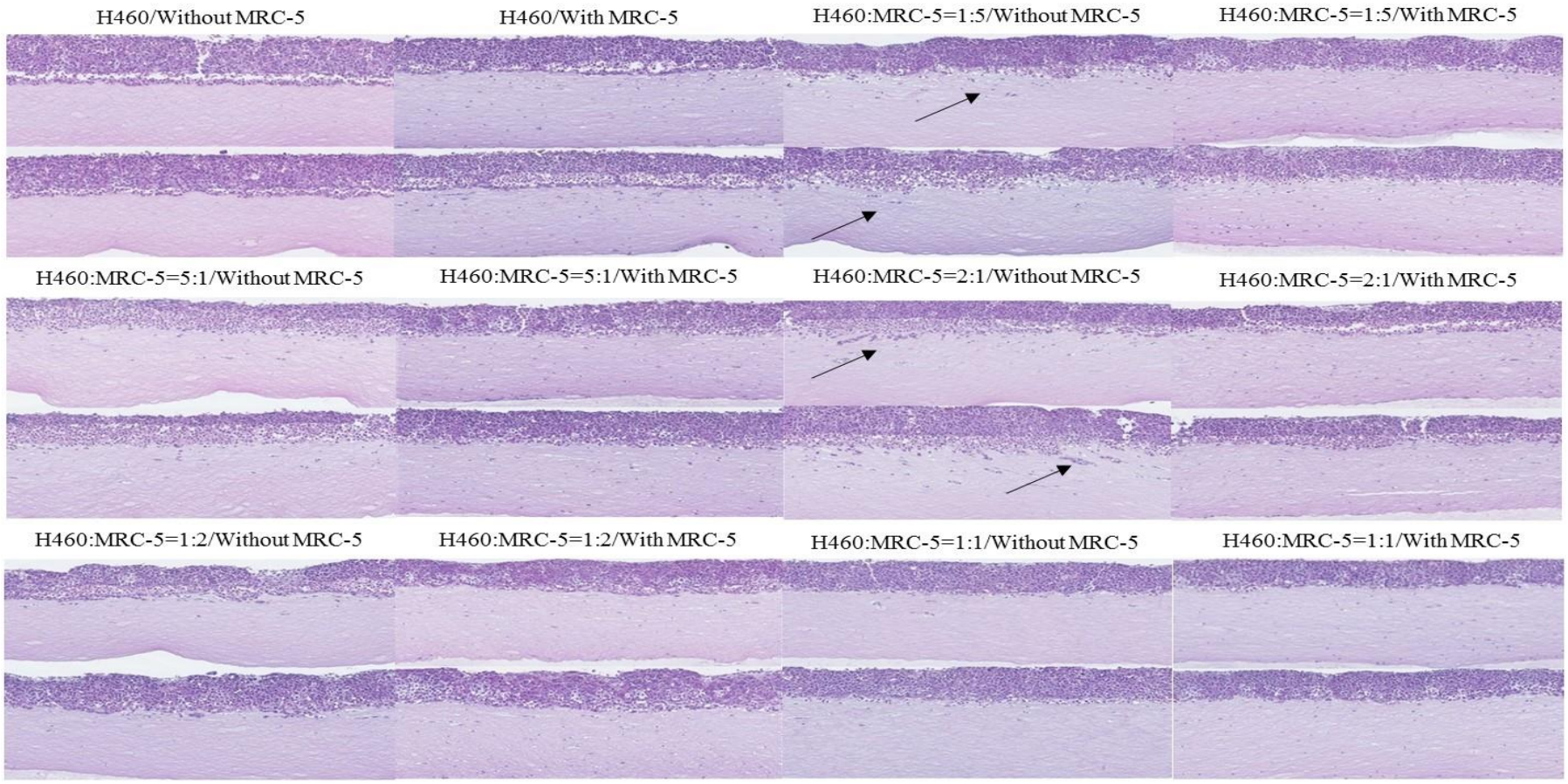

Figure 4. 9 H&E staining for comparison of appropriate ratios of H460 and MRC-5 cells for cell invasion of H460

All ratio groups include control models (H460/without MRC-5 and H460/with MRC-5), 1:5-ratio groups (H460: MRC-5=1:5/without MRC-5 and H460: MRC-5=1:5/with MRC-5), 5:1-ratio groups (H460: MRC-5=5:1/without MRC-5 and H460: MRC-5=5:1/with MRC-5), 2:1-ratio groups (H460: MRC-5=2:1/without MRC-5 and H460: MRC-5=2:1/with MRC-5), 1:2-ratio groups (H460: MRC-5=1:2/without MRC-5 and H460: MRC-5=1:2/with MRC-5) and 1:1-ratio groups (H460: MRC-5=1:1/without MRC-5 and H460: MRC-5=1:1/with MRC-5). Invasive cancer cells in gels are pointed out with black arrows.

4.4.3. H596: MRC-5 RATIO DETERMINATION

The same cell mixtures were used as for the H460 models (Figures 4.10). The highest degree of invasion was once again observed using a ratio of H596: MRC-5=2:1/ without MRC-5 in the gel. Hence, the ratio of 2:1/ without MRC-5 in the gel was selected as the appropriate ratio for assessing drug potencies in this model.

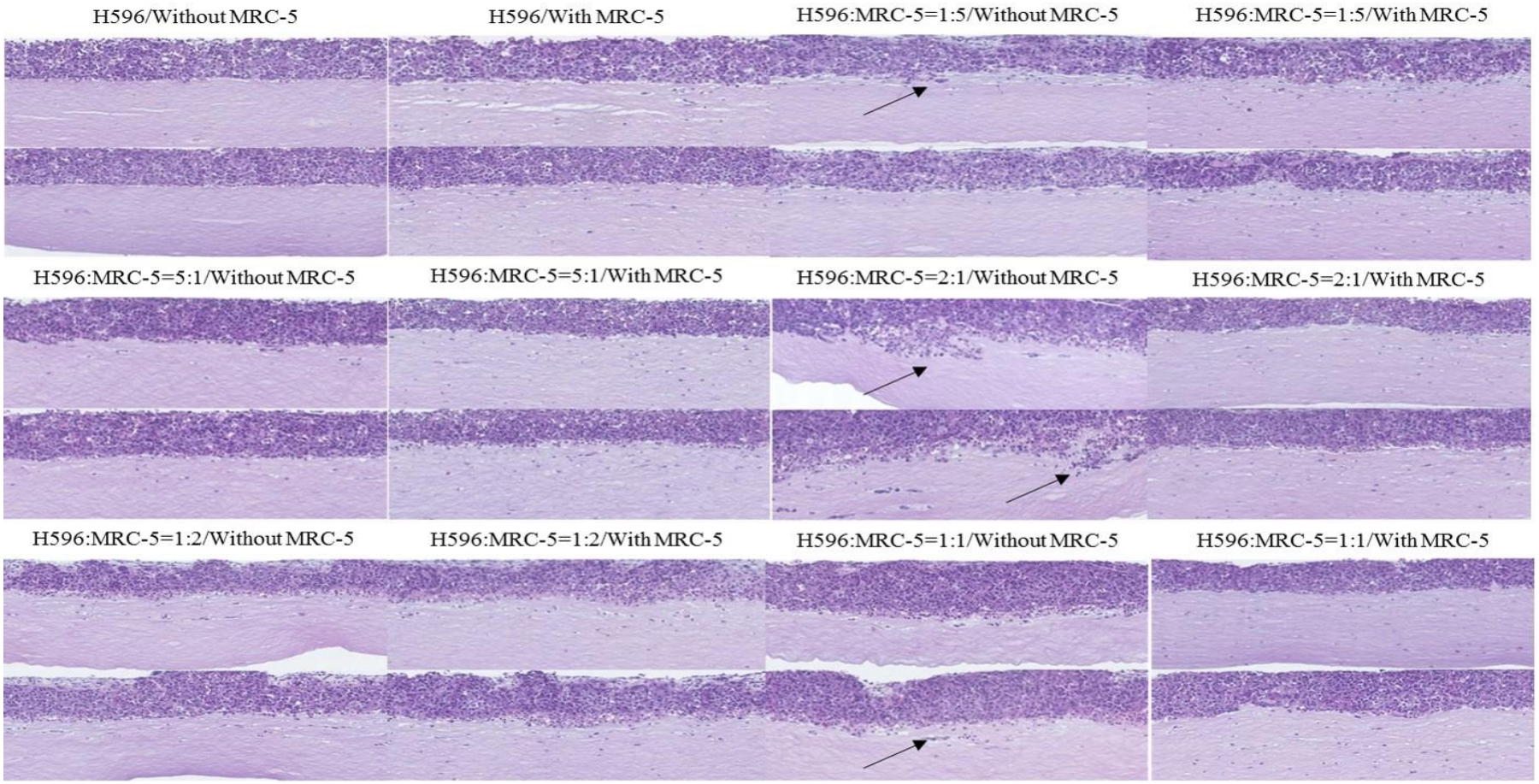

Figure 4. 10 Comparison of appropriate ratios of H596 and MRC-5 cells for cell invasion model

H&E staining was shown for histology of control models (H596/without MRC-5 and H596/with MRC-5), 1:5-ratio groups (H596: MRC-5=1:5/without MRC-5 and H596: MRC-5=1:5/with MRC-5), 5:1-ratio groups (H596: MRC-5=5:1/without MRC-5 and H596: MRC-5=5:1/with MRC-5), 2:1-ratio groups (H596: MRC-5=2:1/without MRC-5 and H596: MRC-5=2:1/with MRC-5), 1:2-ratio groups (H596: MRC-5=1:2/without MRC-5 and H596: MRC-5=1:2/with MRC-5) and 1:1-ratio groups (H596: MRC-5=1:1/without MRC-5 and H596: MRC-5=1:1/with MRC-5). Invasive cancer cells in gels are pointed out with black arrows.

4.5. EFFECT OF COMBINATION TREATMENTS ON THE ORGANOTYPIC MODEL

For the A549 model, the cancer: MRC-5=1:5-ratio group without MRC-5 cells in the gel was selected. The 2:1-ratio of cancer: MRC-5 cells (2:1-ratio group) without MRC-5 cells in the gel was selected for both H460 and H596 models. Due to difficulties encountered with maintaining the models, data from each treatment group was summarized across the entirety of 2 separate gels for 24 hr and 72 hr treatments. Cisplatin in combination with GDC-0941 or MK-2206 as previously determined in 2D cell and 3D spheroid cultures was further assessed within the organotypic culture models. For GDC-0941 combined with cisplatin, a 1 µM dose was used for both cisplatin and GDC-0941 on all models at 24 and 72 hr. The doses of MK-2206 combined with 1 µM cisplatin were used at 3 µM for all models at 24 hr and for both H460 and H596 cells at 72 hr. MK-2206 doses used for A549 at 72 hr were 3, 12 and 21 µM.

4.5.1. BASAL EXPRESSION LEVELS OF ANTIGENS OF INTEREST

The representative sections for baseline staining of antigens previously investigated in 2D models via in-cell westerns are shown for all models (A549, H460 and H596) at 24 hr (Figure 4.11). The cancer cells invading inside the gels stained by different antigen-specific antibodies were the targets of interest, rather than those on the top-most layer of the gels. The staining of CK that showed the majority of invasive cells in the gel were cancer cells , along with the H&E staining was also applied to distinguish invasive cancer cells from the MRC-5 cells within the gel matrix layer. All models showed low basal levels of P53 and cleaved caspase-3. In contrast, both Akt and PTEN were highly expressed in all models. For pAkt expression, the A549 model appeared to show a higher basal level of this antigen in the invasive cancer cells than did the other two models.

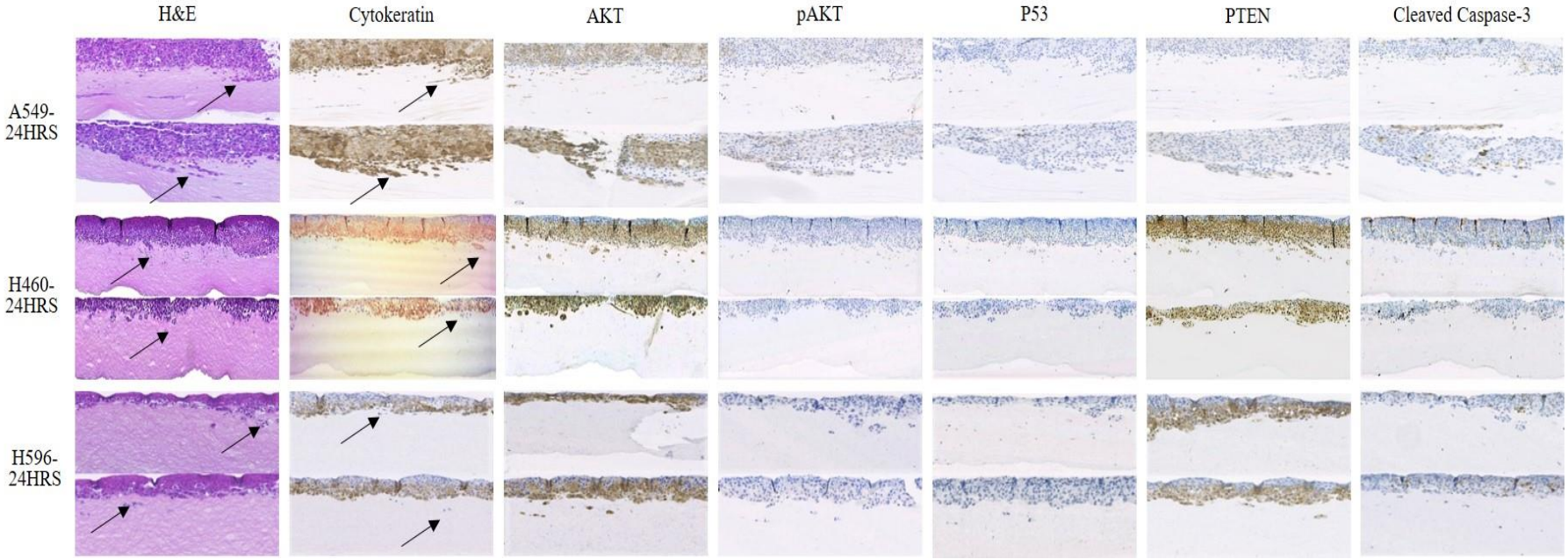

Figure 4. 11 Representative sections showing H&E and immunostaining for detection of CK, Akt, p-Akt, P53, PTEN and cleaved caspase-3 for A549, H460 and H596 models.

Immunostaing shows the control group for each cell model during 24 hr treatment with cisplatin (1µM), GDC-0941 (1µM), MK-2206 (3µM) and cisplatin-based dual-drug combinations. The invasive cancer cells in gels are pointed out with black arrows.

4.5.2. POTENCIES OF CISPLATIN-GDC-0941 OR MK-2206 COMBINATION TREATMENT AT 24 AND 72 HR

After 24 or 72hr-treatment, all groups were detected with various molecular expression, which was Akt, pAkt, P53, PTEN and cleaved caspase-3. Individual data for each organotypic culture model as well as the averaged value of all models are summarized in Table 4.2. Only Akt and PTEN expression (immunoratio) showed a high concentration of protein expression with an average of nearly 100%, whereas the rest of molecular expression showed a less than 10% of cells detected for the antigens, although H460 model showed a high expression of cleaved caspase-3 at cisplatin treatment with a Immunoratio of 44%, compared with approximately 10% at other treatment or control group. Moreover, P53 protein was poorly expressed at any group with a merely 1-2%, observed in all models. There were no significant alterations to the levels (presented as the averaged values) of Akt, PTEN, P53 and cleaved caspase-3 between control group and any treatment. Only pAkt expression was significantly induced at cisplatin treatment across all model with an average of 23%, significantly different from that of control group.

For the comparison to cisplatin treatment (Figure 4.12), the pAkt expression at cisplatin treatment was also significantly higher than that of combination treatment with GDC-0941 or MK-2206. Similarly as shown in the table, there were no significant changes to the expression of the rest antigens of interest.

In contrast to the expression at 24-hr, the 72-hr treatment (Table 4.3) showed a significant increase in the expression of Akt at GDC-0941 single agent and cisplatin-MK-2206 combination across all models, which had an averaged immunoratio of 92% and 88% respectively compared to control group (59%). Moreover, the Akt phosphorylation at cisplatin treatment was less expressed at 72 hr compared to that at 24 hr. The 72-hr treatment also showed a low expression in pAkt protein (nearly 0%) at any treatment at 72 hr, similarly as that observed in the 24-hr treatment and was significantly different from that of control group (7%). Moreover, the P53 expression at 72 hr was still low at all treatments with 1% cells exhibiting this protein in models. The PTEN expression was at a high concentration with an average of 70% across all groups, which was slightly lower than that at 24-hr treatment and there was no significant difference in the antigen expression between control and any treatment. The expression of cleaved caspase-3 was dramatically increased at 72 hr across all groups compared to that at 24 hr and the control

group showed a relatively higher expression of cleaved caspase-3 with an average of 42% across all models non-significantly compared to any treatment.

Table 4. 2 The detection of Akt, pAkt, P53, PTEN and cleaved caspase-3 expression on all cell line models after treatment with cisplatin-GDC-0941 or MK-2206 combinations at 24 hr

Data were analyzed by prism (one-way ANOVA) presented as average of all models and '*' denotes significant comparison between control and each treatment meaning P<0.05.

24 hr treatment	Cell lines	CONTROL	CISPLATIN	GDC-0941	CISPLATIN +GDC-0941	MK-2206	CISPLATIN +MK-2206
	Average	99	92	92	98	93	96
AKT	A549	97	100	97	99	96	99
	H460	100	84	87	96	83	97
	H596	100	93	93	100	99	93
pAKT	Average	3	23*	1	1	2	1
	A549	4	29	0	2	6	3
	H460	2	34	1	0	1	0
	H596	3	7	1	0	0	0
P53	Average	2	2	1	1	1	1
	A549	3	3	1	2	1	1
	H460	2	1	3	1	1	2
	H596	2	0	0	0	1	1
PTEN	Average	99	95	98	99	94	94
	A549	99	99	96	99	94	100
	H460	100	90	97	97	90	84
	H596	98	96	100	100	98	97
Cleaved caspase-3	Average	3	17	9	6	11	10
	A549	2	1	5	6	5	4
	H460	6	44	11	8	23	15
	H596	2	7	10	5	6	11

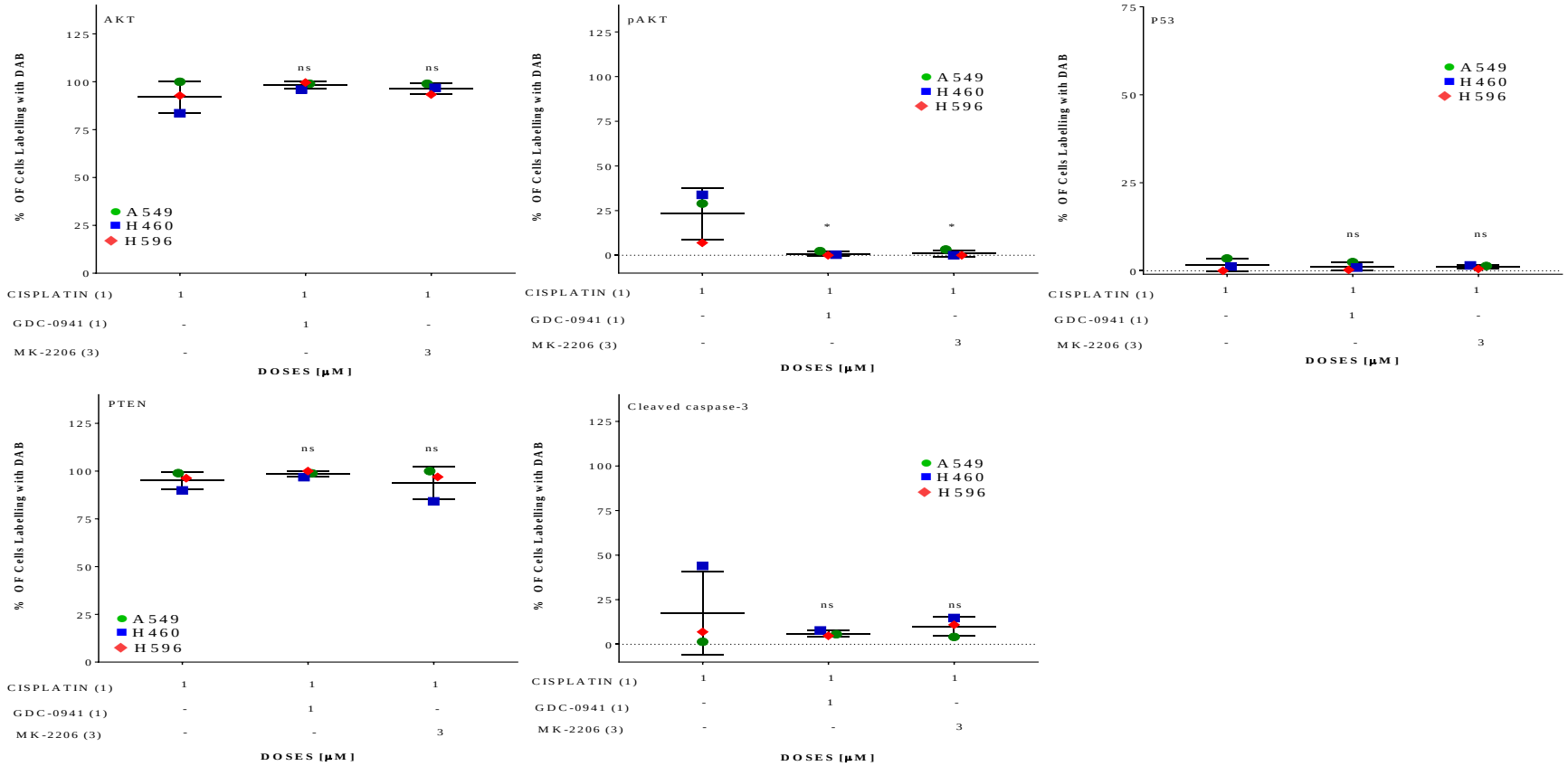

Figure 4. 12 Comparison of Akt, pAkt, P53, PTEN and cleaved casepase-3 expression between cisplatin and cisplatin combined with GDC-0941 and MK-2206 at 24 hr The data were summarized as the average of all model treatments as M ± SD with N=3. The comparison was analyzed by one-way ANOVA with prism and '*' denotes significantly different whereas 'ns' means non-significant.

Table 4. 3 The detection of Akt, pAkt, P53, PTEN and cleaved caspase-3 expression on all cell line models after treatment with cisplatin-GDC-0941 or MK-2206 combinations at 72 hr

Data were analyzed by prism (one-way ANOVA) presented as average of all models and '*' denotes significant comparison between control and each treatment meaning P<0.05.

72 hr treatment	Cell lines	CONTROL	CISPLATIN	GDC-0941	CISPLATIN +GDC-0941	MK-2206			CISPLATIN +MK-2206		
	Average	59	42	92*	76	83			88*		
AKT	A549	46	61	88	64	3 μM	12 μM	21 μM	3 μM	12 μM	21 μM
						91	78	78	81	96	98
	H460	58	59	97	85	87			90		
	H596	73	8	90	78	82			77		
pAKT	Average	7	2	0*	0*	0*			0*		
	A549	14	3	0	0	3 μM	12 μM	21 μM	3 μM	12 μM	21 μM
						0	1	0	0	1	0
	H460	2	5	0	0	0			0		
	H596	4	0	0	0	0			1		
P53	Average	0.5099	0.434	0.5488	0.9282	0.66			2.51		
	A549	0	0	0	0	3 μM	12 μM	21 μM	3 μM	12 μM	21 μM
						0	0	0	1	0	2
	H460	0	0	0	1	1			2		
	H596	1	1	1	2	2			8		
PTEN	Average	49	59	90	66	78			79		
	A549	7	77	90	80	3 μM	12 μM	21 μM	3 μM	12 μM	21 μM
						96	79	78	67	97	100
	H460	55	40	96	52	69			60		
	H596	86	60	84	67	67			72		
Cleaved caspase-3	Average	41	37	18	27	34			25		
	A549	50	38	21	29	3 μM	12 μM	21 μM	3 μM	12 μM	21 μM
						19	35	35	28	12	10
	H460	50	56	20	23	46			34		
	H596	24	19	13	29	34			39		

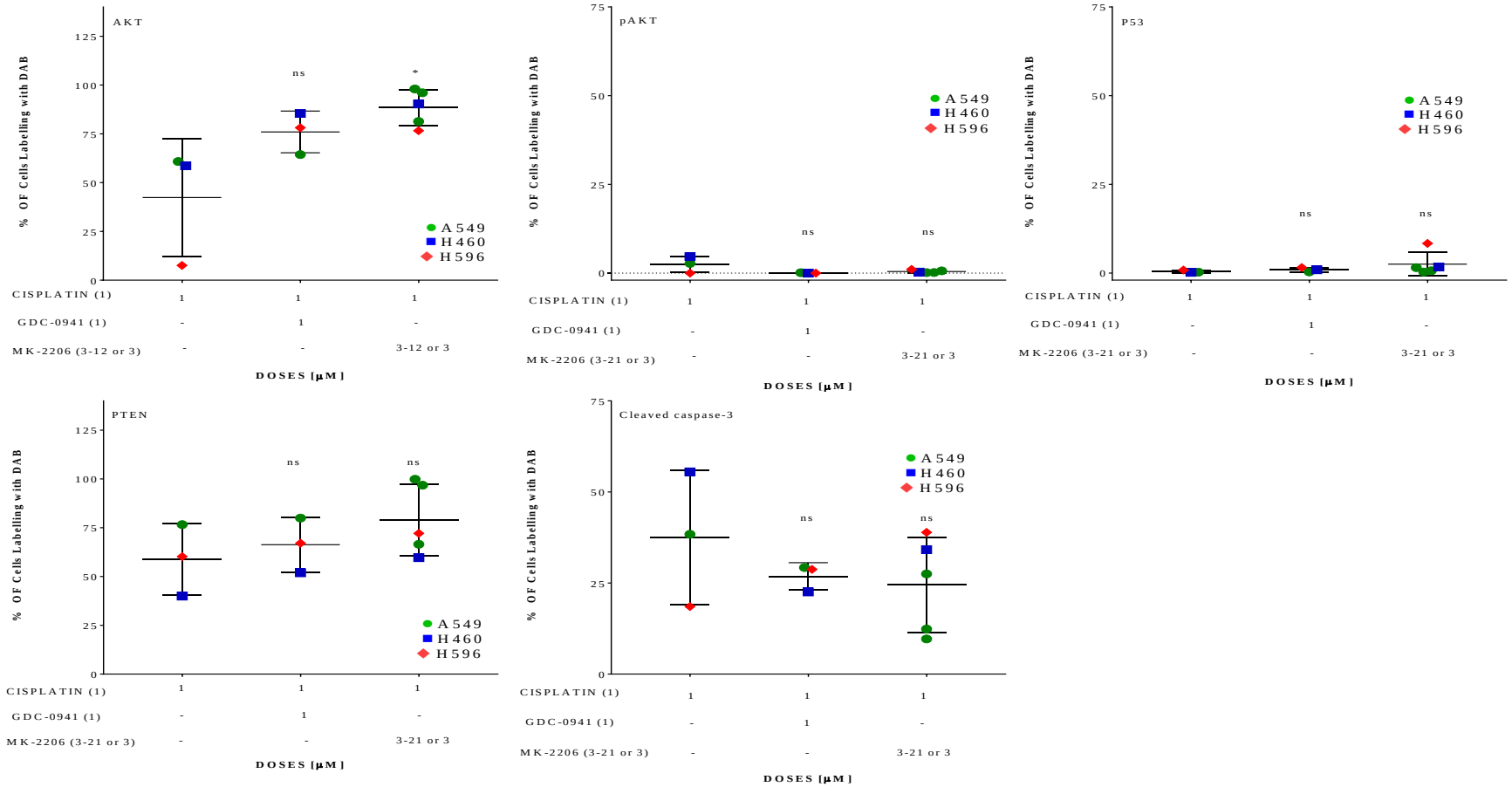

Figure 4. 13 Comparison of Akt, pAkt, P53, PTEN and cleaved casepase-3 expression between cisplatin and cisplatin combined with GDC-0941 and MK-2206 at 72 hr The data were summarized as the average of all models as M ± SD with N=3. The comparison was analyzed by one-way ANOVA with prism and '*' denotes significantly different whereas 'ns' means non-significant.

4.5.3. SUMMARY

Cisplatin single treatment showed a significant induction of pAkt at 24 hr only, whereas the 72-hr treatment saw a basal expression in the antigen. P53 was similarly expressed at both 24 and 72 hr and was not significantly induced by any treatment. Akt and PTEN were the most highly expressed of all antigens, but levels were lower at 72 hr treatment compared to 24 hr treatment. Cleaved caspase-3 was increased at 72 hr in particularly in the control group compared with the 24 hr-treatment, although there were no further increases to cleaved caspase-3 expression observed at 72 hr for any combination treatment compared to cisplatin alone.

4.6. DISCUSSION

4.6.1. COMPARISON OF DRUG RESPONSE BETWEEN 2D CELL LINES AND SPHEROIDS

The uniformity of spheroids' volumes and shapes is an important determinant in drug response, and so reducing variability to a minimum has been shown to benefit the reproducibility of data from experiments using 3D spheroids (Zanoni, et al., 2016). In the study presented here, spheroids were seeded at a concentration of 8000 cells per 200 µL and their uniformity enhanced by centrifuging cells to create a centralized finger-like shape (shown in Figure 2.1) with just one spheroid cultured centrally in each well of low-attachment 96-well microplates. Spheroids were cultured overnight to reach a maximal length of approximately 1-2 mm, at which point a necrotic core might exist.

Culture of 3D multicellular spheroids is of increasing interest to better mimic drug responses than traditional 2D cultures. Within a multicellular spheroid, interactions with surrounding cells and spatial arrangement of receptors critical to key signaling processes are more in keeping with the way cells naturally spatially arrange themselves when not under artefactual influences, such as those found in 2D adherent cell culture. Once spheroids have grown above a certain size, then they are likely to comprise of an outer layer of rapidly proliferating cells surrounding an inner hypoxic core of cells which are more likely to be quiescent due to deprivation of oxygen and nutrients (Edmondson, et al., 2014). In addition, the 3D environment changes the biological behaviors of cancer cells, including alterations in cell signaling, gene expression and protein levels (Lovitt, et al., 2014). A number of studies have shown that 3D cultures exhibit increased drug

resistance to traditional chemotherapeutic agents such as irinotecan, 5-FU (Fluorouracil) and oxaliplatin (Karlsson , et al., 2012), yet few have looked at responses to targeted agents. A study conducted on breast cancer showed that the potencies of targeted or combination therapies were significantly attenuated when treating on the matrix-culturing 3D spheroids compared to 2D cell culture (Gangadhara, et al., 2016). It is likely that the reorganization of cell surface receptors in 3D spheroid culture may play a role in resistance to targeted therapies, in addition to the enhanced quiescent cellular populations present in the more hypoxic spheroid core.

For potencies of drug combination treatments on spheroids, the potency of cisplatin combined with GDC-0941 or MK-2206 was less active when tested on spheroids compared to the 2D cells. Both 24- and 72-hr experiments showed a more potent treatment with cisplatin combined with GDC-0941 or MK-2206, with the spheroid viability significantly decreased by up to 34% and 55% respectively compared to control group, although the difference in the viability compared to cisplatin alone was not greatly enhanced at the combination treatments with less than 30% compared to that in 2D culture. Nearly all treatments including cisplatin treatment at 72 hr emerged to be more active than the counterparts at 24 hr and this was similarly observed in 2D cancer cells which appeared to be refractory to cisplatin single and combination treatments at 24 hr. Change in response to treatments in 3D model compared to 2D culture further indicates that the complex 3D culture environment could actively attenuate drug potencies as discussed above.

There may exist other effects that could change drug sensitivity in 3D culture environment. Multidrug resistance (MDR) in spheroids derived from the lung cancer cell lines INER-37 and INER-51 have been characterized (Barrera-Rodríguez & Fuentes, 2015). Here the authors found that drug sensitivity was determined not only by the decreased proliferation observed upon 3D culture, but also by upregulation of MDR-related genes. However, the authors also suggest that the mechanisms of spheroid-induced MDR-acquisition may be cell-type specific. Zanoni et al. describe how differing spheroid shapes may be a reflection of cell viability within spheroids, with spherical rather than irregular-shaped spheroids exhibiting the greatest degree of drug resistance (Zanoni, et al., 2016).

4.6.2. EFFECT OF DRUG COMBINATIONS ON MRC-5 CELLS

Inclusion of MRC-5 cells into the panel of lung cancer cell lines served to provide insight regarding sensitivities of non-cancer cells in response to combinations of cisplatin with the PI3K/Akt inhibitors. This was important with respect to developing the organotypic co-culture models which takes the simplistic spheroid model approach one step further by the addition of fibroblasts in to a 3D culture system.

The MRC-5 cells were equally sensitive to MK-2206 and GDC-0941-containing combinations as those cancer cells, most notably following a 72 hr treatment with cisplatin-MK-2206 combination therapy. Fibroblasts are able to exert numerous influences on localized cancer cell populations. MRC-5-conditioned media has been shown to influence the behavior of hepatocellular carcinoma cells by potentiating migration and invasion through promoting redistribution of tumor cell cadherins and upregulation of matrix metalloproteases (MMPs) (Ding, et al., 2015). In addition, normal fibroblasts can be transformed to tumor-activated or cancer-associated fibroblasts (CAFs) within tumor stroma, which have a different characterization compared to their normal counterparts and play a role in driving tumor development (Mahale , et al., 2016). Wang et al. investigated the influence of fibroblasts in the response of lung cancer cells with activating EGFR mutations to gefitinib treatment; Here, fibroblast-induced HGF production was thought to mediate the drug resistance in lung cancer cells (Wang , et al., 2009), suggesting fibroblastts to be a suitable therapeutic target in the treatment of lung cancer. Hence, sensitivity of MRC-5 cells to the cisplatin/PI3K/Akt inhibitor treatments may greatly influence co-cultured tumor cell response. The activation of PI3K/Akt signaling pathway also plays a role in regulation of cell survival for fibroblasts. It has been reviewed that PI3K signaling can promote CAF-mediated tumor progression (Yamamura , et al., 2015) and was shown to correlate with CAF-mediated drug resistance (Ying , et al., 2015). The use of Akt inhibitors in reversal of the fibrotic phenotype in diseases such as idiopathic pulmonary fibrosis is of increasing interest. Several studies have shown that inhibition of cell signaling pathways, such as PI3K/Akt signaling could help to decrease fibroblast proliferation, collagen deposition and attenuate mitogenic responses of fibroblasts (Mercer, et al., 2016) (Xu , et al., 2009) (Bujor , et al., 2008). This suggests further that inhibition of fibroblast proliferation and thus their contribution to the pro-carcinogenic microenvironment, may be of benefit.

4.6.3. EFFECT OF DRUG COMBINATIONS ON ORGANOTYPIC CULTURES

Development of the organotypic model across a variety of pathologies has been ongoing for the past decade, and has been shown to better reflect cell invasion observed *in vivo* than more standard 2D cell invasion assays (Nyström, et al., 2005). Many of the older organotypic models incorporated gels consisting mainly of collagen, whereas more modern methods also incorporate Matrigel™, which contains many basement membrane components (as reviewed in 1.6.3). However, a high variability in the composition of Matrigel™ between different batches was observed, impeding reproducibility and complicating drug screening (Fecher, et al., 2016). Whilst the role of stromal fibroblasts has been shown to be critical for invasion of a variety of differing cancer cell types *in vitro* (Nyström, et al., 2005) (Okawa, et al., 2007) (Daly , et al., 2008), fewer studies have been conducted on lung cancer cells using the organotypic model. Here, we showed that the combination of MRC-5 cells with lung cancer cells was critical for tumor cell invasion into the gel, but that the presence of MRC-5 cells embedded in the gel was not a contributing factor to this invasion process. As previously discussed, the presence of MRC-5 cells is likely to contribute to a mix of pro-proliferative and invasion signals including secreted factors such as HGF and Stromal cell-derived factor 1 (SDF-1). In the A549, H460 and H596 models, it is likely that paracrine signaling between the close proximity fibroblasts and tumor cells was sufficient to establish invasive characteristics, without the further requirement of matrix remodeling and invasion signaling from fibroblasts embedded within the gel.

Three dimensional cultures that incorporate a basement membrane mix have also been shown to promote morphological characteristics of invasive and metastatic cancer cells through activation of Akt and mTOR signaling (Nguyen, et al., 2013). It is well established that Akt plays a critical role in cell survival and that its activity correlates to cisplatin resistance in addition to its ability to promote cell invasion of fibroblasts and cancer cells in NSCLC (Lee , et al., 2011) (Kim, et al., 2001). Conversely, the study conducted on breast cancer showed that PI3K/Akt signaling was significantly knocked down in the 3D matrices-culturing model whereas the MAPK signaling was gained in function (Gangadhara, et al., 2016). This may be existing in the study as Akt activation was only significantly observed at cisplatin treatment at 24 hr, whereas the rest of groups including the control group showed a poor expression of pAkt. This suggests that

activation of Akt signaling may not be highly involved in the drug resistance in the 3D culture. it is notable to see that PTEN levels were highly (80%) expressed across all treatments and the low expression of pAkt may be correlated to the high expression of PTEN. P53 expression remained at a modest level (less than 10%) across all treatments, far less than that of PTEN, which further confirmed as suggested in 2D culture that crosstalk between P53 and PTEN does not predominate in the lung cancer setting, highlighting that the interrelationship of these two tumor suppressors is highly dependent on the cancer-specific environment. The expression of cleaved caspase-3 in organotypic model was not shown to be dramatically increased at cisplatin combined with GDC-0941 or MK-2206 compared to cisplatin alone, which was opposite to the observation in 2D cancer cells. Moreover, the 72-hr treatment showed a high expression of cleaved caspase-3 at control group compared to the 24-hr treatment and this may be explained that the increased cell death during a longer incubation period, may be associated with a falsely good drug sensitivity observed in 2D and 3D spheroid models. Hence, it was difficult to assess whether combination of cisplatin with the targeted drugs may provide benefit in terms of decreasing overall cell viability in this model at a longer time point. For future work, immunofluorescent co-staining of cell death/proliferation markers with specific markers for epithelial and fibroblast components may provide insight as to whether the fibroblast populations are still more sensitive to the combined treatments in the co-culture model. Furthermore, longer term treatments with the drugs of interest would also determine whether inhibition of Akt activity (in the fibroblasts or cancer cells) would be sufficient to inhibit matrix remodelling and concomitant invasive capacity of tumor cells. Moreover, the MAPK signaling activation may be examined to detect if there exists a switch of PI3K/Akt to MAPK signaling.

The use of primary cells derived from lung cancer tissues would have further enhanced this organotypic model. Deriving primary cells from tumors would have specifically provided tumor cells with relevant phenotypic and genotypic characteristics, but would also have provided cancer associated fibroblasts (that possess an activated myofibroblast-like phenotype) to be used instead of the normal-derived MRC-5 fibroblasts. Indeed, a significant amount of time was dedicated to trying to grow different populations of cells from lung tumors, but unfortunately with little success. However, use of more relevant primary tissues is addressed in chapter 5.

4.7. CONCLUSION

In summary, both 2D and spheroid models showed a better sensitivity to cisplatin treatment combined with GDC-0941 or MK-2206, among which 2D cells were the most sensitive compared to 3D spheroids. Hence, direct inhibition of PI3K/Akt signaling provided the most significant benefit in terms of the ability to decrease cell viability. Nevertheless, the sensitivities of cells to the combination of cisplatin with GDC-0941 or MK-2206 was not constantly observed among different *in vitro* models, particularly in 3D organotypic model and this may be related to a change in the activation of PI3K/Akt signaling, which was far less activated in the organotypic culture model compared to 2D cells. Moreover, the cisplatin combined with GDC-0941 or MK-2206 on organotypic models seemed not to be suitable for being tested at 72 hr compared to 24 hr due to a high cell death induction at a longer incubation time. There was concurrence between differing cell culture models regarding the protein expression, which was that P53-PTEN crosstalk was not significantly observed in all models and this further confirm the interrelationship between these molecules is more likely tumor-type dependent.

5. CHAPTER FIVE: THE EXPLANT MODEL

5.1. INTRODUCTION

We ultimately sought to determine whether the cellular models and their response to drug treatments presented here, would be translatable to a more clinically relevant paradigm; namely the use of explanted tissues derived from lung cancer patients. Within this chapter, lung cancer tissues exhibiting different mutations would have been utilized to determine whether drug treatments elicited effects on key signaling pathways in a similar manner to that observed in the *in vitro* models. It is acknowledged that tumor heterogeneity is complex, and that tissue samples help to provide a snapshot not just of this genotypic complexity, but also the intricacy of tumor immune and stromal interactions which cannot be recapitulated *in vitro*. However, there are numerous issues associated with use of primary human tissue samples to perform more accurate drug screening assays, not least that of being able to obtain sufficient material and quality of material to give consistent and meaningful data. The comparison between *in vitro* and *ex vivo* drug responses therefore remains important in order to help determine more suitable pre-clinical models for drug screening assays, that may provide better representation of tumor response than simple 2D monolayer cultures. We ultimately wish to translate results of *in vitro* studies to explant models in order to determine whether molecularly targeted agents may be a useful addition to conventional cisplatin-based regimens.

Due to the difficulty in obtaining enough tissues to investigate cisplatin-based combinations undertaken in the previous chapters, this chapter focuses purely on tissue responses to cisplatin. Additionally, the explant model was a continuation of work presented in the thesis undertaken by Dr Karekla (Karekla , 2014), all methods and data analysis were uniformly performed in order that they could be combined with the previous data analyzed by Dr Karekla. From chapter 4, it was concluded that phospho-Akt could be significantly induced in response to cisplatin treatment at 24 hr, compared with GDC-0941 or MK-2206-containing treatments. Here, the explant samples after cisplatin treatment were further analyzed for pAkt and Akt expression in order to evaluate whether Akt activation may play a role in the response to cisplatin and whether a correlation between Akt phosphorylation and other biomarkers of cell proliferation (Ki67) and cell death (cPARP).

5.2. SUMMARY OF CLINICAL CASES OF EXPLANTS

As shown in Table 5.1, the most common subtype of lung cancer for clinically collected samples is SCC, belong to which are cases LT31, LT38, LT84, LT88, LT92, LT98, LT103, LT104, LT105, LT106 and LT107. The cases belonging to ADC include LT33, LT36, LT83 and LT104.The rest of two cases-LT89 and LT116 are atypical carcinoid (AC) of lung cancer. The cases collected by the author include LT98, LT103, LT104, LT105, LT106, LT107 and LT116. Clinical details encompassing patient's gender, tumor stage and survival status is also included in the table.

5.2.1. DETECTION OF COMMON MUTATIONS

The detection for P53 phenotype can be simply achieved via immunohistochemistry staining of P53 nuclear protein. WT P53 was expressed at low levels in small numbers of tumor cells prior to any treatment and was inducible following cisplatin treatment. In contrast, mutant P53 was more likely to be highly expressed in most tumor cells. In those cases exhibiting a P53 deletion, no staining in any tumor area was observed. It is notable to see that both AC cases contained inducible WT P53, as did cases LT33, LT38 and LT83. *KRAS* and *PIK3CA* mutations were detected with the common mutant hotspots (reviewed in chapter 2.3.2.4). The cases collected by the author contain *KRAS*-mutant (*34G>A*) LT104 and LT106 cases, and *PIK3CA*-mutant (*G1633A*) LT105 case, whereas those collected Dr Karekla include *KRAS*-mutant (34G> C or A) LT83 case, and *PIK3CA*-mutant (*A3140G*) LT38 case and *PIK3CA*-mutant (*G1633A*) LT92 case. Overall, the summary of the most common genetic mutations in this small cohort gives a prevalence of 71% TP53, 24% *KRAS* and 24% *PIK3CA* mutations (Table 5.1).

Table 5. 1 Summary of all tissue cases presented for data analysis of antigen expression

Cases collected by Dr Karekla and by the author were summarized in the table below and those cases collected, treated and analyzed by the author are in red, as well as the detected *KRAS* and *PIK3CA* mutations and IHC-detected protein expression. The cases treated by Dr Karekla were all handled by herself including the detection of mutations by qPCR and antigen expression (CK, P53, KI67 and cPARP). Only the expression of Akt and pAkt was later analyzed by the author with IHC.

Case Number	Histology	TNM Staging	Stage	Sex	TP53 Status	Positive Mutation	Antigens detected
LT31	SCC	pT2a, pN0	IB	F	Mutant		CK, P53, Ki67, cPARP, Akt, pAkt
LT33	ADC	pT3, pN0	IIB	F	WT		CK, P53, Ki67, cPARP
LT36	ADC	pT2a, pN0	IB	M	Mutant		CK, P53, Ki67, cPARP
LT38	SCC	pT2b, pN0	IIA	M	WT	PIK3CA A3140G	CK, P53, Ki67, cPARP, Akt, pAkt
LT83	ADC	pT2b, pN1	IIB	M	WT	KRAS 34G>T, C or A	CK, P53, Ki67, cPARP, Akt, pAkt
LT84	SCC	pT2a, pN1	IIA	F	Mutant		CK, P53, Ki67, cPARP, Akt, pAkt
LT88	SCC	pT1b, pN0	IA	F	Mutant		CK, P53, Ki67, cPARP, Akt, pAkt
LT89	AC	pT2a, pN0	IB	F	WT		CK, P53, Ki67, cPARP, Akt, pAkt
LT92	SCC	pT2b, pN1	IIB	F	Deleted	PIK3CA G1633A	CK, P53, Ki67, cPARP,
LT98	SCC	pT3, pN0	IIB	M	Mutant		CK, P53, Ki67, cPARP, Akt, pAkt
LT103	SCC	pT2a, pN0	IB	F	Mutant		CK, P53, Ki67, cPARP, Akt, pAkt
LT104	ADC	pT2a, pN0	IB	M	Deleted	KRAS 34G>A	CK, P53, Ki67, cPARP, Akt, pAkt
LT105	SCC	pT3, pN0	IIB	M	Mutant	PIK3CA G1633A	CK, P53, Ki67, cPARP, Akt, pAkt
LT106	SCC	pT2a, pN1	IIA	F	Mutant	KRAS 34G>A	CK, P53, Ki67, cPARP, Akt, pAkt
LT107	SCC	pT4, pN0	IIIA	F	Mutant		CK, P53, Ki67, cPARP,
LT116	AC	pT2b, pN0	IIA	F	WT		CK, P53, Ki67, cPARP, Akt, pAkt

5.3. RESPONSE OF EXPLANTS TO CISPLATIN

As reviewed in 2.3.2.1, each tumor case was processed for the explant model and was treated with cisplatin (1, 10 and 50 µM) for 24hr, along with two control (untreated) groups (under the same culture conditions with drug vehicle only). Following 24 hr culture, all groups were fixed and embedded for a series of tissue sections, which were visualised using H&E stains and were immunohistochemically stained for the detection of CK, Ki67, cPARP, P53, Akt and pAkt antigens within tissues. All cases were analyzed

for Ki67, cPARP and P53 expression, but due to the lack of explant tissues only certain cases could be stained for Akt and pAkt. WT P53 cases are presented in order to show induction of P53 following treatment with a range of concentrations of cisplatin (1, 10 and 50 µM).

5.3.1. IMMUNOHISTOCHEMISTRY STAINING FOR ANTIGEN EXPRESSION

Figures 5.1 and 5.2 shows the representative photomicrographs of cases with WT P53 (LT116 case) and those with mutant P53 (LT103) respectively. These figures show immunohistochemistry staining of comparative areas for all biomarkers (CK, Ki67, cPARP, Akt, pAkt and P53, along with H&E staining across control and all treatment group. H&E staining was shown to present histology. CK staining was used to select the majority of tumor cells from other cell types.

As a brief overview, LT103 had a higher expression in most biomarkers than that observed in case LT116. Specifically, P53-mutant LT103 case showed a dose response for decreasing Ki67 levels whereas the P53-WT LT116 case showed a low concentration of Ki67 across all cisplatin treatments. Both LT103 and LT116 cases showed a gradual increase in cleaved PARP with concentration of cisplatin rising from 1 µM to 50 µM, whereas the cell death in LT103 emerged to be higher than that in LT116 case. Similarly, both two cases showed no changes to Akt and pAkt expression following treatment with any concentration of cisplatin, among which LT103 case showed a high expression of Akt and pAkt compared to that observed in LT116 case. For P53 expression, LT103 case had an equally high concentration of P53 observed in all groups including the untreated group, whereas LT116 showed a gradually slight induction of P53 expression in response to the increasing concentrations of cisplatin treatments.

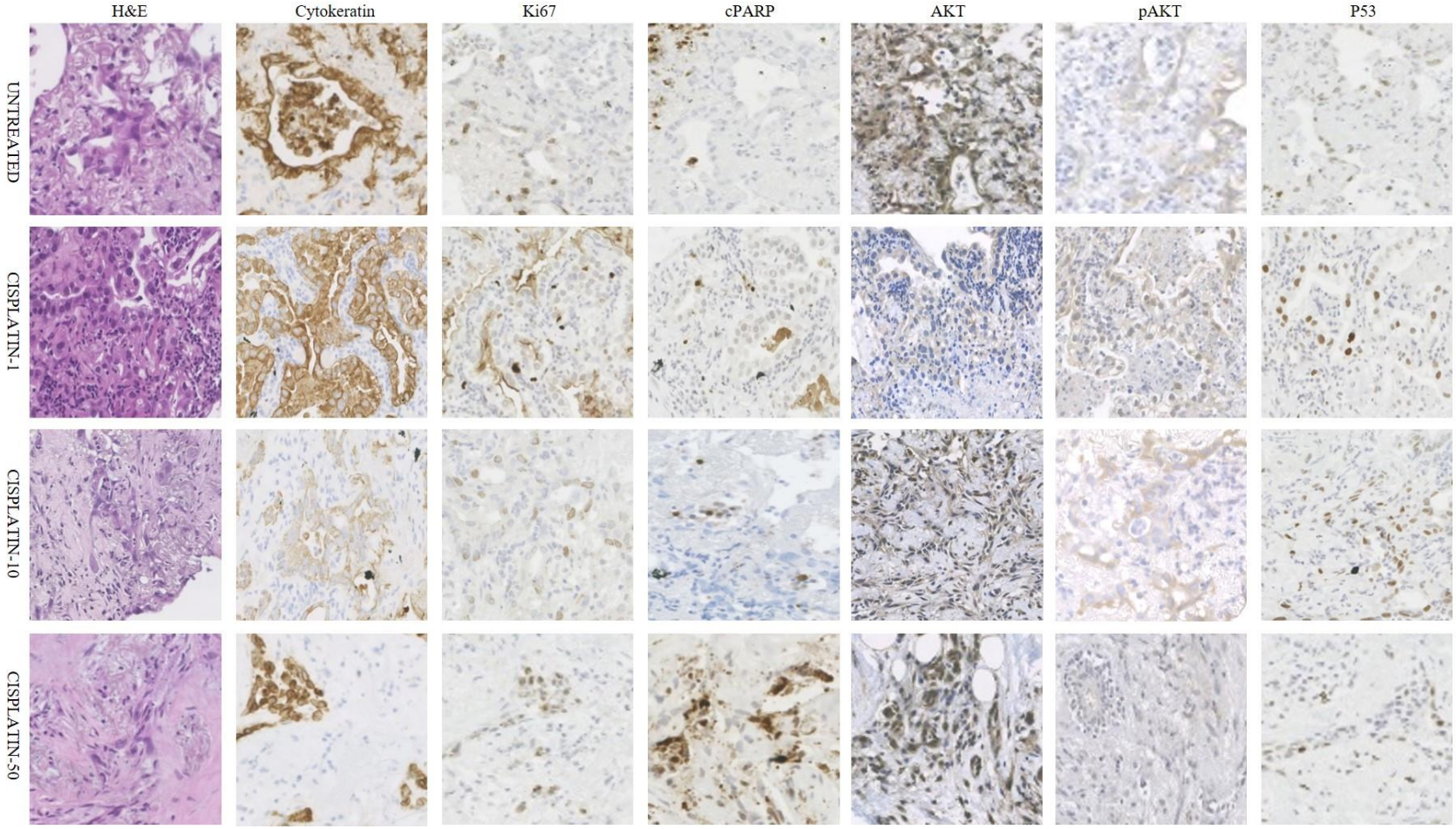

Figure 5. 1 LT103 case showing the comparative areas of explants from untreated group and 1, 10 and 50 µM cisplatin treatment groups for presenting H&E staining and immunohistochemistry staining of CK, Ki67, cPARP, Akt, pAkt and P53

It is shown that nearly all biomarkers are highly expressed in LT103 case particularly for cPARP, Akt, pAkt and P53 expression.

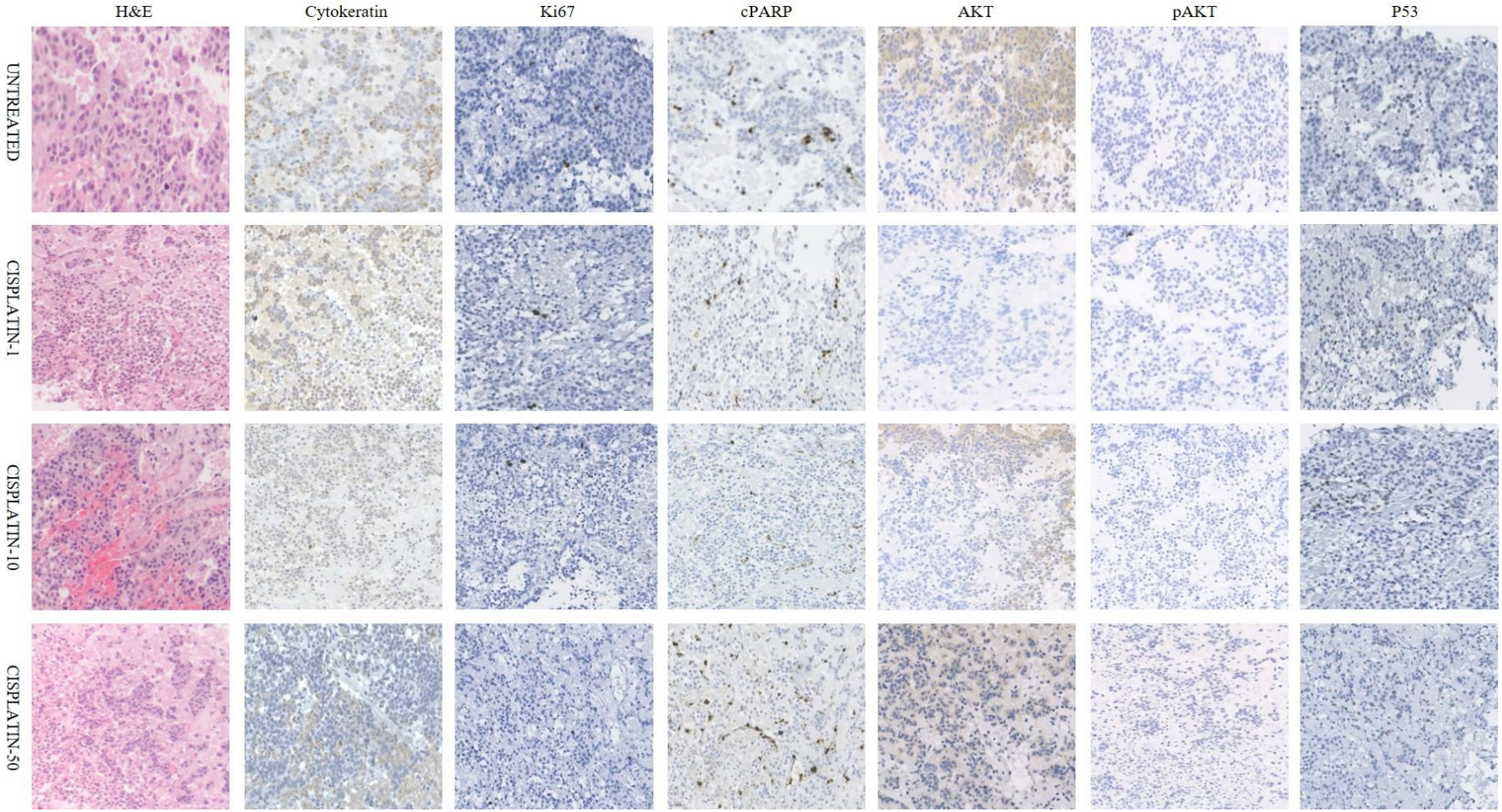

Figure 5. 2 LT116 case showing the comparative areas of explants from untreated group and 1, 10 and 50 µM cisplatin treatment groups for presenting H&E staining and immunohistochemistry staining of CK, Ki67, cPARP, Akt, pAkt and P53

This case showed low concentrations in most biomarkers, such as Ki67, pAkt and P53.

5.3.2. ANTIGEN EXPRESSION RESPONDING TO CISPLATIN TREATMENT

The Figure 5.3 shows the results for Ki67, cPARP, P53 expression (only the WT P53 cases) and pAkt/Akt ratio, summarized from all cases, which are further grouped into SCC, ADC and AC subtypes.

The majority of cases, whether they were P53 WT or mutant, underwent a positive response to cisplatin treatment (particularly at the highest concentration), namely the induction of cPARP-mediated apoptosis in conjunction with a decrease in Ki67-indicated proliferation . It was notable to observe that WT P53 cases had only a modest response to cisplatin treatment; only cases LT38 and LT83 showed a significant increase in cleaved PARP across the range of cisplatin doses, whereas the rest of the cases (LT33, LT89 and LT116) showed a small change to cPARP expression in response to any concentration of cisplatin treatment. Moreover, the induction of cell death at 50 µM cisplatin treatment observed in WT P53 cases was lower than most cases with P53 mutation.

Amongst all P53 mutant cases, cases LT31, LT36, LT84, LT88, LT92, LT105, LT106 and LT107 exhibited the greatest sensitivity to cisplatin treatment, with cPARP expression (immunoratio) increasing above 80%. There exists a dose response to cisplatin treatment observed in most SCC cases, although the LT98 case showed an increase in Ki67 expression, rising from approximately 30% at 1 µM cisplatin to 60% at 50 µM cisplatin. Nearly all SCC cases showed a relatively higher expression of cPARP than those ADC and AC cases in response to cisplatin treatment. In contrast to this, K67 levels decreased, from approximately 70% to less than 20%, whereas the other subtypes' cases showed an only slight change in Ki67 expression by up to 10%. In the cases that expressed WT P53 there appeared overall, to be a gradual increase in P53 expression with increasing concentrations of cisplatin from 1 µM to 50 µM. Case LT33 showed the highest expression of P53 across all cisplatin treatment groups, with the level of P53 increasing up to approximately 60% at 50 µM cisplatin. Case LT38 case also showed a relatively higher expression of P53 at 50 µM cisplatin with an immunoratio of about 20%.

Akt activity is presented as pAkt/Akt ratio that was calculated from pAkt immunoratio divided by Akt immunoratio. Amongst all cases, only LT84 case with P53 mutation showed a significant increase in the ratio of pAkt/Akt in response to cisplatin treatment,

with a maximal ratio increase of between 5 and 8. However, cisplatin sensitivity was still observed in this case.

In contrast, the rest of other cases with or without P53 mutations, showed a lower pAkt/Akt ratio less than 1 but still exhibited sensitivity to cisplatin treatment.

The data analysis was further summarized in Figure 5.4. The cPARP expression was expressed as cPARP increase in fold as compared to control group and the data showed a significant ($P<0.05$) increase in cPARP-mediated apoptosis at 50 µM cisplatin alone with cPARP expression increasing between 2 and 16-fold increase compared to a less than 4-fold increase at 1µM cisplatin treatment. The data for the rest of antigen expression were presented as immunoratios (%) for each case. For Ki67 expression, 50 µM cisplatin showed a significant decrease in the protein compared to that at 1 µM cisplatin alone, decreasing from around 40% at 1 µM cisplatin to 20% at 50 µM cisplatin. P53 expression was significantly induced at the highest concentration of cisplatin (about 35%) compared to control (0%) and 1 µM cisplatin (10%) alone. In contrast, there were no significant changes to pAkt/Akt ratio by any concentration of cisplatin treatment.

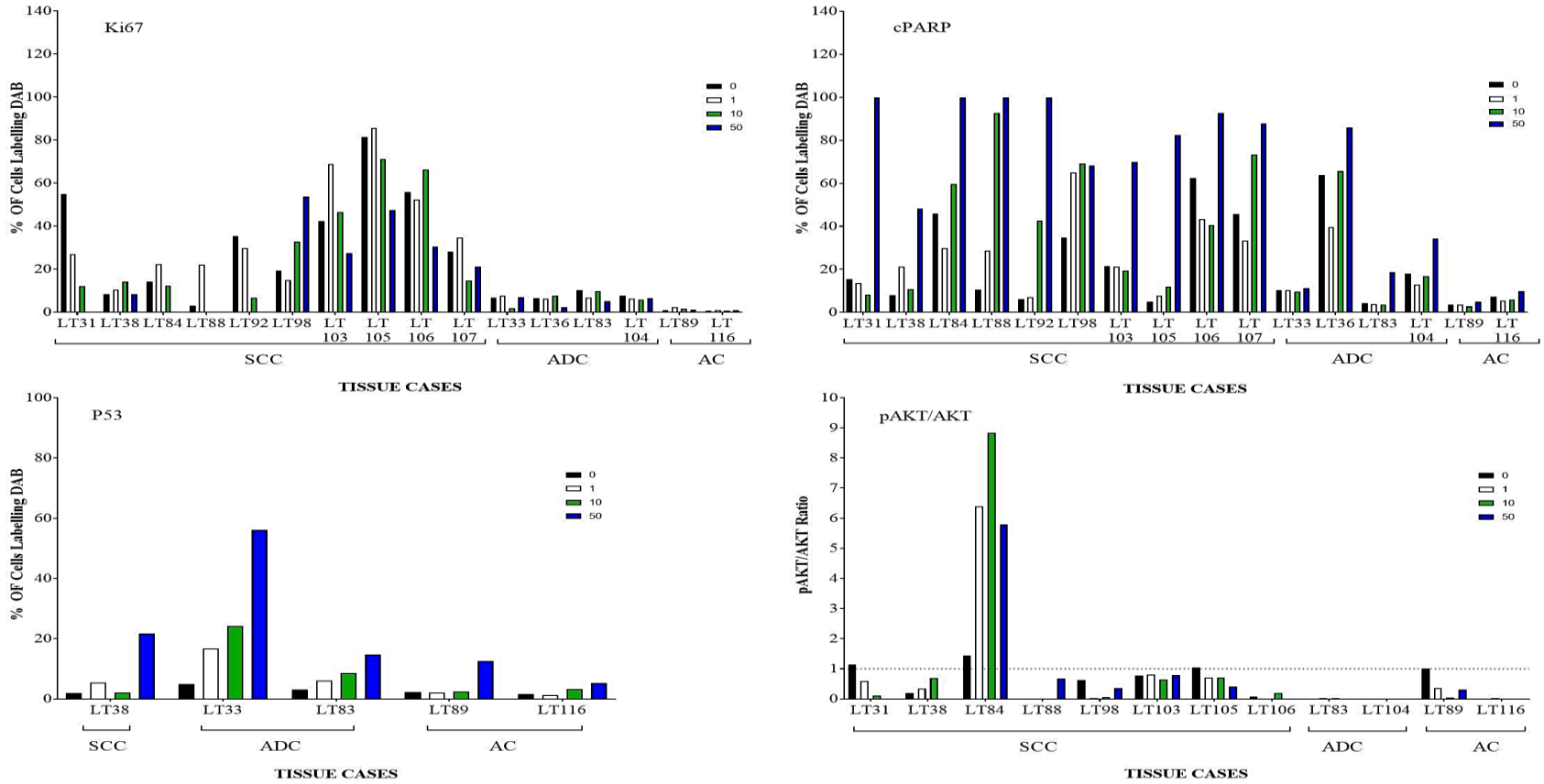

Figure 5. 3 Summary of cases for expression of KI67, cPARP, P53 and pAkt/Akt ratio with respect to cisplatin treatment

The untreated group is labelled with '0' and increasing concentrations of cisplatin treatment are labelled with 1, 10 and 50 respectively. Cases are categorized according to the tumor subtypes, which are SCC, ADC and AC respectively. The result for antigen expression is presented as immunoratio (%). pAkt/Akt ratio is calculated from the division of pAkt immunoratio to Akt immunoratio.

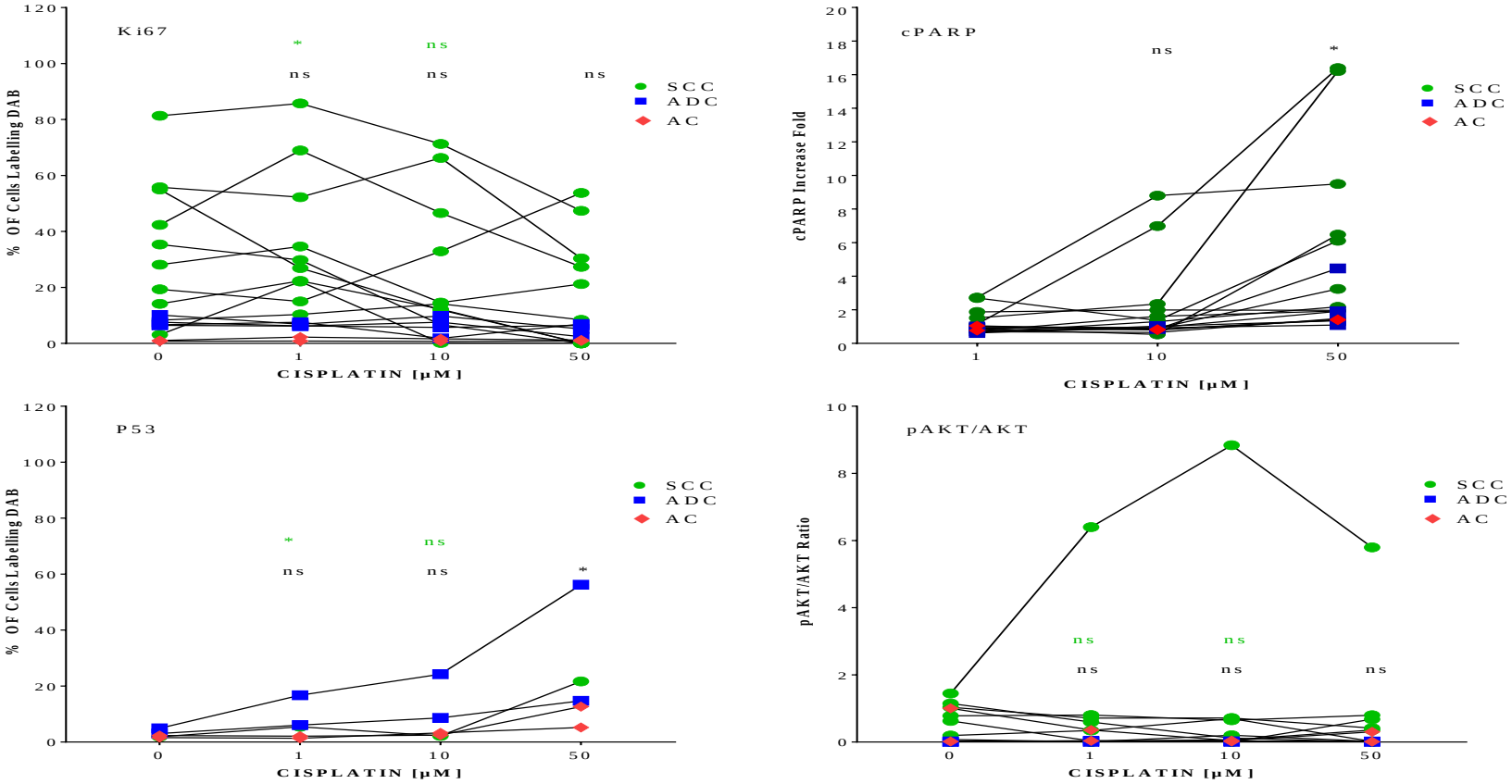

Figure 5. 4 Drug Response to cisplatin treatment with respect to expression of Ki67, cPARP and P53 and the pAkt/Akt ratio

The data were summarized from all cases and analyzed by two-way ANOVA (prism) to compare control vs cisplatin treatment and the difference between 50 µM cisplatin and the rest of cisplatin treatment. For cPARP expression, the increase in fold was presented to indicate the comparison of 1 µM cisplatin with 10 or 50 µM cisplatin. P<0.05 and 'ns' means non-significant. The significance (* or ns) is shown in black for comparing control vs each treatment and green for 50 µM cisplatin treatment vs 1 or 10 µM cisplatin treatment.

5.3.3. THE COMPARISON OF CISPLATIN RESPONSE BY P53 STATUS

As the majority of cases showed a P53 mutation (about 70%), it is interesting to evaluate the difference in response to cisplatin treatment between P53 inducible (WT P53) and P53 non-inducible cases (mutant and deleted P53).

The result, as shown in 5.3.2 was that at 50 µM cisplatin there was a significant increase in cPARP-mediated cell death in conjunction with a significant decrease in cell proliferation (Ki67) compared to 1 µM cisplatin alone. Thus, only the comparison in the changes to Ki67, cPARP expression and pAkt/Akt ratio following 50 µM cisplatin treatment compared to control was shown between WT and mutant P53 cases (Figure 5.5). Similarly as shown above, the majority of SCC cases with mutant P53 showed a significant increase in cPARP level concurrently with a significant decrease in Ki67 expression in response to 50 µM cisplatin compared to untreated, in contrast to that in WT P53 cases. No significant difference in pAkt/Akt ratio was observed in response to 50 µM cisplatin treatment compared to untreated between WT and mutant P53 cases.

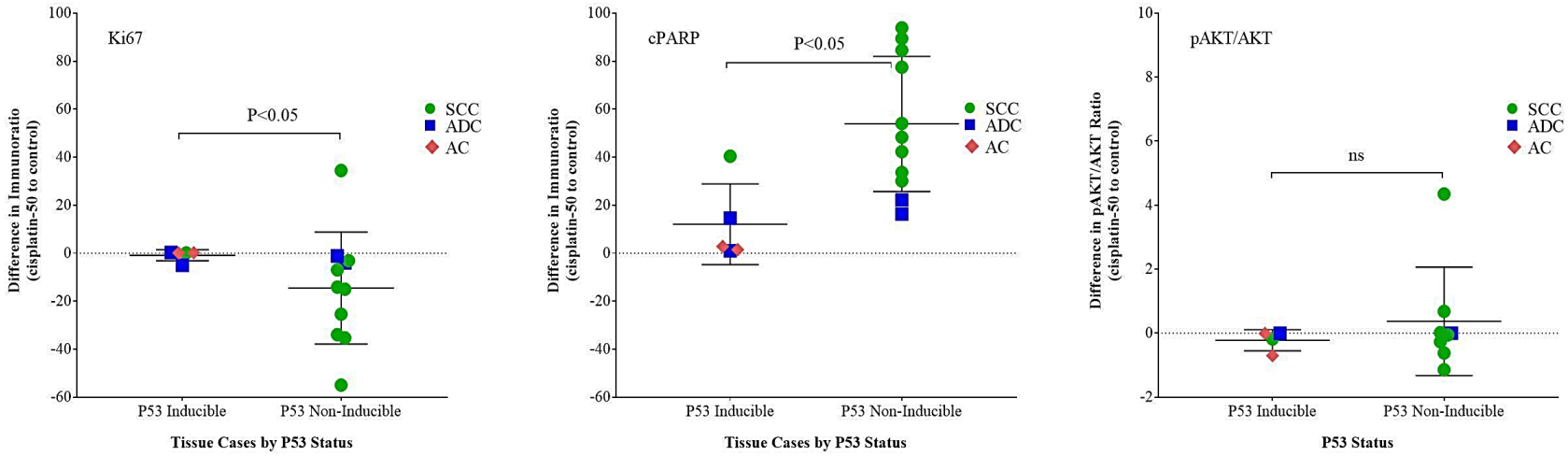

Figure 5. 5 The comparison in changes to Ki67, cPARP and pAkt/Akt ratio by 50 µM cisplatin compared to control between P53-induciable and non-inducible cases The figure shows the changes to the expression of Ki67, cPARP and pAkt/Akt ratio (t-test by prism) between P53 inducible and non-inducible cases following 50 µM cisplatin treatment compared to untreated group. All cases were summarized according to the tumor subtypes (SCC, ADC and AC). Results are shown as M ± SD of all cases with non-inducible P53 cases more than those with a functional P53. '*' means P<0.05 and 'ns' means non-significant.

Following the results shown in Figure 5.5, it was interesting to evaluate whether a correlation existed between pAkt and cPARP or other biomarkers (Ki67 and Akt) with respect to cisplatin treatment. As shown in Figure 5.6, WT P53 cases showed a significantly inverse correlation between pAkt and cPARP expression at 50 µM cisplatin compared to untreated group. In contrast, no other significant correlations were observed between pAkt to Ki67 or Akt expression at the cisplatin treatment. Moreover, there appeared to be a zero correlation between pAkt and Ki67 expression at 50 µM cisplatin compared to untreated group observed in WT P53 cases, with a linear regression slope nearly parallel to the x axis (0). In contrast, those P53 mutant cases showed a clearer correlation, although not significant, between pAkt and Ki67 expression at 50 µM cisplatin compared to untreated group. Similarly as shown for WT P53 cases, there was also an inverse interrelationship, although not significant, between pAkt and cPARP at 50 µM cisplatin compared to control observed in the mutant P53 cases. This indicates that Akt inactivation may be likely to promote PARP cleavage in response to cisplatin treatment. For the correlation between pAkt to Akt, both WT and mutant P53 cases showed a similar trend between these two molecules which, however, was not significantly correlated with each other.

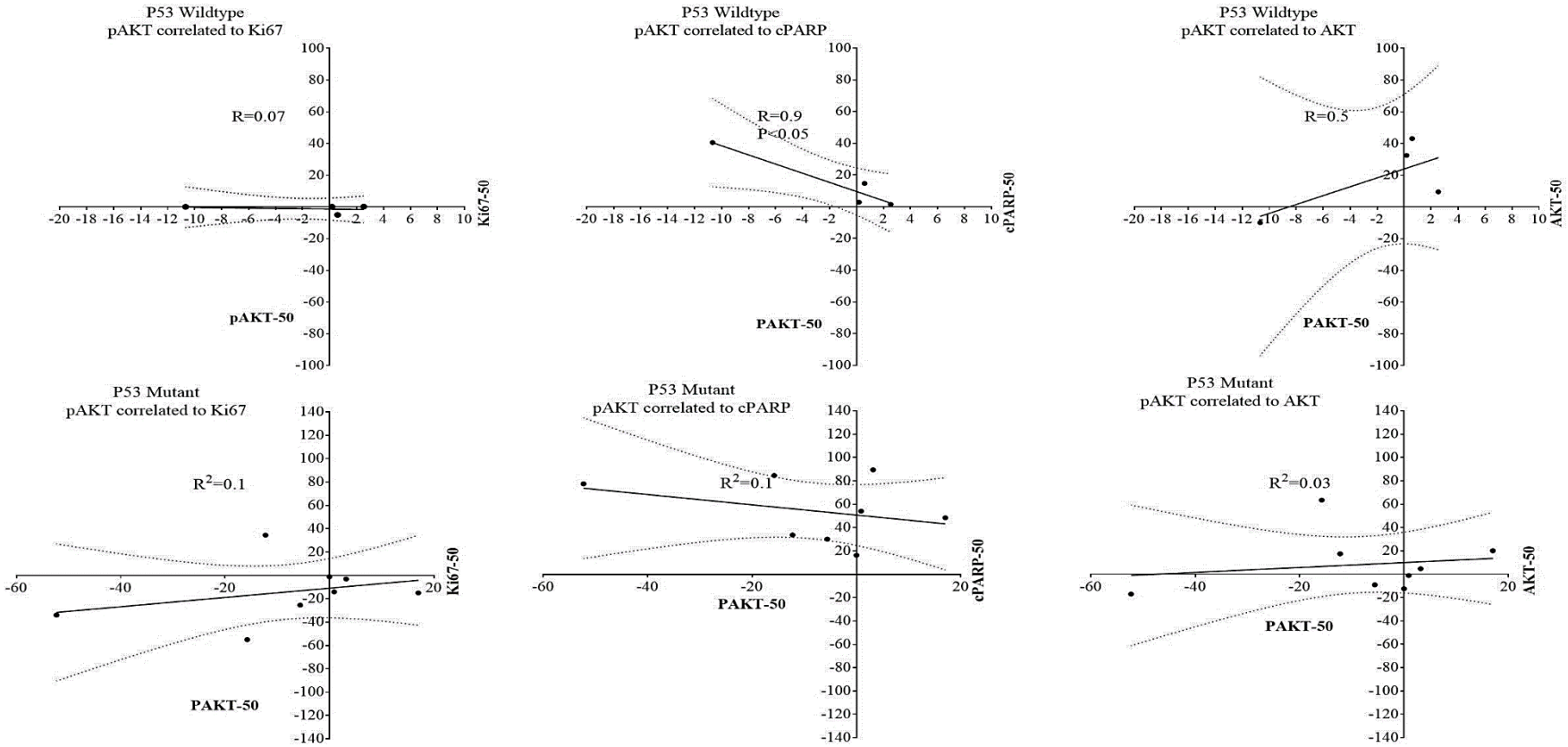

Figure 5. 6 The correlations between pAkt to Ki67, cPARP and Akt expression in P53 WT and mutant cases

Figure shows the correlation between pAkt and respectively Ki67, cPARP and Akt with respect to changes in response to 50 µM cisplatin compared to untreated group in WT or mutant P53 cases. The significant correlation was expressed as '*', which means $P<0.05$ and R^2 is used to assess linear regression for each correlation. An R^2 close to 1 presents a good a correlation.

Due to limited cases with *KRAS* or *PIK3CA* mutations, it was not possible to evaluate the comparison of these biomarker expression between *KRAS/PIK3CA* mutant and WT cases.

In summary, cisplatin treatment at the highest concentration (50 µM) showed the greatest potency in the explant model with a significant induction of cPARP expression. The majority of cases sensitive to cisplatin treatment appeared to be the squamous cell carcinoma subtype concurrently possessing a P53 mutation. The majority of cisplatin-sensitive cases showed a lower pAkt/Akt ratio with the exception of LT84 case, which had a higher pAkt/Akt ratio increasing to more than 5 following cisplatin treatment, whereas the drug sensitivity was still observed in that case. Moreover, the WT P53 cases showed a significantly inverse correlation between pAkt and cPARP expression at 50 µM cisplatin compared to untreated group.

5.4. DISCUSSION

5.4.1. ADVANTAGES AND DISADVANTAGES OF THE EXPLANT MODEL COMPARED TO IN VITRO CULTURES

Explants were sourced directly from patients undergoing surgical resection for their lung cancer. Explants offer a distinct advantage in their cellular composition compared with simpler forms of 2D and 3D tissue culture models, as they display a well-preserved microenvironment such as would be observed within the original tumors. In contrast, 2D adherent and 3D cell models are unable to recapitulate the complex intercellular communication that is integral in maintaining the TME, which likely to play a critical role in drug response. Like explants, several similar tissue-derived models, such as organ-slices cultures have been developed recently (Shamir & Ewald , 2014). The *ex vivo* model culture of human tissues has been shown to be useful in predicting drug response from tumors (Vaira, et al., 2010). The animals-sourced organs and tissue slice models have also developed to offer the closest *in vitro* models of the *in vivo* state (Antoni , et al., 2015). However, such animal models are expensive, the organs have limited availability, and maintaining the tissue's viability *ex vivo* is difficult. Moreover, animal-based models may fail to predict the therapeutic response outcomes in patients (Antoni , et al., 2015) .

A study has used an *ex vivo* culture of tumor sections that well preserve the heterogeneity of TME to successfully predict the clinical response to therapeutic efficacy of targeted and cytotoxic drugs in patients with HNSCC and colorectal cancer (Majumder , et al.,

2015). In the study presented here, the *ex vivo* explant model was initially developed by Dr Karekla (Karekla , 2014) and has undergone substantial method development for the study of drug treatments, with further investigation focussing on whether *ex vivo* responses may be predictive of patient response. Her studies showed that there was a significant correlation between clinical response of patients and response of explant model to cisplatin. Furthermore, the survival curve of patients after clinical treatments was significantly associated with *ex vivo* response to cisplatin treatment. The work has been successfully published (Karekla , et al., 2017). This thesis contributed to this publication and included data from explants prepared by Dr Karekla.

The study presented here further analyze the correlation between Akt activity and response to cisplatin treatment, and demonstrated that decreased pAkt expression was significantly associated with induction of cPARP-mediated cell death at 50 µM cisplatin compared to untreated group, which was only observed in WT P53 cases compared to P53-mutant cases. This was similarly observed in 2D and 3D spheroid cultures that cisplatin treatment combined with PI3K/Akt inhibitors appeared to be more potent in the WT P53 cell lines (A549 and H460) than the mutant P53 cell line (H596). Moreover, the majority of cisplatin-sensitive explant models were P53-mutant squamous cell carcinoma cases. This bears similarity to the simplistic 2D cultures of the H596 cell line which is derived from an adenosquamous carcinoma subtype, harbours P53 mutation and showed the greatest sensitivity to cisplatin treatment compared to other cell lines. Taken together, there was concurrence in observations between the explants model and the *in vitro* 2D and 3D cultures. Moreover, preliminary data have proven promising and expansion of this model to incorporate PI3K/Akt targeted drugs in combination with cisplatin is of considerable interest.

Despite this, there are a number of limitations inherent with the explant model that still dictate a viable niche for the more simplistic cellular models within the drug discovery pathway.

Not only is the collection of explants limited by the local resection rate (with further limitations also created by hospital bed availability, cancelations etc), availability of pathology staff to cut tissue samples and competing for tissue with numerous other studies, explant success also relies heavily on tissue quality and integrity. Tissue with highly necrotic areas is unsuitable for explant culture, and the volume of tissue must be sufficient

such that all treatment and controls can be included for completeness of each experimental observation. In addition, explant tissues are easily damaged during the dissection and fixation processes, and so attrition rates from all samples remain relatively high. Out of the 7 cases (just including all collected by the author) presented here, 18 case of tissues were actually collected showing that more than 60% of cases were lost as they were not suitable for analysis. The thicknesses of tissues in some cases also limited the amount of sections that could be cut for immunohistochemical analysis, and so evaluation of all required antigens was not always feasible. Lung cancers often exhibit regions of dense stroma, meaning that there is little epithelial tumor tissue present in which to evaluate expression of pertinent proteins, ultimately resulting in loss of data within that particular group. For keeping consistency in data comparison between control and treatments, two control groups were usually prepared to assess whether the explants were responding to the drug treatments of interest. Mutation profiling was undertaken after completion of explant treatments, with P53 WT samples accounting for only 29% of all tissues. *KRAS* and *PIK3CA* mutations were even less common, and so difficulties may further be encountered when trying to factor in relevant controls for specific genotypes.

Due to the heterogeneity between patients (genotype, stage, histology, survival), the protein expression was evaluated by IHC on a case-by-case basis. This means that a large number of pulmonary explant cases are required in order to achieve robust datasets from which appropriate conclusions can be drawn.

However, the lack of material available means that the 2D, 3D and organotypic cultures have an important role to play in determining pertinent dose- and time-responses to take forward into resource-limited explant cultures.

5.4.2. P53 EXPRESSION IN RESPONSE TO CISPLATIN TREATMENT

Previous validation work has revealed that tissues which are P53 WT may offer an indicator of response to cisplatin treatment, due to its known induction in response to genotoxic stressors. However, the study presented herein showed the opposite observation, in that most cases with P53 mutation exhibited a greater sensitivity to cisplatin treatment than those WT P53 cases with high proportion of cPARP-mediated cell death; Moreover, most of the P53 mutant cases with the exception of LT98 showed a significant decrease in Ki67 with the highest concentration of cisplatin treatment compared to the lowest dose of cisplatin alone. This suggested that cisplatin-induced

cytotoxicity could be P53 independent, which was also observed in 3.5.1. The P53-indepent induction of cell death in response to cisplatin treatment could be a switch from BAK-dependent apoptotic pathway in P53 WT-expressing NSCLC cells to a BAX-dependent cell death in the P53-loss-of-function cells (Matsumoto, et al., 2016).

A correlation may also exist between cisplatin-induced P53 expression and pAkt downregulation. This study presented herein showed that at 50 µM cisplatin where there was an inverse correlation between pAkt expression and cPARP in WT P53 cases only. Moreover, there was a P53 mutant case (LT84) showed an increase in the cell death concurrently with an observation of the highest pAkt/Akt ratio. Similarly to that, cisplatin treatment on 2D cells at 24 hr (see appendix 7.2) caused an increase in pAkt expression in H596 (P53 mutant) compared to other two cell lines (P53 WT). Taken together, hyperactivation of Akt is more likely to exist in mutant P53 cases in comparison to WT P53 cases, whereas in P53-WT cases, downregulation of Akt phosphorylation significantly correlated with induction of cPARP-mediated apoptosis. This potentially highlight the role of pAkt as a useful biomarker for predicting response to cisplatin treatment.

5.4.3. FURTHER USE OF THE EXPLANT AND ORGANOTYPIC MODELS

Due to time and tissue limitations, further drug screening of the combination therapies between cisplatin, GDC-0941 and MK-2206 inhibitors failed be undertaken within the context of this thesis. Use of specific PI3K/Akt inhibitors would help to increase understanding of the relationship between Akt activity and P53 induction by cisplatin within the explant model. The 2D and 3D cultures (including spheroid and organotypic culture models) showed the combined inhibition of PI3K/Akt with cisplatin treatment exerted a minor effect on P53 induction compared with cisplatin treatment. This result should be further assessed in the explant model in the future.

5.5. SUMMARY

To summarize, P53 induction in the WT P53 cases was not associated with the sensitivity to cisplatin treatment compared to P53 mutant cases. However, there was a significant inverse correlation between pAkt downregulation and induction of cell death at 50 µM cisplatin observed in P53 WT cases, suggested that a decrease in Akt phosphorylation may be associated with cisplatin-induced P53 accumulative expression.

6. CHAPTER SIX: CONCLUSION AND FURTHER WORK

In the project presented here, various preclinical models including 2D adherent cell culture, 3D homogeneous -cell spheroids, the 3D co-culture model of cancer and stromal cells, and human tissue-derived explants were respectively tested for drug response following cisplatin treatment or combined with agents that directly or indirectly target Akt. Due to the time limitation and poor availability of human tissues, explants were tested with cisplatin treatment only. Sufficient amount of time will be needed in order to finish the assessment of various cisplatin-based combination treatments.

Nevertheless, the result from the explant model showed the majority of P53 mutant explant cases exhibited the greatest sensitivity to cisplatin treatment, with the levels of cPARP increasing up to 100%, compared to that observed for WT P53 cases. The 2D adherent and 3D spheroid cultures could predict similar such responses, revealed that the mutant P53 cell line (H596) was the most sensitive to cisplatin treatment compared to the other two cell lines (A549 and H460), This has recently been reviewed in the literature (Matsumoto, et al., 2016). In opposite to that, previous studies have demonstrated that the chemosensitivity of *P53* mutant NSCLC cell lines could be restored by improving P53 function (Lai, et al., 2000) (Guntur, et al., 2010). The tissue-specific subtype may play a role in responding to cisplatin treatment, as the majority of explant cases were the SCC subtype that showed a better response to cisplatin treatment compared to that observed at ADC and AC. In contrast to that, the genomics of drug sensitivity database showed there was no significant difference in the sensitivity to cisplatin treatment between P53 mutant and WT lung ADC cells (http://www.cancerrxgene.org/translation/Drug/1005#t_scatter_1005).

As for the correlation of Akt activity to drug response to cisplatin treatment, the study presented here showed a significantly inverse correlation between Akt phosphorylation and PARP cleavage in response to cisplatin treatment at high concentration of cisplatin treatment compared to control group. Although this was only demonstrated in WT P53 cases compared to the P53 mutant cases, this highlights that Akt could be a potential drug target to enhance cisplatin treatment. As shown in 2D culture, the combination of cisplatin with PI3K/Akt inhibitors appeared to more potent on both WT P53 A549 and H460 cells

than the P53 mutant H596 cells with high induction of caspase-3-dependent apoptosis. However, the level of pAkt was not shown to be highly expressed (A549 and H460) with respect to cisplatin treatment prior to combination with PI3K/Akt inhibitors. The results from 3D organotypic culture model showed a significant decrease in pAkt expression at cisplatin combined with GDC-0941 or MK-2206 compared to cisplatin alone, which did not appear to correlate with an induction of cell death (caspase-3 cleavage). Additionally, there may exist an equipment-specific problem (i.e. ICW showed a high variance in the data). Therefore, it is valuable to assess the Akt activity in explants model in response to cisplatin treatment and to the combination with Akt-targeted agents in the future in order to assess whether a correlation may exist between Akt activity and sensitivity to the cisplatin-based combination treatments.

As for P53 crosstalk with PTEN/PI3K/Akt signaling, this study showed no significant relationship between P53 expression and Akt inactivation; Moreover, PTEN expression appeared to be independent of P53 expression. This highlights that the crosstalk between PTEN and P53 is tumor type-specific, which has been reviewed recently (Chalhoub & Baker, 2009). Nevertheless, this observation should be further analyzed in the explant model in the future work, which will include the detection of PTEN with IHC in the explants cases. Moreover, cell lines used in the project are all PTEN-intact and PTEN function may be associated with low activity of PI3K signaling and thus maybe slightly affected by P53 function. It would be interesting to study further on PTEN-loss-of-function-mediated PI3K/Akt signaling activation and the association with P53 function by using PTEN dysfunctional cell lines.

Furthermore, mutations in *KRAS* and *PIK3CA* may affect the response to cisplatin treatment that is independent on P53 status. As shown in 2D culture, the *KRAS* WT cell line-H596 showed greatest response to cisplatin treatment, whereas A549 with *KRAS* mutation only showed the least sensitivity. Similarly as shown in the explant model, two of the three cases (LT83 and LT104) with *KRAS* mutation all showed a modest response to cisplatin treatment. Whereas there exists a debate whether KRAS mutation could efficiently predict the response to chemotherapy (Hames, et al., 2016) (Chan & Hughes, 2015) (Riely , et al., 2009). Akt activation may be associated with *KRAS* driven cell survival, as KRAS is an upstream activator of PI3K and thus mediate Akt downstream signaling. Both *KRAS* mutant cell lines (A549 and H460) showed a high sensitivity to

cisplatin treatment in combination with Akt inhibition. The concurrent *KRAS* and *PIK3CA* mutations may promote Akt activity compared with the context with either of single mutation only. This was shown in 2D and 3D spheroid models that both mutation-containing cells showed a high sensitivity to PI3K/Akt inhibitors and the combinations with cisplatin treatment. Preclinical study has reviewed that the combined PI3K and MEK inhibition showed an enhancement in apoptosis compared with either single agent treatment (Zou , et al., 2012). In the future work, the analysis of *KRAS* and *PIK3CA* mutations will be continually conducted in explant cases following cisplatin single or combination treatments in order to analyze whether there is a correlation between the gene status and response to the treatments. Moreover, the correlation of Akt phosphorylation to other biomarkers expression (cPARP and Ki67) will also be studied and compared between *KRAS/PIK3CA* WT and mutant cases. Lastly, PI3K-MEK dual targeted treatments combined with cisplatin would be interesting to be tested on the *in vitro* models for further improving cisplatin toxicity compared to the cisplatin-GDC-0941 or MK-2206 doublet.

APPENDIX

7.1 The drug efficacy of cisplatin treatment and dose selection at 48 hr for A549, H460 and H596 cell lines.

Results are shown as M ± SD of over 21 replicates and '*' means P<0.05 and 'ns' means non-significant

Drugs	Doses (μM)	Time-point (hr)	A549			H460			H596		
			M	SD	N	M	SD	N	M	SD	N
Cisplatin	0	48	100	12	22	100	16	22	100	23	21
	1		101	11	21	90	8	21	83*	12	21
	5		89*	9	21	64*	7	21	58*	10	21
	10		79*	11	21	51*	6	20	44*	8	21
	20		73*	14	21	34*	6	21	31*	8	21
STA-9090	0	48	100	21	30	100	16	30	100	16	37
	0.002		88*	10	28	96	10	28	88	27	35
	0.02		82*	12	28	92	13	28	76*	14	35
	0.2		65*	13	28	66*	12	28	38*	9	35
	2		55*	9	28	60*	12	28	45*	24	35
nmx5023	0	48	100	13	35	100	9	28	100	12	29
	0.3		104	16	35	102	16	28	106	10	25
	0.6		91*	15	35	95	13	28	102	12	27
	1		70*	8	35	93*	16	28	96	11	27
	10		48*	14	35	62*	7	28	48*	17	28
nmx5034	0	48	100	10	49	100	9	28	100	9	28
	0.3		82*	12	49	95	15	28	75*	9	28
	0.6		73*	17	48	86*	9	28	66*	8	28
	1		73*	9	49	85*	7	28	53*	13	28
	10		44*	15	46	66*	13	28	33*	7	28
GDC0941	0	48	100	8	21	100	9	21	100	11	21
	1		45*	7	21	91	11	21	84*	19	21
	5		26*	5	21	65*	10	21	60*	12	21
	10		25*	9	21	63*	8	21	56*	13	21
MK2206	0	48	100	8	21	100	9	21	100	11	21
	3		64*	19	21	80*	10	21	79*	11	21
	12		49*	15	21	75*	9	21	76*	14	21
	21		25*	16	21	66*	10	21	63*	15	21
AZD6244	0	48	100	8	21	100	9	21	100	11	21
	10		56*	12	21	75*	9	21	79*	14	21
	50		51*	12	21	78*	13	21	78*	10	21
	100		47*	13	21	80*	12	21	76*	11	21

7.2 The detection of Akt, pAkt, P53 by ICW for cisplatin treatment at 24 hr in A549, H460 and H596 cell lines

Akt and pAkt expression was analyzed in all cell lines while P53 expression was only analyzed in A549 and H460, both of which harbour WT P53, compared to the mutant P53 cell line (H596). Result for each cell line is shown as mean.

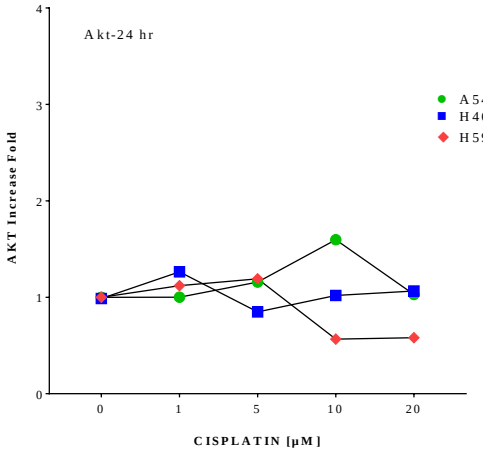

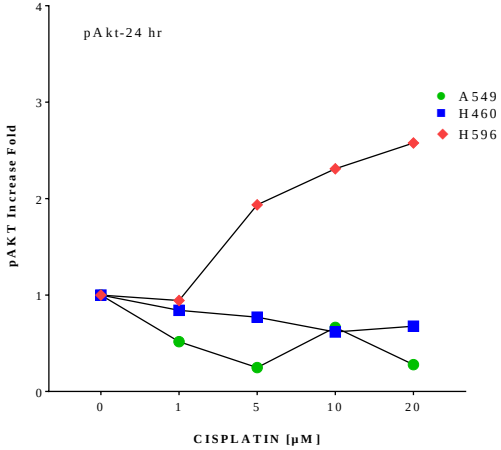

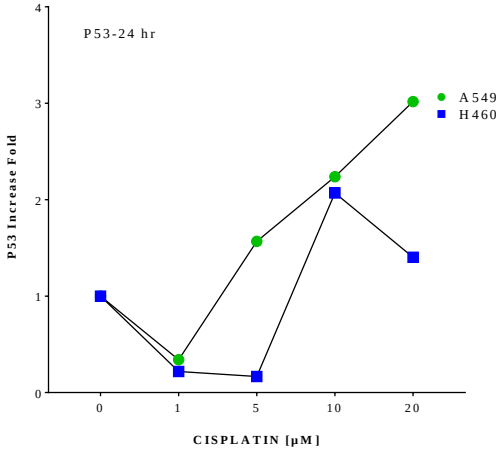

7.3 The published paper by Dr Karekla in 2017

Karekla , E. et al., 2017. Ex vivo explant cultures of non-small cell lung carcinoma enable evaluation of primary tumor responses to anticancer therapy. *Cancer Research*

Therapeutics, Targets, and Chemical Biology

Cancer Research

Ex Vivo Explant Cultures of Non-Small Cell Lung Carcinoma Enable Evaluation of Primary Tumor Responses to Anticancer Therapy

Ellie Karekla[1], Wen-Jing Liao[1], Barry Sharp[2], John Pugh[2], Helen Reid[2], John le Quesne[1,3], David Moore[1], Catrin Pritchard[1], Marion MacFarlane[3], and Howard Pringle[1]

Abstract

To improve treatment outcomes in non-small cell lung cancer (NSCLC), preclinical models that can better predict individual patient response to novel therapies are urgently needed. Using freshly resected tumor tissue, we describe an optimized *ex vivo* explant culture model that enables concurrent evaluation of NSCLC response to therapy while maintaining the tumor microenvironment. We found that approximately 70% of primary NSCLC specimens were amenable to explant culture with tissue integrity intact for up to 72 hours after explant. Variations in cisplatin sensitivity were noted with approximately 50% of cases responding *ex vivo*. Notably, explant responses to cisplatin correlated significantly with patient survival ($P = 0.006$) irrespective of tumor stage. In explant tissue, cisplatin-resistant tumors excluded platinum ions from tumor areas in contrast to cisplatin-sensitive tumors. Intact TP53 did not predict cisplatin sensitivity, but a positive correlation was observed between cisplatin sensitivity and TP53 mutation status ($P = 0.003$). Treatment of NSCLC explants with the targeted agent TRAIL revealed differential sensitivity with the majority of tumors resistant to single-agent or cisplatin combination therapy. Overall, our results validated a rapid, reproducible, and low-cost assay to assess drug responses in patient tumors *ex vivo*, thereby enabling preclinical testing of novel drugs and helping stratify patients using biomarker evaluation. *Cancer Res; 1–13. ©2017 AACR.*

Introduction

Non-small cell lung cancer (NSCLC) is a leading cause of cancer death worldwide. Patients with stage I–III tumors are surgically resected and given adjuvant chemotherapy or radiotherapy. Patients with stage IV disease receive palliative chemotherapy only unless they can be stratified for targeted therapy. Most patients receive combination chemotherapy based on clinical parameters of cisplatin or carboplatin with at least one other drug such as vinorelbine, gemcitabine, or paclitaxel. Unfortunately, only approximately 5% of patients receiving adjuvant therapy show 5-year average survival benefit (1, 2). Therefore, more accurate methods for predicting chemotherapeutic benefit are urgently required to improve clinical outcomes.

The era of personalized medicine has heralded the development of targeted therapies for NSCLC, some of which rely on preselection of cancers according to genetic mutation. For example, selective EGFR inhibitors gefitinib and erlotinib provide clinical benefit over standard chemotherapy for NSCLC tumors bearing *EGFR* mutations (3, 4), whereas the ALK inhibitor crizotinib benefits *ALK*-mutated cases (5). A global industry is centered on assessing additional mono- or combinatorial treatments in NSCLC clinical trials. Despite this momentum, late-stage failures are a reality and there is less than 11% success in bringing a drug to market (6), attributable in part to nonpredictive preclinical drug platforms (7, 8). The incorporation of patient-derived xenograft (PDX) mouse models (9, 10) into preclinical studies has improved predictive accuracy somewhat (11, 12). However, PDX efficacy studies are expensive, requiring large numbers of mice. Furthermore, not all primary human tumors generate PDXs and, of those that do, serial propagation can select tumors that adapt to grow in an immunocompromised environment.

An alternative approach is to use 3-dimensional *ex vivo* culture of fresh human tumors. Methods for *ex vivo* culture of human tumors have been available for many years, and evidence shows that they can reliably reflect tumor growth *in vivo* (13–19). Here, we have developed and perfected an *ex vivo* culture method for NSCLC tumor samples that is both simple and reproducible. We have optimized culture conditions and show that tumor and stroma are retained intact and are viable. As proof-of-concept, NSCLC explant response to the standard-of-care chemotherapy drug cisplatin was examined, as well as response to the targeted agent TRAIL. We also illustrate how

[1]Department of Cancer Studies, University of Leicester, Leicester, United Kingdom. [2]Centre for Analytical Science, Department of Chemistry, Loughborough University, Loughborough, Leicestershire, United Kingdom. [3]MRC Toxicology Unit, Leicester, United Kingdom.

Note: Supplementary data for this article are available at Cancer Research Online (http://cancerres.aacrjournals.org/).

C. Pritchard, M. MacFarlane, and J.H. Pringle contributed equally to this article.

Corresponding Authors: Catrin Pritchard, Department of Cancer Studies, University of Leicester, Lancaster Road, Leicester LE1 9HN, United Kingdom. Phone: 4411-6229-7061; Fax: 4411-6229-7018; E-mail: cap8@le.ac.uk; and Marion MacFarlane, MRC Toxicology Unit, Hodgkin Building, Lancaster Road, Leicester LE1 9HN, United Kingdom. E-mail: mm2@le.ac.uk

doi: 10.1158/0008-5472.CAN-16-1121

REFERENCES

A.D.A.M., 2013. *Lung Cancer - Non-Small Cell.* [Online] Available at: http://www.nytimes.com/health/guides/disease/lung-cancer-non-small-cell/chemotherapy-treatments.html
[Accessed 25 October 2016].

About Lung Cancer, 2016. *IASLC-International Association for the Study of Lung Cancer*. [Online]
Available at: https://www.iaslc.org/about-lung-cancer
[Accessed 15 October 2016].

Acquaviva, J. et al., 2012. Targeting KRAS-mutant non-small cell lung cancer with the Hsp90 inhibitor ganetespib. *Molecular cancer therapeutics*, 11(12), pp. 2633-2643.

American Cancer Society, 2014. *A Guide to Palliative or Supportive CareWhat is palliative care?*. [Online]
Available at: http://www.cancer.org/treatment/treatmentsandsideeffects/palliativecare/supportive-care
[Accessed 25 October 2016].

American Cancer Society, 2016. *Chemotherapy for non-small cell lung cancer*. [Online]
Available at: http://www.cancer.org/cancer/lungcancer-non-smallcell/detailedguide/non-small-cell-lung-cancer-treating-chemotherapy
[Accessed 25 October 2016].

American Cancer Society, 2016. *Treatment choices by stage of small cell lung cancer*. [Online]
Available at: http://www.cancer.org/cancer/lungcancer-smallcell/detailedguide/small-cell-lung-cancer-treating-by-stage
[Accessed 23 October 2016].

American Cancer Society, 2016. *Types of cancer immunotherapy*. [Online]
Available at: http://www.cancer.org/treatment/treatmentsandsideeffects/treatmenttypes/immunotherapy/immunotherapy-what-is-immunotherapy
[Accessed 26 October 2016].

American Cancer Society, 2016. *What's new in non-small cell lung cancer research?-Maintenance therapy.* [Online] Available at: http://www.cancer.org/cancer/lungcancer-non-smallcell/detailedguide/non-small-cell-lung-cancer-new-research
[Accessed 26 October 2016].

American Joint Committee on Cancer, 2009. *Lung Cancer Staging-7th Edition.* [Online] Available at: http://cancerstaging.org/references-tools/quickreferences/documents/lungmedium.pdf
[Accessed 23 October 2016].

Amoêdo , N. et al., 2011. Energy Metabolism in H460 Lung Cancer Cells: Effects of Histone Deacetylase Inhibitors. *PLoS ONE ,* 6(7), p. e22264.

Anon., 2012. Targeting MEK for the Treatment of Non–Small-Cell Lung Cancer. *Journal of Thoracic Oncology,* 7(16), pp. S377-378.

Antoni , D., Burckel , H., Josset , E. & Noel , G., 2015. Three-dimensional cell culture: a breakthrough in vivo. *International journal of molecular sciences,* 16(3), pp. 5517-5527.

AstraZeneca, 2016. *AstraZeneca provides update on Phase III trial of Selumetinib in non-small cell lung cancer.* [Online] Available at: https://www.astrazeneca.com/media-centre/press-releases/2016/AstraZeneca-provides-update-on-Phase-III-trial-of-Selumetinib-in-non-small-cell-lung-cancer-09082016.html
[Accessed 05 March 2017].

AstraZeneca, 2017. *AZD8186 First Time In Patient Ascending Dose Study (NCT01884285).* [Online] Available at: https://clinicaltrials.gov/ct2/show/NCT01884285?term=NSCLC+PI3K&rank=7
[Accessed 2 March 2017].

Bach, P. B. et al., 2012. *ASCO-The role of CT screening for Lung Cancer in clinical practice.* [Online] Available at: https://www.asco.org/practice-guidelines/quality-guidelines/guidelines/lung-cancer#/10211
[Accessed 21 October 2016].

Balmanno, K. et al., 2009. Intrinsic resistance to the MEK1/2 inhibitor AZD6244 (ARRY-142886) is associated with weak ERK1/2 signaling and/or strong PI3K signaling in colorectal cancer cell lines. *International journal of cancer,* 125(10), pp. 2332-2341.

Barbie, D. A. et al., 2009. Systematic RNA interference reveals that oncogenic KRAS-driven cancers require TBK1. *Nature,* Volume 462, pp. 108-112.

Barbone, D. et al., 2011. The Bcl-2 repertoire of mesothelioma spheroids underlies acquired apoptotic multicellular resistance. *Cell death & disease,* Volume 2, p. e174.

Barrera-Rodríguez , R. & Fuentes, J., 2015. Multidrug resistance characterization in multicellular tumor spheroids from two human lung cancer cell lines. *Cancer cell international,* Volume 15, pp. 47 (1-11).

Bekki, H. et al., 2015. Elevated expression of HSP90 and the antitumor effect of an HSP90 inhibitor via inactivation of the Akt/mTOR pathway in undifferentiated pleomorphic sarcoma.(Research article)(Report). *BMC Cancer,* 15(1), pp. 804-814.

Benton , G., Kleinman , H., George, J. & Arnaoutova , I., 2011. Multiple uses of basement membrane-like matrix (BME/Matrigel) in vitro and in vivo with cancer cells. *International journal of cancer,* 128(8), pp. 1751-1757.

Besse, B. et al., 2011. A phase Ib study to evaluate the PI3-kinase inhibitor GDC-0941 with paclitaxel (P) and carboplatin (C), with and without bevacizumab (BEV), in patients with advanced non-small cell lung cancer (NSCLC). *Journal of Clinical Oncology,* Volume 29, p. Abstract 3044.

Bhattacharya, S., Socinski, M. A. & Burns, T. F., 2015. KRAS mutant lung cancer: progress thus far on an elusive therapeutic target. *Clinical and translational medicine ,* Volume 4, pp. 35 (1-11).

BMJ Best Practice , 2016. *Non-small cell lung cancer-Pathophysiology.* [Online] Available at: http://bestpractice.bmj.com/best-practice/monograph/1082/basics/pathophysiology.html
[Accessed 27 October 2016].

Bonomi, P. D., 2010. Implications of key trials in advanced nonsmall cell lung cancer. *Cancer,* 116(5), pp. 1155-1164.

Borczuk, A. C., Toonkel, R. L. & Powell, C. A., 2009. Genomics of Lung Cancer. *Proceedings of the American Thoracic Society,* 6(2), pp. 152-158.

Bouwman , P. & Jonkers, J., 2012. The effects of deregulated DNA damage signaling on cancer chemotherapy response and resistance. *Nature Reviews Cancer* , Volume 12, pp. 587-598.

Bradford, C. et al., 2003. P53 mutation correlates with cisplatin sensitivity in head and neck squamous cell carcinoma lines. *Head neck,* 25(8), pp. 654-661.

Bremnes , R. et al., 2011. The role of tumor stroma in cancer progression and prognosis: emphasis on carcinoma-associated fibroblasts and non-small cell lung cancer. *Journal of thoracic oncology,* 6(1), pp. 209-217.

Brognard, J., Clark, A. S., Ni, Y. & Dennis, P. A., 2001. Akt/protein kinase B is constitutively active in non-small cell lung cancer cells and promotes cellular survival and resistance to chemotherapy and radiation. *Cancer research,* 61(10), pp. 3986-3997.

Bujor , A. et al., 2008. Akt blockade downregulates collagen and upregulates MMP1 in human dermal fibroblasts. *The Journal of investigative dermatology,* 128(8), pp. 1906-1914.

Busacca, S. et al., 2016. Resistance to HSP90 inhibition involving loss of MCL1 addiction. *Oncogene,* 35(12), pp. 1483-1492.

Caiola, E. et al., 2015. Base excision repair-mediated resistance to cisplatin in KRAS(G12C) mutant NSCLC cells. *Oncotarget,* 6(30), pp. 30072-30087 .

Cancer Research UK, 2014. *Chemotherapy for non small cell lung cancer.* [Online] Available at: http://www.cancerresearchuk.org/about-cancer/type/lung-cancer/treatment/chemotherapy/about-chemotherapy-for-lung-cancer#adjuvant [Accessed 25 October 2016].

Cancer Research UK, 2014. *Endoscopic Ultrasound Scan and Mediastinoscopy.* [Online] Available at: http://www.cancerresearchuk.org/about-cancer/type/lung-cancer/diagnosis/further-tests-for-lung-cancer#media [Accessed 21 October 2016].

Cancer Research UK, 2014. *MRI scan.* [Online] Available at: http://www.cancerresearchuk.org/about-cancer/type/lung-

cancer/diagnosis/further-tests-for-lung-cancer#ctscan
[Accessed 21 October 2016].

Cancer Research UK, 2014. *Types of biological therapy.* [Online] Available at: http://www.cancerresearchuk.org/about-cancer/type/lung-cancer/treatment/biological-therapy-for-lung-cancer
[Accessed 25 October 2016].

Cancer Research UK, 2016. *Lung Cancer Incidence by Stage at Diagnosis.* [Online] Available at: http://www.cancerresearchuk.org/health-professional/cancer-statistics/statistics-by-cancer-type/lung-cancer/incidence#heading-Three
[Accessed 23 October 2016].

Carpeño, J. d. C. & Belda-Iniesta, C., 2013. KRAS mutant NSCLC, a new opportunity for the synthetic lethality therapeutic approach. *Translational lung cancer research,* 2(2), pp. 142-151.

Chalhoub , N. & Baker, S. J., 2009. PTEN and the PI3-Kinase Pathway in Cancer. *Annual review of pathology,* Volume 4, pp. 127-150.

Chan, B. A. & Hughes, B. G., 2015. Targeted therapy for non-small cell lung cancer: current standards and the promise of the future. *Translational lung cancer research,* 4(1), pp. 36-54.

Chatterjee, S., Bhattacharya, S., Socinski, M. A. & Burns, T. F., 2016. HSP90 Inhibitors in Lung Cancer: Promise Still Unfulfilled. *Clinical Advances in Hematology & Oncology,* 14(5), pp. 346-356.

Chen , F. et al., 2015. New horizons in tumor microenvironment biology: challenges and opportunities. *BMC Medicine,* Volume 13, pp. p45:1-13.

Cheng, H. et al., 2014. Targeting the PI3K/Akt/mTOR pathway: potential for lung cancer treatment. *Lung cancer management,* 3(1), pp. 67-75.

Chen, J. et al., 2011. Resistance to platinum-based chemotherapy in lung cancer cell lines. *Cancer Chemotherapy and Pharmacology,* 66(6), pp. 1103-1111.

COSMIC Cell Lines Project, 2016. *Wellcome Trust Sanger Institute, Genome Research Limited.* [Online]

Available at: http://cancer.sanger.ac.uk/cosmic/ [Accessed 20 August 2016].

Daly , A. J., Mcilreavey, L. & Irwin, C. R., 2008. Regulation of HGF and SDF-1 expression by oral fibroblasts – Implications for invasion of oral cancer. *Oral Oncology,* 44(7), pp. 646-651.

Dasari , S. & Tchounwou, P. B., 2014. Cisplatin in cancer therapy: molecular mechanisms of action. *European Journal of Pharmacology,* Volume 740, pp. 364-378.

di Pietro, A. et al., 2012. Pro- and anti-apoptotic effects of p53 in cisplatin-treated human testicular cancer are cell context-dependent. *Cell cycle,* 11(24), pp. 4552-4562.

Ding, S. et al., 2015. MRC-5 fibroblast-conditioned medium influences multiple pathways regulating invasion, migration, proliferation, and apoptosis in hepatocellular carcinoma. *Journal of Translational Medicine,* Volume 13, pp. 237 (1-13).

Djuzenova, C. et al., 2016. Dual PI3K- and mTOR-inhibitor PI-103 can either enhance or reduce the radiosensitizing effect of the Hsp90 inhibitor NVP-AUY922 in tumor cells: The role of drug-irradiation schedule. *Oncotarget,* 7(25), pp. 38191-38209.

Downward, J., 2008. Targeting RAS and PI3K in lung cancer. *Nature Medicine ,* Volume 14, pp. 1315-1316.

Edmondson, R., Broglie, J. J., Adcock, A. F. & Yang, L., 2014. Three-Dimensional Cell Culture Systems and Their Applications in Drug Discovery and Cell-Based Biosensors. *Assay and drug development technologies,* 12(4), pp. 207-218.

Ersahin, T., Tuncbag, N. & Cetin-Atalay, R., 2015. The PI3K/Akt/mTOR interactive pathway. *Molecular BioSystems,* 11(7), pp. 1946-1954.

Farhat , F. S. & Houhou, W., 2013. Targeted therapies in non-small cell lung carcinoma: what have we achieved so far?. *Therapeutic advances in medical oncology,* 5(4), pp. 249-270.

Fasano, M. et al., 2015. Pulmonary Large-Cell Neuroendocrine Carcinoma: From Epidemiology to Therapy. *Journal of Thoracic Oncology,* 10(8), pp. 1133-1141.

FDA, 2015. *FDA approves Keytruda for advanced NSCLC.* [Online] Available at:

http://www.fda.gov/NewsEvents/Newsroom/PressAnnouncements/ucm465444.htm [Accessed 04 August 2016].

Fecher, D. et al., 2016. Human Organotypic Lung Tumor Models: Suitable For Preclinical 18F-FDG PET-Imaging. *PloS one* , 11(8), p. e0160282.

FLEMING, J. M. et al., 2010. Local Regulation of Human Breast Xenograft Models. *Journal of Cellular Physiology,* 224(3), pp. 795 - 806.

Fumarola , C., Bonelli , M., Petronini, P. & Alfieri , R., 2014. Targeting PI3K/Akt/mTOR pathway in non small cell lung cancer. *Biochemical pharmacology,* 90(3), pp. 197-207.

Funai, K. et al., 2003. Clinicopathologic Characteristics of Peripheral Squamous Cell Carcinoma of the Lung. *The American Journal of Surgical Pathology,* 27(7), pp. 978-984.

Gangadhara, S., Smith, C., Barrett-Lee, P. & Hiscox, S., 2016. 3D culture of Her2+ breast cancer cells promotes Akt to MAPK switching and a loss of therapeutic response. *BMC cancer* , Volume 16, pp. 345(1-12).

Garon , E. et al., 2010. Identification of common predictive markers of in vitro response to the Mek inhibitor selumetinib (AZD6244; ARRY-142886) in human breast cancer and non-small cell lung cancer cell lines. *Molecular cancer therapeutics,* 9(7), pp. 1985-94.

Genentech clinical data (Phase I) (NSCLC) (2011) R & D Focus Drug News.

Genentech clinical data (Phase I) (solid tumor) (2012) R & D Focus Drug New.

Gibbons, D. L., Byers, L. A. & Kurie, J. M., 2014. Smoking, p53 Mutation, and Lung Cancer. *Molecular cancer research* , 12(1), pp. 3-13.

Glatter, R., 2015. *Pharma & Healthcare.* [Online] Available at: http://www.forbes.com/sites/robertglatter/2015/02/16/medicare-to-cover-low-dose-ct-scanning-for-those-at-high-risk-for-lung-cancer/#56148954a141 [Accessed 21 October 2016].

Godwin, P. et al., 2013. Targeting Nuclear Factor-Kappa B to Overcome Resistance to Chemotherapy. *Frontiers in oncology* , Volume 3, pp. 120 (1-10).

Goldman, J. W. & Garon, E. B., 2012. Targeting MEK for the Treatment of Non Small-Cell Lung Cancer. *Journal of thoracic oncology,* 7(16), pp. S377-S378.

Gomez-Casal, R. et al., 2015. The HSP90 Inhibitor Ganetespib Radiosensitizes Human Lung Adenocarcinoma Cells. *Cancers,* 7(2), pp. 876-907.

González-Cao, M., 2015. Immunotherapy for lung cancer. *Translational lung cancer research,* 4(6), pp. 675-677.

Gottlieb, T. M. et al., 2002. Cross-talk between Akt, p53 and Mdm2: possible implications for the regulation of apoptosis. *Oncogene,* Volume 21, pp. 1299-1303.

Greenberg, A., Yee, H. & Rom , W., 2002. Preneoplastic lesions of the lung. *Respiratory Research,* 3(1).

Guntur, V. P. et al., 2010. Increasing p53 protein sensitizes non-small cell lung cancer to paclitaxel and cisplatin in vitro. *Anticancer research,* 30(9), pp. 3557-3564.

H. Lee Moffitt Cancer Center & Research Institute, 2017. *A Phase I/IB Trial of MEK162 in Combination With Erlotinib in NSCLC Harboring KRAS or EGFR Mutation (NCT01859026).* [Online] Available at: https://clinicaltrials.gov/ct2/show/NCT01859026?term=NSCLC+MEK&rank=1 [Accessed 3 March 2017].

Hames, M. L. et al., 2016. Correlation between KRAS mutation status and response to chemotherapy in patients with advanced non-small cell lung cancer. *Lung cancer,* Volume 92, pp. 29-34.

Harrington , C. et al., 2010. Determination of cisplatin 1,2-intrastrand guanine-guanine DNA adducts in human leukocytes by high-performance liquid chromatography coupled to inductively coupled plasma mass spectrometry. *Chemical research in toxicology,* 23(8), pp. 1313-1321.

Haymarket Media, 2014. *Small Cell Lung Cancer Oncogene Discovered.* [Online] Available at: http://www.cancertherapyadvisor.com/lung-cancer/small-cell-lung-cancer-oncogene-discovered/article/368088/ [Accessed 30 October 2016].

Heavey, S. et al., 2014. Strategic targeting of the PI3K-NFκB axis in cisplatin-resistant NSCLC. *Cancer biology & therapy,* 15(10), pp. 1367-1377.

Heavey, S., O'Byrne , K. J. & Gately, K., 2014. Strategies for co-targeting the PI3K/Akt/mTOR pathway in NSCLC. *Cancer Treatment Reviews,* 40(3), pp. 445-456.

Helwick, C., 2014. *The ASCO Post-Targeting KRAS Mutations in Lung Cancer: No Longer Impossible.* [Online] Available at: http://www.ascopost.com/issues/september-1-2014/targeting-kras-mutations-in-lung-cancer-no-longer-impossible.aspx [Accessed 1 March 2017].

Hirai, H. et al., 2010. MK-2206, an allosteric Akt inhibitor, enhances antitumor efficacy by standard chemotherapeutic agents or molecular targeted drugs in vitro and in vivo. *Molecular cancer therapeutics,* 9(7), pp. 1956-1967.

Hirschhaeuser, F. et al., 2010. Multicellular tumor spheroids: an underestimated tool is catching up again. *Journal of Biotechnology,* Volume 148, pp. 3-15.

Holderfield, M., Deuker, M. M., McCormick, F. & McMahon, M., 2014. Targeting RAF kinases for cancer therapy: BRAF mutated melanoma and beyond. *Nature reviews. Cancer,* 14(7), pp. 455-467.

Huang, L. & Fu, L., 2015. Mechanisms of resistance to EGFR tyrosine kinase inhibitors. *Acta Pharmaceutica Sinica B,* 5(5), pp. 390-401.

Iida, M. et al., 2013. Targeting Akt with the allosteric Akt inhibitor MK-2206 in non-small cell lung cancer cells with acquired resistance to cetuximab. *Cancer biology & therapy,* 14(6), pp. 481-491.

Iida, M. et al., 2013. Targeting Akt with the allosteric Akt inhibitor MK-2206 in non-small cell lung cancer cells with acquired resistance to cetuximab. *Cancer biology & therapy,* 14(6), pp. 481-91.

Jiang , H. et al., 2009. The combined status of ATM and p53 link tumor development with therapeutic response. *Genes & development,* 23(16), pp. 1895-1909.

Johnstone, T. C., Park, G. Y. & Lippard, S. J., 2014. Understanding and Improving Platinum Anticancer Drugs – Phenanthriplatin. *Anticancer research,* 34(1), pp. 471-476.

Kadaba, R. et al., 2013. Imbalance of desmoplastic stromal cell numbers drives aggressive cancer processes. *The Journal of Pathology,* 230(1), pp. 107-117.

Karekla , E., 2014. Improving therapeutic approaches for the treatment of Non-small Cell Lung Cancer using an ex-vivo explant culture system. *University of Leicester (Thesis).*

Karekla , E. et al., 2017. Ex vivo explant cultures of non-small cell lung carcinoma enable evaluation of primary tumor responses to anticancer therapy. *Cancer Research.*

Karlsson , H., Fryknäs , M., Larsson , R. & Nygren , P., 2012. Loss of cancer drug activity in colon cancer HCT-116 cells during spheroid formation in a new 3-D spheroid cell culture system. *Experimental cell research,* 318(13), pp. 1577-1585.

Kim, D. et al., 2001. Akt/PKB promotes cancer cell invasion via increased motility and metalloproteinase production. *FASEB journal ,* 15(11), pp. 1953-1962.

Kim, J., 2005. Three-dimensional tissue culture models in cancer biology. *seminars in cancer biology,* Volume 15, pp. 365-77.

Kim, J., Beg , A. & Haura , E., 2013. Non-canonical IKKs, IKKϵ and TBK1, as novel therapeutic targets in the treatment of non-small cell lung cancer. *Expert opinion on therapeutic targets,* 17(10), pp. 1109-1112.

Kong , L. et al., 2015. MEK Inhibition Overcomes Cisplatin Resistance Conferred by SOS/MAPK Pathway Activation in Squamous Cell Carcinoma. *Molecular cancer therapeutics,* 14(7), pp. 1750-1760.

Ku, B. M. et al., 2015. BYL719, a selective inhibitor of phosphoinositide 3-Kinase α, enhances the effect of selumetinib (AZD6244, ARRY-142886) in KRAS-mutant non-small cell lung cancer. *Investigational new drugs,* 33(1), pp. 12-21.

Lai, S., Perng , R. & Hwang , J., 2000. p53 gene status modulates the chemosensitivity of non-small cell lung cancer cells. *Journal of biomedical science,* 7(1), pp. 64-70.

Lama, R. et al., 2013. Development, validation and pilot screening of an in vitro multi-cellular three-dimensional cancer spheroid assay for anti-cancer drug testing. *Bioorganic & medicinal chemistry,* Volume 21, pp. 922-931.

Langer, C., Dresler, C., Goldberg, M. & Movsas, B., 1996. 3. Stage-directed treatment guidelines. *Current Problems in Cancer,* 20(3), pp. 157-178.

Lee , M. et al., 2011. Roles of Akt1 and Akt2 in non-small cell lung cancer cell survival, growth, and migration. *Cancer science,* 102(10), pp. 1822-1828.

Lee, M. W., Kim, D. S., Min, N. Y. & Kim, H. T., 2008. Akt1 inhibition by RNA interference sensitizes human non-small cell lung cancer cells to cisplatin. *International Journal of Cancer,* 122(10), pp. 2380-2384.

Lin , F. et al., 2016. The association between human papillomavirus infection and female lung cancer. *Medicine,* 95(23), p. e3856.

Little , J. B., 2000. Radiation carcinogenesis. *Carcinogenesis,* 21(3), pp. 397-404.

Liu, L.-Z.et al., 2007. *Akt1* amplification regulates cisplatin resistance in human lung cancer cells through the mammalian target of rapamycin/p70S6K1 pathway. *Cancer research,* 67(13), pp. 6325-6332.

Li, W. et al., 2015. IKBKE Upregulation is Positively Associated with Squamous Cell Carcinoma of the Lung In Vivo and Malignant Transformation of Human Bronchial Epithelial Cells In Vitro. *Medical science monitor ,* Volume 21, pp. 1577-1586.

Lovitt, C. J., Shelper, T. B. & Avery, V. M., 2014. Advanced Cell Culture Techniques for Cancer Drug Discovery. *Biology,* 3(2), pp. 345-367.

Lovly, C., Horn, L. & Pao, W., 2015. *Akt1 in Non-Small Cell Lung Cancer (NSCLC).* [Online]
Available at: https://www.mycancergenome.org/content/disease/lung-cancer/akt1/23/ [Accessed 01 November 2016].

Lovly, C., Horn, L. & Pao, W., 2015. *KRAS in Non-Small Cell Lung Cancer (NSCLC).* [Online]
Available at: https://www.mycancergenome.org/content/disease/lung-cancer/kras/ [Accessed 29 October 2016].

Lovly, C., Horn, L. & Pao, W., 2015. *PTEN in Non-Small Cell Lung Cancer (NSCLC).* [Online]
Available at: https://www.mycancergenome.org/content/disease/lung-cancer/pten/ [Accessed 30 October 2016].

Lovly, C., Horn, L. & Pao, W., 2016. *Molecular Profiling of Lung Cancer.* [Online] Available at: https://www.mycancergenome.org/content/disease/lung-cancer/ [Accessed 28 October 2016].

Lung Cancer Fact Sheet - 2015 - Europe, 2015. *IASLC-International Association for the Study of Lung Cancer.* [Online] Available at: https://www.iaslc.org/lung-cancer-fact-sheet-2015-europe [Accessed 15 October 2016].

Lung Cancer Fact Sheet - 2016 - Asia, 2016. *IASLC-International Association for the Study of Lung Cancer.* [Online] Available at: https://www.iaslc.org/lung-cancer-fact-sheet-2016-asia [Accessed 16 October 2016].

Lung Cancer Incidence by Age, 2016. *Cancer Research UK.* [Online] Available at: http://www.cancerresearchuk.org/health-professional/cancer-statistics/statistics-by-cancer-type/lung-cancer/incidence#heading-One [Accessed 16 October 2016].

Lung Cancer Mortality by Age, 2016. *Cancer Research UK.* [Online] Available at: http://www.cancerresearchuk.org/health-professional/cancer-statistics/statistics-by-cancer-type/lung-cancer/mortality#heading-One [Accessed 16 October 2016].

Madrigal pharmaceuticals, 2012. *Synta Announces First Patients Treated in Two ALK Positive Lung Cancer Trials.* [Online] Available at: http://phx.corporate-ir.net/phoenix.zhtml?c=147988&p=irol-newsArticle_Print&ID=1721499 [Accessed 16 March 2017].

Mahajan, K. & Mahajan, N. P., 2012. PI3K-independent Akt activation in cancers: A treasure trove for novel therapeutics. *Journal of Cellular Physiology,* 227(9), pp. 3178-3184.

Mahale , J. et al., 2016. The role of stromal fibroblasts in lung carcinogenesis: A target for chemoprevention?. *International journal of cancer,* 138(1), pp. 30-44.

Mahale, J., 2016. Preclinical evaluation of Meriva (a formulation of curcumin) as a putative agent for chemoprevention of lung cancer. *University of Leicester (Thesis).*

Maione, P. et al., 2010. Treating advanced non-small cell lung cancer in the elderly. *Therapeutic Advances in Medical Oncology,* 2(4), pp. 251-260.

Majumder , B. et al., 2015. Predicting clinical response to anticancer drugs using an ex vivo platform that captures tumor heterogeneity. *Nature communications,* Volume 6, pp. 6169 (1-14).

Martini, M., Ciraolo, E., Gulluni, F. & Hirsch, E., 2013. Targeting PI3K in Cancer: Any Good News?. *Frontiers in oncology* , Volume 3, pp. 108 (1-9).

Matsumoto, M. et al., 2016. Cisplatin-induced apoptosis in non-small-cell lung cancer cells is dependent on Bax- and Bak-induction pathway and synergistically activated by BH3-mimetic ABT-263 in p53 wild-type and mutant cells. *Biochemical and Biophysical Research Communications,* 473(2), pp. 490-496.

Matsusaki, M., Case, C. P. & Akashi, M., 2014. Three-dimensional cell culture technique and pathophysiology. *Advanced Drug Delivery Reviews,* Volume 74, pp. 95-103.

McArthur, G. A., 2015. *Exploring the Pathway: The RAS/RAF/MEK/ERK Pathway in Cancer: Combination Therapies and Overcoming Feedback.* [Online] Available at: https://am.asco.org/exploring-pathway-rasrafmekerk-pathway-cancer-combination-therapies-and-overcoming-feedback
[Accessed 31 October 2016].

Mccubrey, J. A. et al., 2007. Roles of the Raf/MEK/ERK pathway in cell growth, malignant transformation and drug resistance. *BBA - Molecular Cell Research,* 1773(8), pp. 1263-1284.

Mellema , W. et al., 2013. KRAS mutations in advanced nonsquamous non-small-cell lung cancer patients treated with first-line platinum-based chemotherapy have no predictive value. *Journal of thoracic oncology* , 8(9), pp. 1190-5.

Meng, J. et al., 2010. Combination Treatment with MEK and Akt Inhibitors Is More Effective than Each Drug Alone in Human Non-Small Cell Lung Cancer In Vitro and In Vivo. *PLoS ONE,* 5(11), pp. e14124 (1-10).

Meng, J. et al., 2009. High level of Akt activity is associated with resistance to MEK inhibitor AZD6244 (ARRY-142886). *Cancer Biology & Therapy,* 8(21), pp. 2073-2080.

Mercer, P. et al., 2016. Exploration of a potent PI3 kinase/mTOR inhibitor as a novel anti-fibrotic agent in IPF. *Thorax,* 71(8), pp. 701-711.

Minguet, J., Smith, K. H. & Bramlage, P., 2016. Targeted therapies for treatment of non-small cell lung cancer—Recent advances and future perspectives. *International Journal of Cancer,* 138(11), pp. 2549-2561.

Mirsadraee, S. et al., 2012. The 7th lung cancer TNM classification and staging system: Review of the changes and implications. *World Journal of Radiology* , 4(4), pp. 128-134.

Mogi, A. & Kuwano, H., 2011. TP53 Mutations in Nonsmall Cell Lung Cancer. *Journal of Biomedicine and Biotechnology,* Volume 2011, pp. 1-9.

Molife, L. R. et al., 2014. Phase 1 trial of the oral Akt inhibitor MK-2206 plus carboplatin/paclitaxel, docetaxel, or erlotinib in patients with advanced solid tumors.(Research)(Report). *Journal of Hematology & Oncology,* Volume 7, pp. 1-12.

Morrow, J. K. et al., 2011. Recent Development of Anticancer Therapeutics Targeting Akt. *Recent Patents on Anti-Cancer Drug Discovery* , 6(1), pp. 146-159.

Mountain, C. F., 1986. A New International Staging System for Lung Cancer. *Chest,* 89(4), pp. 225S-233S.

National Cancer Institute (NCI) , 2016. *MK2206 and Erlotinib Hydrochloride in Treating Patients With Advanced Non-Small Cell Lung Cancer Who Have Progressed After Previous Response to Erlotinib Hydrochloride Therapy.* [Online] Available at: https://clinicaltrials.gov/ct2/show/results/NCT01294306?sect=X798b0156&term=NSCLC+MK2206&rank=2#outcome1
[Accessed 16 March 2017].

National Cancer Institute (NCI) , 2017. *Erlotinib Hydrochloride and Hsp90 Inhibitor AT13387 in Treating Patients With Recurrent or Metastatic EGFR-Mutant Non-small Cell Lung Cancer (NCT02535338).* [Online] Available at: https://clinicaltrials.gov/ct2/show/NCT02535338?term=Heat+Shock+Proteins+90+nsclc&rank=1
[Accessed 3 March 2017].

National Cancer Institute, 2015. *Types of Immunotherapy.* [Online] Available at: https://www.cancer.gov/about-cancer/treatment/types/immunotherapy [Accessed 26 October 2016].

National Cancer Institute, 2016. *Non-Small Cell Lung Cancer Treatment (PDQ®)–Patient Version-Treatment Option Overview.* [Online] Available at: https://www.cancer.gov/types/lung/patient/non-small-cell-lung-treatment-pdq#section/_164
[Accessed 23 October 2016].

National Cancer Institute, 2016. *Non-Small Cell Lung Cancer Treatment (PDQ®)–Patient Version-Treatment Options by Stage.* [Online] Available at: https://www.cancer.gov/types/lung/patient/non-small-cell-lung-treatment-pdq#link/_212_toc
[Accessed 23 October 2016].

National Cancer Institute, 2016. *Non-Small Cell Lung Cancer Treatment (PDQ®)–Patient Version-Treatment Options for Recurrent Non-Small Cell Lung Cancer.* [Online] Available at: https://www.cancer.gov/types/lung/patient/non-small-cell-lung-treatment-pdq#section/_231
[Accessed 25 October 2016].

National Cancer Institute, 2016. *Small Cell Lung Cancer Treatment (PDQ®)–Patient Version-Treatment Option Overview.* [Online] Available at: https://www.cancer.gov/types/lung/patient/small-cell-lung-treatment-pdq#section/_92
[Accessed 23 October 2016].

National Cancer Institute, 2016. *Small Cell Lung Cancer Treatment (PDQ®)–Patient Version-Treatment Options for Recurrent Small Cell Lung Cancer.* [Online] Available at: https://www.cancer.gov/types/lung/patient/small-cell-lung-treatment-pdq#section/_121
[Accessed 25 October 2016].

National Collaborating Centre for Cancer (UK), 2011. *The Diagnosis and Treatment of Lung Cancer (Update).* [Online] Available at: https://www.nice.org.uk/guidance/cg121/evidence/full-guideline-

181636957
[Accessed 21 October 2016].

Nguyen, H. et al., 2013. Src-mediated morphology transition of lung cancer cells in three-dimensional organotypic culture. *Cancer Cell International* , 13(1), p. 16.

Niederst, M. J. & Engelman, J. A., 2013. Bypass Mechanisms of Resistance to Receptor Tyrosine Kinase Inhibition in Lung Cancer. *Science signaling* , 6(294), pp. p:1-10.

Nyström, M. et al., 2005. Development of a quantitative method to analyse tumor cell invasion in organotypic culture. *The Journal of Pathology*, 205(4), pp. 468-475.

Okawa, T. et al., 2007. The functional interplay between EGFR overexpression, hTERT activation, and p53 mutation in esophageal epithelial cells with activation of stromal fibroblasts induces tumor development, invasion, and differentiation. *GENES & DEVELOPMENT* , Volume 21, pp. 2788-2803.

Other Risk Fctors-Exposure to Radon Gas, 2014. *Cancer Research UK.* [Online] Available at: http://www.cancerresearchuk.org/about-cancer/type/lung-cancer/about/lung-cancer-risks-and-causes#other
[Accessed 16 October 2016].

Ou, Y.-H.et al., 2011. TBK1 Directly Engages Akt/PKB Survival Signaling to Support Oncogenic Transformation. *Molecular Cell*, 41(4), pp. 458-470.

Pal, S., Reckamp, K., Yu, H. & Figlin, R., 2010. Akt inhibitors in clinical development for the treatment of cancer. *Expert opinion on investigational drugs*, 19(11), pp. 1355-1366.

Pao, W. & Girard, N., 2011. New driver mutations in non-small-cell lung cancer. *Lancet Oncology*, 12(2), pp. 175-180.

Papadimitrakopoulou, V., 2012. Development of PI3K/Akt/mTOR Pathway Inhibitors and Their Application in Personalized Therapy for Non–Small-Cell Lung Cancer. *Journal of Thoracic Oncology*, 7(8), pp. 1315-1326.

Passive Smoking, 2016. *Cancer Research UK.* [Online] Available at: http://www.cancerresearchuk.org/about-cancer/causes-of-cancer/smoking-and-cancer/passive-smoking
[Accessed 16 October 2016].

PiercePharma, 2012. *Synta Provides Clinical Update and Reports Second Quarter 2012 Financial Results.* [Online] Available at: http://www.fiercepharma.com/pharma/synta-provides-clinical-update-and-reports-second-quarter-2012-financial-results [Accessed 16 March 2017].

Pillai, R. N. & Ramalingam, S. S., 2012. Hsp90 Inhibitors. *Journal of thoracic oncology,* 7(12), pp. S407-S408.

Pillai, R. N. & Ramalingam, S. S., 2014. Heat shock protein 90 inhibitors in non-small-cell lung cancer. *Current Opinion in Oncology,* 26(2), pp. 159-164.

Pirnia, F. et al., 2006. Ex vivo assessment of chemotherapy-induced apoptosis and associated molecular changes in patient tumor samples. *Anticancer Research,* Volume 26, pp. 1765-1772.

Polo , V. & Besse, B., 2014. Maintenance strategies in stage IV non-small-cell lung cancer (NSCLC): in which patients, with which drugs?. *Annals of Oncology,* 25(7), pp. 1283-1293.

Porta, M. et al., 2009. Cigarette smoking and K- ras mutations in pancreas, lung and colorectal adenocarcinomas: Etiopathogenic similarities, differences and paradoxes. *Mutation Research-Reviews in Mutation Research,* 682(2), pp. 83-93.

Puglisi, M. et al., 2014. Akt inhibition synergistically enhances growth-inhibitory effects of gefitinib and increases apoptosis in non-small cell lung cancer cell lines. *Lung Cancer,* 85(2), pp. 141-146.

Pumonary Imaging, 2010. *SlideShare.* [Online] Available at: http://image.slidesharecdn.com/channa6thfeb10cxrppt-100206131403-phpapp01/95/pulmonary-imaging-71-728.jpg?cb=1265462258 [Accessed 22 October 2016].

Ramalingam, S. et al., 2015. A randomized phase II study of ganetespib, a heat shock protein 90 inhibitor, in combination with docetaxel in second-line therapy of advanced non-small cell lung cancer (GALAXY-1). *Annals of oncology ,* 26(8), pp. 1741-1748.

Riely , G., Marks , J. & Pao , W., 2009. KRAS mutations in non-small cell lung cancer. *Proceedings of the American Thoracic Society,* 6(2), pp. 201-205.

Riely, G. J., Marks, J. & Pao, W., 2009. KRAS Mutations in Non–Small Cell Lung Cancer. *Proceedings of the American Thoracic Society,* 6(2), pp. 201-205.

Rivlin, N., Brosh, R., Oren, M. & Rotter, V., 2011. Mutations in the p53 Tumor Suppressor Gene. *Genes & Cancer,* 2(4), pp. 466-474.

Roberts, P. & Der, C., 2007. Targeting the Raf-MEK-ERK mitogen-activated protein kinase cascade for the treatment of cancer. *Oncogene,* Volume 26, pp. 3291-3310.

Sackett, M. K. et al., 2010. Diagnostic concordance of histologic lung cancer type between bronchial biopsy and cytology specimens taken during the same bronchoscopic procedure. *Archives of Pathology & Laboratory Medicine,* 134(10), pp. 1504-1512.

Sankaranarayanan , R., Swaminathan , R., Jayant , K. & Brenner , H., 2011. Chapter 32: An overview of cancer survival in Africa, Asia, Caribbean and Central America: the case for investments in cancer health services. *IARC scientific publications,* Volume 162, pp. 257-291.

Sato, S., Fujita, N. & Tsuruo, T., 2000. Modulation of Akt kinase activity by binding to Hsp90. *Proceedings of the National Academy of Sciences of the United States,* 97(20), pp. 10832-10837.

Scrima, M. et al., 2012. Signaling Networks Associated with Akt Activation in Non-Small Cell Lung Cancer (NSCLC): New Insights on the Role of Phosphatydil-Inositol-3 kinase (Molecular Alterations in NSCLC). *PLoS ONE,* 7(2), pp. e30427(1-15).

Selleck Chemicals, 2017. *Ganetespib (STA-9090)-Catalog No.S1159.* [Online] Available at: http://www.selleckchem.com/products/ganetespib-sta-9090.html [Accessed 3 March 2017].

Selleck Chemicals, 2017. *Pictilisib (GDC-0941) (Catalog No.S1065).* [Online] Available at: http://www.selleckchem.com/products/GDC-0941.html?gclid=CL_0iJftutICFU0Q0wodvgsCUw
[Accessed 3 March 2017].

Selleck Chemicals, 2017. *Selumetinib (AZD6244)-Catalog No.S1008.* [Online] Available at: http://www.selleckchem.com/products/AZD6244.html [Accessed 4 March 2017].

Shamir, E. R. & Ewald , A. J., 2014. Three-dimensional organotypic culture: experimental models of mammalian biology and disease. *Nature Reviews Molecular Cell Biology,* Volume 15, p. 647–664 .

Sharma, P., Singh, H., Basu, S. & Kumar, R., 2013. Positron emission tomography-computed tomography in the management of lung cancer: An update. *South Asian Journal of Cancer,* 2(3), pp. 171-178.

Shen, R. R. & Hahn, W. C., 2011. Emerging roles for the non-canonical IKK[epsilon] in cancer.(Report). *Oncogene,* 30(6), pp. 631-641.

Shimamura, T. et al., 2012. Ganetespib (STA-9090), a nongeldanamycin HSP90 inhibitor, has potent antitumor activity in in vitro and in vivo models of non-small cell lung cancer. *Clinical cancer research ,* 18(18), pp. 4973-85.

Shimamura, T. & Shapiro, G. I., 2008. Heat Shock Protein 90 Inhibition in Lung Cancer. *Journal of thoracic oncology ,* 3(602), pp. S152-159.

Shi, Y. et al., 2014. Platinum(IV) cisplatin derivative trans, cis, cis-bis(heptanoato)amine(cyclohexylamine)dichloridoplatinum(IV) has an enhanced therapeutic index compared to cisplatin for the treatment of non-small cell lung cancer. *Inorganica Chimica Acta,* Volume 423, pp. 215-219.

Singh, B. et al., 2002. p53 regulates cell survival by inhibiting PIK3CA in squamous cell carcinomas. *Genes & development,* 16(8), pp. 984-993.

Smith , D. et al., 2015. The HSP90 inhibitor ganetespib potentiates the antitumor activity of EGFR tyrosine kinase inhibition in mutant and wild-type non-small cell lung cancer. *Targeted Oncology,* 10(2), pp. 235-245.

Soria , J. et al., 2002. Lack of PTEN expression in non-small cell lung cancer could be related to promoter methylation. *Clinical cancer research ,* 8(5), pp. 1178-1184.

Spira, A., Halmos, B. & Powell, C. A., 2015. Update in Lung Cancer 2014. *American journal of respiratory and critical care medicine,* 192(3), pp. 283-294.

Spoerke, J. M. et al., 2012. Phosphoinositide 3-kinase (PI3K) pathway alterations are associated with histologic subtypes and are predictive of sensitivity to PI3K inhibitors in lung cancer preclinical models. *Clinical cancer research ,* 18(24), pp. 6771-83.

Sputum cytology, 2016. *American Cancer Society.* [Online] Available at: http://www.cancer.org/cancer/lungcancer-smallcell/detailedguide/small-cell-lung-cancer-diagnosis
[Accessed 22 October 2016].

Staging, 2015. *National Cancer Institute.* [Online] Available at: https://www.cancer.gov/about-cancer/diagnosis-staging/staging [Accessed 22 October 2016].

Steven, A., Fisher, S. A. & Robinson, B. W., 2016. Immunotherapy for lung cancer. *Respirology,* 21(5), pp. 821-833.

Stevenson, M., 2016. *Non-Small Cell Lung Cancer Treatment Protocols.* [Online] Available at: http://emedicine.medscape.com/article/2007153-overview#a1 [Accessed 1 March 2017].

Stewart, B. W., 2014. *World Cancer Report 2014.* 1st ed. s.l.:International Agency for Research on Cancer .

Stewart, E. L., Tan, S. Z., Liu, G. & Tsao, M.-S., 2015. Known and putative mechanisms of resistance to EGFR targeted therapies in NSCLC patients with EGFR mutations-a review. *Translational lung cancer research,* 4(1), pp. 67-81.

Stinchcombe , T. & Johnson , G., 2014. MEK inhibition in non-small cell lung cancer. *Lung cancer,* 86(2), pp. 121-5.

Suda , K., Tomizawa , K. & Mitsudomi , T., 2010. Biological and clinical significance of KRAS mutations in lung cancer: an oncogenic driver that contrasts with EGFR mutation. *Cancer metastasis reviews,* 29(1), pp. 49-60.

Sun , D. et al., 2015. MK2206 potentiates cisplatin-induced cytotoxicity and apoptosis through an interaction of inactivated Akt signaling pathway. *Urologic oncology,* 33(3), pp. 111.e17-26.

Survival for NCLC and SCLC by Stage, 2014. *Cancer Research UK.* [Online] Available at: http://www.cancerresearchuk.org/about-cancer/type/lung-cancer/treatment/statistics-and-outlook-for-lung-cancer#outcome
[Accessed 17 August 2016].

Survival for non small cell lung cancer by stage, 2014. *Cancer Research UK.* [Online] Available at: http://www.cancerresearchuk.org/about-cancer/type/lung-cancer/treatment/statistics-and-outlook-for-lung-cancer#outcome
[Accessed 17 August 2016].

Synta Pharmaceuticals Corp. , 2016. *A Phase 3 Study of Ganetespib in Combination With Docetaxel Versus Docetaxel Alone in Patients With Advanced NSCLC (Galaxy 2) (NCT01798485).* [Online]
Available at: https://clinicaltrials.gov/ct2/show/results/NCT01798485?sect=X870156&term=NSCLC+GANETESPIB&rank=4#outcome2
[Accessed 05 March 2017].

The Cancer Genome Atlas Research Network, 2012. Comprehensive genomic characterization of squamous cell lung cancers. *Nature,* Volume 489, pp. 519-525.

The Cancer Genome Atlas Research Network, 2014. Comprehensive molecular profiling of lung adenocarcinoma. *Nature,* Volume 511, pp. 543-550.

Torre, L. A. et al., 2015. Global Cancer Statistics, 2012. *CA: A Cancer Journal for Clinicians,* Volume 65, pp. 87-108.

Toulany, M. & Rodemann, H. P., 2015. Phosphatidylinositol 3-kinase/Akt signaling as a key mediator of tumor cell responsiveness to radiation. *Seminars in Cancer Biology,* Volume 35, pp. 180-190.

Travis, W. et al., 2013. Diagnosis of Lung Cancer in Small Biopsies and Cytology Implications of the 2011 International Association for the Study of Lung Cancer/American Thoracic Society/European Respiratory Society Classification. *Archives Of Pathology & Laboratory Medicine,* 137(5), pp. 668-684.

Travis, W. D. et al., 2015. The 2015 World Health Organization Classifiation of Lung Tumors-Impact of Genetic, Clinical and Radiologic Advances Since the 2004 Classifiation. *Journal of Thoracic Oncology,* 10(9), pp. 1243-1260.

Travis, W. D. et al., 2011. International Association for the Study of Lung Cancer/American Thoracic Society/European Respiratory Society International

Multidisciplinary Classification of Lung Adenocarcinoma. *Journal of Thoracic Oncology* , 6(2), pp. 244-285.

Tsurutani , J. et al., 2006. Evaluation of two phosphorylation sites improves the prognostic significance of Akt activation in non-small-cell lung cancer tumors. *Journal of clinical oncology* , 24(2), pp. 306-14.

Union for International Cancer Control, 2011. *TNM Classification of Malignant Tumours-7th ed.-Changes between the 6th and 7th editions.* [Online] Available at: http://www.uicc.org/sites/main/files/private/TNM_Classification_of_Malignant_Tumours_Website_15%20MAy2011.pdf
[Accessed 23 October 2016].

University of Birmingham , 2016. *National Lung Matrix Trial: Multi-drug Phase II Trial in Non-Small Cell Lung Cancer (NCT02664935).* [Online] Available at: https://clinicaltrials.gov/ct2/show/NCT02664935?term=NSCLC+AKT&rank=16
[Accessed 2 March 2017].

Vaira, V. et al., 2010. Preclinical model of organotypic culture for pharmacodynamic profiling of human tumors. *Proceedings of the National Academy of Sciences of the United States of America,* Volume 107, pp. 8352-6.

van Boerdonk , R. et al., 2013. High-risk human papillomavirus-positive lung cancer: molecular evidence for a pattern of pulmonary metastasis. *Journal of Thoracic Oncology* , 8(6), pp. 711-718.

Vasan, N., Boyer , J. & Herbst , R., 2014. A RAS renaissance: emerging targeted therapies for KRAS-mutated non-small cell lung cancer. *Clinical cancer research* , 20(15), pp. 3921-30.

Wang , W. et al., 2009. Crosstalk to stromal fibroblasts induces resistance of lung cancer to epidermal growth factor receptor tyrosine kinase inhibitors. *Clinical cancer research,* 15(21), pp. 6630-6638.

Wang , X., Martindale, J. L. & Holbrook, N. J., 2000. Requirement for ERK activation in cisplatin-induced apoptosis. *The Journal of biological chemistry,* 275(50), pp. 39435-39443.

Wang, L. et al., 2014. PIK3CA mutations frequently coexist with EGFR/KRAS mutations in non-small cell lung cancer and suggest poor prognosis in EGFR/KRAS wildtype subgroup. *PloS one,* 9(2), pp. e88291(1-10).

Wang, M. et al., 2013. Activation of ERK1/2 and Akt is associated with cisplatin resistance in human lung cancer cells. *Journal of Chemotherapy,* 25(3), pp. 162-169.

Weng , S. et al., 2012. Inhibition of thymidine phosphorylase expression by using an HSP90 inhibitor potentiates the cytotoxic effect of cisplatin in non-small-cell lung cancer cells. *Biochemical pharmacology,* 84(1), pp. 126-36.

White, M. C. et al., 2014. Age and Cancer Risk. *American Journal of Preventive Medicine,* 46(301), pp. S7-15.

WHO Media Centre , 2015. *WHO-World Health Organization.* [Online] Available at: http://www.who.int/mediacentre/factsheets/fs297/en/ [Accessed 15 October 2016].

Why Non-smokers Sometimes Get Lung Cancer, 2015. *American Cancer Society.* [Online]
Available at: http://www.cancer.org/cancer/news/why-lung-cancer-strikes-nonsmokers [Accessed 16 October 2016].

Wilson, S. M. et al., 2008. mTOR Mediates Survival Signals in Malignant Mesothelioma Grown as Tumor Fragment Spheroids. *American Journal of Respiratory Cell and Molecular Biology,* Volume 39, pp. 576-83.

Worldwide Cancer Factsheet, 2014. *Cancer Research UK.* [Online] Available at: http://publications.cancerresearchuk.org/cancerstats/statsworldwide/worldfactsheet.html [Accessed 15 October 2016].

Wu , X. et al., 2005. Cell Cycle Checkpoints, DNA Damage/Repair, and Lung Cancer Risk. *Cancer Research,* 65(1), pp. 349-357.

Xu , S. et al., 2009 . Rac inhibition reverses the phenotype of fibrotic fibroblasts. *PLoS One,* 4(10), p. e7438.

Yamamura , Y. et al., 2015. Akt-Girdin signaling in cancer-associated fibroblasts contributes to tumor progression. *Cancer research,* 75(5), pp. 813-823.

Yang, L. et al., 2014. Blocking the PI3K pathway enhances the efficacy of ALK-targeted therapy in EML4-ALK-positive nonsmall-cell lung cancer. *Tumor Biology,* 35(10), pp. 9759-9767.

Yang, T., Barbone, D., Fennell, D. & Broaddus, V., 2009. Bcl-2 family proteins contribute to apoptotic resistance in lung cancer multicellular spheroids. *American journal of respiratory cell and molecular biology,* Volume 41, pp. 14-23.

Yang, X. et al., 2008. Regulation of apoptosis-inducing factor-mediated, cisplatin-induced apoptosis by Akt. *British Journal of Cancer,* 98(4), pp. 803-808.

Ying , L. et al., 2015. Cancer Associated Fibroblast-Derived Hepatocyte Growth Factor Inhibits the Paclitaxel-Induced Apoptosis of Lung Cancer A549 Cells by Up-Regulating the PI3K/Akt and GRP78 Signaling on a Microfluidic Platform. *PLoS One,* 10(6), p. e0129593.

Yip, P. Y., 2015. Phosphatidylinositol 3-kinase-Akt-mammalian target of rapamycin (PI3K-Akt-mTOR) signaling pathway in non-small cell lung cancer. *Translational lung cancer research,* 4(2), pp. 165-176.

Zambetti, G. P., 2005. *The p53 Tumor Suppressor Pathway and Cancer.* 1st ed. Boston: Springer Science Business Media.

Zanoni, M. et al., 2016. 3D tumor spheroid models for in vitro therapeutic screening: a systematic approach to enhance the biological relevance of data obtained. *Scientific Reports,* Volume 6, pp. 19103 (1-11).

Zhang, Y., Lu, H. & Xu, G., 2014. Effect of PI3K/Akt pathway on cisplatin resistance in non-small cell lung cancer. *Chinese journal of lung cancer,* 17(8), pp. 635-642.

Zhu, Z. et al., 2014. Inhibition of KRAS-driven tumorigenicity by interruption of an autocrine cytokine circuit. *Cancer discovery,* 4(4), pp. 452-465.

Zhu, Z. & Golay, H. G., 2014. Targeting pathways downstream of KRAS in lung adenocarcinoma. *Pharmacogenomics,* 15(11), pp. 1507-1518.

Zou , Z. et al., 2012. The novel dual PI3K/mTOR inhibitor GDC-0941 synergizes with the MEK inhibitor U0126 in non-small cell lung cancer cells. *Molecular medicine reports*, 5(2), pp. 503-508.